UNIVERSITÀ DEGLI STUDI DI PADOVA

Dipartimento di Medicina Animale, Produzioni e Salute

Dipartimento di Biomedicina Comparata ed Alimentazione

Corso di laurea magistrale a ciclo unico in

MEDICINA VETERINARIA

Array Comparative Genomic Hybridization (aCGH) analysis in Canine Acral Melanoma (CAM)

Relatore:
Prof. Massimo Castagnaro

Correlatore:
Dott.ssa Ginevra Brocca

Laureanda:
Giovanna Miani

Matricola n.
1166854

ANNO ACCADEMICO 2021-2022

Da’ al mondo gli inchini dovuti

A . Schopenhauer

Summary

Abstract

Melanomas are malignant neoplasms developing from melanocytes that have been described in human beings and in several animal species, including dogs. Due to its clinical aggressiveness and tendency to metastasize, human melanoma (HM) is a leading cause of skin cancer mortality in people. In dogs, it accounts for 4% of all tumours and, as in humans, it carries a bad prognosis. Both genetic and environmental factors are involved in its development. Although most of HMs are caused by UV exposure, others can arise from sun-shielded locations such as the eye, digits and mucosa. Therefore, based on their location, HMs can be differentiated into melanomas of sun-exposed sites and sun-shielded sites. Melanomas of sun-exposed locations are classed as either chronically sun damaged (CSD) or non-CSD, while mucosal and acral melanomas belong to the sun-shielded category.

A high level of aggressiveness is a common feature of melanomas, particularly mucosal and acral melanomas, which generally leads to a poor prognosis. Additionally, these cancers frequently resist treatments like radiotherapy and chemotherapy. Naturally arising canine melanomas can be used as models for human ones since in both species these tumours develop in presence of an intact immune system, are characterized by tumour growth over a protracted period and include inter-individual and intra-tumoural heterogeneity, metastasis, cancer recurrence and therapy resistance. Furthermore, dogs and humans share similar environments and, as a consequence, environmental factors that can contribute to tumour development. Finally, dogs have shorter lifespan which allows for earlier assessments of the impacts of the disease progression and overall survival.

This thesis project focused on Canine Acral Melanoma (CAM), a malignant tumour that arises on the glabrous skin of the palms, soles and nail apparatus (subungual). The aim was to investigate its whole genome landscape through the pathway enrichment analysis, an important recent new approach to cancer genomic investigations. This procedure allows to look at multiple aberrated genes as well as pinpoint the regions where it is essential to search for biological processes

associated with cancer that are disrupted. As a result, it enables the development of new targeted therapies as well as more accurate diagnostic standards.

To achieve this goal, we used a molecular technique called Array Comparative Genomic Hybridization (aCGH) that enabled a genome-wide analysis of large size tumour aberrations. Amplifications and deletions of DNA sequences detected by aCGH were then analysed through ClueGo plugin for the software Cytoscape 3.9.0 which allows to gain new insights and perspectives on tumours, discovering enriched biological pathways that would otherwise go unnoticed if only single aberrations, and associated genes, were characterized.

Ten samples of CAM underwent this analysis and revealed the disruption of 182 pathways derived from lost genes and 159 pathways derived from gained genes. The pathways were then grouped depending on their main function, revealing numerous pathways related to the loss of cell cycle control and DNA damage response, pro-survival mitogenesis, angiogenesis, ultraviolet radiation response and immune system resistance. Interestingly, these groups represent the main features of tumours alterations.

Whitin the loss of cell cycle control and DNA damage response, many disruption concerned the p53 pathways, a commonly aberrated pathway in both COM and hAM. The most relevant genetic alterations were detected in MDM2, CDK4 (gained), MTBP and Tp53BP2 (deleted) in contrast with what is mostly know for COM. Pro-survival mitogenic pathways were mostly disrupted through the alteration of tyrosine kinases receptor that are known to be dysregulated in many cancers. Among these, amplifications of PDGFR-α and KIT were detected, consistently with canine and human mucosal melanoma. Angiogenetic pathways were highly enhanced and relevant amplifications that contributed to it were found in PDGFR-α, PTK2, ANGPT1 and ANGPTLs genes, similarly for what is so far known for other melanomas. Interestingly, the gain of ultraviolet-response genes suggests a possible role of ultraviolet radiation in the development of the tumor, in contrast with the hypothesis that CAM and hAM belong to the sun-shielded category of melanomas. Moreover, the detected alteration of the immune system response are also consistent with what reported in melanomas. Among these it was seen that the

pathways mostly disrupted are the ones of coinhibitory checkpoint molecules of T cells and of cytokines as IFN-γ and IL-12.

Riassunto

I melanomi sono tumori maligni che derivano dai melanociti, riportati sia nell'uomo e in molte specie animali, incluso il cane. A causa della sua aggressività dal punto di vista clinico e la tendenza a sviluppare metastasi, il melanoma umano (HM) è una delle principali cause di morte per tumori cutanei nell'uomo. Nei cani rappresenta il 4% di tutti i tumori e, come nell'uomo, è caratterizzato da una prognosi infausta. Nel suo sviluppo sono coinvolti sia fattori genetici che ambientali. Nonostante la maggior parte dei HM sia causato dall'esposizione ai raggi UV, vi sono melanomi che possono insorgere in posizioni protette dai raggi solari, come l'occhio, le dita e le mucose. Pertanto, in base alla loro posizione, gli HM possono essere divisi in melanomi delle zone esposte al sole e delle zone protette dal sole. I melanomi delle zone esposte al sole sono classificati in base al danno solare che subiscono e si dividono pertanto in danneggiati cronicamente dal sole (CSD) e danneggiati non cronicamente dal sole (non-CSD).

L'elevato livello di aggressività è una caratteristica comune dei melanomi, in particolar modo per quanto riguarda i melanomi mucosali ed acrali, che comunemente comportano una prognosi infausta. In aggiunta, questi tumori sono spesso resistenti a trattamenti standard con radioterapia e chemioterapia. I melanomi che insorgono naturalmente nei cani possono essere usati come modelli per l'uomo poiché in entrambe le specie questi tumori insorgono in presenza di un sistema immunitario intatto, sono caratterizzati da una crescita protratta nel tempo, una spiccata eterogeneità interindividuale ed intratumorale, metastasi frequenti, recidive e resistenza alle terapie. Inoltre, cani e umani condividono ambienti simili e, pertanto, fattori ambientali che possono contribuire allo sviluppo del tumore. Infine, i cani hanno una durata di vita inferiore all'uomo che permette di valutare prima gli impatti dello sviluppo della patologia e la sopravvivenza.

Questo progetto di tesi si focalizza sul melanoma acrale canino (CAM), un tumore maligno che insorge sulla pelle glabra di palmo, suole e apparato ungueale (subungueale). L'obiettivo era quello di investigare il suo panorama genomico attraverso la *pathway enrichment analysis*, un importante nuovo approccio allo

studio genomico dei tumori. Questa procedura permette di valutare l'alterazione di molteplici geni e di individuare le regioni in cui possono essere alterati processi biologici associati al tumore. Questo approccio permette lo sviluppo di nuove terapie con target specifici e l'individuazione di nuovi standard diagnostici.

Per raggiungere l'obiettivo abbiamo applicato una tecnica molecolare che prende il nome di *Array Comparative Genomic Hybridization* (aCGH) che permette l'analisi genomica delle aberrazioni del tumore. L'aCGH ha permesso l'individuazione di amplificazioni e delezioni di DNA che sono poi state analizzate tramite il ClueGo plugin del software Cytoscape 3.9.0; quest'ultimo permette di ottenere nuove informazioni e prospettive sui tumori tramite la scoperta di *pathway* biologici arricchiti che passerebbero inosservati con tecniche focalizzate solo su singole aberrazioni e i geni associati.

Dieci campioni di CAM sono stati sottoposti a tale analisi e hanno rivelato l'alterazione di 182 *pathway* derivanti dalla delezione di geni e di 159 *pathway* derivanti dall'amplificazione di geni. I *pathway* sono stati raggruppati in base alla loro funzione principale e, tra essi, sono stati rilevati *pathway* relativi alla perdita del controllo del ciclo cellulare e della risposta a danni al DNA, mitogenesi, angiogenesi, risposta ai raggi ultravioletti e resistenza al sistema immunitario. E' interessante rilevare come queste funzioni sono tutte incluse negli *hallmarks* dei tumori maligni.

All'interno dei *pathway* riguardanti la perdita di controllo del ciclo cellulare e della risposta ai danni al DNA, molte alterazioni riguardano i *pathway* associati a p53, comunemente riscontrati anche nel melanoma orale del cane (COM) e nel melanoma acrale dell'uomo (hAM). All'interno di questo gruppo e in contrasto con quanto riportato nel COM, i principali geni alterati sono MDM2, CDK4 (amplificati), MTBP and Tp53BP2 (deleti). I *pathway* mitogenetici interessano principalmente i recettori tirosin-chinasici, noti per essere alterati in molti tumori. Tra questi sono state individuate amplificazioni di PDGFR-α e KIT, in modo analogo a quello che è stato riscontrato anche nei melanomi mucosali di cane e uomo. Analogamente anche i *pathway* angiogenici sono risultati fortemente potenziati, in particolare con amplificazioni genetiche di PDGFR-α, PTK2, ANGPT1 e ANGPTLs. Ancora, alcuni risultati sembrano suggerire che anche i raggi ultravioletti possano giocare un ruolo

nello sviluppo del tumore, in contrasto con l'ipotesi che CAM e hAM appartengano alla categoria dei melanomi delle zone protette dal sole. Infine, alterazioni della risposta del sistema immunitario sono state riscontrate, coerentemente con ciò che è noto nei melanomi. Tra queste, i *pathway* principalmente alterati sono quelli riguardanti le molecole co-inibitorie dei checkpoint delle cellule T e le citochine quali IFN-γ e IL-12.

1. Introduction

1.1 Human and canine melanoma

Melanomas are malignant neoplasms that develop from melanocytes, skin pigment cells located in the epidermal and dermal layers of the skin that generate and store melanin. These tumours have been described in human beings and in several animal species, including dogs, cats, horses, and also in wild terrestrial and marine animals (Nishiya et al., 2016).

Melanocytes are dendritic cells that originate from the neuroectoderm and melanoblasts of the neural crest that during embryogenesis migrate to dermis and epidermis, mucous membranes and eyes. In adults, they are located in the basal layer of keratinocytes and are anchored to the basal membrane of the epidermis. A healthy melanocyte is an unpigmented cell that does not interact with other cells of its kind. Melanin is actually packaged in melanosomes and is transferred to keratinocytes through the dendritic processes of melanocytes. In addition, Epithelial cadherin (E-cadherin) molecules allow each melanocyte to attach to five to eight keratinocytes without being connected to other melanocytes (Smith et al., 2002). During their cancerous development, melanocytic cells tend to lose their non-pigmented and isolated characteristics and become pigmented and clustered neoplastic melanocytes through a multistep process consisting of initiation, promotion, transformation and metastasis (Smith et al., 2002). Throughout this process, there are variations in the expression of cell-to-cell adhesion molecules such as a decreased expression of E-cadherin and V-CAM 1 (vascular cell adhesion molecule-1), as well as increased expression of N-cadherin, Mel-CAM 1, ICAM 1, and integrins (Li et al., 2002). The interaction between melanocytes and keratinocytes provided by the E-cadherin is required for the growth and phenotypic control of melanocytes by keratinocytes. During the developmental process of melanoma, shown in Figure 1, there is a shift in the cadherin profile from E- to N- which rids cells of epidermal keratinocytes and imparts new adhesive properties. Furthermore, N-cadherin-expressing melanoma cells are able to form an N-cadherin-mediated adherent junction and a connexin-mediated gap junction with vascular endothelial

cells and with fibroblasts. In addition two other adhesion complexes, implicated in the progression of melanoma, can be found: Mel-CAM and its ligand, L1- CAM and integrin avb3 (Li et al., 2002).

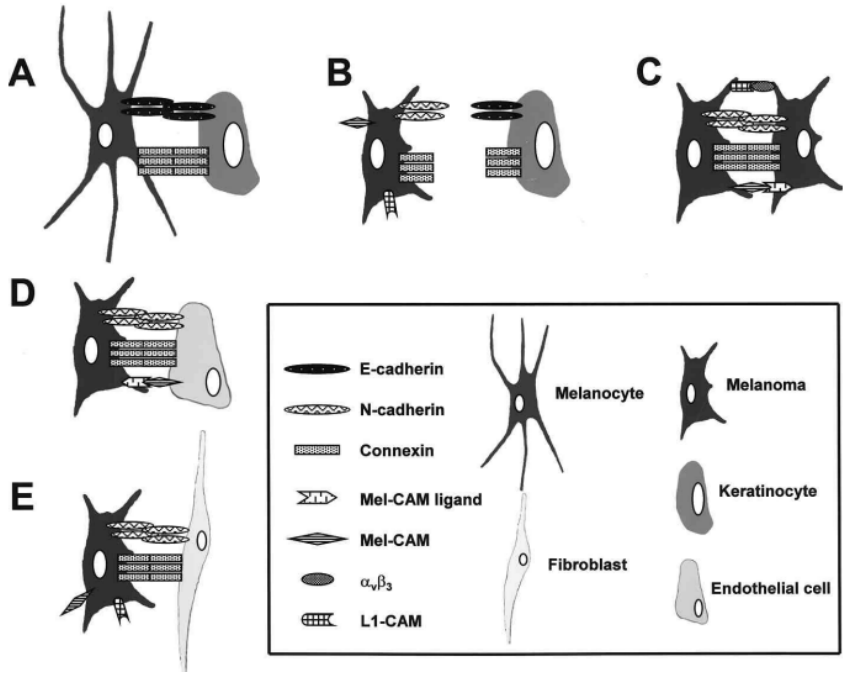

Figure 1: cell interaction and communication during melanoma development.

(A) The physiological interaction between a keratinocyte and a melanocyte.
(B) Cadherin shift from E to N that allows the cell to move from the epidermal keratinocytes.
(C) Communication between melanoma cells through a variety of adhesion junctional receptors.
(D) New adhesive properties conferred by the cadherin switch that allows adhesion to endothelial cells and fibroblasts (E) (Li et al., 2002)

According to Curtin et al.(2005), HM can be classified into four types based on their development region, localisation on either sun-shielded or sun-exposed sites, and genomic characterization, as shown in Figure 2. Melanomas on skin with chronic sun-induced damage (CSD), melanomas on skin without chronic sun-induced damage (non-CSD), mucosal melanomas, and acral melanomas (palms, soles, and subungual sites) are the tumours that can be encountered (Curtin et al., 2005).

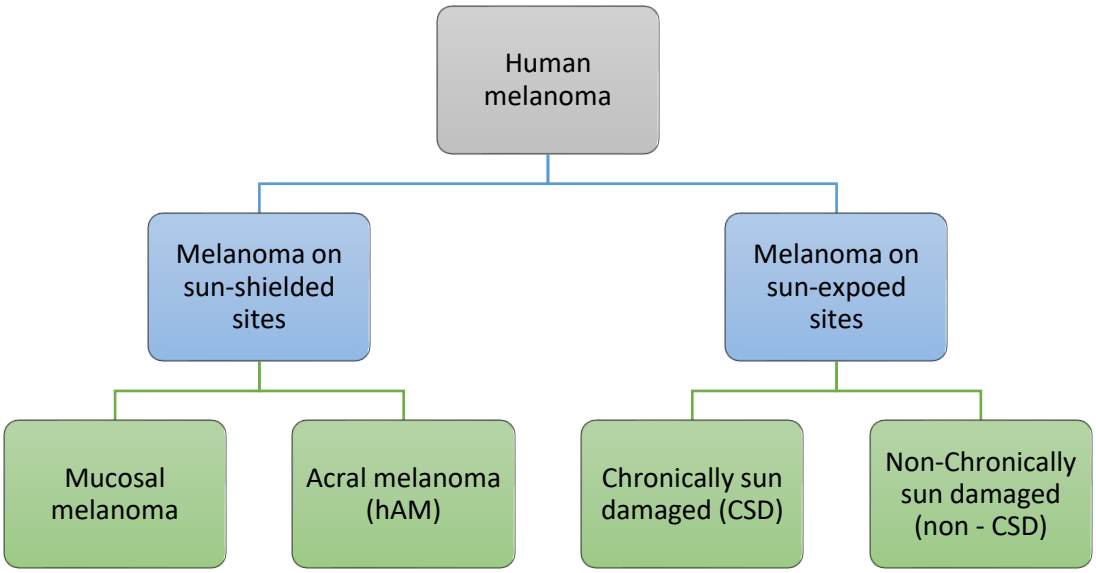

Figure 2: Classification of the melanoma types according to Curtin et al. (2005) genetic characterization (Curtin et al., 2005)

Among human cancers, melanoma is the one that has been increasing in incidence the most (Bergman et al., 2020). Malignant melanoma is also found in dogs and is responsible for nearly 4% of all tumours (Manley et al., 2011). While relatively prevalent in dogs, particularly those with considerable degrees of skin pigmentation, melanoma is rather uncommon in cats. The hairy skin is the most frequent location for canine melanoma, where they grossly present as little brown to black masses, but can also look like big, flat, and/or wrinkled masses. Other areas where primary melanoma can develop are the oral cavity, nailbed, footpad, eye, gastrointestinal tract, nasal cavity, anal sac, and mucocutaneous junction. Furthermore locations were metastases arise mostly are lymphnodes (LNs), lungs, liver, meninges, and adrenal glands (Bergman et al., 2020).

Recent studies on the etiology of human melanoma have found numerous separate mechanisms in addition to the UV-associated mutagenesis. UV-associated melanoma is less likely to be the primary cause of the disease in dogs because the majority of canine breeds have a thick coat of hair that presumably provides them with protection from the sun. Canine melanoma risk factors, however, are not well understood (Bergman et al., 2020). Up to know it has been shown that the pathogenesis of this tumour in the canine population is connected to the site where it arises and the coat colour. Furthermore, the tumour malignancy, prognosis,

occurrence, and breed propensity are all influenced by the tumour development location (Conrad et al., 2022). The mortality incidence is in fact related to the site of development and can be split into three levels, according to Spangler & Kass (2006): oral melanomas have the highest mortality rate and their benign counterpart is rarely found. Digital and labial melanomas have instead an intermediate value of mortality, while the ones affecting the eye and all other cutaneous body sites have the least amount and usually affect the head, ventral abdomen, scrotum or the eye (Conrad et al., 2022). Although, localization is not a perfect predictor of local invasiveness and predisposition for metastatic disease (Bergman et al., 2020).

1.2 Human acral melanoma (hAM)

Acral melanoma (AM) is an uncommon form of melanoma that develops from the glabrous skin of the palms, soles and nail apparatus (subungual). In humans the etiological role of ultraviolet (UV) radiation induced mutations appears less significant when compared to other non-acral cutaneous melanomas. Its annual incidence is the same among all racial groups in the human population (1 case per 100.000 individuals), but it seems to be more prevalent in Asian, African, and Hispanic populations than in the European-derived ones. Human Acral Melanoma (hAM) has a quite poor prognosis, with a five-year overall survival (OS) rate that ranges from 59% to 70%. This is largely due to the rare location, which delays detection, as well as the effects of the various histotypes and molecular backgrounds. The four histological subtypes of acral melanoma (AM) that can be identified from a pathological point of view are acral lentiginous melanoma (ALM), the most common and aggressive form, superficial spreading melanoma (SSM), nodular melanoma (NM) and nevoid melanoma (Elefanti et al., 2021)

1.3 Canine acral melanoma (CAM)

1.3.1 Incidence, localization and clinical aspects

CAM accounts for 5-8% of canine melanomas, in fact the most common sites of melanoma development are the oral cavity and mucous membranes of the lips, which together with cutaneous neoplasms account for about 90% of melanomas (Gillard et al., 2014; Hardwick, 2021). Although, it is the second most common tumour of the digit in the canine population (Manley et al., 2011) accounting for a 24% incidence among tumours of this area (Bergman et al., 2020). A number of studies examining various digital lesions in dogs, including Grassingers' (2021), discovered that they were tumoural in more than half of the cases, with melanoma being the second most prevalent one after subungual squamous cell carcinoma (SCC) (Grassinger et al., 2021; Wobeser et al., 2007; Henry et al., 2005). This tumour has a reported prevalence of approximately 16% and most of them appear to have an aggressive behaviour, often related to bone invasion (Grassinger et al., 2021; Henry et al., 2005). However, the incidence of this tumour remains uncertain because the veterinary literature on the subject is still scarce, as it is generally for neoplasms affecting the digit of various histogenesis, with the exception of squamous cell carcinoma (Wobeser et al., 2007).

The occurrence likelihood is based on breed and coat colour (Conrad et al., 2022; Grassinger et al., 2021; Smith et al., 2002). In fact, Rottweilers and Labrador Retrievers have been found to be at a higher risk of developing acral melanoma, especially when compared to mixed breeds (Grassinger et al., 2021). A general predisposition of these two breeds to develop melanomas has already been noted by authors such as Gillard et al. (2014), implying that, given to the high amount of DNA sequence shared and their close relationship, there could be a common genetic component causing the same vulnerability (Grassinger et al., 2021). A higher predisposition has also been found in Schnauzers, Irish Setters, Golden Retrievers and Poodles (Conrad et al., 2022; Grassinger et al., 2021; Henry et al., 2005; Nishiya et al., 2016) and, despite of their breed, black-coated dogs seem overrepresented (Conrad et al., 2022; Grassinger et al., 2021). In contrast, Grassinger et al. (2021) found that Dachshunds and Rhodesian ridgebacks were rarely affected, although

Dachshunds are at higher risk for oral and dermal melanoma and Rhodesian Ridgebacks have a proclivity for cutaneous melanocytoma. This prompted the author to state the need for further investigations regarding the possibility of the existence of a breed-related tumour resistance to specific digital neoplasms. The distribution of the nature of digital lesions for each breed found by Grassinger et al. (2021) is shown in Figure 3.

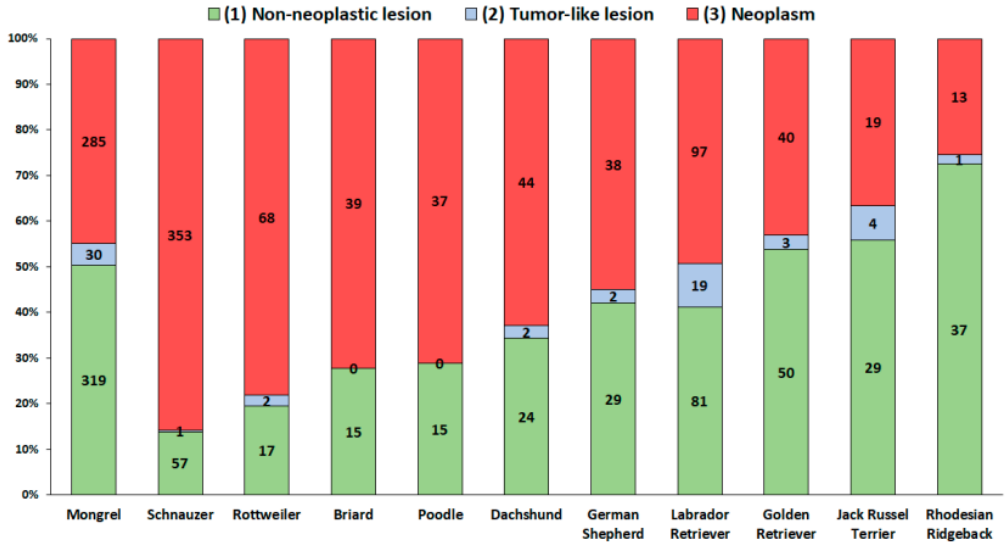

Figure 3: Analysis of the distribution of digital lesions, including non-neoplastic lesions, tumor-like lesions, and neoplasms divided by the most common breeds that included at least 50 dogs (Grassinger et al., 2021)

Additionally, melanoma is more common in older dogs, with an average age of over 10 years (Smith et al., 2002). Although, the incidence of melanocytic tumours in male dogs is higher, as in humans (Smith et al., 2002). Wobeser et al. (2007) were the firsts, and only, to identify a higher incidence of acral melanoma in females. Malignant tumours affecting the digits, such as melanoma, tend to occur more often on the forelimbs than on the hindlimbs (Henry et al., 2005). One hypothesis to justify melanoma tendency to primarily affect the forelimbs could be related to the greater weight they carry and possible exposure to trauma and carcinogens during activities such as digging (Wobeser et al., 2007). Aside from being less likely to have the dewclaw (first finger) affected by neoplasms, there has not been any evidence of a higher involvement of other digits (Wobeser et al., 2007) while in humans the great toe and thumb are more commonly affected (Elefanti et al., 2021).

Regardless of the underlying cause, whether neoplastic or inflammatory, dogs with finger lesions share common clinical signs (Henry et al., 2005). The presence of a digital mass, typically accompanied with lameness, is usually the presenting complaint of owners. Ulceration of the toe and breaking or splitting of the toenail are also usually associated clinical signs (Grassinger et al., 2021; Henry et al., 2005).

1.3.2 Macroscopical and microscopical aspects

Gross pathology of melanoma can vary considerably, regardless of the site where it occurs (Smith et al., 2002) which can be the skin of the digits, the footpad or the nail bed (Prouteau & André, 2019). Pigmentation can range from grey to brown to black, red, or even dark blue, and does not represent a discriminating trait since other lesions, whether cancerous or not, might have a similar appearance. Melanomas vary in size, but most are between one and three centimetres in diameter (Smith et al., 2002).

Melanomas of the digits frequently result in nail deformity, as in the case in Figure 4, and the mass usually grows from the nailbed or paronychia (Smith et al., 2002). Phalangeal bone destruction can be detected in 5% to 58% of dogs affected by this disease and is related to the tumour ability of invading bones and causing bony lysis (Nishiya et al., 2016; Smith et al., 2002). The third phalanx is usually the most involved in the lytic phenomena and is often detected via radiographic examination (Goldschmidt & Goldschmidt, 2016).

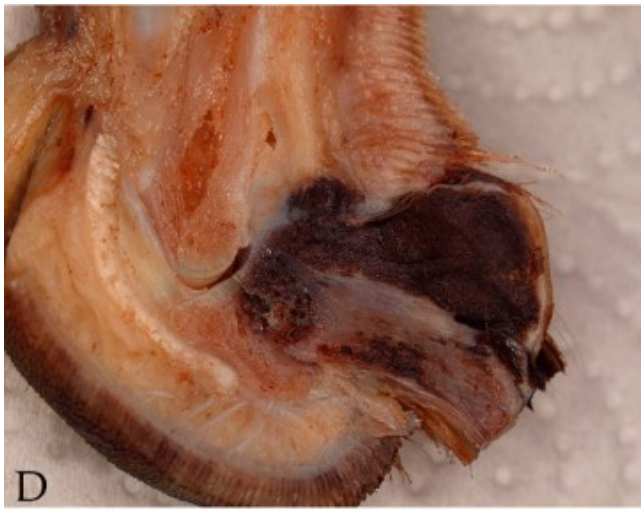

Figure 4: Finger section of an 11-year-old Labrador retriever affected by acral malignant melanoma (diameter 1,6 cm) (Grassinger et al., 2021)

Moreover, regional and distant metastases are frequently observed (Nishiya et al., 2016). Around 58% of digital melanoma exhibits radiographic evidence of metastatic processes in various visceral organs, and it can reach them through vessels of the lymphatic or blood system. The regional lymph node appears to be the first to be targeted by metastatic processes, and, while any visceral organ might be impacted, the lungs (Figure 5) are more commonly afflicted (Nishiya et al., 2016; Smith et al., 2002). Serosal surfaces, such as pericardium, pleura and peritoneum, are rarely involved (Smith et al., 2002).

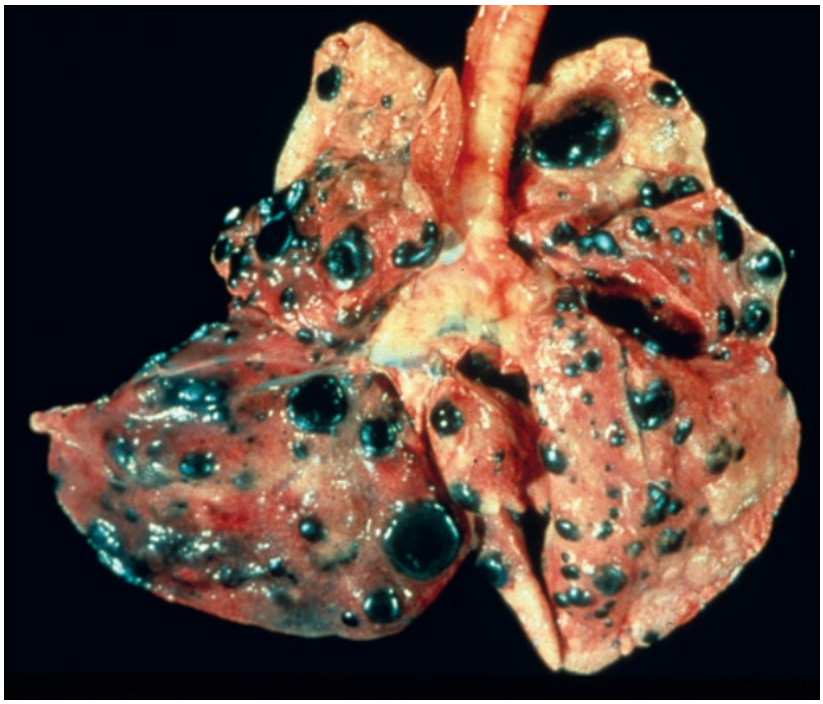

Figure 5: metastasis of melanoma in the lungs of a dog. The distribution of the tumor nodules is multifocal (embolic), characteristic of metastasis that derive from hematogenous spread (Newkirk et al., 2017)

Gross pathology cannot distinguish malignant melanoma from its benign counterpart. In both circumstances, the tumour can appear pigmented or unpigmented, and pigmentation is not a reliable predictor of the neoplasm malignancy degree. However, malignancy should be diagnosed and further histological examination performed anytime the neoplasm invades the subcutaneous tissue and deeps along the fascial planes (Goldschmidt & Goldschmidt, 2016).

When observing melanomas histologically (Figure 6), neoplastic melanocytes in the epidermal component, within the basal portion of the epidermis or its upper layers, appear isolated or in small groups. The presence of melanocytes in the upper layer of the epidermis, also known as pagetoid infiltration, is a feature that distinguishes melanomas from melanocytomas and can be highly helpful in diagnosing melanoma, especially when it is unpigmented (Goldschmidt & Goldschmidt, 2016).

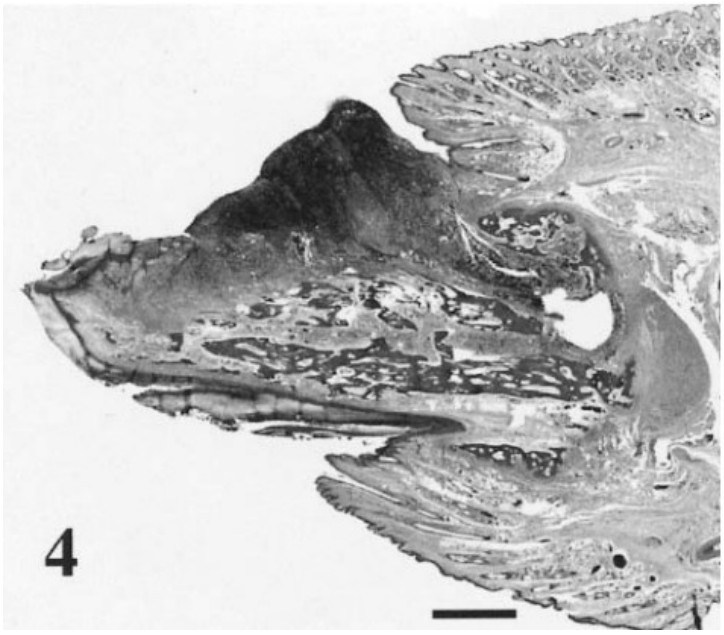

Figure 6: Subgross appearance of a canine digital melanoma. Malignant melanocytes are forming and exophytic protrusion that meanwhile invades the underlying phalangeal bone (Smith et al., 2002).

Melanoma cells in this area have bigger nuclei, prominent and often multiple nucleoli, and more frequent mitosis than cells in melanocytomas. Nucleoli can be irregularly shaped and situated eccentrically inside the nucleus. The key trait utilized by pathologists to distinguish a benign neoplasm from a malignant one is nuclear atypia, although this feature can be highly subjective. Tumoural cells in the dermal component can have a polygonal/epithelioid or fusiform (spindle or fibrous) shape, and the tumour can be formed by a single or mixed kind of cells. Melanoma cells are typically more anaplastic and pleomorphic than in melanocytoma and have a varying concentrations of melanin. Nests of epithelioid cells can be surrounded by a fine, fibrovascular stroma, while fusiform cells have patterns that often can resemble those of fibrosarcoma, malignant nerve sheath neoplasms and hemangiopericytomas. Subungual melanoma presents all of these general

characters that can be found in melanomas, but cells morphology is mostly epithelioid (Goldschmidt & Goldschmidt, 2016).

1.3.3 Diagnosis and staging

The diagnostic and clinical staging in dogs with melanoma is rather straightforward. A thorough physical examination, a full blood count, a biochemical profile, and a urinalysis should all be part of the minimum database. Gross melanoma characteristics, such as pigmentation of the tumour, should prompt a melanoma diagnosis. Fine-needle aspiration (FNA) and cytology are quick and simple methods for confirming pigmented melanomas. Evaluation of the regional LNs and of the thoracic cavity, using either three-view thoracic radiography or a thoracic CT scan, are typical clinical staging investigations. Whether lymphadenomegaly is present or not, regional LNS should be evaluated because metastases at this level are found in about 70% of dogs with lymphadenomegaly and in 40% of dogs with normal sized LNs. Despite their rare descriptions, abdominal ultrasonography or CT scans should be utilized to evaluate dogs with melanomas, particularly non-cutaneous ones, by looking for any signs of potential metastasese to the abdominal LNs, liver, adrenal glands, and other intraabdominal locations (Bergman et al., 2020). Simpson et al. (2014) recommend determining the tumour stage initially using imaging devices such as ultrasound of lymph nodes to detect metastases and CT or MRI with particular attention to the lungs, lymph nodes, abdomen and brain (Bergman et al., 2020). Moreover biopsy of the lymph nodes or of the palpable mass is recommended, both for staging and understanding the tumour development and response to therapy (Simpson et al., 2014). The TNM staging system elaborated by the World Health Organization (WHO) can be used for staging the oral melanoma. It takes in account the size of the tumour, lymph node involvement and presence of metastases, even though none of these aspects is considered to be a prognostic factor (Nishiya et al., 2016).

Making a diagnosis of melanoma via histopathology can be complicated, especially if it is amelanotic, as in a third of all cases. Moreover its histology can mirror other tumours as carcinomas, sarcomas, lymphomas and osteogenic tumours (Nishiya et al., 2016). These challenges to diagnose melanoma through histopathology,

combined with the fact that despite all of the characteristics that can be identified none of them has a prognostic significance, immunohistochemistry is necessary to obtain a broader view on the tumour nature (Goldschmidt & Goldschmidt, 2016; Nishiya et al., 2016). Immunohistochemistry is a very useful tool especially when there is an amelanotic tumour or the melanoma is mainly composed by spindle cells. These tumours may require histochemical stains as Fontana-Masson or a single or combined immunohistochemical stain as Melan-A, PNL2, TRP – 1 and TRP – 2 (Goldschmidt & Goldschmidt, 2016). Melan-A is a monoclonal antibody (mAb) used in human and veterinary pathology. It is a melanocyte-differentiating protein targeted by the human cytotoxic T lymphocytes when they are infiltrating a tumour. Its staining intensity is interestingly linked to biological behaviour and it appears stronger in more differentiated neoplasms than in amelanotic and undifferentiated ones. PNL2 reacts with normal and neoplastic human melanocytes in both benign and malignant lesions. Even if its targeted protein is yet unknown, it represent a useful marker for the immunohistochemical diagnosis of melanocytic lesions. These two stains are more effective for epithelioid cell melanomas than for spindle cell ones, and this makes it difficult to distinguish spindle cell amelanotic melanomas from other spindle cell cancers such as sarcomas (Giudice et al., 2010). TRP-1 and TRP-2, on the other hand, are novel tyrosinase antibodies still under investigation (Ohsie et al., 2008). When these four stains are used together, they provide the highest sensitivity for detecting amelanotic melanomas while also preserving 100% specificity (Smedley et al., 2011).

Finding histological traits that are directly related to the tumour aggressiveness is challenging and debated. Spangler and Kass (2006) created a tumour scoring system that included mitotic index, nuclear atypia, deep inflammation, intralesional necrosis of tumour cells and tumour size/volume as factors that directly contribute to death. Other attributes such as cell types, nuclear diameter, intraepithelial melanocyte proliferation, junctional activity, giant cells that do not contribute to mortality were not included in the scoring system. This method appears to be capable of predicting mortality within a year with a 66% accuracy while also predicting survival for at least one year with a 90% accuracy (Spangler & Kass, 2006).

1.3.4 Therapy

For all melanomas, surgery is the most common local therapy option: wide surgical excision, as the one showed in Figure 7, is the treatment of choice (Henry et al., 2005; Morris & Dobson, 2001; Wobeser et al., 2007). This treatment is recommended for both benign and malignant tumours, with a good prognosis for melanocytomas and a guarded to poor one for melanomas (Morris & Dobson, 2001). Amputation of the digit is the first line of treatment when acral melanoma is discovered with no evidence of metastases (Henry et al., 2005; Wobeser et al., 2007). When one toe is afflicted, excision at the level of the proximal phalanx or disarticulation through the phalangeal-metacarpal/tarsal joint should be undertaken. Nonetheless, tumour site, clinical stage, owner requirements, and the surgeon's ability to do a wide excision in challenging area, should all be taken into consideration when evaluating the surgical option. Unplanned or limited attempts of excision frequently result in residuals of macroscopic or microscopic tumoural tissue, hence these procedures should be avoided (Bergman et al., 2020). The possibility of local fast recurrence is higher when a more conservative resection is performed; alternatively, operating on intact anatomy usually results in the best chance of obtaining margins (Bergman et al., 2020; Dobson et al., 2003).

Figure 7: CAM located between third and fourth digit. The blue line shows the surgical margins that were between 1 and 2 cm. In this case partial foot amputation was performed achieving a complete histologic excision (Bergman et al., 2020)

Unfortunately, the Mean Survival Time (MST) following surgery remains low: 12 months, with 42-57 % of dogs alive after a year and 11-13 % after two years (Prouteau & André, 2019). These values indicate that the tumour is highly aggressive, and systemic therapy should be investigated, particularly to minimize the tumour metastatic rate (Nishiya et al., 2016). The application of therapies like radiation (RT) or other adjuvant therapies should be taken into consideration, particularly if a wide resection is cannot be accomplished during surgery and as a result histologic margins are incomplete. Although historically surgery has not been advised if a metastatic process is discovered during staging, the combination of adjuvant therapy (chemotherapy or immunotherapy) with cytoreductive surgery is currently being explored for metastatic melanoma (Bergman et al., 2020).

Chemotherapy and radiation therapy are often ineffective against both human and canine melanomas. There is no standard treatment for this condition in dogs; nevertheless, surgery is frequently used in association with hypofractionated or definitive radiotherapy and platinum chemotherapy (Hernandez et al., 2018). With some debate, melanoma is thought to be a relatively radioresistant tumour form, and it is therefore assumed that, in order to obtain local control, a higher dose in each fraction must be used. Although the optimal dose per fraction in hypofractionated protocols, as well as the relative radiosensitivity of melanoma in domestic animal species, has not been established, most procedures tend to adopt higher dose per fraction protocols. The most important benefits of hypofractionated protocols are less treatments with a consequent decrease in the number of anaesthesia, reduced costs, lower obligation for the owners, and less severe acute effects. These protocols, on the other hand, have a lower overall and biologic equivalent dose, which in theory leads to lower possibilities of local control and a higher risk for late adverse effects. Lower dose per fraction methods can be utilized for dogs who have a better prognosis to reduce the chance of late effects. However, when treating gross illness, responses are typically quick, and within a few weeks of initiating therapy, substantial reductions in the tumour volume can be observed (Bergman et al., 2020). However, even with that being said, it is important to remember that the majority of trials and retrospective studies focus on COM.

In dogs with a moderate to high risk of metastasis, such as those with oral, digit, or pad melanomas, systemic therapy is advised (Bergman et al., 2020). Among these, chemotherapy does not appear to be an effective treatment (Bergman et al., 2020; Brockley et al., 2013), in particular when using single agents like dacarbazine, melphalan, vinorelbine, or doxorubicin (Bergman et al., 2020). Patients who received cisplating and piroxicam or carboplatin treatments are instead the ones that reported the best therapeutic outcomes (Bergman et al., 2020). However, even when responding to chemotherapy, the survival rate does not appear to be significantly increased (Bergman et al., 2020; Brockley et al., 2013).

Other potential systemic therapies strategies for the adjuvant treatment of melanoma are represented by immunotherapy, cyclooxygenase inhibitors and xenogenetic DNA vaccine. A variety of immunotherapy strategies and targets have been used for canine melanoma. Although immunotherapies have produced some clinical antitumour responses, the processes for developing these products are typically costly and time-consuming, as well as difficult to replicate consistently. Currently, none of these methods is commercially accessible (Bergman et al., 2020). The use of cyclooxygenase (COX)-2 inhibitors is also a potential clinical therapy strategy that has not gotten much attention yet for canine melanoma. However, the results so far indicate the need for additional research (Bergman et al., 2020). Even the use of xenogenic DNA vaccination as an adjuvant therapy is a promising area for further research and evaluation (Bergman et al., 2020). It has so far been demonstrated to be safe and potentially therapeutic (Bergman et al., 2020; Manley et al., 2011), but its limitations, as its inability to prevent the formation of metastases in half of the cohort examined by Manley et al. (2011), must be considered.

1.3.5 Prognostic factors

At the time of presentation, around 40% of dogs with a digital lesion, later diagnosed as melanoma, already have developed metastases (Henry et al., 2005). When compared to other tumours of the digital region or melanomas in other cutaneous sites such as hairy skin, digital melanoma has a higher likelihood of detecting metastases at the time of diagnosis (Henry et al., 2005; Wobeser et al., 2007). Therefore, due to their aggressive nature and proclivity to disseminate, canine

digital melanomas frequently necessitate digital amputation. Even subjects who have no metastases and are treated with amputation have a one-year survival rate: roughly half of the individuals affected by this malignancy live for one year, and about a 13% live for two. Unfortunately, even when amputation is performed, 30 to 40% of dogs with this condition develop metastases following the excision (Henry et al., 2005; Nishiya et al., 2016; Wobeser et al., 2007). Despite the use of surgical treatment, the tumour mortality rate suggests a poor prognosis at the time of diagnosis. Even in humans the prognosis is poor, with an overall survival rate ranging from 59 to 70 % after five years. These rates are primarily due to delayed diagnosis (the average is about 60 years), to the atypical localisation and the effect of the various histotypes and molecular background (Elefanti et al., 2021; van der Weyden et al., 2020).

1.4 The dog as a potential model for human melanoma

Melanoma represents a significant threat to human health since it is one of the most lethal forms of skin cancer and because its prevalence is steadily rising. Its development is influenced by both genetic and environmental elements. Although UV exposure is the primary cause of the great majority of HM, other types can develop on sun-protected areas such the eye, digit, and mucosa (Gillard et al., 2014). Animal models are typically employed in studies to better understand melanoma, and the laboratory mouse is the most widely used one. It is used to investigate basic mechanisms and test novel therapeutics in a pre-clinical setting. However, because no animal model is flawless, even mice with induced tumours have limitations (Gillard et al., 2014; van Der Weyden et al., 2016). In fact, when employing laboratory mouse models, a few considerations must be made. Human melanoma has a high heterogeneity that cannot be recreated in inbred laboratory mice, and melanoma natural occurrence cannot be developed in a laboratory setting. Furthermore, because melanocytes in humans are found in the epidermis, whereas in mice they are found in the dermis, there is a different melanocyte microenvironment, which may account for differences in melanoma development and progression between the two species (van der Weyden et al., 2020). As a result, new models that are more human-like and allow for more information on diagnosis,

prognostic factors, and novel treatment options are being researched. Domestic animals, particularly dogs with naturally occurring tumors, are the primary species studied for this purpose because the anatomical locations and physiopathology of their tumors are similar to that of humans. (Gillard et al., 2014). They are a helpful tool because they produce positive outcomes in terms of genetical, practical, clinical and histological factors that can be useful both as a comparative and preclinical model (Gillard et al., 2014; van der Weyden et al., 2020).

The spontaneous insurgence in dogs is similar to what occurs in humans: it takes place in the presence of an intact immune system and is characterized by tumour growth over a protracted period. As in humans, canine cancer features include inter-individual and intra-tumoural heterogeneity, metastasis, cancer recurrence, and therapy resistance. Further consistency is given by the fact that dogs and humans share similar environments and, as a consequence, environmental factors that can contribute to tumour development. (Hernandez et al., 2018). Dog trials have the added benefit of allowing for an earlier assessment of the effects on illness progression and overall survival. This is due to the fact that dogs have a shorter lifespan, melanoma advances faster, and hence the illness timeline is shortened. Furthermore, preliminary safety and, in some cases, pharmacodynamics and pharmacokinetics of therapies have been already examined in laboratory testing on dogs (van Der Weyden et al., 2016). Moreover, because canine DNA and protein sequences are more comparable to human DNA than those of mouse, molecular tools for researching canine disorders are fairly advanced, especially since many antibodies generated against human antigens also act against canine proteins.

The differences between CSD and non-CSD tumours suggest that additional pathogenetic factors, such as phototypes, may exist. The fact that these subtypes are distributed differently in various populations backs this up: non-CSD melanoma is more common in Asian and dark-skinned African people, while cutaneous melanoma (CSD) is more common in Caucasians. Similarly, in dogs, a considerable breed predisposition to melanoma subtypes has been discovered. This genetic tendency is the outcome of years of breed selection that resulted, as a side effect,

in an increased breed-related vulnerability to melanoma. However, research into the genetic variables that predispose to the development of melanoma can aid the discovery of new driver mutations in human melanomas. The occurrence of a varied risk associated with specific breeds represents the opportunity of using different breeds for a more specific identification of melanoma subtypes and their distinctive drivers implicated in homologous subtypes in humans (Gillard et al., 2014).

Prouteau & André (2019) compared also human and canine histopathology. A good amount of homologies for melanocytic tumours from oral, cutaneous, and ocular locations were found and 4 categories resembling human histological subtypes were identified: animal-type melanoma, melanoma simulating nevus, melanoma with epithelioid cells, and melanoma with composite cells. Unfortunately nothing is yet been identified for acral melanoma.

Even though literature (Prouteau & André, 2019; Simpson et al., 2014; van Der Weyden et al., 2016) strongly supports the existence of a broad range of similarities between human and dog it focuses mainly on cutaneous, mucosal and uveal melanoma. Less is known for acral melanoma apart for some significant mutations have been identified as for BRAF, NRAS and NF1 (Prouteau & André, 2019)

1.5 Pathway and genes

The molecular basis of carcinogenesis has been the main focus of pathological studies on tumours for many years. Four types of normal regulatory genes, that are the main targets of genetic damage, have received particular attention: the growth-promoting protooncogenes, the growth-inhibiting tumour suppressor genes, the genes that control programmed cell death (apoptosis) and the genes involved in DNA repair (Kumar et al., 2004). Figure 8 shows the different steps that lead to the tumour occurrence and development, while Figure 9 shows localisation and functions of the genes involved.

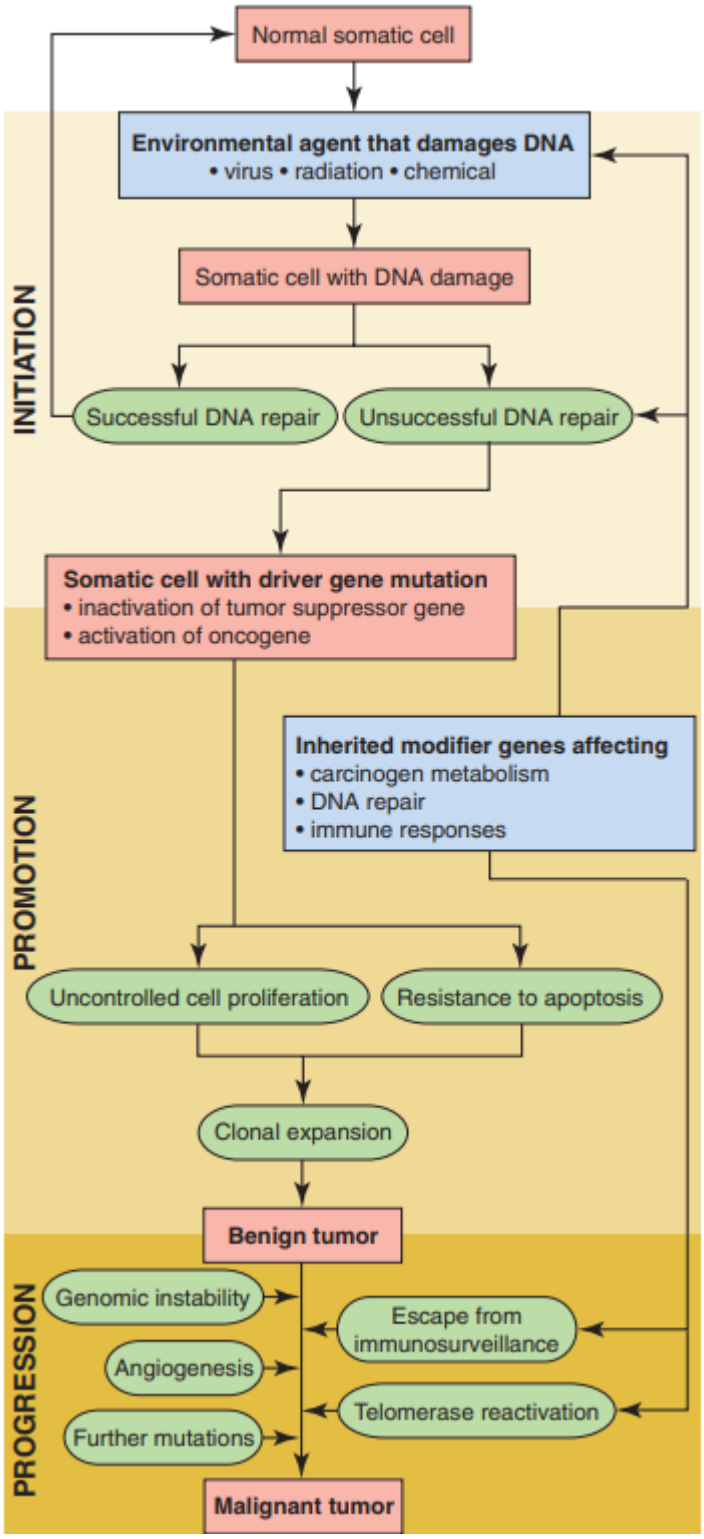

Figure 8: the scheme describes and summarizes the multistep development of cancer (Kumar et al., 2004).

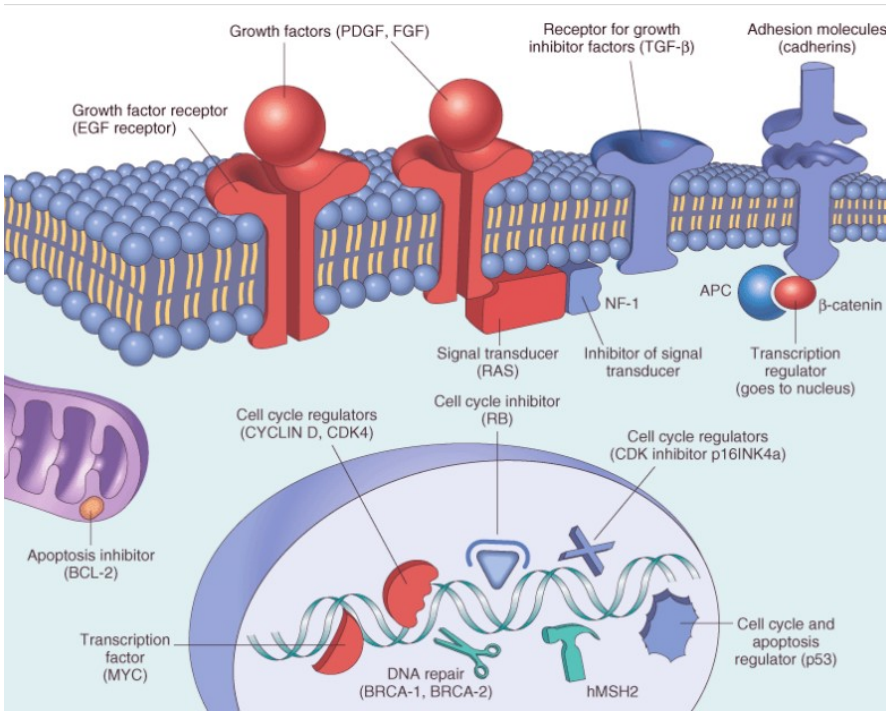

Figure 9: Locations and functions of the main types of cancer-associated genes. Protooncogenes are coloured in red, while cancer suppressor genes are in blue, DNA repair ones in green and the genes responsible for apoptosis regulation in purple (Kumar et al., 2004).

Protooncogenes are physiologic regulators of cell proliferations and differentiation that find their oncologic counterpart in oncogenes that are instead genes that promote autonomous cell growth in cancer cells without the need of conventional mitogenic signals (Kumar et al., 2004). Therefore, although proto-oncogenes can be altered to cause malignancy, they do not have the transforming potential to create tumours in their natural condition. Their sites and mechanisms of activity in the normal cell can be divided into 5 groups: growth factors, growth factor receptors, protein kinases, signal transducers and nuclear proteins and transcription factors (Argyle et al., 2020). Among these groups, the genes that are mostly affected by abnormalities in human tumours are the RAS family genes that, due to point mutations, become oncogenes that cause a pathologic activation of the mitogenic signalling pathway since they are related to G-protein signal transduction (Argyle et al., 2020; Kumar et al., 2004). More than 60% of melanomas and more than 80% of benign nevi have been shown to have BRAF mutations, part of the RAS family. This shows that although it is insufficient to produce carcinogenesis on its own, disruption of the RAS/RAF/MAP kinase pathway may be one of the initial steps in the development of melanomas (Kumar et al., 2004).

Moreover, uncontrolled growth can be caused both by stimulatory effects caused by proto-oncogenes and loss of inhibitory functions associated with another class of cellular genes called the Tumour Suppressor (TS) genes (Argyle et al., 2020). The p53 TS gene is a key TS gene, contributing to the progression of the cell cycle, regulation of gene expression, and cellular response mechanism against to DNA damage. Tumour suppression is mediated by p53-mediated processes, which also limit the build-up of potentially cancer-causing mutations and genomic instability. Under normal circumstances, the p53 protein can bind to precise DNA sequences and control the transcription of many genes implicated in the cell cycle and apoptotic pathways as p21 /cip1 and Bax. These biological functions might not be activated as a result of p53 disruption, which could lead to abnormal uncontrolled cell growth that eventually results in tumoural transformation. P53 can be both altered by gene mutational events and nonmutational mechanisms, as the overexpression of the cellular oncogene MDM2. Both p53 and MDM2 homologs have been found in domestic animal species, and numerous studies suggest that this gene is also crucial for the development of veterinary cancers (Argyle et al., 2020).

Studies of tumours have traditionally focused on the study of single genes, such as those previously mentioned, but they have recently undergone a revolution thanks to the advent of novel techniques that can concurrently detect the expression of many genes. The DNA microarray technology is one of them that is most frequently employed for large-scale analyses of gene expression. This technology allows to group genes together, based on how similar their gene expression patterns are, by using a method called hierarchical clustering (Kumar et al., 2004). Comparative genomic hybridization (CGH) is a microarray-based technique that, rapidly and with highly reproducible results, identifies gains and losses in chromosome number in tumour specimens. It makes it possible to identify the areas where it is crucial to look for cancer-related genes, allowing for the creation of precise diagnostics, therapies, and management techniques (Argyle et al., 2020).

1.5.1 Array Comparative Genomic Hybridization and Pathway enrichment analysis

The Array Comparative Genomic Hybridization (aCGH) procedure consists in labelling genomic DNA fragments from tumour and healthy tissue with two fluorescently coloured probes. The labelled DNA is then hybridized to a spotted array that consists of short oligonucleotide probes that together span the entire genome. The level of hybridization is then determined by measuring the fluorescence with a laser scanner. A chromosomal duplication in the region of the genome covered by the probe is indicated if there is a higher level of hybridization of the tumoural DNA, which indicates a higher binding of the tumoural DNA to the probe. Similarly, a stronger binding of normal individual DNA implies chromosomal loss in the region, instead an equal degree of hybridization between pathological and healthy DNA reflects a normal copy number (Argyle et al., 2020). Each location on the array will specifically be coloured red or green based on whether a particular gene is expressed more or less in the tumour, or black or yellow (depending on the type of fluorescent scanning) if there is no difference in gene expression between the tumour and control sample (Kumar et al., 2004).

The long gene list obtained by aCGH can then be condensed into a shorter list of more understandable pathways using pathway enrichment analysis. A pathway is a group of genes that cooperate to carry out a biological function whereas pathway enrichment analysis is a statistical technique to find pathways that are significantly represented in a gene list. The pathways can be found in a variety of substantial, easily accessible, open-access pathway databases that provide the greatest benefit for pathway enrichment analysis (Reimand et al., 2019). Pathway analysis gives complementary insights to gene-focused driver discovery since it enables to find pathways and processes that stand out when the data are combined but are not obvious in any single studied dataset (Paczkowska et al., 2020).

2. Aim of the study

Acral and mucosal melanomas have shown considerable genetic differences from cutaneous melanoma and are more similar to one another than other melanomas (Furney et al., 2014; Hayward et al., 2017). First off, the primary mutation processes in these tumours do not involve UV radiation, raising the possibility of other carcinogenic exposures that are shared with tumours other than those of the skin (Hayward et al., 2017). In addition to point mutations, larger-scale genomic rearrangements may also activate acral melanoma drivers, according to the pattern of somatic alterations between acral and mucosal melanoma drivers (Furney et al., 2014). In order to identify and understand the major cellular pathways and functions that are crucially dysregulated during oncogenesis, a wider perspective on the tumoural behaviour is needed.

This can be achieved through pathway enrichment analysis, which enables a description of the behaviour of the tumour while highlighting how genes interact with one another and thereby provides a better understanding of what single gene mutation analysis could accomplish (Paczkowska et al., 2020). Additionally, pathway analysis aids the development of novel therapeutic approaches, which can be particularly beneficial for tumours like melanomas that frequently fail to respond to currently available treatments (Hernandez et al., 2018). The most successful targeted therapies will be those that interfere with the processes and pathways that cancer cells exploit, in order to interrupt pathways that are specific to cancer cell biology. This has the additional benefit of reducing systemic adverse effects (Hardwick, 2021). Additionally, by comparing CAM with the molecular pathogenesis of human acral melanoma and canine oral melanoma, a greater understanding of melanoma biology can be achieved, leading to the development of additional targeted therapy (Hardwick, 2021).

The aim of the study is to deepen the whole-genome landscape to better understand pathogenetic pathways underlying acral melanoma, consequently helping to achieve all of the benefits that this type of analysis may offer. To achieve this goal, we used aCGH (Array Comparative Genomic Hybridization) molecular techniques

that enable a genome-wide analysis of large size tumour aberrations (amplifications and deletion of DNA sequences). The identification of enriched tumour pathways was then performed by a specific, commercially available software (ClueGo plugin for the software Cytoscape 3.9.0) which allows to gain new insights and perspectives on tumour biology by identifying tumour characteristics that would otherwise go unnoticed if only single aberrations, and associated genes, were characterized. The last goal was to compare the most recent findings from studies on hAM and COM, similarly to what has already been done in COM studies, in order to have a more comprehensive understanding of AM behaviour and peculiarities.

3. Materials and methods

3.1 Sample collection and selection

The research was conducted with formalin-fixed, paraffin-embedded (FFPE) samples obtained from the archives of the Department of Comparative Biomedicine and Food Science of the University of Padua and the Department of Veterinary Medicine of the University of Perugia.

FFPE samples were selected in order to perform a genomic extraction of healthy and tumoural DNA to be further analysed through aCGH. To be included in the study, the pathological samples had to be diagnosed histologically as CAM. The diagnoses were made through the evaluation of slides stained with routine Hematoxylin and Eosin protocol, and evaluated by ECVP Diplomates from the Universities of Padova and Perugia. Further inclusion criteria were the presence of sufficient material for the extraction procedure. In the case of amelanotic melanomas, the samples were subjected to an immunohistochemical evaluation with the antibodies anti Melan-A, TRP-1, TRP-2, and PNL-2, to assess the melanocytic origin of the neoplasm. The presence of healthy tissue, adjacent to the neoplastic mass, was also assessed during the recruiting phase. When possible, all the additional clinical information about the dogs were also collected.

Ideally, for aCGH analysis, healthy and pathological tissue, and therefore DNA, should derive from the same individual. Since the same individual whose pathological tissue was selected could not be used, a healthy pool was made. Ideally, the pool must be composed of a number of samples equal to or greater than that of the pathological group and be balanced between males and females. When available, the DNA was extracted from the healthy tissue adjacent to the acral melanomas selected. More samples were then enrolled and healthy DNA was extracted from archival FFPE samples containing healthy lymph nodes and liver. Finally, healthy DNA already available from previous studies, originating from the healthy mucosal tissue adjacent to mucosal melanomas, was also included in the selection. The selected FFPE samples were cut in 5 sections 10 µm-thick from the

blocks using a microtome with disposable blades. The sections obtained by each sample were put into 1,5 ml Eppendorf to be extracted.

3.2 Nucleic acid extraction and purification from FFPE tissue

The All-Prep DNA-RNA FFPE KIT (Qiagen R®) was used to extract genomic DNA according to the manufacturer's instructions, with the use of a heptane solution for deparaffinization steps. This kit is the best choice for FFPE tissue due to its yield and quality (Patel et al., 2017). The whole protocol can be found in paragraph 8.1 named as "Protocol A".

The tissue obtained by trimming underwent a process of deparaffination trough different steps of exposure to heptane, methanol and ethanol solutions mixed by vortexing and then centrifugated. Supernatant was then removed by pipetting and the tubes were incubated with the lid open to allow ethanol excess vaporisation. Afterwards a digestion buffer (Buffer PKD) and proteinase K were added to complete the process. Deparaffination is an essential step since paraffin can inactivate proteinase K. This proteinase allows the digestion of contaminating proteins and the inactivation of nuclease (DNAse and RNAase), and therefore is a key enzyme since it prevents the destruction of nucleic acids. All these steps allowed the separation of tissue pellets then used as input for DNA extraction. The supernatant can be utilized instead for RNA extraction, but this was not necessary for the purpose of the study. Afterwards, purified DNA was obtained through additional steps as the addition of various buffers and enzymes, centrifugation, and isolation, all conducted according to the protocol (steps 10 to 20 in "Protocol A").

3.3 Assessment of extracted DNA quality, quantity and integrity

The extracted DNA quality and quantity were determined using a Nanodrop ND-1000 (Life Technologies®) spectrophotometer, and its integrity was verified using an agarose gel electrophoresis.

3.3.1 Quantification

The spectrophotometer absorbance measurement is used to evaluate quality and quantity of the extracted DNA. Nucleic acids have in fact intrinsic absorptivity

properties represented in Figure 10. The purity of DNA can be therefore evaluated through ratios that consider its absorbance properties together with the buffer ones. Since they have a distinctive peak at 260 nm, proteins of 280 nm, and solvents of 230 nm the purity of DNA can be determined by the 260/280 and 260/230 ratios. Moreover, this technique allows to evaluate concentration values that are determined automatically by the computer connected to the system. The data obtained by spectrophotometry was elaborated using a specialized software, which provided results and charts for each sample (ThermoFisher Scientific, 2022c).

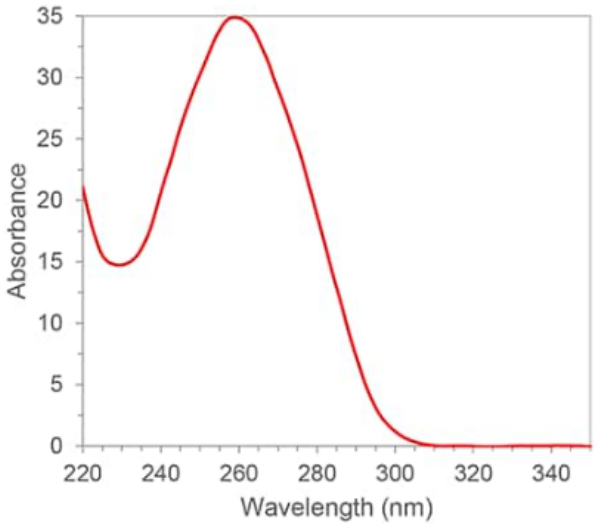

Figure 10: typical RNA/DNA absorbance spectrum (Desjardins & Conklin, 2010)

The 260 nm to 280 nm ratio, with a value equal or greater of 1,8, is an good level of DNA purity. If the ratio is much lower, proteins, phenol, or other components that absorb strongly at or near 280 nm may be present. The second measure of nucleic acid purity given by 260 nm and 230 nm ratio has usually greater values than the 260/280. Expected 260/230 values normally fall between 2,0 and 2,2. Contaminants that absorb at 230 nm may be dominant if the ratio is much lower than expected. Purity ratios that, in general, are much lower than projected values, might require further improvement of the isolation method (Desjardins & Conklin, 2010). Only samples (both pathological and healthy sections) having a yield of DNA of at least 450ng and an A260/A230 ratio of at least 1,5 underwent the following steps.

3.3.2 Electrophoresis

To evaluate their DNA integrity, samples were analysed with an agarose gel electrophoresis. The gel was prepared using an 1% agarose gel matrix. Agarose comes in a form of white powder that is purified from agar, a carbohydrate structural component of the cell wall of marine reg algae. 0,5 g of it was combined with 50ml of TAE buffer (Tris-acetate-EDTA). The mixture was heated to help the agarose particles melt, then 5 µl of SYBER Safe (Invitrogen), a phosphorescent dye, were added. This stain is a DNA–intercalator that produces fluorescence when exposed to UV light, and it has a detection sensitivity similar to ethidium bromide, but with far lower toxicity and mutagenicity.

The compound was then cooled and hardened in an electrophoresis tank with a removable comb to create wells. Only when the gel was totally solidified, the gel comb was lifted upward, smoothly and steadily, to avoid damaging the gel and altering the wells. After that, the gel was placed in an horizontal electrophoresis gel box with a running buffer (TAE 1x). After adding the buffer and removing the comb, extra care was taken to eliminate any trapped air bubbles in the wells.

The samples were made by combining 5 µl of each of them with 5 µl of loading dye. This dye, which combines bromophenol blue and xylene cyanol, provides colour for an easier sample loading and electrophoretic run progress monitoring. In each well 10 µl of dyed DNA were located, while a DNA ladder (molecular weight size marker) was placed in the two lateral wells. Samples were placed in agarose wells and exposed to an electric field (80-100V), which caused the negatively charged nucleic acids to migrate toward the positive electrode. Shorter DNA fragments run faster, while the longest fragments stay closer to the gel origin, resulting in size separation.

Electrophoresis was completed in 50 minutes after which the gel was positioned under a trans illuminator (BioRad®) to visualise stained DNA. DNA cannot be seen under normal light but the UV light emitted by this illuminator was reflected by DNA linked to SYBER Safe dye, which absorbs light with a wavelength of 280-520 nm and emits it at 522 nm. The intensity of fluorescence correlates to the amount of nucleic acid bound, which is the basis for detection and quantitation of nucleic acids in

electrophoresis. The two controls in the lateral wells, thanks to their pre-determined molecular weight, provided size and concentration indications (ThermoFisher Scientific, 2022a, 2022b).

Gel electrophoresis determined if the fragments and their sizes were appropriate for aCGH analysis. Typically, fragmented DNA is extracted from FFPE samples, although restriction digestion might be used when the integrity is too much preserved (van Beers et al., 2006).

3.4 Array Comparative Genomic Hybridization

The SureTag DNA Labeling Kit (Agilent) was used to cyanine label the samples. Prior to labelling, samples that had a higher integrity underwent Restriction Digestion, according to the SureTag DNA protocol. Cyanine are synthetic dyes widely used in biotechnology and that can be applied for nucleic acid labelling in order to visualise and quantify them. Cyanine 5-deoxyuridine triphosphate (Cy5) and cyanine 3-deoxyuridine triphosphate (Cy3) were used to stain pathological and healthy DNA, respectively. The final cyanine incorporation and concentration, along with the sample specific activity, were assessed via spectrophotometry using a Nanodrop ND-1000. Samples with a suitably matched ratio of healthy and malignant Cy3 and Cy5 were selected for further investigation and therefore co-hybridized to a 180,000-feature SurePrint G3 Canine CGH Microarray (4–180 K, Agilent Technologies).

Sample hybridization was made by pairing pathological and healthy labelled DNA samples. The volume of DNA paired with the pathological sample was withdrawn from the healthy pool and was calculated in order to obtain the same amount (in nanograms) of pathological and healthy DNA.

The microarray is composed of repeat-masked 60-mer oligonucleotides distributed at ~2,7 Kb intervals throughout the dog CanFam3 genome assembly. After 24 hours of incubation at 65° and 20 rpm, arrays were washed and scanned at 3µm using an Agilent G2565CA scanner, following manufacturer's instructions. All of the steps are summarized in Figure 11. The obtained images and data were

processed using specific Feature Extraction (FE) version 11.5 and Genomic Workbench version 7.0.

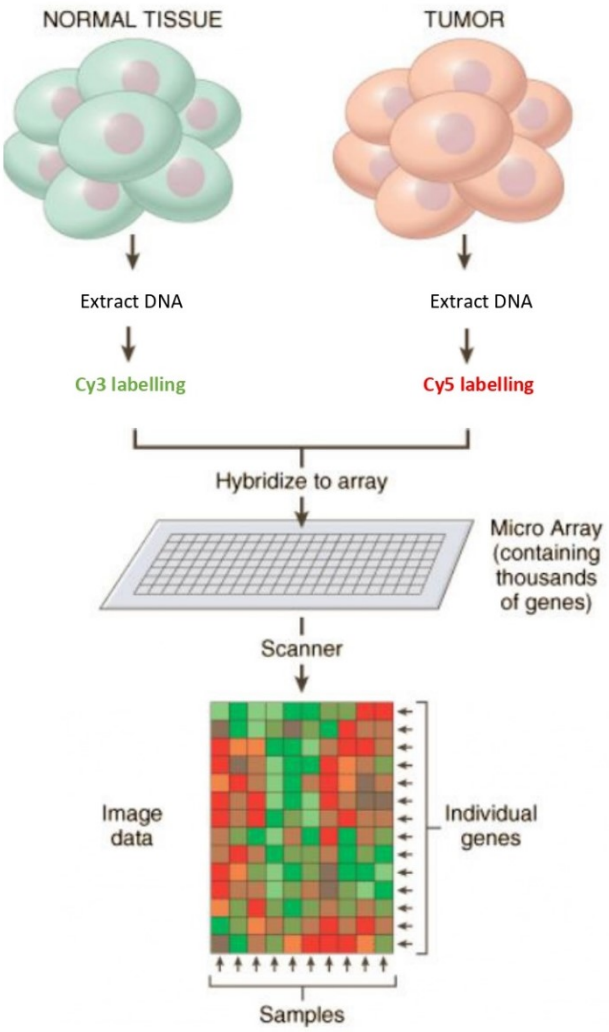

Figure 11: aCGH process overview (Kumar et al., 2004)

3.5 Copy Number Aberrations (CNAs) Analysis

The data obtained by the laser scanner were analysed using the Agilent Genomic Workbench. All sample florescence data were normalized using the centralization algorithm with a threshold of eight and fuzzy ON in order to remove probes that exhibited non-uniform hybridization or signal saturation. Sexual chromosomes were not included in our study and only the outcomes related to autosomes were examined.

The Aberration Detection Method 2 (ADM- 2 or “adam- two”) algorithm was used to define Copy Number Aberrations (CNAs) for each sample with the "three probes minimum" filter. Based on a statistical score, this algorithm finds all aberrant intervals in a sample that have consistently high or low log ratios. It searches for intervals where a statistical score, derived from the average quality weighted log ratio of the sample and reference channels, exceeds a user-specified threshold and then identifies contiguous genomic regions of any size as aberrant regions. To define the user specified threshold the Cy5/Cy3 intensity ratio of each spot was translated into a log2 ratio. Therefore, the threshold applied allowed to identify the aberrant regions in the chromosomes and determined whether a copy number gain or loss was assigned to those regions where the log2 ratio was either more than 0.25 (>0.25) or less than -0.25 (<-0.25). Megabase (Mb) positions were used to designate chromosomal locations. The aberrant regions identified by the ADM-2 analysis then underwent the Fuzzy zero correction which applies a “Global error model” to each of them. This is a more realistic error model that allows to identify erroneous aberrations when the errors are correlated.

Instead, the entire samples subset underwent the Context corrected common Aberration Analysis (CAA), which identifies significant CNAs by detecting the regions of the genome noticeably gained or lost across samples. To maximize the score of the CNAs it in fact finds the common aberrations in a selection of samples that for this study are represented by the results of all the arrays. It takes into consideration all of the aberrations found in the genome together with the likelihood of discovering a common aberration. In the end the report displays statistically significant common aberrant regions among the samples subset.

3.6 Pathway Enrichment Analysis

The procedure generated five distinct lists of aberration: lost regions in more than 40% of samples, lost regions in more than 70% of samples, gained regions in more than 40% of samples, statistically significant lost regions and statistically significant gained regions. The statistically significant lost and gained regions were the ones obtained through CAA.

The Ensemble Genome Browser (http://www.ensembl.org/index.html) allowed to find all of the genes corresponding to the aberrated regions. The applied tool was BioMart with Ensembl genes 104 as the chosen database. CanFam 3.1 served as the dataset and the selected attributes were gene stable ID and gene name. The obtained stable ID was then used to identify the orthologous human genes. The Ensemble Genome Browser's BioMart tool was also used for this. Human Gene stable ID and Human Gene name were the attributes for orthologous genes that were chosen to obtain the data. As a result five lists of genes, corresponding to the aberrated regions, were produced: lost genes in more than 40% of samples (LG40), lost genes in more than 70% of samples (LG70), gained genes in more than 40% of samples (GG40), statistically significant lost genes (LGSS), and statistically significant gained regions (GRSS).

The five gene lists were further processed by the ClueGo plugin for Cytoscape 3.9.0, an open-source Java application that identifies non-redundant biological data for big gene clusters. Genes were entered into the program as Human Gene name and were therefore analysed with homo sapiens as the control species. Each gene was assigned to a specific pathway based on the information of five different databases: KEGG, GO Biological process, GO Immuno, REACTOME, and WIKIPATHWAYS. The standard hyergeometric two-sided test was employed to assess each term significance and each network was created using a kappa score threshold of 0,5 and a minimum of three genes that made up at least 10% of all the related genes in that specific network. In ClueGO, the kappa score is used to define term-term interrelations (edges), and functional groups based on shared genes between terms. Additionally, the "fusion" option was implemented to minimize redundancy, and the Benjamini-Hochberg adjustment was performed on each pathway P-value.

4. Results

4.1 Sample extraction and selection

The healthy and pathological samples selected for our study are listed in Table 1, Table 2 and Table 3, where also the results of the quality and quantity of DNA extracted are shown. The absorption ratios (260/280 and 260/230) and the concentration of DNA, measured in nanograms per microliter (ng/ul), are listed in the columns.

Table 1: The 12 CAM samples selected with their DNA concentration and absorption ratios (260/280 and 260/230)

SAMPLE ID	ng/ul	260/280	260/230
D01	54,11	1,76	2,1
D02	124,03	1,76	3,05
D03	100,04	1,9	1,71
D04	144,83	1,68	2,16
D07	121,32	1,86	2,51
D08	59,25	1,72	1,71
D09	42,85	1,63	1,67
D10	94,87	1,87	2,16
D11	103,2	1,93	1,79
D12	63,74	1,76	2
D13	169,44	1,83	2,13
D15	149,19	1,7	1,99

Table 2: The 8 healthy male samples selected with their DNA concentration and absorption ratios (260/280 and 260/230)

SAMPLE ID	ng/ul	260/280	260/230
A3_S	126,24	1,94	2,2
C12_S	898,98	1,84	2,32
A34_S	182,41	1,80	1,86
D11_S	92,05	1,95	2,36
D13_S	104,91	1,77	1,99
D10_S	84,77	1,59	1,90
M1	196,33	1,86	2,09
C11_S	92,78	1,83	2,45

Table 3: The 8 healthy female samples selected with their DNA concentration and absorption ratios (260/280 and 260/230)

SAMPLE ID	ng/ul	260/280	260/230
A24_S	98,11	1,92	2,11
A35_S	91,08	1,90	2,92
A1_S	129,89	1,80	1,52
D16_S	86,4	1,64	1,77
F1_II	143,46	1,90	1,99
F4	93,83	1,86	2,40
F7	44,99	1,90	1,62
D7_S	48,2	1,86	2,43

For aCGH high molecular weight genomic DNA must be fragmented into suitable-sized fragments (van Beers et al., 2006). Gel electrophoresis was used on the samples to assess fragmentation as shown in the example in Figure 12. In most cases, DNA extracted from FFPE samples is sufficiently fragmented as a result of the archiving process, therefore extra steps like sonication or restriction digestion are not required (van Beers et al., 2006).

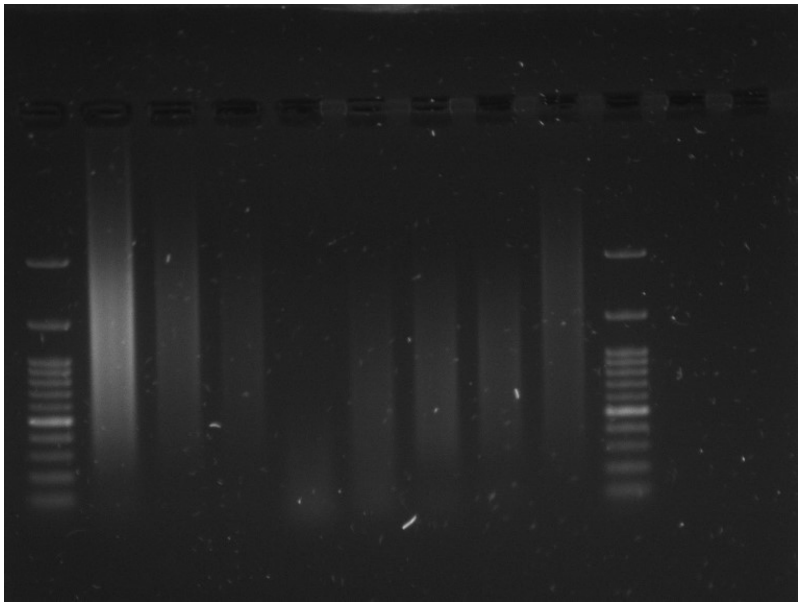

Figure 12: Example of gel electrophoresis results for healthy samples. The first and last well are DNA ladder (100 bp), lane 2,3, 4 and 8 show partially degraded DNA (> 500bp) that furtherly underwent digestion, while lane 5, 6 and 7 show severely degraded DNA.

However, electrophoresis revealed that fragmentation was insufficient for the healthy samples and for pathological samples D7, D11, D13 and D10. Therefore these samples underwent an extra step of restriction digestion.

Quality and quantity evaluations allowed the selection of 16 healthy DNA samples and 12 pathological DNA samples that underwent cyanine labelling. Nanodrop ND-1000 (Life Technologies®) spectrophotometer analysis allowed to identify cyanine yield and specific activity. Specific activity was calculated through the ratio of cyanine yield with the DNA concentration and then multiplied by 1000. The samples demonstrated sufficient yield and specific activity to be further processed through aCGH analysis. The healthy sample pool was created, by equimolarly pooling samples listed in Table 2 and Table 3, and once again evaluated through nanodrop. The pool had a total volume of 170 uL, an amount of DNA of 44676 ng and Nanodrop revealed a cyanine yield of 7,6 and a specific activity of 28,92. Cyanine yield and specific activity were measured through the average values obtained by two Nanodrop measurements, visible in Table 4.

Table 4: Healthy sample DNA pool parameters. Ng/ul indicates concentration of DNA, Cyanine indicates the cyanine yield, Spec Act. indicates cyanine specific activity, ul indicates the volume obtained by mixing all the healthy samples and ng tot indicates the total amount of labelled DNA.

Sample ID	ng/ul	Mean ng/ul	Cyanine	Mean cyanine	Spec Act.	ul	ng tot
Healthy pool	262,3	262,8	7,6	7,6	28,91933	170	44676
Healthy pool	263,3		7,6				

4.2 Array Comparative Genomic Hybridization (aCGH)

Two DNA samples are needed for each array: one from the pathological tissue and one from the healthy tissue. The amount of healthy and pathological DNA (measured in nanograms) must be equal. Based on the extracted amount of available extracted pathological DNA, the maximum amount that could be used for array was estimated. This amount is listed on the “ng” column in Table 5, Table 6 and Table 7. After that, calculations were made to determine the volume needed to produce the same amount of healthy DNA as pathological DNA. The concentration of healthy DNA pool was equal to 262,8 ng/ul. As a result, the volume (ul) required was determined by dividing the DNA quantity (ng) and its concentration (ng/ul).

The healthy and pathological samples are shown in Table 5, Table 6 and Table 7. The “Pool_S” sample ID indicates a sample obtained by the healthy pool. Each

pathological sample is associated with the “Pool_S” sample listed above them. Samples are separated into three tables that each correspond to an array slide (listed in the column “array code”) where hybridization took place. Each slide had four arrays on it and the position of each sample is listed in the “Position” column.

After that, calculations were made to determine the volume needed to produce the same amount of healthy DNA as pathological DNA. The concentration of healthy DNA pool was equal to 262,8 ng/ul. As a result, the volume (ul) required was determined by dividing the DNA quantity (ng) and its concentration (ng/ul).

Table 5: Array slide 1 (code 706)

Sample ID	Mean Conc (ng/ul)	Spec Act.	ng	vol sample	Vol TE	Array code	Position	Res
Pool_S	262,8	28,92	4500	17,12	10	706	**1**	**1**
D7_P	272,4		4500	16,52				
Pool_S	262,8	28,92	4000	15,22	3	706	**2**	**2**
D9_P	155,5		4000	25,72				
Pool_S	262,8	28,92	3500	13,32	1	706	**3**	**3**
D15_P	118,7		3500	29,49				
Pool_S	262,8	28,92	3000	11,42	9	706	**4**	**4**
D4_P	128		3000	23,44				

Table 6: Array slide 2 (code 707)

Sample ID	Mean Conc (ng/ul)	Spec Act.	ng	vol sample	Vol TE	Array code	Position	Res
Pool_S	262,8	28,92	4000	15,22	15	707	**1**	**1**
D11_P	284,95	30,00	4000	14,04				
Pool_S	262,8	28,92	3300	12,56	5	707	**2**	**2**
D8_P	122,65	19,50	3300	26,91				
Pool_S	262,8	28,92	3000	11,42	8	707	**3**	**3**
D10_P	120,3	15,00	3000	24,94				
Pool_S	262,8	28,92	2000	7,61	13	707	**4**	**4**
D1_P	85	21,80	2000	23,53				

Table 7: Array slide 3 (code 708)

Sample ID	Mean Conc (ng/ul)	Spec Act.	ng	vol sample	Vol TE	Array code	Position	Res
Pool_S	262,8	28,92	2400	9,13	7	708	**1**	**1**
D2_P	85,45	24,50	2400	28,09				
Pool_S	262,8	28,92	2100	7,99	11	708	**2**	**2**
D3_P	84,5	26,00	2100	24,85				
Pool_S	262,8	28,92	3500	13,32	8	708	**3**	**3**
D13_P	155,35	18,90	3500	22,53				
Pool_S	262,8	28,92	3500	13,32	8	708	**4**	**4**
D12_P	152,1	17,00	3500	23,01				

A total of 12 healthy-pathological pairs of samples were therefore obtained. They were placed onto three slides, each containing 4 arrays, and submitted for aCGH analysis.

After the laser scanning, hybridisation quality was assessed through Agilent Feature Extraction 11.5 and Agilent Genomic Workbench 7.0.

A quality report (QC report) was developed by Agilent Feature Extraction (FE) and reported quality metrics important for CGH applications. Agilent has identified the FE Stats that make up the best metrics for monitoring the processing of Agilent arrays. Additionally, it determines whether these measures fall within certain limits by giving them three different grades: "Excellent," "Good," or "Evaluate". QC reports were obtained from all of the samples and allowed to identify which samples could undergo further analysis. It was in fact seen that D2 and D3 had a poor quality of hybridization and were therefore excluded by the study.

The sample that had the highest levels of the metrics was D11 and they are reported in Figure 13, while the worst metrics were found in sample D2 (Figure 14)

Evaluation Metrics for CGH_QCMT_Sep17
Excellent (6) ; Good (6) ; Evaluate (1)

Metric Name	Value	Excellent	Good	Evaluate
IsGoodGrid	1.00	>1	NA	<1
AnyColorPrcntFeatNonU...	0.00	<1	1 to 5	>5
DerivativeLR_Spread	0.27	<0.20	0.20 to 0.30	>0.30
gRepro	0.11	0 to 0.05	0.05 to 0.20	<0 or >0.20
g_BGNoise	4.22	<5	5 to 15	>15
g_Signal2Noise	52.49	>100	30 to 100	<30
g_SignalIntensity	221.67	>150	50 to 150	<50
rRepro	0.12	0 to 0.05	0.05 to 0.20	<0 or >0.20
r_BGNoise	5.23	<5	5 to 15	>15
r_Signal2Noise	37.16	>100	30 to 100	<30
r_SignalIntensity	194.22	>150	50 to 150	<50
RestrictionControl	-1.00		0.80 to 1	<0.80 or >1
LogRatioImbalance	-0.19	-0.26 to 0.26	(-0.75 to -0.2...	<-0.75 or >0.75

• Excellent • Good • Evaluate

Figure 13: evaluation metrics for sample D11

Evaluation Metrics for CGH_QCMT_Sep17
Excellent (5) ; Good (3) ; Evaluate (5)

Metric Name	Value	Excellent	Good	Evaluate
IsGoodGrid	1.00	>1	NA	<1
AnyColorPrcntFeatNonU...	0.04	<1	1 to 5	>5
DerivativeLR_Spread	0.86	<0.20	0.20 to 0.30	>0.30
gRepro	0.11	0 to 0.05	0.05 to 0.20	<0 or >0.20
g_BGNoise	4.51	<5	5 to 15	>15
g_Signal2Noise	33.85	>100	30 to 100	<30
g_SignalIntensity	152.54	>150	50 to 150	<50
rRepro	0.09	0 to 0.05	0.05 to 0.20	<0 or >0.20
r_BGNoise	4.02	<5	5 to 15	>15
r_Signal2Noise	1.52	>100	30 to 100	<30
r_SignalIntensity	6.12	>150	50 to 150	<50
RestrictionControl	-1.00		0.80 to 1	<0.80 or >1
LogRatioImbalance	-21.38	-0.26 to 0.26	(-0.75 to -0.2...	<-0.75 or >0.75

• Excellent • Good • Evaluate

Figure 14: evaluation metrics for sample D2

The QC report includes two histograms (as in Figure 15) that display the distribution of measured colour intensity of red and green. The distribution should be gaussian in both channels (red and green) and, preferentially, with comparable intensity between the two channels.

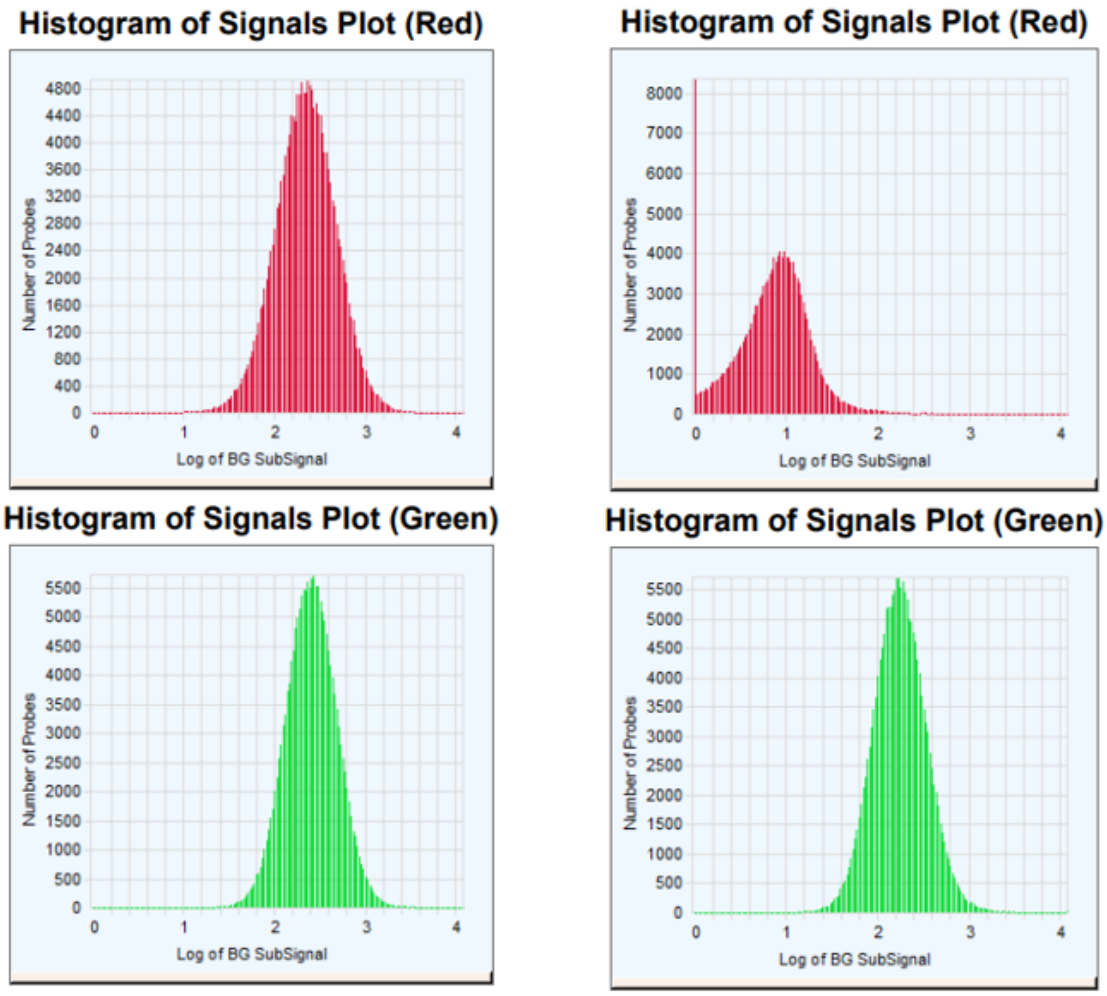

Figure 15: Histogram of red and green signal for sample D11 (on the left) and sample D2 (on the right)

QC report also shows a plot of the log of the red background-corrected signal versus the log of the green background-corrected signal for all non-control inlier features. The plot should be linear, and the linearity or curvature of the plot reflects the suitability of the background method selections. The location of the median signal is indicated by the point where the red vertical and horizontal lines connect. Figure 16 shows two examples: sample D11 (on the left), which was the best did, in fact, show a linear relationship between the two channels, whereas sample D2 (on the right) did not and was therefore discarded.

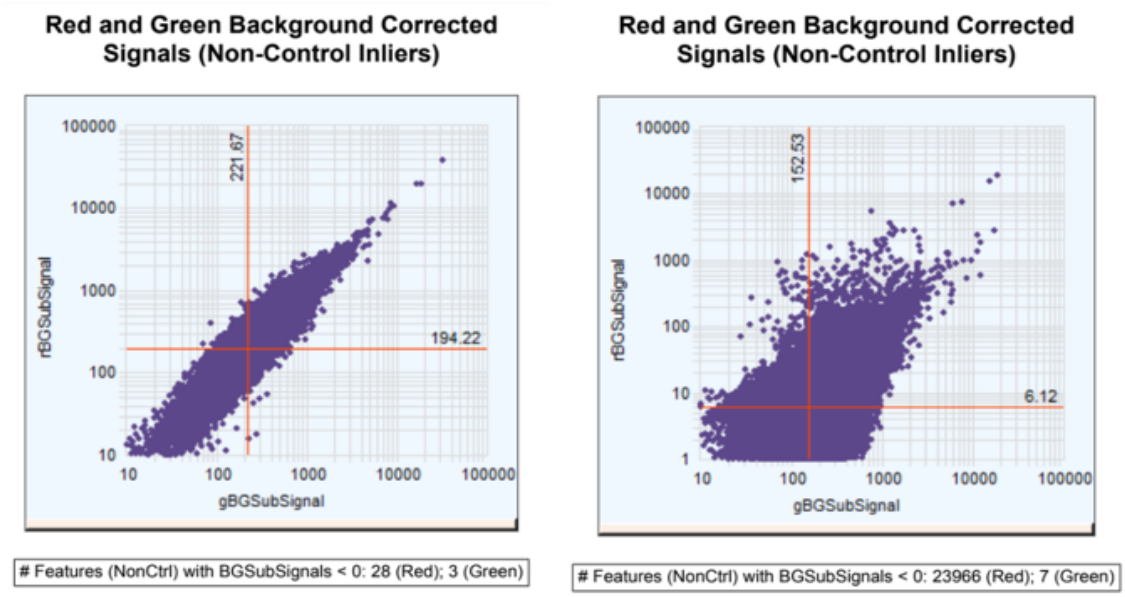

Figure 16: Sample D11 (left) and D2 (right) plot of the log of the red background-corrected signal versus the green background corrected signal

Agilent Genomic Workbench 7.0 enables the evaluation of several array parameters to determine the quality of the microarray data. Some of these parameters come from the CGH module itself, while others come via the Agilent Feature Extraction program. There are four possible ratings for each parameter: Excellent (yellow), Good (turquoise), Evaluate (pink), or NA (white). The graphs obtained are shown in Figure 17 and represent, for each parameter, its rating for each sample. The samples that are represented are, according to the graphs ordered from left to right: D1, D4, D7, D8 ,D9, D10, D11, D12, D13 and D15. The first graph shows signal to noise green, which is considered good for all samples except D1 where it is termed as “evaluate”; the second graph shows signal to noise red, which is termed as evaluate for all samples except D11 where it is good. Green signal intensity, in the third graph, is for 9 samples excellent. Instead, the red signal intensity ranges from evaluate to excellent, with the mean (seen as a black dot in the boxplot) falling somewhere between poor and good. The background noise values for green and red (fifth and sixth graphs) are mostly around excellent and each plot background colour is determined by quality standards created by Agilent based on typical ranges seen during analysis of well-established cell lines carried out using standard Agilent protocols. It should be noted that the standards derive from excellent quality DNA samples and therefore obtaining good and excellent results when using FFPE samples is challenging. The repeatability values (seventh and eight graph) for green and red are all good.

On the right of each graph there is a boxplot were the 25th and 75th percentiles are shown by the box lower and upper margins, respectively. The median is depicted in the box as the black horizontal line and the mean is represented by the black dot. The range of values that are not outliers is represented by the "whiskers." Values that are more than 150% beyond the 25th to 75th percentile range are considered outliers, and if they plot out of the available space on the graph they are represented as open triangles, as for the second and fourth graph. This report confirms that D11 is the best quality sample available.

Eventually the 10 total samples obtained by aCGH underwent further analysis and were comprised of 10 tumoural samples matched with the healthy tissue pool.

Figure 17: Agilent Genomic Workbench 7.0 quality results. The samples represented are from left to right D1, D4, D7, D8, D9, D10, D11, D12, D13 and D15. The graphs are referred to, from the top, as Graph 1, 2, 3, 4, 5, 6, 7, 8

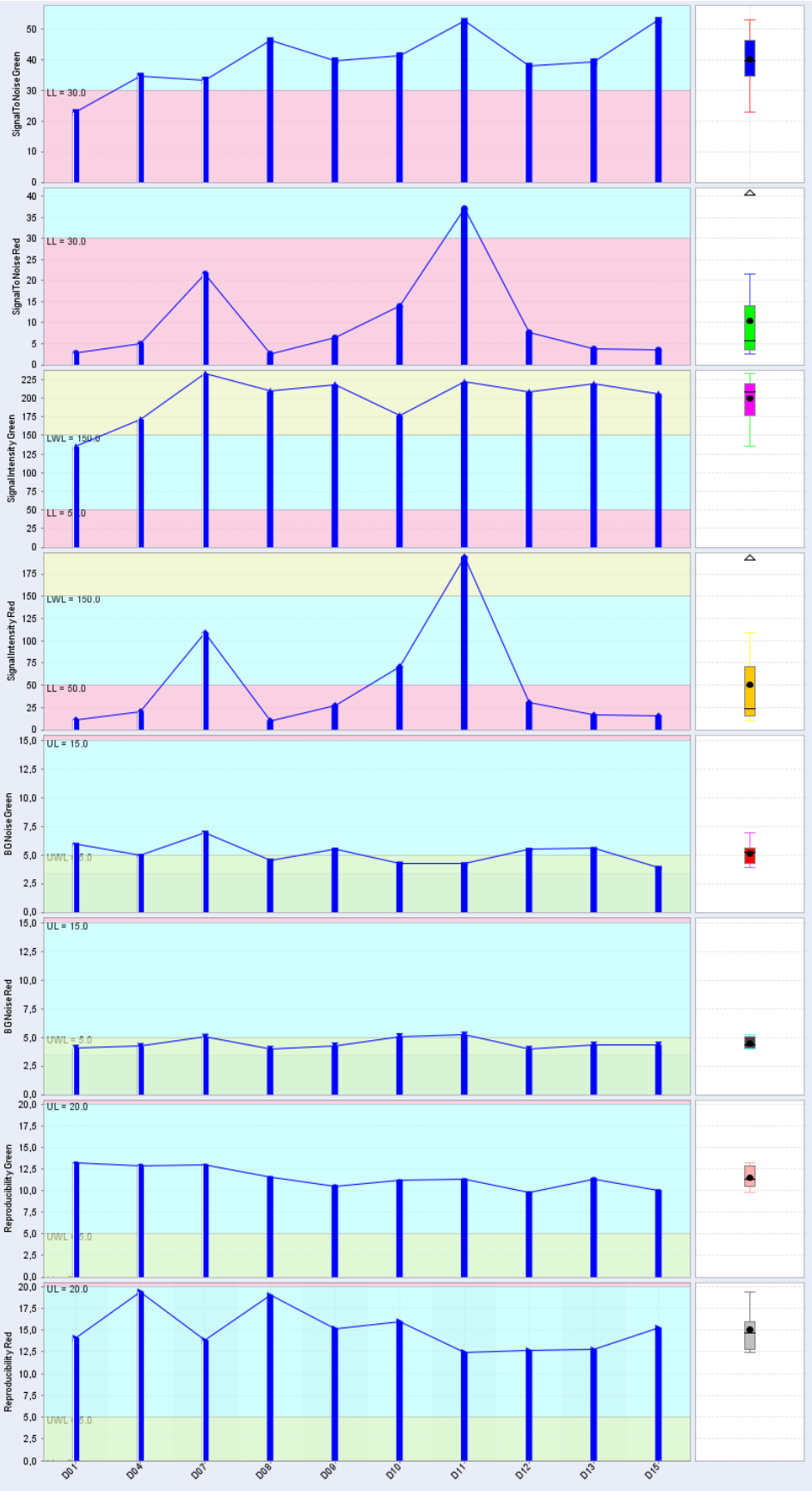

4.3 Genomic Pattern of Aberration

CNA analysis revealed both focal and broad chromosomal aberrations (reaching a 55 Mb length in chr14), which were characterized by gains and losses. All of the samples had aberrations, with a mean of 25,1 aberrations each, ranging from 5 to 88, with sample D11 having the highest number. Only regions with a penetrance ≥ 20% were chosen from a total of 333 genomic alterations (autosomes only). The selected ones consisted of 65 gained regions and 60 lost regions, with size ranging from 2bp to 55Mb (with a mean length of 5,2 Mb) for gains and from 6,3Kb to 31,1 Mb (mean length of 3,3 Mb) for losses. Chromosomes (CFA) 5, 9, 13 and 20 were the ones with more gained regions (penetrance ≥20%), while lost regions involved most frequently chromosomes CFA 10 and 30 (penetrance ≥20%).

Among the gained regions, 8 showed a penetrance ≥40% in chromosomes 13, 20 and 36 and had a size ranging from 0,9 Mb to 27Mb (mean length of 11,9Mb). On chromosome 20 the region chr20: 21823094-22727104 showed 50% penetrance and therefore represents the region with the highest penetrance within the gained ones.

Among regions with losses, 18 had a penetrance ≥40% in chromosomes 8,10 and 30 with a size ranging from 8 kb to 0,7 Mb (mean length = 0,18 kb). 12 regions reached penetrance over 70% in chromosomes 10 and 30, with a size ranging from 8 kb to 0,7 Mb (mean length = 0,19 kb). In both of these chromosomes there were aberrations of 100% of the samples affecting regions chr10:49340369-49840587 (500218 bp) and chr30:16663301-17417119 (753818 bp).

Chromosomes that appeared to be more affected by gains and losses were CFA 9, 10 and 30, all presenting 15 or more aberration sites. CFA 9 has a total of 19 aberrations (each with a prevalence of 20 or 30%), comprising of 18 gained regions and one lost region. CFA 10 and 30 have respectively 16 and 15 aberrations, all derived by the loss of regions. In CFA 10 of the lost regions, two of them (chr10:49332254:49340369 and chr10:49840587:49887075) are detected in 90% of the samples and one (chr10:49340369-49840587) in 100% of them. CFA 30 showed instead 9 lost regions with a prevalence of 70% or higher and within them two

regions (chr30:16117390-16663301 and chr30:17417119-17473667) can be found in 90% of the samples and one (chr30:16663301-17417119) in 100% of them.

The CAA was then used to determine CNAs that have a statistically significant frequency (pvalue < 0.05). A total of 26 significant aberrated regions were identified. Of the identified regions 21 were lost regions and 5 gained ones.

The chromosomes affected by losses were CFA 5, 8, 10, 18, 19, 26, 29 and 30 and had lost regions of a size ranging from 0,1kb to 55Mb (average 4,2 Mb). Each of the cited chromosomes had one lost region while CFA 10 and CFA 30 had respectively 7 and 8. CFA 10 presented 3 regions (chr10: 10933922 – 11037045, chr10:49268194-49840587 and chr10:49332254-49911945) that were significantly lost in at least 50% of samples. The aberrated regions in CFA 30 were instead all present in 50% or more samples with 2 regions (chr30: 15916428- 16633792 and chr30: 16117390 – 17417119) detected in 90% of them and one (chr30:16663301- 17417119) in all of the samples.

CFA 6, 7, 13, 14 and 20 were the chromosomes that the algorithm identified as significantly affected by gained regions. Each chromosome had one gained region with a size ranging from 1,6 Mb to 80Mb (average size 52Mb). Every alteration was found in 20% of the samples, apart for the one in CFA 13 that was detected in 40% of samples.

4.4 Pathway Enrichment Analysis

Five different lists were submitted to the ClueGO program to find significantly enriched pathways in order to create a summary of the pathways that are most likely involved in the carcinogenesis of AMs. Any pathway that had an adjusted Benjamini-Hochberg P < 0.05 was deemed significant.

The list that underwent analysis were composed by five groups of orthologous human genes: lost genes in ≥ 40% of samples (LG40), lost genes in ≥ 70% of samples (LG70), gained genes in ≥ 40% of samples (GG40), statistically significant lost genes (LGSS) and statistically significant gained genes (GGSS). The amount of orthologous human gene names in LG40 was 289, in LG70 25, in GG40 1131, in LGSS was 1192 and in GGSS 2351.

The enrichment analysis identified three significant pathways from the LG40 group, no significant pathway for the LG70 group, 186 significant pathways from GG40, 182 significant pathways for LGSS and 159 significant pathways for GGSS. Since the latter two lists (LGSS and GGSS) were created from data that underwent a statistical significance evaluation, only those pathways were taken into consideration for further study. Table 15 and Table 16 (in paragraph 9) contain all of the pathways discovered using respectively GGSS and LGSS, whereas the tables discussed in paragraph 5 list the ones involved in melanoma processes and thus the most relevant for the aim of this study. The results are all grouped according to ClueGo criteria. However, some of the clusters of pathways were manually associated when they had the same biological function.

Results were compared with the most recent published data on COM and hAM.

5 Discussion

The pathways discovered in our study that are more representative and descriptive of cancer behaviour and, as a result, are more interesting from a therapeutical perspective were grouped into five main functions. The main altered functions discovered are the loss of cell cycle control and response to DNA damage, the ability to promote mitogenesis and angiogenesis, the response to UV radiation, and the ability to evade the immune system. The majority of them reflects cancer hallmarks.

5.1 Loss of Cell Cycle Control and DNA Damage Response

Cells have a large number of defence systems to protect themselves from damage. These mechanisms are activated in response to stress signals, such as DNA damage, and have the ability to stop the cell cycle or trigger apoptosis. The different surveillance checkpoints occur at various times during the cell cycle, including the G1 phase in response to DNA damage, the S phase to monitor DNA replication efficiency and DNA damage occurrence, and the G2/M phase to assess the spindle condition. When DNA is damaged, two significant protein kinases, ATM and ATR, are activated. They activate several signalling pathways that interrupt cell cycle progression and promote the activation of genes involved in DNA repair. One of the primary genes whose expression is increased by these pathways is p53, a negative cell cycle regulator that helps cells to react to stress or DNA damage. P53 acts as a transcriptional regulator when activated: it binds to DNA regulatory regions and transactivates various genes, leading the cell to arrest its cycle in G1. This stops damaged DNA from being replicated, allowing the cell to repair the DNA before restarting the cell cycle (Argyle et al., 2020). If the entire repair process is successful, the cell continues with its cycle; if not, p53 activates the BAX gene, which induces cell apoptosis. In situations where p53 is either lost or altered there is no DNA repair or cell-cycle arrest brought on by DNA damage. Thus, DNA-damaged cells continue to multiply and give rise to malignant neoplasms (Argyle et al., 2020; Kumar et al., 2004; Newkirk et al., 2017). This process is summarized in Figure 18.

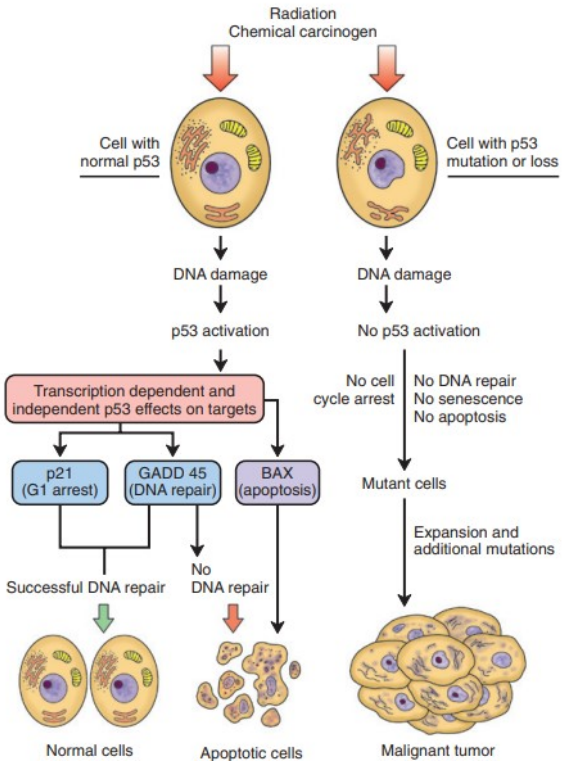

Figure 18: p53 and Maintenance of Genome Integrity. Normal p53 is activated by DNA damage, causing G1 arrest through transcription-dependent and transcription-independent mechanisms. This is accomplished through the activation of p21, growth arrest, and DNA damage-inducible 45. (GADD45). Successful DNA repair enables cells to continue their cycle. However, BCL2-associated X protein (BAX) induces apoptosis if DNA repair fails. Cell cycle arrest or DNA repair, on the other hand, are not brought on by DNA damage in cells that have lost or mutated p53. These cells that have a damaged DNA therefore proliferate and accumulate mutations that can eventually give rise to tumors (Newkirk et al., 2017).

In our study five pathways, shown in Table 8, were found to be related to the loss of cell cycle control and DNA damage: three pathways related to the p53 mechanism (R-HSA:5633008, R-HSA:6803211, KEGG:04115), one pathway related to the control of the G1 to S cell cycle (WP:45), and one pathway related to DNA damage response (WP:707). This suggests that the CAM samples had a disruption of the DNA repairing system that, as a consequence, allows it to maintain chronic proliferation. This trait is a hallmark of the pathophysiology of cancer. An aberration of the p53 pathway can be caused by a variety of mutations as focal amplification of p53 inhibitor MDM2, increases in p53 binding protein, truncating mutations in the p53 protein or mislocation of wild-type p53 protein with nuclear exclusion. In oral and cutaneous melanomas, in both dogs and humans, it was seen that this pathway is compromised (Hardwick, 2021).

Table 8: pathways related to cell damage response

Pathway ID	Pathway term
R-HSA:5633008	TP53 Regulates Transcription of Cell Death Genes
R-HSA:6803211	TP53 Regulates Transcription of Death Receptors and Ligands
KEGG:04115	p53 signaling pathway
WP:707	DNA damage response
WP:45	G1 to S cell cycle control

MDM2 amplifications are frequently observed in COMs and are frequently related with CDK4 and mutually exclusive with Tp53 inactivating mutations (Hardwick, 2021). Because MDM2 functions primarily as a negative regulator of p53 activity, it has become a target for new treatments. However, MDM2 and CDK4 regions were deleted in our samples, and the TP53 gene had no alterations. Although, copy number increases in Mdm2 binding protein (MTBP) and Tp53 binding protein (Tp53BP2) can be seen in COM in the absence of MDM2 amplification. In our study, it was discovered that both of them were amplified, consistently for what was already seen by Brocca et al. (2019). However, this appears to be different from what is so far know in COM (Hardwick, 2021), but even if the reason for this discrepancy is not clear, all of these aberrations confirm a disruption in the p53 pathway and, therefore, with the cells cycle control and DNA damage response (Brocca et al., 2019).

In Elefanti et al. (2021) study on the molecular landscape of hAM, TP53 mutation was also discovered. They hypothesized that TP53 mutations might occur early in the development of AM, leading to an accumulation of the many structural rearrangements and copy number changes that are typically seen in this kind of melanoma. In fact, hAM presents a significant percentage of genome modification, especially in those cases with poor histologic prognostic factors (thick lesion, presence of ulceration, and high mitotic count).

5.2 Pro-Survival Mitogenic Pathways

Another distinguishing feature of tumours is their ability to maintain chronic proliferation in the absence of external mitogenic stimuli. To become independent of exogenous signals, tumour cells severely disrupt normal cell homeostasis and become capable of autonomously promoting signals (typically via intracellular kinase domains) for cell cycle progression, cell growth, cell survival, and metabolism changes. These mechanisms can be acquired through a variety of events, such as cancer cells producing growth factor ligands on their own or inducing stromal cells to produce ligands. Increased concentrations of cell surface ligands can also cause cells to become hyperresponsive to ligands. Otherwise, they can enhance signalling pathways, as the PI3K-Akt pathway, by either activating them or by disrupting their negative feedback mechanisms, as for Ras and PTEN gene modifications (Argyle et al., 2020).

Tyrosine kinases (TKs), a group of proteins that tightly regulates cell growth and differentiation, are important players in normal cell signal transduction. In normal cells, tyrosine kinases respond to growth factors or other stimuli by initiating a phosphorylation cascade, which results in changes in gene transcription that affect cell proliferation and survival. Kit, Met, Axl, and epithelial growth factor receptor (EGFR) are examples of tyrosine kinases receptor (RTK) that are known to be dysregulated in certain types of cancer. Furthermore, tyrosine kinase receptors play an important role in tumour angiogenesis; in fact, their family includes the vascular endothelial growth factor receptor (VEGFR), platelet derived growth factor receptor (PDGFR), fibroblast growth factor receptor (FGFR), and Tie1/2 (London, 2009).

Our research led to the discovery of the amplification of the KIT gene, which is involved in a variety of pathways leading to cell proliferation, including vascular and epithelial proliferation, as well as epithelial and endothelial migration. However, the pathways (listed in Table 9) are made up of several amplified genes, ranging in number from 36 to 352 (with the average number of genes equal to 134,6).

Table 9: pathways related to cell proliferation and migration

Pathway ID	Pathway term
GO:0032879	regulation of localization
GO:0040012	regulation of locomotion
GO:0048870	cell motility
GO:0090132	epithelium migration
GO:0016477	cell migration
GO:0051270	regulation of cellular component movement
GO:2000145	regulation of cell motility
GO:0001667	ameboidal-type cell migration
GO:0010632	regulation of epithelial cell migration
GO:0030334	regulation of cell migration
GO:0043542	endothelial cell migration
GO:0042127	regulation of cell population proliferation
GO:0008284	positive regulation of cell population proliferation
GO:0050673	epithelial cell proliferation
GO:0050679	positive regulation of epithelial cell proliferation
R-HSA:9006934	Signaling by Receptor Tyrosine Kinases

Both in COM and in human melanoma, KIT amplification has been found (Hardwick, 2021). Older studies claimed that this was the most common molecular mutation in hAM, however more current investigations demonstrate that this amplification is rare (Elefanti et al., 2021). Furthermore, its role in COM is still unknown, and there has not been any evidence of a substantial relationship between KIT expression and any histopathologic characteristic, WHO stage, or total patient survival periods (Hardwick, 2021). As a result, the efficacy of using Tyrosine Kinase Inhibitors (TKIs) as solo-treatments is still unreliable. In a recent study masitinib mesylate, a type of TKI, was examined for its efficiency in treating canine advanced malignant melanoma, and it was shown to be only moderately effective. However additional research with larger cohorts at earlier stages of the disease and in conjunction with other treatments may result in a more efficient disease control (Giuliano & Dobson, 2020; Hardwick, 2021). In addition, we found that the platelet-derived growth factors receptor alpha (PDGFR-α) gene was amplified in our samples and involved in most of the pathways listed in Table 9, as well as in the ones in Table 10. PDGFRs (PDGFR-α and PDGFR-β) are physiologically expressed in a variety of cell types, including fibroblasts, vascular smooth muscle cells, and endothelial cells and, by activating signal transduction pathways, they stimulate fibroblast and endothelial

cell proliferation. This suggests that they might also be involved in the interaction of cancerous cells with the stromal compartment during the growth and invasion of tumours. PDGFRs have been observed to be commonly altered in human cancers, and a copy number gain of PDGFR-α was found in human melanoma. Additionally, it was discovered that PDGFRs may contribute to the pathogenesis of canine malignant melanoma, and the co-expression of both PDGFRs (PDGFR-α and PDGFR-β) should be considered as a negative prognostic marker (Iussich et al., 2017).

Table 10: angiogenesis pathways

Pathway ID	Pathway term
GO:0048646	anatomical structure formation involved in morphogenesis
GO:0022603	regulation of anatomical structure morphogenesis
GO:0035295	tube development
GO:0035239	tube morphogenesis
GO:0072359	circulatory system development
GO:0001944	vasculature development
GO:0001568	blood vessel development
GO:0001525	angiogenesis
GO:0048514	blood vessel morphogenesis
GO:0045765	regulation of angiogenesis
GO:0045766	positive regulation of angiogenesis
GO:0050793	regulation of developmental process
GO:0022603	regulation of anatomical structure morphogenesis
GO:0035239	tube morphogenesis
GO:0001525	angiogenesis
GO:0048514	blood vessel morphogenesis
GO:0045765	regulation of angiogenesis

In both human and canine cutaneous melanomas, epidermal growth factor receptors (EGFRs) overexpression is linked to aggressive behaviour. However, in COM, it was not discovered to be amplified or prognostic (Hardwick, 2021). In line with this, it was discovered that our samples had deleted EGFR.

The MAPK and phosphoinositide-3-OH kinase (PI3K) signalling pathways, represented in Figure 19, are two crucial mitogenic cascades involved in melanoma since their disruption increases the tumour capacity to proliferate on its own. Their role is in fact the stimulation of cell proliferation and survival as well as the promotion of protein synthesis and angiogenesis.

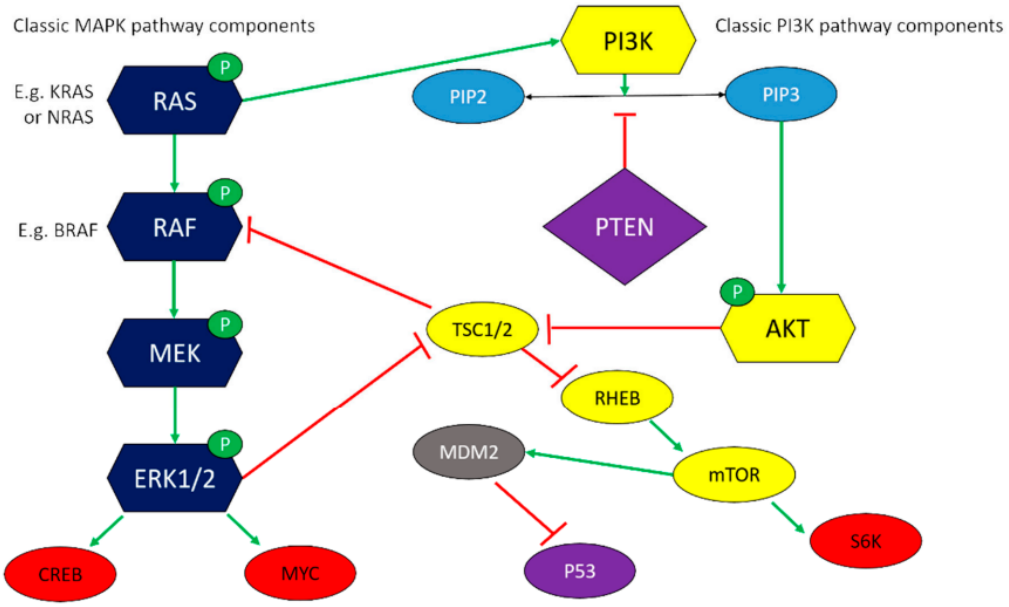

Figure 19: MAPK and PI3K pathway components. The inhibitory effects are represented by the red bars, whereas activating effects are represented by green arrows. Critical transcription factors driving cell proliferation, growth, and survival are shown in red forms, while key tumour suppressor proteins are shown in purple shapes. (Hardwick)

The MAPK signalling cascade is made up of many elements such the RAS, RAF, MEK1/2, and ERK1/2 signalling cascade, and it causes the transcription of genes like CREB and MYC that promote cell division (Hayward et al., 2017). Our research revealed that the MYC gene was amplified and implicated in multiple proliferation pathways (Table 9 and Table 10). In contrary to what is typically observed in human non-acral cutaneous melanoma, no abnormality in the BRAF genes was found, although this is consistent with the findings in COM (Elefanti et al., 2021; Hardwick, 2021). However, compared to other cutaneous melanomas, BRAF mutations are typically less frequent in hAM. Furthermore, it has recently been revealed that BRAF mutations are more prevalent in European-derived patients and are associated with favourable prognostic indicators including low thickness, low mitotic count, and patients with early-stages of AM. Since BRAF-mutated tumours can be candidates for the addition of anti-BRAF targeted therapy within the treatment, this represents a significant benefit for therapy selection in humans (Elefanti et al., 2021; Vanella et al., 2019).

The PI3K/mTOR/AKT signalling pathway was discovered to be disrupted, as shown in Table 11. In addition to the direct disruption of this route, changes in the insulin receptor signalling cascade, which typically stimulates PI3K, were also found. FGFs, EIF4G1, HRAS, KRAS, NRAS, and RPTOR are examples of core pathway members found in the MAPK and PI3K pathways (Hendricks et al., 2018). Due to the fact that several of their constituents, including FGFs (especially FGF3, FGF4, and FGF19), and HRAS, were shown to be deleted in the genome landscape, it was discovered in our study that the PI3K and the Insulin receptor signalling cascade pathways were actually suppressed. None of the other genes cited above had any alteration as well as PTEN, a PI3K suppressor that is typically down-regulated in canine and human melanoma.

These findings demonstrate that, in contrast to COM, where MAPK and PI3K participation appears to play a significant role in carcinogenesis, this does not appear to exist in CAM.

Table 11: PI3K-related pathways

Pathway ID	Pathway term
KEGG:05218	Melanoma
R-HSA:2219528	PI3K/AKT Signaling in Cancer
R-HSA:5674400	Constitutive Signaling by AKT1 E17K in Cancer
R-HSA:6811558	PI5P, PP2A and IER3 Regulate PI3K/AKT Signaling
R-HSA:74751	Insulin receptor signalling cascade
R-HSA:74752	Signaling by Insulin receptor
WP:3844	PI3K-AKT-mTOR signaling pathway and therapeutic opportunities

5.3 Angiogenesis

Angiogenesis is another hallmark of cancer and is necessary for its proliferation and metastasis. Growth factors like VEGF recruit circulating endothelial cells that construct new vascular tubes and organize themselves to maintain blood flow. This results in the formation of a new vasculature in the tumour that is usually characterised by an abnormal structure with a disorganized, leaky vascular system that is poorly structured, has limited adventitial growth, and has an excessive amount of branching. VEGFRs, PDGFRs, FGFRs, and Tie-1 and Tie-2 (receptors for angiopoietin) are the RTKs implicated in this process. The vascular endothelium

expresses VEGFRs, which are responsible for promoting endothelial migration and proliferation and that work along with the FGFR-1 and -2 that increase VEGF expression. PDGFR-α and -β are instead on stroma and pericyte and contribute to the maintenance of new blood vessels. Tie-1 and Tie-2 are expressed on tumoural blood vessels and recruit pericytes and smooth muscle cells for the new vessels (Argyle et al., 2020; London, 2020).

It was discovered that the pathways shown in Table 10 are all involved in the development of blood vessels and are enhanced by the amplification of several genes. Each pathway has 119 amplified genes on average, with a range of 31 to 311. Among these, ANGPT1 was found to be amplified. This gene, which is a member of the angiopoietin family, is essential for the regulation of angiogenesis, endothelial cell survival, proliferation, migration, adhesion and cell spreading (GeneCards, 2022)

Additionally, it was discovered that Angiopoietin-Like Proteins (ANGPTL) as ANGPTL1, 4 and 6 were increased and implicated in these pathways. ANGPTL are engaged in a variety of biological processes and their balance plays a role in angiogenesis, inflammation, apoptosis, metabolism, and cancer progression. Although their significance in the development of cancer is still not fully understood, it appears that they are crucial to the proliferative and invasive characteristics of cancer cells. In particular, ANGPTL1, 4 and 6 likely regulate angiogenesis and have been seen to be involved in human cancers (Carbone et al., 2018). In addition, the Protein Tyrosine Kinase 2 (PTK2), another important gene involved in endothelial and vascular cell proliferation, was found to be amplified and involved in these pathways as well as in the ones listed in Table 9. PDGFRA amplification and involvement was also found, as already seen in paragraph 5.1.

ANGPT, PDGFRA and PTK2 amplifications are consistent with Brocca et al. (2019) while no aberration was found for VEGFRs in contrast with COM (Hayward et al., 2017).

5.4 Ultraviolet radiation response

Table 12: UV radiation pathways

Pathway ID	Pathway term
GO:0009416	response to light stimulus
GO:0009411	response to UV
GO:0071482	cellular response to light stimulus
GO:0034644	cellular response to UV

The pathways mentioned in Table 12 refer to any process that, in response to an ultraviolet radiation (UV light) stimulation, causes a change in the state or activity of a cell in terms of movement, secretion, enzyme production, or gene expression (EMBL-EBI, 2022).

Mutations brought on by frequent and severe exposure to UV light can frequently result in the development of human cutaneous melanoma. However, several etiological factors have been discovered in addition to UV-associated mutagenesis. Dogs are less prone to get UV-associated melanoma because of their thick coats of hair, which possibly shield them from the sun (Bergman et al., 2020). However, the UV exposure associated risk must be taken in account. UVA (320–400 nm), UVB (280–320 nm), and UVC (200 to 280 nm) are the three wavelength ranges that make up the UV portion of the sun spectrum. Since UVB stimulates the formation of pyrimidinedimers in DNA, as shown in Figure 20 (Cancer Council NSW, 2022), it is thought to be the cause of the development of cutaneous tumours. As a result, this may have a variety of effects on cells, including cell division inhibition, enzyme deactivation, mutation induction, and even direct cell death. The most significant mutations that UVB can cause are those involving oncogenes and tumour suppressor genes. RAS and p53 gene alterations have been found in both human skin malignancies and UVB-induced tumours in animals. Additionally, it was discovered that these mutations primarily affect DNA dipyrimidine sequences, confirming the role of UVB radiation as the causal agent (Kumar et al., 2004).

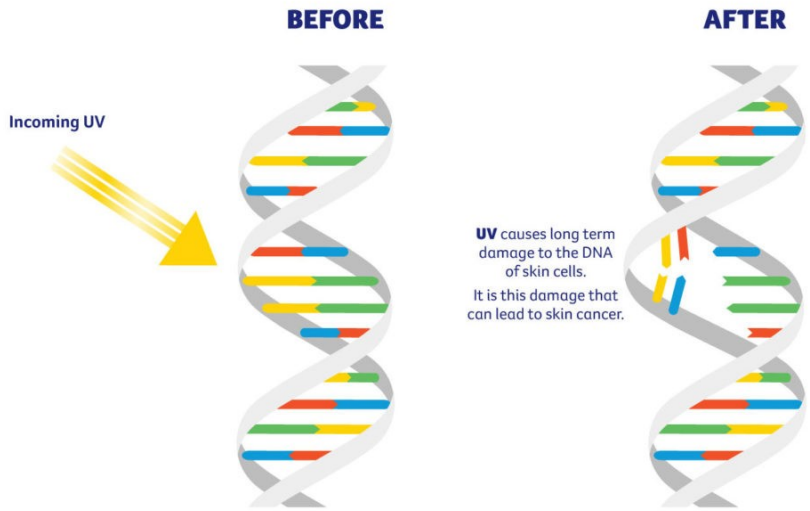

Figure 20: UV induced DNA damage (Cancer Council NSW, 2022)

Our discovery in CAM is in contrast with what has previously been observed in COM (Hardwick, 2021), indicating that these tumours may differ in certain ways. When compared to mucosal sites, the area where CAM develops may actually justify a significant risk of UV-related damage. hAM, compared to other non-acral cutaneous melanomas, also exhibits less UV-induced mutations. The TERT gene is often present in the majority of melanomas that develop on sun-exposed skin, indicating a potential causal role for UV radiation. As hAM exhibits a low incidence of TERT mutation, UV-correlated pathophysiology may be discarded. Furthermore, in humans, a significant protection against sun damage could be acquired due to the tumour position and the substantial amount of stratum corneum that covers it (Elefanti et al., 2021).

5.5 Alteration of the immune microenvironment

The first step in the immune response against the development of a tumour is the elimination of cancerous cells by immune system cells as cytotoxic CD8+ T cells. After the initial reaction of the immune system there is an equilibrium where the development of the tumour is held stationary. Tumours like COM also have a final stage where they become able to evade the immune response either by suppressing it or making it become tolerant to their antigens (Hardwick, 2021; Porcellato et al., 2020).

Tumours can evade the immune system through a number of different methods, shown in Figure 21. The ones that are currently better understood are those that interact with the inhibition of infiltrating cytotoxic T cells or natural killer (NK) cells, the recruitment of immunosuppressive inflammatory cells, as regulatory T cells (Treg) or myeloid-derived suppressor cells (MDSC), and tumour-promoting macrophages, alteration of the antigen presentation, the creation of tolerance thanks to the absence of co-stimulatory molecules expressed by cancer and the production of molecules, as CTLA-4 or programmed-death-1 ligand/receptor (PD/PDL-1) that interact with immune checkpoints inhibiting the T-cell function (Argyle et al., 2020).

The immune profile induced by the tumour can represent a prognostic factor. This has been observed in human cutaneous melanoma tumor infiltrating lymphocytes (TLI) that infiltrate the tumor or come into direct contact with its cells, but less is known about dogs. As a consequence, the observation of the immune system profile induced by the tumour leads to a better understanding of its pathophysiology and contributes to the selection of suitable therapies (Hardwick, 2021; Porcellato et al., 2020).

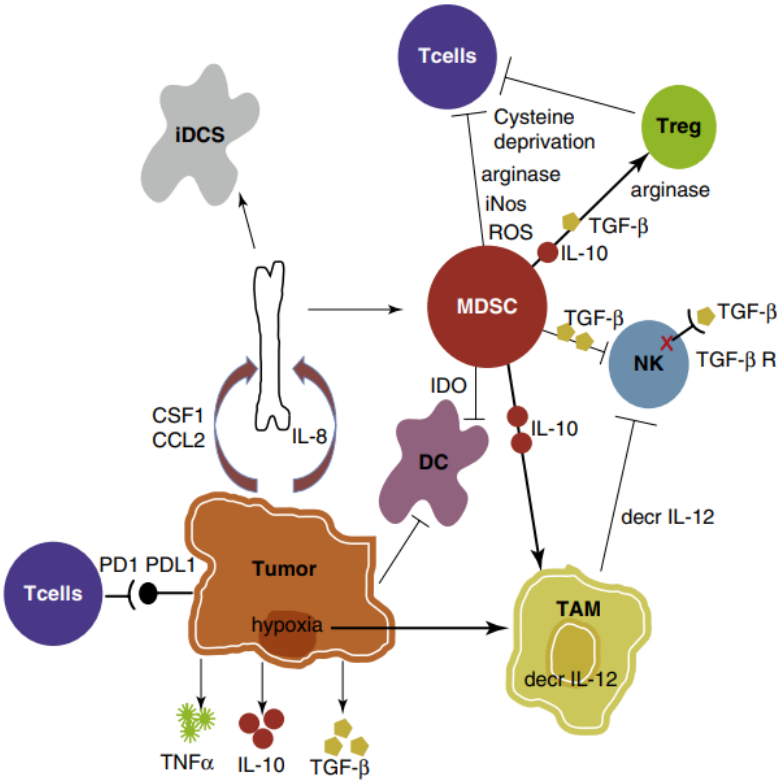

Figure 21: Immune system evasion mechanisms operated by tumor cells. DC: Dendritic cell; iDC: immature dendritic cell; MDSC: myeloid-derived suppressor cell; TAM: tumor-associated macrophage; Treg: regulatory T-cell (Dow & Guth, 2020)

Many discovered pathways reveal a general disturbance of the immune system response and are listed in Table 13 and Table 14. Particularly, those in Table 13 suggest a significant enhancement of the negative regulation of the immune system, which supports the idea that CAM, like COM, alters the immunological microenvironment. Being aware of the modifications brought on by this tumour enables the identification of potential immunotherapeutic treatments. Immunotherapy is one of the key foundations for treating cancer in humans since it enhances the patient's ability to respond to tumour development. However, its application to veterinary medicine has not yet been thoroughly investigated and comprehended. Targeting immune checkpoint inhibitors and melanoma vaccination have received the majority of attention recently.

Table 13: immune system pathways disrupted by gained genes

Pathway ID	Pathway term
GO:0002698	negative regulation of immune effector process
GO:0002822	regulation of adaptive immune response based on somatic recombination of immune receptors built from immunoglobulin superfamily domains
GO:0002823	negative regulation of adaptive immune response based on somatic recombination of immune receptors built from immunoglobulin superfamily domains
GO:0002890	negative regulation of immunoglobulin mediated immune response
GO:0030368	interleukin-17 receptor activity

Table 14: immune system pathways disrupted by deleted genes

Pathway ID	Pathway term
GO:0006956	complement activation
GO:0010324	membrane invagination
GO:0002455	humoral immune response mediated by circulating immunoglobulin
GO:0006911	phagocytosis, engulfment
GO:0016064	immunoglobulin mediated immune response
GO:0030449	regulation of complement activation
GO:0050864	regulation of B cell activation
GO:0050871	positive regulation of B cell activation
R-HSA:447115	Interleukin-12 family signaling
R-HSA:8950505	Gene and protein expression by JAK-STAT signaling after Interleukin-12 stimulation
R-HSA:9020591	Interleukin-12 signaling
GO:0035722	interleukin-12-mediated signaling pathway
KEGG:05235	PD-L1 expression and PD-1 checkpoint pathway in cancer

5.5.1 Evasion of T cell response

The immune system is regulated by checkpoint molecules that are mostly expressed by T cells. These molecules can be grouped into two categories: molecules that activate T cells (costimulatory checkpoint molecules) and molecules that inhibit T cells (coinhibitory checkpoint molecules). It is possible for the tumour to escape the immune system by enhancing coinhibitory immune checkpoint receptors. One of these receptors, known as programmed death 1 (PD-1), is essential because it regulates T-cell activity in response to its ligand PD-L1, thereby preventing tissue damage when the immune system is engaged in response to an infection. Tumours like melanoma induce a decreased T cell response by increasing this mechanism. Therefore, inhibiting the PD-1 pathway may offer antitumour immunity, particularly in cancers that are PD-L1 positive (Dolan & Gupta, 2014; Dow & Guth, 2020; Hardwick, 2021). This pathway (KEGG:05235) was shown to be disturbed in our investigation, indicating that CAM might be a candidate for these treatments.

However, no evidence of PD-1 or PD-L1 gene increase or loss was detected. Nevertheless, the possibility of targeting this pathway is unaffected by the absence of gene alterations, supporting the idea that pathway analysis can expand therapeutic options for melanoma and tumours in general. Numerous new monoclonal antibody (mAb) drugs that target PD-1 have been licensed for the treatment of human melanoma, like Keytruda (pembrolizumab) and Opdivo (nivolumab). Since these human antibodies do not cross-react with canine antigens, these therapies are not available for dogs. However, efforts are being made to produce analogous canine mAbs as a canine chimeric anti-PD-L1 mAb that has shown clinical efficacy on COM (Almela & Ansón, 2019; Dow & Guth, 2020; Maekawa et al., 2017).

5.5.2 Interleukin-12

Table 14 lists the pathways that we discovered were affected by gene loss, and four of them (R-HSA:447115, R-HSA:8950505, R-HSA:9020591 and GO:0035722) are connected to Interleukin-12 function (IL-12). In response to the antigen presentation, dendritic cells (DCs), macrophages, and B cells release this interleukin, which enhances T cell proliferation and function and increases NK cell and T cell cytolytic activity that synthesize Interferon-γ (IFN- γ) and tumour necrosis factor-alpha (TNF-α). TNF-α induces tumour apoptosis and plays a role as proinflammatory cytokine while IFN- γ promotes the differentiation of naïve CD4+ T cells to Th1 phenotype, activates macrophages and enhances MHC Class I/II expression (Dow & Guth, 2020). The IFNG gene, that codes for IFN- γ, was found to be deleted in our study and to contribute to the disruption of the IL-12 pathways.

Therefore IL-12 represents a crucial mediator for tumour suppression and its reduction contributes to melanoma ability to evade the immune system, as shown in Figure 21. In order to enhance the immune response, IL-12 aid may therefore be utilized in the treatment of melanoma. Dog studies on therapies using NHS-IL12, a immunocytokine related to IL-12 that targets necrotic tumour regions revealed that, when given subcutaneously, it can be a therapeutic alternative for treating melanoma (Paoloni et al., 2015).

6 Conclusions

This is the first report on genetic alterations in canine acral melanoma (CAM), aiming to gain insight into its whole-genome landscape. This was accomplished through the identification of genetic anomalies using array Comparative Genomic Hybridization. Furthermore, we examined the amplified and deleted genes using pathway enrichment analysis, a novel technique that enables to highlight tumoral disrupted biological pathways, providing new insights into the description and comprehension of the tumor peculiar behaviour.

Our findings show that CAM, consistently with pathways alterations in canine oral melanoma (COM) and knowledge of human acral melanoma (hAM), induces alterations that reflect cancer hallmarks. It impacts cell cycle control and DNA damage response, which are primarily related to the p53 pathway, mitosis and angiogenesis, and immune system resistance. Interestingly, enhanced ultraviolet (UV) radiation response pathways may play a role in the development of this tumor and may be associated with the specialised unspecific melanocytes response or, less likely, it indicates a potential role of UV exposure.

The sole analysis of gained or deleted genes would have not been able to underline crucial biological alterations. In fact, within CAM, crucial genes that are frequently altered in COM and hAM had no aberrations, whereas the pathways in which these genes are involved did.

As a result, both a single gene mutation and a pathway dysregulation have the same biological effect. This demonstrated that pathway enrichment analysis, being able to capture the complex interaction between several genes, provides a broader view of the tumor behaviour and development. This new approach could lead to a more effective selection of targeted therapies that, even by still targeting a specific protein, would be chosen in order to interrupt a pathway that is strongly related to the tumor development and aggressiveness.

The comparison with hAM, and thus the potential use of CAM as a model for human studies, is limited by the fact that hAM studies focus on gene alterations rather than

pathway enrichment analysis. Finally, larger sample size studies on CAM, with additional clinical information, should be conducted in order to further analyse its differences and similarities with the human counterpart and COM.

7 References

Almela, R. M., & Ansón, A. (2019). A Review of Immunotherapeutic Strategies in Canine Malignant Melanoma. *Veterinary Sciences*, *6*(1), 15. https://doi.org/10.3390/vetsci6010015

Argyle, D. J., Khanna, C., & Giancristofaro, N. (2020). Tumor Biology and Metastasis. In D. M. Vail, D. H. Thamm, & J. M. Liptak (Eds.), *Withrow & MacEwen's Small Animal Clinical Oncology* (Sixth). Elsevier Inc. https://doi.org/https://doi.org/10.1016/C2016-0-01939-3

Bergman, P. J., Selmic, L. E., & Kent, M. S. (2020). Melanoma. In D. M. Vail, D. H. Thamm, & J. M. Liptak (Eds.), *Withrow and Macewen's small animal clinical onocology* (Sixth). Elsevier Inc. https://doi.org/https://doi.org/10.1016/C2016-0-01939-3

Brocca, G., Ferraresso, S., Zamboni, C., Martinez-merlo, E. M., Ferro, S., Goldschmidt, M. H., & Castagnaro, M. (2019). Array Comparative Genomic Hybridization Analysis Reveals Significantly Enriched Pathways in Canine Oral Melanoma. *Frontiers in Oncology*, *9*, 1397. https://doi.org/10.3389/fonc.2019.01397

Brockley, L. K., Cooper, M. A., & Bennett, P. F. (2013). Malignant melanoma in 63 dogs (2001-2011): the effect of carboplatin chemotherapy on survival. *New Zealand Veterinary Journal*, *61*(1), 25–31. https://doi.org/10.1080/00480169.2012.699433

Cancer Council NSW. (2022). *How UV radiation increases skin cancer risk*. www.cancercouncil.com.au

Carbone, C., Piro, G., Merz, V., Simionato, F., Santoro, R., Zecchetto, C., Tortora, G., & Melisi, D. (2018). Angiopoietin-Like Proteins in Angiogenesis , Inflammation and Cancer. *International Journal of Molecular Sciences*, *19*(2), 431. https://doi.org/10.3390/ijms19020431

Conrad, D., Kehl, A., Beitzinger, C., Metzler, T., Steiger, K., Pfarr, N., Fischer, K., Klopfleisch, R., & Aupperle-Lellbach, H. (2022). Molecular Genetic Investigation of Digital Melanoma in Dogs. *Veterinary Sciences*, *9*(2), 56. https://doi.org/10.3390/vetsci9020056

Curtin, J. A., Fridlyand, J., Kageshita, T., Patel, H. N., Busam, K. J., Kutzner, H., Cho, K.-H., Aiba, S., Bröcker, E.-B., LeBoit, P. E., Pinkel, D., & Bastian, B. C. (2005). Distinct Sets of Genetic Alterations in Melanoma. *The New England Journal of Medicine*, *353*(20), 2135–2147. https://doi.org/10.1056/nejmoa050092

Desjardins, P., & Conklin, D. (2010). NanoDrop Microvolume Quantitation of Nucleic Acids. *Journal of Visalized Experiments*, *45*, 2565. https://doi.org/10.3791/2565

Dobson, J. M., Duncan, B., & Lascelles, X. (2003). *BSAVA manual of canine and feline oncology*.

Dolan, D. E., & Gupta, S. (2014). PD-1 Pathway Inhibitors : Changing the Landscape of Cancer Immunotherapy. *Cancer Control : Journal of the Moffitt Cancer Center*, *21*(3), 231–237. https://doi.org/10.1177/107327481402100308

Dow, S., & Guth, A. (2020). Cancer Immunotherapy. In D. M. Vail, D. H. Thamm, & J. M. Liptak (Eds.), *Withrow & MacEwen's Small Animal Clinical Oncology*. Elsevier Inc. https://doi.org/https://doi.org/10.1016/C2016-0-01939-3

Elefanti, L., Zamuner, C., Fiore, P. Del, Stagni, C., Pellegrini, S., Olmo, L. D., Fabozzi, A., Senetta, R., Ribero, S., Salmaso, R., & Mocellin, S. (2021). The Molecular Landscape of Primary Acral Melanoma : A Multicenter Study of the Italian Melanoma Intergroup (IMI). *International Journal of Molecular Sciences*, *22*(8), 3826.

EMBL-EBI. (2022). *GO:0034644*. https://www.ebi.ac.uk/QuickGO/term/GO:0034644

Furney, S. J., Turajlic, S., Stamp, G., Thomas, J. M., Hayes, A., Strauss, D., Gavrielides, M., Xing, W., Gore, M., Larkin, J., & Marais, R. (2014). The mutational burden of acral melanoma revealed by whole-genome sequencing and comparative analysis. *Pigment Cell & Melanoma Research*, *27*(5), 835–838. https://doi.org/10.1111/pcmr.12279

GeneCards. (2022). *ANGPT1 Gene - Angiopoietin 1*. www.genecards.org

Gillard, M., Cadieu, E., De Brito, C., Abadie, J., Vergier, B., Devauchelle, P., Degorce, F., Dréano, S., Primot, A., Dorso, L., Lagadic, M., Galibert, F., Hédan, B., Galibert, M. D., & André, C. (2014). Naturally occurring melanomas in dogs as models for non-UV pathways of human melanomas. *Pigment Cell & Melanoma Research*, *27*(1), 90–102. https://doi.org/10.1111/pcmr.12170

Giudice, C., Ceciliani, F., Rondena, M., Stefanello, D., & Grieco, V. (2010). Immunohistochemical investigation of PNL2 reactivity of canine melanocytic neoplasms and comparison with Melan A. *Ournal of Veterinary Diagnostic Investigation : Official Publication of the American Association of Veterinary Laboratory Diagnosticians, Inc*, *22*(3), 389–394. https://doi.org/10.1177/104063871002200307

Giuliano, A., & Dobson, J. (2020). Prospective clinical trial of masitinib mesylate treatment for advanced stage III and IV canine malignant melanoma. *Journal of Small Animal Practice*,

61(3), 190–194. https://doi.org/10.1111/jsap.13111

Goldschmidt, M., & Goldschmidt, K. (2016). Epithelial and Melanocytic Tumors of the Skin. In D. J. Meuten (Ed.), *Tumors in Domestic Animals* (5th editio). Wiley-Blackwell.

Grassinger, J. M., Floren, A., Müller, T., Cerezo-Echevarria, A., Beitzinger, C., Conrad, D., Törner, K., Staudacher, M., & Aupperle-Lellbach, H. (2021). Digital lesions in dogs: A statistical breed analysis of 2912 cases. *Veterinary Sciences*, *8*(7), 136. https://doi.org/10.3390/vetsci8070136

Hardwick, L. (2021). A comparative view on molecular alterations and potential therapeutic strategies for canine oral melanoma. *Veterinary Sciences*, *8*(11), 286. https://doi.org/10.3390/vetsci8110286

Hayward, N. K., Wilmott, J. S., Waddell, N., Johansson, P. A., Field, M. A., Nones, K., Patch, A. M., Kakavand, H., Alexandrov, L. B., Burke, H., Jakrot, V., Kazakoff, S., Holmes, O., Leonard, C., Sabarinathan, R., Mularoni, L., Wood, S., Xu, Q., Waddell, N., … Mann, G. J. (2017). Whole-genome landscapes of major melanoma subtypes. *Nature*, *545*(7653), 175–180. https://doi.org/10.1038/nature22071

Hendricks, W. P. D., Zismann, V., Sivaprakasam, K., Legendre, C., Poorman, K., Tembe, W., Perdigones, N., Kiefer, J., Liang, W., DeLuca, V., Stark, M., Ruhe, A., Froman, R., Duesbery, N. S., Washington, M., Aldrich, J., Neff, M. W., Huentelman, M. J., Hayward, N., … Trent, J. M. (2018). Somatic inactivating PTPRJ mutations and dysregulated pathways identified in canine malignant melanoma by integrated comparative genomic analysis. *PLoS Genetics*, *14*(9), e1007589. https://doi.org/10.1371/journal.pgen.1007589

Henry, C. J., Brewer, W. G., Whitley, E. M., Tyler, J. W., Ogilvie, G. K., Norris, A., Fox, L. E., Morrison, W. B., Hammer, A., Vail, D. M., & Berg, J. (2005). Canine digital tumors: a veterinary cooperative oncology group retrospective study of 64 dogs. *Journal of Veterinary Internal Medicine*, *19*(5), 720–724. https://doi.org/10.1892/0891-6640(2005)19[720:CDTAVC]2.0.CO;2

Hernandez, B., Adissu, H. A., Wei, B. R., Michael, H. T., Merlino, G., & Simpson, R. M. (2018). Naturally Occurring Canine Melanoma as a Predictive Comparative Oncology Model for Human Mucosal and Other Triple Wild-Type Melanomas. *International Journal of Molecular Sciences*, *19*(2), 394. https://doi.org/10.3390/ijms19020394

Iussich, S., Maniscalco, L., Di Sciuva, A., Iotti, B., Morello, E., Martano, M., Gattino, F., Buracco,

P., & De Maria, R. (2017). PDGFRs expression in dogs affected by malignant oral melanomas: correlation with prognosis. *Veterinary and Comparative Oncology*, *15*(2), 462–469. https://doi.org/10.1111/vco.12190

Kumar, V., Abbas, A. K., & Fausto, N. (2004). *ROBBINS AND COTRAN PATHOLOGIC BASIS OF DISEASE*. Elsevier Inc.

Li, G., Satyamoorthy, K., & Herlyn, M. (2002). Dynamics of cell interactions and communications during melanoma development. *Critical Reviews in Oral Biology and Medicine : An Official Publication of the American Association of Oral Biologists*, *13*(1), 62–70. https://doi.org/10.1177/154411130201300107

London, C. A. (2009). Tyrosine Kinase Inhibitors in Veterinary Medicine. *Topics in Companion Animal Medicine*, *24*(3), 106–112. https://doi.org/10.1053/j.tcam.2009.02.002

London, C. A. (2020). Molecular/Targeted Therapy of Cancer Section B: Signal transduction and cancer. In D. M. Vail, D. H. Thamm, & J. M. Liptak (Eds.), *Withrow & MacEwen's Small Animal Clinical Oncology*. Elsevier Inc. https://doi.org/https://doi.org/10.1016/C2016-0-01939-3

Maekawa, N., Konnai, S., Takagi, S., Kagawa, Y., & Okagawa, T. (2017). A canine chimeric monoclonal antibody targeting PD-L1 and its clinical efficacy in canine oral malignant melanoma or undifferentiated sarcoma. *Scientific Reports*, *7*(1), 8951. https://doi.org/10.1038/s41598-017-09444-2

Manley, C. A., Leibman, N. F., Wolchok, J. D., Rivière, I. C., Bartido, S., Craft, D. M., & Bergman, P. J. (2011). Xenogeneic Murine Tyrosinase DNA Vaccine for Malignant Melanoma of the Digit of Dogs. *Journal of Veterinary Internal Medicine*, *25*(1), 94–99. https://doi.org/10.1111/j.1939-1676.2010.0627.x

Morris, J., & Dobson, J. (2001). *Small Animal Oncology* (1st editio). Wiley Blackwell.

Newkirk, K. M., Brannick, E. M., & Kusewitt, D. F. (2017). Neoplasia and Tumor Biology. In J. F. Zachary (Ed.), *Pathologic Basis of Veterinary Disease* (Sixth). Elsevier Inc.

Nishiya, A. T., Massoco, C. O., Felizzola, C. R., Perlmann, E., Batschinski, K., Tedardi, M. V., Garcia, J. S., Mendonça, P. P., Teixeira, T. F., & Dagli, M. L. Z. (2016). Comparative aspects of canine melanoma. *Veterinary Sciences*, *3*(1), 7. https://doi.org/10.3390/vetsci3010007

Ohsie, S. J., Sarantopoulos, G. P., Cochran, A. J., & Binder, S. W. (2008). Immunohistochemical characteristics of melanoma. *Journal of Cutaneous Pathology*, *35*(5), 433–444.

https://doi.org/10.1111/j.1600-0560.2007.00891.x

Paczkowska, M., Barenboim, J., Sintupisut, N., Fox, N. S., Zhu, H., Abd-Rabbo, D., Mee, M. W., Boutros, P. C., PCAWG Drivers and Functional Interpretation Working Group, Reimand, J., & PCAWG Consortium. (2020). Integrative pathway enrichment analysis of multivariate omics data. *Nature Communications*, *11*(1), 735. https://doi.org/10.1038/s41467-019-13983-9

Paoloni, M., Mazcko, C., Selting, K., Lana, S., Barber, L., Phillips, J., Skorupski, K., Vail, D., Wilson, H., Biller, B., Avery, A., Kiupel, M., Leblanc, A., Bernhardt, A., & Brunkhorst, B. (2015). Defining the Pharmacodynamic Profile and Therapeutic Index of NHS-IL12 Immunocytokine in Dogs with Malignant Melanoma. *PLoS ONE*, *10*(6), e0129954. https://doi.org/10.1371/journal.pone.0129954

Patel, P. G., Selvarajah, S., Guérard, K. P., Bartlett, J. M. S., Lapointe, J., Berman, D. M., Okello, J. B. A., & Park, P. C. (2017). Reliability and performance of commercial RNA and DNA extraction kits for FFPE tissue cores. *PLoS ONE*, *12*(6), e0179732. https://doi.org/10.1371/journal.pone.0179732

Porcellato, I., Silvestri, S., Menchetti, L., Recupero, F., Mechelli, L., Sforna, M., Iussich, S., Bongiovanni, L., Lepri, E., & Brachelente, C. (2020). Tumour-infiltrating lymphocytes in canine melanocytic tumours: An investigation on the prognostic role of CD3+ and CD20+ lymphocytic populations. *Veterinary and Comparative Oncology*, *18*(3), 370–380. https://doi.org/10.1111/vco.12556

Prouteau, A., & André, C. (2019). Canine melanomas as models for human melanomas: Clinical, histological, and genetic comparison. *Genes*, *10*(7), 501. https://doi.org/10.3390/genes10070501

Reimand, J., Isserlin, R., Voisin, V., Kucera, M., Tannus-Lopes, C., Rostamianfar, A., Wadi, L., Meyer, M., Wong, J., Xu, C., Merico, D., & Bader, G. D. (2019). Pathway enrichment analysis and visualization of omics data using g:Profiler, GSEA, Cytoscape and EnrichmentMap. *Nature Protocols*, *14*(2), 482–517. https://doi.org/10.1038/s41596-018-0103-9

Simpson, R. M., Bastian, B. C., Michael, H. T., Webster, J. D., Prasad, M. L., Conway, C. M., Prieto, V. M., Gary, J. M., Goldschmidt, M. H., Esplin, D. G., Smedley, R. C., Piris, A., Meuten, D. J., Kiupel, M., Lee, C. C. R., Ward, J. M., Dwyer, J. E., Davis, B. J., Anver, M. R., … Hewitt, S. M. (2014). Sporadic naturally occurring melanoma in dogs as a preclinical

model for human melanoma. *Pigment Cell and Melanoma Research*, *27*(1), 37–47. https://doi.org/10.1111/pcmr.12185

Smedley, R. C., Spangler, W. L., Esplin, D. G., Kitchell, B. E., Bergman, P. J., Ho, H. Y., Bergin, I. L., & Kiupel, M. (2011). Prognostic markers for canine melanocytic neoplasms: A comparative review of the literature and goals for future investigation. *Veterinary Pathology*, *48*(1), 54–72. https://doi.org/10.1177/0300985810390717

Smith, S. H., Goldschmidt, M. H., & Mcmanus, P. M. (2002). A Comparative Review of Melanocytic Neoplasms. *Veterinary Pathology*, *39*(6), 651–678. https://doi.org/10.1354/vp.39-6-651

Spangler, W. L., & Kass, P. H. (2006). The histologic and epidemiologic bases for prognostic considerations in canine melanocytic neoplasia. *Veterinary Pathology*, *43*(2), 136–149. https://doi.org/10.1354/vp.43-2-136

ThermoFisher Scientific. (2022a). *DNA Electrophoresis*. www.thermofisher.com

ThermoFisher Scientific. (2022b). *Nucleic Acid Electrophoresis Workflow—5 Main Steps*. www.thermofisher.com

ThermoFisher Scientific. (2022c). *RNA/DNA Quantification*. www.thermofisher.com

van Beers, E. H., Joosse, S. A., Ligtenberg, M. J., Fles, R., Hogervorst, F. B., Verhoef, S., & Nederlof, P. M. (2006). A multiplex PCR predictor for aCGH success of FFPE samples. *British Journal of Cancer*, *94*(2), 333–337. https://doi.org/10.1038/sj.bjc.6602889

van der Weyden, L., Brenn, T., Patton, E. E., Wood, G. A., & Adams, D. J. (2020). Spontaneously occurring melanoma in animals and their relevance to human melanoma. *Journal of Pathology*, *252*(1), 4–21. https://doi.org/10.1002/path.5505

van Der Weyden, L., Patton, E. E., Wood, G. A., Foote, A. K., Brenn, T., Arends, M. J., & Adams, D. J. (2016). Cross-species models of human melanoma. *Journal of Pathology*, *238*(2), 152–165. https://doi.org/10.1002/path.4632

Vanella, V., Festino, L., Trojaniello, C., Vitale, M. G., Sorrentino, A., Paone, M., & Ascierto, P. A. (2019). The Role of BRAF-Targeted Therapy for Advanced Melanoma in the Immunotherapy Era. *Current Oncology Reports*, *21*(9), 76. https://doi.org/10.1007/s11912-019-0827-x

Wobeser, B. K., Kidney, B. A., Powers, B. E., Withrow, S. J., Mayer, M. N., Spinato, M. T., &

Allen, A. L. (2007). Diagnoses and clinical outcomes associated with surgically amputated canine digits submitted to multiple veterinary diagnostic laboratories. *Veterinary Pathology*, *44*(3), 355–361. https://doi.org/10.1354/vp.44-3-355

8. Protocols

8.1 Protocol A, AllPrep® DNA/RNA FFPE Kit

A. Procedure

1. Using a scalpel, trim excess paraffin off the sample block.
2. Cut sections 10–20 µm thick. Do not use more than four 10 µm sections of 150 mm^2 surface area or two 20 µm sections of 150 mm^2 surface area. Discard the first 2–3 sections.
3. Immediately place the sections in a 1.5 ml Safe-Lock microcentrifuge tube (not supplied), and close the lid.
4. Deparaffinization using heptane (more compact sample pellets in step 8):
    - Add 500 µl of heptane, vortex vigorously for 10 s, and incubate for 10 min at room temperature;
    - Add 25 µl methanol, vortex vigorously for 10 s, and centrifuge for 2 min at 9000 x g;
    - Carefully remove the supernatant by pipetting without disturbing the pellet. Carefully remove any residual heptane/methanol using a fine pipet tip;
    - Add 1 ml ethanol (96-100%) to the pellet, mix by vortexing, and centrifuge at full speed for 2 min;
    - Carefully remove the supernatant by pipetting without disturbing the pellet. Carefully remove any residual ethanol using a fine pipet tip;
    - Keep the lid open, and incubate at room temperature or at up to 37°C for 10 min or until all residual ethanol has evaporated.
    - Proceed to step 5.
5. Resuspend the pellet by adding 150 µl Buffer PKD; Flick the tube to loosen the pellet;Add 10 µl proteinase K, and mix by vortexing.
6. Incubate at 56°C for 15 min. (The sample may not be completely lysed. This does not affect the procedure).
7. Incubate on ice for 3 min.
8. Centrifuge for 15 min at 14,000 rpm.
9. Carefully transfer the supernatant, without disturbing the pellet, to a new 1.5 ml Safe-Lock microcentrifuge tube for RNA purification in steps 10–24.

10. Keep the pellet for DNA purification in steps 25–35. The DNA-containing pellet can be stored for 2 h at room temperature, for up to 1 day at 2–8°C, or for longer periods at –15 to –30°C.

B. DNA purification

The pellet should be equilibrated to room temperature prior to resuspension.

11. Resuspend the pellet from step 9 in 180 µl Buffer ATL; Add 40 µl proteinase K; Mix by vortexing.

12. Incubate at 56°C for 1 h.

13. Incubate at 90°C for 2 h without agitation. Keep the sample at room temperature until the heating block has reached 90°C.

14. Briefly centrifuge the microcentrifuge tube to remove drops from the inside of the lid.

    Allow the sample to cool to room temperature; Add 4 µl RNase A (100 mg/ml); Incubate for 2 min at room temperature before proceeding.

15. Add 200 µl Buffer AL; Mix thoroughly by vortexing; Add 200 µl ethanol (96–100%); Mix thoroughly again by vortexing or pipetting.

16. Transfer the entire sample to a QIAamp MinElute spin column placed in a 2 ml collection tube (supplied); Close the lid gently, and centrifuge for 1 min at ≥10,000 rpm;

    Discard the collection tube with the flow-through.

    If the sample has not completely passed through the membrane after centrifugation, centrifuge again at a higher speed until the QIAamp MinElute spin column is empty.

17. Place the QIAamp MinElute spin column in a new 2 ml collection tube (supplied); Add 700 µl Buffer AW1 to the spin column; Close the lid gently, and centrifuge for 15 s at ≥10,000 rpm to wash the spin column membrane;

Discard the flow-through.

Reuse the collection tube in next step.

18. Add 700 µl Buffer AW2 to the QIAamp MinElute spin column; Close the lid gently, and centrifuge for 15 s at ≥10,000 rpm to wash the spin column membrane;

    Discard the flow-through.

    Reuse the collection tube in next step.

19. Add 700 µl ethanol (96–100%) to the QIAamp MinElute spin column;

    Close the lid gently, and centrifuge for 15 s at ≥10,000 rpm;

    Discard the collection tube with the flow-through.

20. Place the QIAamp MinElute spin column in a new 2 ml collection tube (supplied); Open the lid of the spin column, and centrifuge at full speed for 5 min;

    Discard the collection tube with the flow-through.

21. Place the QIAamp MinElute spin column in a new 1.5 ml collection tube (supplied); Add 60 µl Buffer ATE directly to the spin column membrane; Close the lid gently, and incubate for 5 min at room temperature; Centrifuge at full speed for 1 min to elute the DNA.

    Important: Ensure that Buffer ATE is equilibrated to room temperature. If using small elution volumes (<50 µl), pipet Buffer ATE onto the center of the membrane to ensure complete elution of bound DNA.

8.2 Protocol B, Cy3 and Cy5 labelling and labelled DNA purification

A. Labelling with Cy3 and Cy5

1. Get Random Primers (green) and the other reagents and let the defrost on ice;
2. Prepear a stip with 26 µl of sample per tube and spin it
3. Add 5 µl of Random Primers to each sample (total volume of 31 µl, 26+5) and spin;
4. Set the thermocycler 3: user CGH, run “denat” (10 minutes at 98°C) and spin at the end of the denaturation cycle. At the end leave 5 min into ice;
5. Start thermocycler from step 8 (Thermocycler 3: user CGH, run “label” (37°C for 2h, 65°C 10 min));
6. Prepear labelling mix with volumes listed in table below:

Reagent	**1X**	**4,5X (Cy3)**	**4,5X (Cy5)**
5X Reaction Buffer	10.0	45	45
10X dNTPs	5.0	22,5	22,5
Cyanine 3 (SANO) o Cyanine 5 (PATO)	3.0	13,5	/
Cyanine 3 (SANO) o Cyanine 5 (PATO) Exo Klenow	3.0	/	13,5
	1.0	4,5	4,5
Volume finale labeling	19	85,5	85,5

N.B: when withdrawing cyanines be careful to a) protect them from light the whole time; b) withdraw 6.6 µl only from the top and not from the bottom (they are very gluey); c) once withdrawn the cyanine release it in one part of the mix and clean the tip on the other side only once.

7. Add 19 µl of labelling mix (mixing it up and down with the tip, especially the first time) to each sample and remember to add to the healthy one the mix with Cy3 and to the pathological one the mix with Cy5;
8. Thermocycler 3: user CGH, run “label” (37°C 2h, 65°C 10’) and at the end place the samples into ice.

B. Purification of labelled DNA

1. After part A, spin the strip;
2. Add 430 µl of TE buffer in new 1.5ml eppendorf (non in the kit);

3. Move the labelled samples (50 µl) into the Eppendorf with TE
4. Per each sample prepare a labelled spin column and move the volume of labelled DNA and TE (480 µl) into them
5. Centrifuge at 15°C, 10 min, 14000 rcf and remove the eluate
6. Add 480 µl of TE Buffer
7. Centrifuge at 15°C, 10 min, 14000 rcf and remove the eluate
8. Withdrawn spin column and put it in a new Eppendorf (into the kit)
9. Centrifuge for 1 minute at 1000 rcf and keep the eluate on ice. Trash the spin column
10. Measure with the Nanodrop (1.5 µl) every sample twice. Select from the program main window “Microarray” instead of “Nucleic acid” and use TE for the white. At the end save the report.
11. Measure µl of the labelled DNA that remains into the Eppendorf and bring it into a new 1.5 ml Eppendorf (not in the kit)

8.3 Protocol C

A. Hybridization

1. In a fresh 1.5-mL RNase-free Microfuge Tub, combine test and reference sample using the appropriate cyanine-5-labeled sample and cyanine-3-labeled sample for a total mixture volume of 39 µl

(1 b. Prepare the 10× Blocking Agent: add 1,350 µL of DNase/RNase-free distilled water to the vial containing lyophilized 10× aCGH Blocking Agent and leave at room temperature for 60 minutes and mix on a vortex mixer to reconstitute sample before use or storage)

Prepare the labaled DNA for hybridization:

2. Prepare the hybridization master mix:

Component	**Volume (µl)**
Cot-1 DNA	5
10x aCGH Blocking Agent	11
2x HI-RPM Hybridization Buffer	55
Final Volume	71

3. Add 71 µl of the Master Mix to the labeled DNA (total volume 110 µ)

4. Mix the sample by pipetting up and down, then quickly spin in a centrifuge to drive contents to the bottom of the reaction tube.

5. Transfer sample tubes to a thermal cycler (98°C for 3 minutes + 37°C for 30 minutes)

6. Remove sample tubes from the thermal cycler. Spin 1 minute at 6000 × g in a centrifuge to collect the sample at the bottom of the tube.

The samples are ready to be immediately hybridized

7. Load a clean gasket slide into the Agilent SureHyb chamber base with the gasket label facing up and aligned with the rectangular section of the chamber base. Ensure that the gasket slide is flush with the chamber base and is not ajar.

8. Slowly dispense 110 µl of hybridization sample mixture onto the gasket well.

9. Put a microarray slide “active side” down onto the gasket slide, so the numeric barcode side is facing up and the “Agilent”-labeled barcode is facing down. Assess that the sandwich-pair is properly aligned.

10. Put the SureHyb chamber cover onto the sandwiched slides and slide the clamp assembly onto both pieces.

11. Hand-tighten the clamp firmly onto the chamber.

12. Vertically rotate the assembled chamber to wet the slides and assess the mobility of the bubbles. Tap the assembly on a hard surface if necessary to move stationary bubbles.

13. Load each assembled chamber into the oven rotator rack. Start from the center of the rack (position 3 or 4 when counting from the left). Set your hybridization rotator to rotate at 20 rpm.

14. Hybridize at 67°C for 24 hours.

B. Washing

1. Prewarm Agilent Oligo aCGH/ChIP-on-Chip Wash Buffer 2 at 37°C overnight.

2. Completely fill slide-staining dish #1 with Agilent Oligo aCGH/ChIP-on-Chip Wash Buffer 1 at room temperature.

3. Prepare dish #2:

   a. Put a slide rack into slide-staining dish #2.

   b. Add a magnetic stir bar. Fill slide-staining dish #2 with enough Agilent Oligo aCGH/ChIP-on-Chip Wash Buffer 1 at room temperature to cover the slide rack.

   c. Put this dish on a magnetic stir plate.

4. Prepare dish #3:

a. Put the prewarmed 1.5 L glass dish on a magnetic stir plate with heating element.

b .Put the slide-staining dish #3 into the 1.5 L glass dish.

c. Fill the 1.5 L glass dish with pre-warmed Milli-Q ultrapure water.

d. Fill the slide-staining dish #3 approximately three-fourths full with Agilent Oligo aCGH/ChIP-on-Chip Wash Buffer 2 (warmed to 37°C).

e. Add a magnetic stir bar.

f. Turn on the heating element and maintain temperature of Agilent Oligo aCGH/ChIP-on-Chip Wash Buffer 2 at 37°C.

5. Remove one hybridization chamber from the incubator and resume rotation of the others. Record whether bubbles formed during hybridization and if all bubbles are rotating freely.

6. Prepare the hybridization chamber disassembly:

a. Put the hybridization chamber assembly on a flat surface and loosen the thumbscrew, turning counter-clockwise.

b. Slide off the clamp assembly and remove the chamber cover.

c. With gloved fingers, remove the microarray-gasket sandwich from the chamber base by lifting one end and then grasping in the middle of the long sides. Keep the microarray slide numeric barcode facing up as you quickly transfer the sandwich to slide-staining dish #1.

d. Without letting go of the slides, submerge the microarray-gasket sandwich into slide-staining dish #1 containing Agilent Oligo aCGH/ChIP-on-Chip Wash Buffer 1.

7. With the sandwich completely submerged in Agilent Oligo aCGH/ChIP-on-Chip Wash Buffer 1, pry the sandwich open from the barcode end only:

a. Slip one of the blunt ends of the forceps between the slides.

b. Gently twist the forceps to separate the slides.

c. Let the gasket slide drop to the bottom of the staining dish.

d. Remove the microarray slide, grasp it from the upper corners with thumb and forefinger, and quickly put into slide rack in the slide-staining dish #2 containing Agilent Oligo aCGH/ChIP-on-Chip Wash Buffer 1 at room temperature. Minimize exposure of the slide to air. Touch only the barcode portion of the microarray slide or its edges!

8. Repeat the steps for up to four additional slides in the group. A maximum of five disassembly procedures yielding five microarray slides is advised at one time in order to facilitate uniform washing.

9. When all slides in the group are put into the slide rack in slide-staining dish #2, stir at 350 rpm for 5 minutes. Adjust the setting to get good but not vigorous mixing.

10. Wash the slides in Agilent Oligo aCGH/ChIP-on-Chip Wash Buffer 2:

a. Transfer slide rack to slide-staining dish #3, which contains Agilent Oligo aCGH/ChIP-on-Chip Wash Buffer 2 at 37°C:

b. Activate the magnetic stirrer.

c. Wash microarray slides for at least 1 minute and no more than 2 minutes.

Adjust the setting to get thorough mixing without disturbing the microarray slides.

11. Slowly remove the slide rack trying to minimize droplets on the slides. It should take 5 to 10 seconds to remove the slide rack.

12. Discard used Agilent Oligo aCGH/ChIP-on-Chip Wash Buffer 1 and Agilent Oligo aCGH/ChIP-on-Chip Wash Buffer 2.

13. Repeat step 1 through step 11 for the next group of five slides using fresh Agilent Oligo aCGH/ChIP-on-Chip Wash Buffer 1 and Agilent Oligo aCGH/ChIP-on-Chip Wash Buffer 2 warmed to 37°C.

14. Scan slides immediately to minimize the impact of environmental oxidants on signal intensities. If necessary, store slides in orange slide boxes in a N2 purge box, in the dark.

C. Scanning

1. Switch on the computer

2. Switch on the Scanner

3. Start the program

4. Verify the slide position: Start: 1 End slot: 2

5. Verify the setting: Agilent G3_CGH (R+G; 61 x 21,6; 3 µm; 16 bit; 100%; 100%)

6. Verify that the Scanner status in the main window says Scanner Ready.

7. Put assembled slide holders into the scanner cassette.

8. Click Start Scan.

9. Check and save the scan:

    a. D:\ location,

    b. double click on the scanning (ignore the “error” alarm),

    c. copy and paste on the USB key

10. Close the program Scan Control

11. Switch off the Scanner

12. Switch off the computer

9. Annex

The following tables (Table 15 and Table 16) show all the pathways obtained through the analysis. The colour division (grey and white) indicates the groups that ClueGO created depending on the function of the pathways.

Table 15: pathways derived from gained genes (GGSS)

ID	Term	Term PValue Corrected with Benjamini - Hochberg	Group PValue Corrected with Benjamini - Hochberg	% Associated Genes	Nr. Genes	Associated Genes Found
GO:0000393	spliceosomal conformational changes to generate catalytic conformation	0,04	0,00	57,14	4,00	[ISY1, ISY1-RAB43, XAB2, YJU2]
GO:0061519	macrophage homeostasis	0,03	0,00	100,00	3,00	[BAP1, MAGI1, RNF2]
GO:0140053	mitochondrial gene expression	0,04	0,00	17,47	29,00	[COA3, DAP3, DARS2, GADD45GIP1, GARS1, LARS2, MALSU1, METTL4, MPV17L2, MRPL13, MRPL22, MRPL24, MRPL34, MRPL4, MRPL42, MRPL45, MRPL54, MRPL55, MRPS10, MRPS14, MRPS25, MRPS36, MTERF1, NDUFA7, NOA1, POLRMT, RPUSD3, TFB2M, TRNT1]
GO:0140056	organelle localization by membrane tethering	0,05	0,00	17,14	30,00	[AKAP9, CAV2, CEP135, CEP192, CEP41, CEP76, CETN2, CFTR, EXOC4, HAUS1, HAUS8, MBD1, NEK2, ODF1, PRKACA, PSEN2, RAB12, RAB13, RAB3A, RAB3D, RAB8A, SCFD2, SDCCAG8, STX10, STX6, STXBP2, TSNARE1, TUBB, TUBB4A, UNC13A]
GO:1903729	regulation of plasma membrane organization	0,04	0,00	40,00	6,00	[ASAP1, DNM2, FASLG, PRKCD, RAB3A, WASL]
KEGG:05206	MicroRNAs in cancer	0,03	0,00	15,81	49,00	[ABCB1, APC2, CDC25A, CDK6, DNMT1, EFNA1, EFNA3, FOXP1, MAP2K2, MET, MIR1-2, MIR129-1, MIR133A1, MIR135A1, MIR181A1, MIR181B1, MIR181C, MIR183, MIR199A1, MIR199A2, MIR205, MIR214, MIR23A, MIR27A, MIR29A, MIR29B1, MIR29B2, MIR29C, MIR30B, MIR30D, MIR335, MIR7-3, MIR96, MIRLET7G, MYC, NOTCH3, PDGFRA, PIK3R2, PTGS2, RAF1, RASSF1, RHOA, ROCK1, SHC1, SOCS1, TNN, TNR, WNT3A, ZFPM2]
R-HSA:162582	Signal Transduction	0,02	0,00	12,00	307,00	[ABHD17A, ABHD6, ABL2, ADCY10, ADCY8, ADCYAP1, ADCYAP1R1, ADGRE1, ADGRE3, ADGRE5, ADORA1, AGO2, AHCTF1, AKT3, ANGPT1, ANLN, AREG, ARHGAP39, ARHGAP45, ARHGEF11, ARHGEF18, ARHGEF2, ARHGEF3, ARPC4, ARPC5, ATP6V1C1, ATP6V1F, ATP6V1G3, BRK1, C3, CALCA, CALCR, CARM1, CAV1, CAV2, CCL25, CCR1, CCR2, CCR3, CCR5, CCR9, CCRL2, CD55, CDC37, CDC42BPA, CENPF, CENPL, CFTR, CHN2, COL1A2, COL5A3, CRABP2, CRHR2, CSN2, CSNK1G2, CXCL6, CXCL8, CXCR6, DGKB, DNAJB1, DNM2, DNM3, DOCK3, DOCK4, DOCK6, DYNC1I1, E2F4, EBAG9, EEPD1, ELF3, ELMO1, EMC3, EPGN, EPOR, EPS15L1, EREG, F2RL3, FAM91A1, FASLG, FCER2, FGD5, FGF22, FOXH1, FSTL3, FZD1, FZD6, GATAD2A, GATAD2B, GHRHR, GHRL, GMIP, GNA15, GNAI2, GNAL, GNAT1, GNG11, GNGT1, GNRHR, GPNMB, GPR161, GPR25, GPR37, GPR37L1, GREM2, GRM2, GRM3, GRM7, GRM8, GTF2F1, H2BU1, H3-3B, HDAC11, HDAC9, HHAT, HNRNPM, HRH1, HRH4, IFT122, IL17RD, IL5RA, IL6, IL6R, INSR, IQGAP3, ITPR1, JAK3, JUNB, JUND, KCTD6, KDM4B, KDR, KHDRBS3, KIF14, KIT, LAMA1, LAMA3, LAMB2, LAMB3, LAMC1, LAMC2, LAMTOR2, LBR, LEP, LGR6, LPAR2, LRIG1, LYL1, MAF1, MAP2K2, MAPK4, MAPKAPK3, MATK, MBD3, MEF2D, MET, MGLL, MIB1, MKRN1, MOB1B, MSI2, MST1, MST1R, MTX1, MYC, MYL12A, MYO9B, NCF2, NCKIPSD, NDC80, NISCH, NMU, NOTCH3, NPBWR2, NPSR1, NPY, NR5A2, NRTN, NSL1, NTRK1, OBSCN, OPN1SW, OPN3, OXTR, P2RY11, PARP1, PCP2, PDE1C, PDE4A, PDE4C, PDGFRA, PDHB, PDK4, PIK3C3, PIK3R2, PIN1, PIP5K1C, PKN1, PLA2G4A, PLIN3, PLPPR2, PLPPR3, PLXNA1, PLXNB1, PLXND1, POLR2B, POLR2E, POU2F1, PPARG, PPBP, PPP1R12B, PPP2R5A, PRKACA, PRKAR2A, PRKCD, PROK2, PSEN2, PSMA8, PSMD4, PSPN, PTGER1, PTH1R, PTK2, PTPN2, PTPN7, PTPRS, PYGO2, RAB7A, RAD21, RAF1, RALBP1, RASAL2, RASAL3, REST, RGL1, RGS16, RGS22, RGS7, RGS8, RGSL1, RHOA, RHPN1, RIT1, RIT2, RLN3, RNF2, ROCK1, RSPO2, RUVBL1, S100A9, S1PR2, S1PR4, S1PR5, SCRIB, SEC13, SEM1, SEPTIN7, SH2D2A, SH3GL1, SHARPIN, SHC1, SIRT6, SKA1, SMAD2, SMAD7, SMARCA4, SMO, SOCS1, SPC24, SPPL2B, SRGAP3, STAP2, STK11, STK3, STK38, SYDE1, TAC1, TAX1BP1, TBXA2R, TGIF1, THBS3, TLE2, TLR9, TOR1AIP1, TPM4, TRH, TRHR, TRIB1, TRIP10, TUBB4A, TUBB6, TYK2, UBA52, USP4, VAV1, WASL, WDR6, WIPF3, WNT16, WNT2, WNT3A, WNT5A, WNT7A, WNT9A, XCL1, XCL2, XCR1, YES1]
R-HSA:373080	Class B/2 (Secretin family receptors)	0,01	0,00	23,16	22,00	[ADCYAP1, ADCYAP1R1, ADGRE1, ADGRE3, ADGRE5, CALCA, CALCR, CD55, CRHR2, FZD1, FZD6, GHRHR, GNG11, GNGT1, PTH1R, SMO, WNT16, WNT2, WNT3A, WNT5A, WNT7A, WNT9A]
R-HSA:381119	Unfolded Protein Response (UPR)	0,04	0,00	20,21	19,00	[ASNS, ATF3, CALR, CREB3L3, CREB3L4, CXCL8, CXXC1, DCSTAMP, DNAJB9, EDEM1, EXOSC4, EXOSC7, HDGF, KHSRP, LMNA, MYDGF, SHC1, TATDN2, WFS1]
R-HSA:419408	Lysosphingolipid and LPA receptors	0,03	0,00	42,86	6,00	[LPAR2, PLPPR2, PLPPR3, S1PR2, S1PR4, S1PR5]
R-HSA:9006934	Signaling by Receptor Tyrosine Kinases	0,04	0,00	14,23	72,00	[ADCYAP1, ADCYAP1R1, AKT3, AREG, ATP6V1C1, ATP6V1F, ATP6V1G3, BRK1, CAV1, CDC37, COL1A2, COL5A3, CSN2, DNM2, DNM3, DOCK3, ELMO1, EPGN, EPS15L1, EREG, FGF22, GTF2F1, HNRNPM, INSR, ITPR1, JUNB, JUND, KDR, KIT, LAMA1, LAMA3, LAMB2, LAMB3, LAMC1, LAMC2, LRIG1, LYL1, MAP2K2, MAPKAPK3, MATK, MEF2D, MET, MST1, MST1R, NCF2, NTRK1, PDGFRA, PIK3C3, PIK3R2, POLR2B, POLR2E, PRKACA, PRKCD, PSEN2, PTK2, PTPN2, PTPRS, REST, RHOA, RIT1, RIT2, ROCK1, SH2D2A, SH3GL1, SHC1, SOCS1, THBS3, TLR9, TRIB1, UBA52, VAV1, YES1]
WP:2363	Gastric Cancer Network 2	0,03	0,00	30,30	10,00	[AHCTF1, ATAD2, CACYBP, DSCC1, FAM91A1, LBR, LMNB2, MYC, S100A6, SNURF]
WP:306	Focal Adhesion	0,04	0,00	16,83	34,00	[AKT3, CAPN2, CAV1, CAV2, CAV3, COL1A2, COL5A3, COMP, FLNB, FLNC, ITGB8, KDR, LAMA1, LAMA3, LAMB2, LAMB3, LAMC1, LAMC2, MET, MYL12A, PDGFRA, PIK3R2, PIP5K1C, PPP1R12B, PTK2, RAF1, RHOA, ROCK1, SHC1, THBS3, TNN, TNR, TXK, VAV1]
WP:334	GPCRs, Class B Secretin-like	0,01	0,00	37,50	9,00	[ADCYAP1R1, ADGRE1, ADGRE5, ADGRL1, ADGRL3, CALCR, CRHR2, GHRHR, PTH1R]
GO:0006940	regulation of smooth muscle contraction	0,03	0,00	24,19	15,00	[ADORA1, CALCA, CAV1, CHRNA3, CNN1, DAPK3, DOCK4, GHRL, KIT, NMU, OXTR, PROK2, PTGS2, RHOA, TBXA2R]
GO:0007009	plasma membrane organization	0,05	0,00	17,69	26,00	[ABCA7, AKR1B1, AREG, ARL8B, ASAP1, CAV1, CAV2, CAV3, CR1, CRB1, DEGS1, DNM2, EMP2, EPB41L3, FASLG, FER1L6, MTSS1, NDRG1, PRDX6, PRKCD, PTPRC, RAB3A, S100A9, SPAM1, SYT11, WASL]
GO:0071257	cellular response to electrical stimulus	0,03	0,00	42,86	6,00	[ADSS2, CACNA1A, CIITA, GNAT1, PALM, REST]
GO:0009887	animal organ morphogenesis	0,04	0,00	12,72	144,00	[ACP5, ADAM15, AKR1B1, AKT3, AMBN, AMTN, AQP1, AREG, ASH1L, ASXL3, BSG, CAV1, CAV3, CD34, CDH2, CELSR3, COL1A2, COMP, CRB1, CTHRC1, DAG1, DLX5, DLX6, DMTF1, DNAH11, E2F4, EFNA1, ELF3, ENAM, EREG, EXOC4, EXT1, FASLG, FGF22, FLVCR1, FOXH1, FZD1, FZD6, GATA2, GBA, GNAT1, GNGT1, GREB1L, GREM2, GRHL2, GSX2, HAS2, HESX1, HOXA1, HOXA11, HOXA13, HOXA2, HOXA3, HOXA4, HOXA5, HOXA6, HOXA7, HYAL1, HYAL2, IFT122, IGFN1, IL6, INSR, KDM5B, KIF26B, LAMA1, LAMA3, LAMB2, LAMB3, LAMC1, LAMC2, LEFTY1, LHX4, LHX9, LMNB2, LONP1, LRIG1, LTF, LY6E, LY6H, MAPRE2, MBD4, MEF2D, MIB1, MINDY4, MST1, MYC, MYL3, NANOS3, NR5A2, ODAM, OSR2, PAPPA2, PAX4, PBX4, PDGFRA, PLXNA1, PLXND1, PRICKLE2, PROX1, PRRX1, PSMA8, PSMD4, PTK2, PTN, PTPRM, RHOA, RNU6-664P, RSPO2, SCRIB, SCX, SEM1, SETD2, SIRT6, SLC39A1, SLC39A3, SMAD2, SMAD7, SMARCC1, SMO, SNX10, SOSTDC1, SPAM1, SSUH2, TBX20, THBS3, TLE2, TMIE, TNFRSF11B, TNNC1, TNNI1, TNNT2, TREX1, TSPAN12, TTC39C, TWSG1, WNT16, WNT2, WNT3A, WNT5A, WNT7A, WNT9A, ZFPM2, ZHX2]

						[AASS, ABCA7, ABCB1, ABCB4, ABHD17A, ABL2, ACAD9, ACTR8, ADAM15, ADAMTS10, ADAMTS3, ADAMTS9, ADAMTSL5, ADCY8, ADCYAP1, ADGRB1, ADGRL1, ADGRL3, ADIPOR1, AFG3L2, AGO2, AHCTF1, AKAP8, AKAP9, AKR1B1, AKT3, ALAS1, ALDOA, ALKBH7, AMIGO3, ANGPT1, ANLN, AP1M1, AP3D1, APC2, APEH, APOO, APPL1, AQP1, AQP4, AREG, ARF4, ARHGAP28, ARHGAP39, ARHGEF11, ARHGEF18, ARHGEF2, ARIH2, ARL8B, ARPC4, ARPC4-TTL3, ARPC5, ASAP1, ASF1B, ASH1L, ASPM, ASZ1, ATAD2, ATCAY, ATG7, ATP10D, ATP1B1, ATP5F1A, ATP5F1D, ATP5MC3, ATP5PD, ATP6V1C1, ATP6V1F, ATP6V1G3, ATP8A1, ATP8B2, ATXN7, BABAM1, BAP1, BBS9, BCAN, BECN2, BET1, BLZF1, BRD4, BRK1, BRPF1, BSG, BSN, BST2, C3, CACNA1A, CALCA, CALR, CAMK1, CAMKV, CAMSAP2, CAND2, CAPN2, CAPZA2, CARM1, CAV1, CAV2, CAV3, CCDC136, CCDC66, CCN3, CCR5, CCT3, CD34, CDC34, CDC37, CDC42BPA, CDH2, CDKN2D, CELF4, CELF5, CENPF, CENPL, CEP135, CEP192, CEP350, CEP41, CEP76, CETN1, CETN2, CFAP100, CFAP69, CFTR, CHAF1A, CHCHD3, CHCHD4, CHL1, CHRAC1, CHRNA3, CHRNB2, CHTOP, CIDEA, CIDEC, CIRBP, CISH, CLDN12, CLEC16A, CLOCK, CNIH3, CNIH4, CNN1, CNN2, CNTN4, CNTN6, COA3, COL14A1, COL1A2, COL28A1, COL5A3, COL7A1, COLEC12, COLGALT1, COLGALT2, COMP, COX18, COX20, CPA4, CPNE9, CR1, CRABP2, CRACD, CRB1, CRB3, CRBN, CRPPA, CRTC1, CRTC2, CSMD3, CSPG5, CSRP1, CTHRC1, CTTNBP2, CXXC1, CYRIB, DAG1, DAP3, DAPK3, DCAF1, DCSTAMP, DDX49, DEGS1, DEPTOR, DGAT1, DGKB, DHX30, DHX9, DLX5, DMTF1, DNAH1, DNAJB1, DNASE1L3, DNASE2, DNM2, DNM3, DNMT1, DOT1L, DPT, DSCC1, DYM, DYNC1I1, DYRK3, E2F4, EBAG9, ECSIT, EFNA1, EFNA3, EIF3E, EIF3G, EIF3H, EIF3L, ELANE, ELAVL1, ELF3, ELMO1, ELOF1, EMC2, EMC3, EMP2, ENAH, ENPP2, ENY2, EPB41L3, EPG5, EPGN, EPHA5, EPPK1, EPS15L1, ERC2, EREG, ESCO1, ETV1, EVI5L, EVX1, EXO1, EXOC1, EXOC4, EXOSC4, EXT1, F2RL3, F5, FAM107A, FAM83H, FAM91A1, FANCD2, FARSA, FASLG, FBLN2, FBXO43, FCHO1, FER1L6, FEZF2, FGD5, FHOD3, FLNB, FLNC, FRYL, FSCN3, FSD1, FYCO1, FZD1, FZR1, GABRA2, GADD45GIP1, GARS1, GATA2, GATAD1, GATAD2B, GBA, GDF15, GET3, GGCT, GHRL, GNL3, GORAB, GPAA1, GPIHBP1, GPX1, GRHL2, GRM7, GRXCR1, GSDMD, GSPT1, H1-8, H2AW, H2BU1, H3-3B, HAPLN2, HAS2, HAUS1, HAUS8, HAX1, HDAC11, HDAC9, HDGFL2, HEPACAM2, HNRNPA2B1, HNRNPU, HOOK2, HOPX, HOXA13, HOXA2, HSF1, HYAL1, HYAL2, IBA57, ICAM1, ICAM3, ICAM4, ICAM5, IER3IP1, IFT122, IGFBP7, IGFN1, IL10, IL17RB, IL6, IMPACT, INAVA, ING3, INO80C, INSR, INSRR, IP6K2, IQGAP3, IQSEC1, IQUB, ISY1, ISY1-RAB43, ITGB8, JAGN1, JCHAIN, JMJD4, KANK3, KATNAL2, KCND2, KCNS2, KCNV1, KCTD1, KCTD6, KCTD8, KDM4B, KDM5B, KDR, KHDC4, KIAA1614, KIF14, KIF9, KIFAP3, KIFC2, KIT, KLHDC8B, KLHL20, L3MBTL4, LAMA1, LAMA3, LAMB2, LAMB3, LAMC1, LAMC2, LAMTOR2, LAPTM4B, LBR, LDLR, LGR6, LHFPL4, LHX4, LHX9, LIMCH1, LIMD1, LIN9, LIPG, LMNA, LMNB2, LMOD2, LMOD3, LONP1, LRGUK, LRP12, LRRC24, LRRC4, LRRC6, LRRC8E, LRRN1, LRRN3, LRTM1, LSM3, LSM4, LTF, LZTFL1, MADCAM1, MAEL, MAGI1, MANF, MAP1LC3C, MAP1S, MAP2K2, MAP2K7, MAP4, MAPK15, MAPRE2, MAST1, MAST3, MAU2, MBD1, MBD3, MCM2, MCMBP, MET, METTL4, MIB1, MICOS13, MIER2, MINDY4, MISP, MITF, MKLN1, MOCOS, MPND, MPP6, MPV17L2, MRPL13, MRPL22, MRPL24, MRPL34, MRPL4, MRPL42, MRPL45, MRPL54, MRPL55, MRPS10, MRPS14, MRPS25, MRPS36, MST1, MSTO1, MTBP, MTCL1, MTERF1, MTSS1, MTX1, MUC1, MVB12A, MYC, MYO1F, MYO5B, MYOC, MYOG, NANOS3, NAPG, NAV1, NAXE, NCAN, NCKIPSD, NCLN, NDC80, NDRG1, NDUFA11, NDUFA13, NDUFA7, NDUFAF3, NDUFB1, NDUFB7, NDUFB9, NDUFS7, NDUFV2, NEK2, NEK7, NES, NISCH, NME6, NOTCH3, NPC1, NPHS2, NPR1, NPRL2, NPY, NRF1, NRTN, NSL1, NSMCE2, NT5C3A, NTRK1, NUBP1, NUP210, NUSAP1, OBSCN, ODAM, ODF1, OXTR, PALM, PAPPA2, PARP1, PBRM1, PDGFRA, PDZRN3, PEAK3, PET100, PEX1, PEX11G, PHF14, PHF20L1, PHOX2B, PIK3C3, PIN1, PIP5K1C, PKN1, PKP1, PLEC, PLEKHA8, PLIN5, PLK5, PLXNA1, PLXNA2, PLXNA4, PLXNB1, PLXND1, POC1A, PODXL, POLRMT, POT1, PPAN, PPAN-P2RY11, PPARG, PPFIA4, PPP1R9A, PRDX6, PRELID3A, PRKACA, PRKCD, PRKCSH, PROX1, PRRC2C, PRRX1, PSEN2, PSMA8, PSMD4, PSMG2, PSPN, PSTPIP2, PTK2, PTN, PTPN23, PTPRC, PTPRG, PTPRM, PTPRS, PTPRZ1, PUF60, PWWP3A, PYGO2, QSOX1, RAB13, RAB25, RAB31, RAB3A, RAB43, RAB7A, RAB8A, RABIF, RAD21, RAD54L2, RAF1, RALBP1, RASSF1, RBM5, RBSN, RC3H1, RCOR3, REEP6, REST, RFT1, RFX2, RHOA, RIMS2, RIOK3, RIT2, RMI2, RNF165, RNF19A, RNF2, RNU6-664P, ROCK1, RPA3, RPL11, RPL17, RPL23, RPS28, RTP3, RUFY3, RUVBL1, RYBP, S100A6, S100A9, S1PR2, SAFB, SCAP, SCIN, SCRIB, SCX, SDCCAG8, SEC13, SEC16B, SELE, SELP, SEM1, SEMA3B, SEMA3F, SEMA3G, SEMA4A, SEMA6B, SEPTIN7, SET, SETD2, SETD5, SF3A2, SF3A3, SFMBT1, SGTA, SH2D2A, SH3GL1, SHARPIN, SHC1, SHCBP1L, SHFL, SHQ1, SIGLEC15, SIN3B, SIRT6, SKA1, SKAP2, SKOR2, SLAIN2, SLC25A23, SLC4A4, SLC52A1, SLC6A1, SMAD2, SMAD7, SMARCA4, SMARCC1, SMCHD1, SMG5, SMO, SMYD2, SMYD3, SNAP47, SNAPIN, SNRPD1, SNX10, SOAT1, SPAG1, SPAM1, SPATA18, SPC24, SPINK2, SQLE, SRGAP3, SS18, ST7, STAP1, STEAP4, STK11, STRIP2, STX10, STX6, SYBU, SYCE2, SYDE1, SYT11, SYT17, SYT2, SYT4, TAC1, TADA1, TADA3, TASOR, TBX20, TDRD5, TEKT5, TEX264, TF82M, THEG, THSD7A, TICAM1, TIMM17A, TIMM29, TIMM44, TJP3, TLE2, TLE6, TMCC1, TMED1, TMEM106B, TMEM165, TMEM33, TMEM38A, TMEM43, TMEM9, TMF1, TNFRSF11B, TNFSF18, TNN, TNNC1, TNNT2, TNP2, TNR, TOMM7, TOR1AIP1, TOR1AIP2, TP53BP2, TPGS1, TPM4, TPR, TRAPPC9, TREX1, TRIM46, TRIP10, TSNARE1, TSPAN33, TSSK6, TTC39C, TTLL3, TUBB, TUBB4A, TUBB6, TWF2, UBA52, UBA6, UBAP2L, UBL5, UBQLN4, UBR5, UHRF1, UNC13A, UPF1, USE1, USP4, USP46, UTP3, VAMP4, VAPA, VASH2, VAV1, VGLL4, VPS28, WASHC3, WASHC5, WASL, WNT3A, WNT5A, WNT7A, XAB2, XPC, YJU2, YTHDC1, ZBTB7A, ZBTB7B, ZMYND10, ZSWIM4]
GO:0016043	cellular component organization	0,02	0,00	11,05	760,00	
GO:0017156	calcium-ion regulated exocytosis	0,05	0,00	22,06	15,00	[ARL8B, CADPS2, GNAI2, HYAL3, RAB3A, REST, RIMS2, SCIN, SPAM1, SYN2, SYT11, SYT17, SYT2, SYT4, UNC13A]
GO:0019087	transformation of host cell by virus	0,03	0,00	100,00	3,00	[HYAL2, INSR, MYC]
GO:0001618	virus receptor activity	0,03	0,00	21,95	18,00	[BSG, CCR5, CD46, CD55, CLEC4G, CLEC4M, CR1, DAG1, HYAL1, HYAL2, HYAL3, ICAM1, LDLR, NPC1, SLC52A1, SLC52A2, SPAM1, XPR1]
GO:0030368	interleukin-17 receptor activity	0,02	0,00	62,50	5,00	[IL17RB, IL17RC, IL17RD, IL17RE, IL27RA]
GO:0030879	mammary gland development	0,03	0,00	18,52	30,00	[AKR1B1, AREG, CAV1, CAV3, CSN2, CSN3, ELF3, GHRHR, GPX1, HOOK2, HOXA5, IQGAP3, IRF6, KDM5B, MBD4, MST1, MTX1, OXTR, PPAT, PYGO2, SCRIB, SERPINC1, SMO, SOSTDC1, TDGF1, TDGF1P3, WNT2, WNT3A, WNT5A, ZBTB7B]
GO:0071300	cellular response to retinoic acid	0,02	0,00	23,61	17,00	[ABL2, AQP1, BRINP2, HOXA2, LEP, MINDY4, MYC, MYOG, NDUFA13, PPARG, TNNC1, TWF2, WNT2, WNT3A, WNT5A, WNT9A, YES1]
GO:0032984	protein-containing complex disassembly	0,03	0,00	15,45	55,00	[APC2, APEH, ARHGEF2, ATXN7, CAMSAP2, CAPZA2, CAV1, CLEC16A, CRACD, DAP3, DYRK3, EPG5, FYCO1, FZD1, GADD45GIP1, GBA, GSPT1, H2AW, INSR, JMJD4, KIF14, LMOD2, LMOD3, MAP1LC3C, MAP1S, MRPL13, MRPL22, MRPL24, MRPL34, MRPL4, MRPL42, MRPL45, MRPL54, MRPL55, MRPS10, MRPS14, MRPS25, MRPS36, MYC, NES, RNU6-664P, RPL17, RPL23, SCIN, SET, SH3GL1, SHFL, SLC25A23, SMARCA4, SMARCC1, SNAPIN, TWF2, UBQLN4, UPF1, WNT3A]
GO:0033598	mammary gland epithelial cell proliferation	0,04	0,00	29,03	9,00	[AREG, GPX1, HOXA5, IQGAP3, KDM5B, MBD4, MST1, PYGO2, WNT5A]
GO:0001649	osteoblast differentiation	0,04	0,00	16,31	38,00	[ADAR, AREG, CCN4, CDK6, CTHRC1, CXXC1, DHX9, DLX5, FZD1, GARS1, GPNMB, HDAC9, HNRNPU, HOXA2, IL6, IL6R, JUNB, JUND, LIMD1, LTF, MEF2D, MYOC, PPARG, PRKACA, PTH1R, PTK2, REST, RNASEH2A, RSL1D1, RSPO2, SMO, SND1, SUCO, TNN, TNNC1, TPM4, TWSG1, WNT3A]
GO:0040008	regulation of growth	0,03	0,00	13,75	96,00	[ADAM15, ADIPOR1, AFG3L2, AGR2, AKR1B1, AREG, ARHGEF11, BAP1, BST2, CAV3, CCN3, CDKN2D, CISH, CPNE9, CRABP2, CREG1, CSPG5, CXXC1, DCAF1, DCSTAMP, DDX49, DNM2, EBAG9, EPB41L3, EPPK1, EXOSC4, FAM107A, FLVCR1, FYCO1, GDF15, GHRHR, GHRL, H3-3B, HDGFL2, HOPX, HYAL1, HYAL2, IGFBP7, IL17RB, ING3, INSR, IP6K2, KCNK2, KCTD6, KIF14, LAMTOR2, LEP, LONP1, LRP12, MAEL, MAGI1, NDUFA13, NME6, NPR1, NUBP1, PAPPA2, PIN1, PKN1, PLXNA4, PPARG, PROX1, PTPRS, RHOA, RIMS2, RNF2, RUFY3, RUVBL1, S100A9, SEMA3B, SEMA3F, SEMA3G, SEMA4A, SEMA6B, SHC1, SMAD7, SMARCA4, SMO, SOCS1, SPAM1, STK11, STK3, SYT17, SYT2, SYT4, TBX20, TKT, TNR, TRIM46, TWF2, UNC13A, VGLL4, WFS1, WNT2, WNT3A, WNT5A, ZFPM2]
GO:0042045	epithelial fluid transport	0,04	0,00	45,45	5,00	[AQP1, CFTR, ITPR1, MINDY4, SLC26A6]
GO:0044791	positive regulation by host of viral release from host cell	0,04	0,00	57,14	4,00	[CAV2, PODXL, VAPA, ZNF502]
GO:0046641	positive regulation of alpha-beta T cell proliferation	0,05	0,00	33,33	7,00	[CCR2, CD55, EBI3, PTPRC, RASAL3, TNFSF4, XCL1]
GO:0048018	receptor ligand activity	0,03	0,00	14,45	76,00	[ADCYAP1, AMBN, ANGPTL8, AREG, CALCA, CCL25, CCN3, CD320, CD70, COLEC10, CPAMD8, CRLF1, CSPG5, CXCL6, CXCL8, CXXC1, DAND5, EBI3, EPGN, EREG, FAM3C, FAM3D, FASLG, FGF22, FLNB, GDF15, GHRL, GNAI2, GPNMB, GREM2, HDGF, IL10, IL19, IL20, IL24, IL6, LEFTY1, LEFTY2, LEP, LSM4, MACC1, MANF, MYDGF, NPY, NRTN, PPBP, PSPN, PTN, RETN, RLN3, S100A9, SEMA3B, SEMA3F, SEMA3G, SEMA4A, SEMA6B, SLURP1, TAFA1, TAFA4, TDGF1, TDGF1P3, TG, TNFRSF11B, TNFSF14, TNFSF18, TNFSF4, TNFSF9, TRH, WNT16, WNT2, WNT3A, WNT5A, WNT7A, WNT9A, XCL1, XCL2]

GO:0001893	maternal placenta development	0,04	0,00	27,78	10,00	[ASH1L, BSG, CXXC1, DAZAP1, EPOR, GHRL, JUNB, PTGS2, PTN, RNASEH2A]
GO:0048677	axon extension involved in regeneration	0,04	0,00	57,14	4,00	[LAMB2, LAMC1, LMNB2, TNR]
GO:0050794	regulation of cellular process	0,00	0,00	10,89	1267,00	[AASS, ABCA7, ABCB1, ABCB4, ABHD14B, ABHD17A, ABHD6, ABL2, ABRA, ABTB1, ACOX2, ACP5, ACTR8, ADAM15, ADAM22, ADAMTS3, ADAMTS9, ADAR, ADCY10, ADCY8, ADCYAP1, ADCYAP1R1, ADGRB1, ADGRE1, ADGRE3, ADGRE5, ADGRL1, ADGRL3, ADIPOR1, ADORA1, AFP, AGO2, AGR2, AHCTF1, AHR, AKAP8, AKAP9, AKR1B1, AKT3, AMBN, AMIGO3, ANGEL2, ANGPT1, ANGPTL1, ANGPTL4, ANGPTL8, ANKIB1, ANKLE1, ANKRD17, ANLN, AP3D1, APC2, APCDD1, APPL1, AQP1, AREG, ARF4, ARHGAP28, ARHGAP39, ARHGAP45, ARHGEF11, ARHGEF18, ARHGEF2, ARHGEF3, ARID3A, ARIH2, ARL6IP5, ARPC4, ARPC4-TTLL3, ARPC5, ASAP1, ASB14, ASB15, ASB4, ASH1L, ASNS, ASPM, ASXL3, ATAD2, ATCAY, ATF3, ATG7, ATP1B1, ATP5F1A, ATP6V1C1, ATP6V1F, ATP6V1G3, ATP8A1, ATRIP, ATXN7, AZIN1, BABAM1, BAP1, BATF3, BECN2, BEX4, BHLHE40, BMPER, BMT2, BRD4, BRINP2, BRK1, BRPF1, BSG, BSN, BST2, BUD31, C18orf32, C3, C4BPB, CABLES1, CACNA1A, CACNA1D, CACNA1E, CACNA1S, CACNA2D2, CACNA2D3, CACTIN, CACYBP, CADPS2, CALCA, CALCR, CALR, CALR3, CAMK1, CAMKV, CAMP, CAMSAP2, CAND2, CAPN2, CAPS, CAPZA2, CARM1, CAV1, CAV2, CAV3, CC2D1A, CCDC66, CCL25, CCN3, CCN4, CCR1, CCR2, CCR3, CCR5, CCR9, CCRL2, CCT3, CD247, CD320, CD34, CD46, CD55, CD5L, CD70, CDC25A, CDC34, CDC37, CDC42BPA, CDCA7L, CDH2, CDK14, CDK6, CDKN2D, CELF4, CELF5, CELSR3, CENPF, CEP135, CEP192, CEP41, CEP76, CETN2, CFAP69, CFTR, CHERP, CHI3L1, CHL1, CHN2, CHRNA3, CHRNA5, CHRNB2, CHRNB4, CHTOP, CIDEA, CIDEC, CIITA, CIRBP, CISH, CKS1B, CLEC16A, CLEC3B, CLEC4G, CLEC4M, CLK2, CLOCK, CNBP, CNGA1, CNIH3, CNIH4, CNN1, CNN2, CNST, CNTN4, CNTN6, COA3, COL1A2, COL28A1, COL7A1, COLEC10, COLEC12, COLGALT1, COMP, COP1, COPS9, CPAMD8, CPNE9, CR1, CRABP2, CRACD, CRB3, CRBN, CREB3L3, CREB3L4, CREB5, CREG1, CRHR2, CRLF1, CRTC1, CRTC2, CSMD3, CSN2, CSNK1G2, CSPG5, CSRP1, CTHRC1, CTIF, CTTNBP2, CXCL6, CXCL8, CXCR6, CXXC1, CYP51A1, CYRIB, DAD1, DAG1, DAND5, DAP3, DAPK3, DAZAP1, DBF4, DBI, DCAF1, DCAF15, DCAF6, DCP1A, DCST1, DCSTAMP, DCUN1D4, DDA1, DDX49, DENND1B, DENND3, DENND4B, DENND6A, DEPTOR, DERL1, DESI2, DGKB, DHX9, DIRAS1, DLX5, DLX6, DMTF1, DNAH11, DNAJB1, DNAJB9, DNASE1L3, DNM2, DNM3, DNMT1, DOCK3, DOCK4, DOCK6, DOT1L, DPT, DSCC1, DTL, DTNA, DYRK3, E2F4, EBAG9, EBI3, EDEM1, EEF1A1, EEF1AKNMT, EEF1D, EEF2, EEFSEC, EEPD1, EFNA1, EFNA3, EIF3E, EIF3G, EIF3H, EIF3L, EIF4E3, ELANE, ELAVL1, ELF3, ELL, ELMO1, ELOF1, ELP2, ELP6, EMP2, ENPP2, ENY2, EPB41L3, EPG5, EPGN, EPHA5, EPOR, EPPK1, EPS15L1, ERC2, EREG, ESCO1, ETV1, ETV3, ETV3L, EVI5L, EVX1, EWSR1, EXO1, EXOC1, EXOC4, EXOSC4, EXOSC7, EXT1, F2RL3, FAM107A, FAM3C, FAM3D, FAM83A, FAM83H, FANCD2, FASLG, FBLN2, FBXL12, FBXL6, FBXO43, FCER2, FCMR, FCRL1, FCRL2, FCRL4, FCRL5, FERD3L, FEZF2, FGF22, FHIT, FHOD3, FLNB, FOXH1, FOXP1, FOXP2, FSD1, FSTL3, FYCO1, FZD1, FZD6, FZR1, G0S2, GABRA2, GABRA4, GABRG1, GADD45B, GADD45GIP1, GAREM1, GARS1, GATA2, GATAD1, GATAD2A, GATAD2B, GBA, GC, GDF15, GGCT, GHRHR, GHRL, GIPC1, GJC2, GLI4, GLMP, GLUL, GMIP, GNA15, GNAI2, GNAL, GNAT1, GNG11, GNGT1, GNL3, GNRHR, GON4L, GORAB, GPNMB, GPR108, GPR141, GPR161, GPR25, GPR37, GPR37L1, GPR52, GPR62, GPR85, GPT, GPX1, GREM2, GRHL2, GRIN2A, GRINA, GRIP2, GRM2, GRM3, GRM7, GRM8, GRSF1, GSDME, GSPT1, GSX2, GTF2F1, GUF1, H1-8, H2AW, H3-3B, HAS2, HAUS1, HAUS8, HAX1, HCN2, HCN3, HDAC9, HDGF, HDGFL2, HERPUD2, HESX1, HHAT, HMCES, HNRNPA2B1, HNRNPM, HNRNPU, HOMER3, HOOK2, HOPX, HOXA1, HOXA11, HOXA13, HOXA2, HOXA3, HOXA4, HOXA5, HOXA6, HOXA7, HRH1, HRH4, HSF1, HSH2D, HYAL1, HYAL2, HYAL3, ICA1, ICAM1, ICAM3, IER2, IER3IP1, IER5, IFI30, IFRD1, IFT122, IGF2BP3, IGFBP7, IL10, IL12RB1, IL17RB, IL17RC, IL17RD, IL17RE, IL19, IL20, IL24, IL27RA, IL5RA, IL6, IL6R, IL2, IL3, IMPA2, IMPACT, INAVA, ING3, INKA1, INSR, INSRR, INTS3, INTS7, IP6K2, IQCF1, IQGAP3, IQSEC1, IQUB, IRAK2, IREB2, IRF5, IRF6, ITGB8, ITIH1, ITPKB, ITPR1, IVNS1ABP, JAGN1, JAK3, JAZF1, JMJD4, JTB, JUNB, JUND, KANK2, KANK3, KBTBD2, KBTBD8, KCND2, KCNK2, KCNN1, KCNN3, KCNQ3, KCNS2, KCNV1, KCP, KCTD1, KCTD6, KCTD8, KDM4B, KDM5B, KDR, KEAP1, KHDRBS3, KHSRP, KIAA1614, KIF14, KIF26B, KIF9, KIFAP3, KIT, KLF1, KLF10, KLF14, KLF15, KLF16, KLHDC10, KLHL18, KLHL20, KLHL7, KMO, KRIT1, L3MBTL4, LAMA1, LAMA3, LAMC1, LAMC2, LAMTOR2, LAPTM4B, LDHA, LDLR, LEFTY1, LEFTY2, LEP, LGR6, LHFPL4, LHX4, LHX9, LIMCH1, LIMD1, LIN9, LIPG, LITAF, LMCD1, LMNA, LMOD2, LMOD3, LONP1, LPAR2, LPGAT1, LPIN2, LRG1, LRP12, LRRC14, LRRC2, LRRC24, LRRC30, LRRC4, LRRD1, LRRN1, LRRN3, LSM3, LSM4, LSM5, LSM7, LSM8, LTF, LY6E, LY6H, LYL1, LZTFL1, MACC1, MADCAM1, MAEL, MAF1, MAFA, MAGI1, MALSU1, MANF, MAP1S, MAP2K2, MAP2K7, MAP4, MAPK15, MAPK4, MAPKAPK3, MAPRE2, MAST1, MAST3, MATK, MBD1, MBD3, MBD4, MCM2, MDFIC, MED16, MED26, MED30, MEF2B, MEF2D, MET, METTL18, METTL4, MEX3D, MFSD12, MGLL, MIB1, MIDN, MIER2, MINDY4, MIOS, MISP, MITF, MKLN1, MLLT1, MOB1B, MOCOS, MPC2, MPND, MPV17L2, MPZL1, MRPL13, MST1, MST1R, MTBP, MTCL1, MTERF1, MTSS1, MTURN, MUC1, MUC16, MVB12A, MYC, MYDGF, MYO9B, MYOC, MYOG, MYOM1, NACC1, NANOS3, NCALD, NCF2, NCKIPSD, NCLN, NDC80, NDRG1, NDUFA13, NEK2, NEK4, NEK7, NES, NEUROD6, NFE2L3, NFIC, NFIX, NFXL1, NIBAN1, NISCH, NME6, NMU, NOA1, NOD1, NOTCH3, NPBWR2, NPC1, NPR1, NPRL2, NPSR1, NPVF, NPY, NR2C2, NR2F6, NR5A2, NRBP2, NRF1, NRTN, NSMCE2, NTRK1, NUBP1, NUP210, NVL, NWD1, OAZ1, OBSCN, OCIAD1, OCIAD2, ODAM, ODF1, OGG1, OLFM2, OPN1SW, OPN3, OR10H1, OR10H2, OR10H3, OR10H4, OR10H5, OR10X1, OR13G1, OR14I1, OR1I1, OR1M1, OR2AJ1, OR2AK2, OR2G6, OR2L13, OR2L2, OR2L3, OR2L5, OR2L8, OR2M2, OR2M3, OR2M5, OR2M7, OR2T1, OR2T11, OR2T12, OR2T2, OR2T27, OR2T29, OR2T33, OR2T35, OR2T4, OR2T5, OR2T6, OR2T8, OR6F1, OR7A10, OR7A17, OR7A5, OR7C1, OR7C2, OR7D2, OR7D4, OR7E24, OR7G1, OR7G2, OR7G3, OSR2, OXR1, OXTR, P2RY11, P4HTM, PABPC1, PALM, PALM3, PAPPA2, PARP1, PARP3, PAX4, PBRM1, PBX4, PBX1P1, PCBP4, PDC, PDE12, PDE1C, PDE4A, PDE4C, PDGFRA, PDK4, PEAK3, PEAR1, PEG10, PFKFB2, PFKFB4, PGLYRP2, PGPEP1, PHF14, PHF20L1, PHOX2B, PIAS2, PIAS4, PIGR, PIK3C3, PIK3R2, PIN1, PIP5K1C, PKN1, PKP1, PLA2G4A, PLIN5, PLK5, PLP2, PLPP2, PLPPR2, PLPPR3, PLVAP, PLXNA1, PLXNA2, PLXNA4, PLXNB1, PLXND1, PODXL, POGK, POLR2B, POLR2E, PON3, POT1, POU2F1, PPAN-P2RY11, PPARG, PPBP, PPP1R12B, PPP1R17, PPP1R3A, PPP1R9A, PPP2R5A, PPP4R1, PPP4R2, PRCC, PRDX1, PRDX2, PRDX6, PRICKLE2, PRKACA, PRKAR2A, PRKCD, PRKCSH, PROK2, PROX1, PRRX1, PSCA, PSEN2, PSMA8, PSMD4, PSMG2, PSPN, PTGER1, PTGS2, PTH1R, PTK2, PTN, PTP4A3, PTPN14, PTPN2, PTPN23, PTPN7, PTPRC, PTPRG, PTPRM, PTPRS, PTPRZ1, PUF60, PXK, PYGO2, QARS1, QRICH1, QSOX1, RAB11B, RAB12, RAB13, RAB25, RAB31, RAB3A, RAB3D, RAB43, RAB7A, RAB8A, RABIF, RAD18, RAD21, RAD23A, RAF1, RALBP1, RALGPS2, RAPGEF5, RASAL2, RASAL3, RASL11B, RASSF1, RASSF6, RAX2, RBBP8, RBM15B, RBM5, RBSN, RC3H1, RCOR3, REEP6, REST, RETN, RFX1, RFX2, RFXANK, RGL1, RGS16, RGS22, RGS7, RGS8, RHOA, RHPN1, RIDA, RIMS2, RIOK3, RIT1, RIT2, RLN3, RMC1, RMI2, RNASEH2A, RNASEL, RNF113A, RNF125, RNF126, RNF138, RNF139, RNF165, RNF19A, RNF2, RNU6-664P, ROCK1, RPA3, RPL11, RPL17, RPL23, RPL26, RPRD1A, RPS6KC1, RPUSD3, RRM2B, RSL1D1, RSPO2, RUFY3, RUVBL1, RYBP, S100A1, S100A12, S100A13, S100A14, S100A4, S100A6, S100A9, S1PR2, S1PR4, S1PR5, SAFB, SAFB2, SAP18, SBNO2, SCAP, SCIN, SCRIB, SCX, SDCCAG8, SDE2, SEC13, SEC16B, SELE, SELENOK, SELP, SEM1, SEMA3B, SEMA3F, SEMA3G, SEMA4A, SEMA6B, SEPTIN7, SERPINC1, SET, SETD2, SETD5, SF3A2, SFMBT1, SGTA, SH2D2A, SH2D3A, SH3GL1, SHARPIN, SHC1, SHCBP1L, SHFL, SHISA3, SHISA5, SIGLEC15, SIN3B, SIRT6, SKA1, SKAP2, SKOR2, SLA, SLAIN2, SLC25A23, SLC26A6, SLC27A1, SLC30A1, SLC30A8, SLC30A9, SLC35B4, SLC38A3, SLC44A2, SLC4A4, SLC6A1, SLC6A20, SLC6A6, SLMAP, SLURP1, SLURP2, SMAD2, SMAD7, SMARCA4, SMARCC1, SMCHD1, SMG5, SMG7, SMO, SMYD2, SMYD3, SNAP47, SNAPIN, SND1, SNX13, SOAT1, SOCS1, SOSTDC1, SP4, SP8, SPAM1, SPINK2, SPINK8, SPPL2B, SQLE, SRGAP3, SRI, SRP9, SS18, SSBP4, ST3GAL1, ST7, STAP1, STAP2, STIMATE, STK11, STK3, STK38, STX6, STXBP2, SUCO, SULT1E1, SYBU, SYDE1, SYT11, SYT17, SYT2, SYT4, TAC1, TADA1, TADA3, TAF1D, TAF2, TAF4B, TAFA1, TAFA4, TASOR, TATDN2, TAX1BP1, TBX20, TBXA2R, TCF3, TCTA, TDGF1, TDGF1P3, TES, TFB2M, TFEC, TFPI2, TG, TGIF1, THAP5, THOC1, TICAM1, TIMM17A, TIMP4, TIPRL, TLE2, TLE6, TLR9, TMED1, TMEM106B, TMEM115, TMEM161A, TMEM259, TMEM33, TMEM38A, TMEM9, TMF1, TNFAIP8L1, TNFRSF11B, TNFSF14, TNFSF18, TNFSF4, TNFSF9, TNN, TNNC1, TNNT2, TNP2, TNR, TOMM7, TP53BP2, TPR, TPRA1, TRA2A, TRAF5, TRAIP, TRAPPC9, TREX1, TRH, TRHR, TRIB1, TRIL, TRIM11, TRIM46, TRIP10, TRPS1, TSPAN12, TSPAN13, TSSK6, TUBB, TUBB4A, TWF2, TWSG1, TXK, TXNDC2, TXNRD3, TYK2, TYMS, UBA3, UBA52, UBL5, UBQLN4, UBR5, UHRF1, UNC13A, UPF1, USP14, USP19, USP4, USP46, VAMP4, VAPA, VAV1, VGLL4, VN1R5, VPS28, WASHC5, WASL, WDR18, WDR6, WFS1, WIPF3, WIZ, WNT16, WNT2, WNT3A, WNT5A, WNT7A, WNT9A, XCL1, XCL2, XCR1, XPC, XPR1, YES1, YJU2, YOD1, YTHDC1, YY1AP1, ZBTB14, ZBTB18, ZBTB37, ZBTB41, ZBTB7A, ZBTB7B, ZBTB7C, ZC3H3, ZC3HC1, ZCCHC17, ZDHHC3, ZFAT, ZFP41, ZFPM2, ZGLP1, ZHX2, ZMYND10, ZNF101, ZNF16, ZNF177, ZNF195, ZNF24, ZNF250, ZNF266, ZNF277, ZNF281, ZNF317, ZNF333, ZNF34, ZNF358, ZNF396, ZNF397, ZNF414, ZNF429, ZNF502, ZNF517, ZNF519, ZNF521, ZNF555, ZNF556, ZNF557, ZNF558, ZNF559, ZNF559-ZNF177, ZNF57, ZNF572, ZNF623, ZNF648, ZNF653, ZNF699, ZNF7, ZNF706, ZNF846, ZSCAN30, ZSWIM4, ZXDC]
GO:0050808	synapse organization	0,03	0,00	14,66	67,00	[ABHD17A, ADGRB1, ADGRL1, ADGRL3, AFG3L2, AMIGO3, ARF4, ARHGAP39, BCAN, BSG, BSN, C3, CAMK1, CAMKV, CDH2, CHRNB2, CTTNBP2, DAG1, DGKB, DNM3, EFNA1, ERC2, FZD1, FZR1, GABRA2, GHRL, IGFN1, IL10, INSR, LAMB2, LAMC1, LHFPL4, LMNB2, LRRC24, LRRC4, LRRN1, LRRN3, NDRG1, NTRK1, OXTR, PALM, PDZRN3, PIN1, PLXNB1, PLXND1, PPFIA4, PPP1R9A, PTN, PTPRS, RAB3A, REST, RHOA, RNU6-664P, SEMA3F, SEMA4A, SETD5, SLC6A1, SNAPIN, SYBU, TNNC1, TNR, TUBB, UNC13A, WASL, WNT3A, WNT5A, WNT7A]

GO:0051050	positive regulation of transport	0,04	0,00	12,91	129,00	[ABCA7, ABCB1, ABCB4, ADCY8, ADCYAP1, ADCYAP1R1, ADORA1, AKAP9, ANGPT1, APPL1, AQP1, ARIH2, ATP1B1, ATP8A1, AZIN1, BAP1, C3, CACNA1A, CACNA1D, CADPS2, CALCR, CALR, CAMK1, CAV1, CAV3, CCR1, CCR2, CDH2, CFTR, CHRNB2, CNST, CPAMD8, CXXC1, DBI, DHX9, DNM2, DNM3, EDEM1, EEPD1, EXOC1, F2RL3, FASLG, FLNB, FYCO1, FZR1, GATA2, GHRHR, GHRL, GJC2, GLUL, GNAI2, GPNMB, HYAL2, HYAL3, IER3IP1, INSR, KCNN1, KCNN3, KLF15, KMO, LEP, LIPG, LSM4, MAGI1, MBD1, MIB1, MINDY4, MPC2, MTCL1, MYOM1, NMU, NPR1, NPSR1, OAZ1, OPN3, OXTR, PFKFB2, PIK3R2, PIN1, PKN1, PLA2G4A, PPARG, PRKACA, PRKCD, PTGS2, PTPN23, PTPRC, RAB31, RAB3A, RAB3D, RAB7A, RETN, RNASEL, RNF2, RNU6-664P, RUFY3, S100A1, SCIN, SEC16B, SELE, SH3GL1, SLC26A6, SLC30A8, SLC38A3, SLC6A1, SMO, SNAPIN, SPAM1, SRI, STAP1, STIMATE, STK11, SYBU, SYT4, TAC1, TMF1, TOMM7, TP53BP2, TPR, TRH, TRIM46, UBL5, UBR5, VPS28, WASL, WFS1, WNT3A, WNT5A, XCL1]
GO:0072498	embryonic skeletal joint development	0,05	0,00	37,50	6,00	[EXT1, HOXA11, HYAL1, OSR2, SPAM1, WNT9A]
GO:0098926	postsynaptic signal transduction	0,04	0,00	26,83	11,00	[CHRNA3, CHRNB2, CRTC1, GNA15, GNAI2, HRH4, LY6E, LY6H, RGS8, SLURP2, WNT3A]
GO:0095500	acetylcholine receptor signaling pathway	0,05	0,00	28,13	9,00	[CHRNA3, CHRNB2, GNA15, GNAI2, HRH4, LY6E, LY6H, RGS8, SLURP2]
GO:1905153	regulation of membrane invagination	0,03	0,00	36,84	7,00	[ABCA7, C3, GATA2, PPARG, RAB31, STAP1, SYT11]
GO:0060100	positive regulation of phagocytosis, engulfment	0,04	0,00	40,00	6,00	[ABCA7, C3, GATA2, PPARG, RAB31, STAP1]
GO:0061091	regulation of phospholipid translocation	0,03	0,00	66,67	4,00	[ABCB4, ATP8A1, FASLG, PRKCD]
GO:2001138	regulation of phospholipid transport	0,05	0,00	37,50	6,00	[ABCA7, ABCB4, ATP8A1, DBI, FASLG, PRKCD]
GO:0061756	leukocyte adhesion to vascular endothelial cell	0,01	0,00	28,57	14,00	[CCL25, CCR2, ELANE, EXT1, ICAM1, IL6, LEP, MADCAM1, PODXL2, RHOA, ROCK1, SELE, SELL, SELP]
GO:0050901	leukocyte tethering or rolling	0,01	0,00	32,35	11,00	[CCL25, CCR2, ELANE, EXT1, LEP, MADCAM1, PODXL2, ROCK1, SELE, SELL, SELP]
R-HSA:196843	Vitamin B2 (riboflavin) metabolism	0,04	0,00	57,14	4,00	[ACP5, FLAD1, SLC52A1, SLC52A2]
GO:0006771	riboflavin metabolic process	0,04	0,00	57,14	4,00	[ACP5, FLAD1, SLC52A1, SLC52A2]
R-HSA:380108	Chemokine receptors bind chemokines	0,03	0,00	23,73	14,00	[CCL25, CCR1, CCR2, CCR3, CCR5, CCR9, CCRL2, CXCL6, CXCL8, CXCR6, PPBP, XCL1, XCL2, XCR1]
GO:0016493	C-C chemokine receptor activity	0,03	0,00	33,33	8,00	[CCR1, CCR2, CCR3, CCR5, CCR9, CCRL2, CXCR6, XCR1]
R-HSA:8874081	MET activates PTK2 signaling	0,02	0,00	33,33	10,00	[COL1A2, COL5A3, LAMA1, LAMA3, LAMB2, LAMB3, LAMC1, LAMC2, MET, PTK2]
WP:244	Alpha 6 Beta 4 signaling pathway	0,02	0,00	31,43	11,00	[LAMA1, LAMA3, LAMB2, LAMB3, LAMC1, LAMC2, PIK3R2, PRKCD, PTK2, RHOA, SHC1]
R-HSA:217271	FMO oxidises nucleophiles	0,03	0,00	100,00	3,00	[FMO1, FMO2, FMO3]
WP:688	Catalytic cycle of mammalian Flavin-containing MonoOxygenases (FMOs)	0,02	0,00	80,00	4,00	[FMO1, FMO2, FMO3, FMO4]
GO:0042127	regulation of cell population proliferation	0,00	0,00	13,49	235,00	[ADCYAP1, ADGRB1, ADORA1, AHR, AKR1B1, AKT3, AMBN, ANGPT1, AQP1, AREG, ARHGEF2, ASPM, ATF3, ATP5F1A, BAP1, BEX4, BRK1, BSG, BST2, CALR, CAMP, CARM1, CAV1, CAV2, CAV3, CCN3, CCN4, CCR2, CCR3, CD320, CD46, CD55, CD70, CDCA7L, CDH2, CDK6, CDKN2D, CHRNB2, CHTOP, CLEC4G, CNBP, CNN1, CNN2, COMP, COPS9, CPAMD8, CR1, CRLF1, CSRP1, CTHRC1, CXCL8, DAND5, DHX9, DLX5, DLX6, DNMT1, DPT, E2F4, EBI3, ELANE, EMP2, EPGN, EPPK1, EREG, ETV3, FASLG, FEZF2, FGF22, FOXP1, FZR1, GAREM1, GARS1, GATA2, GDF15, GHRHR, GHRL, GJC2, GLUL, GNAI2, GNL3, GPNMB, GPR37L1, GPX1, GSDME, HAS2, HNRNPU, HOXA3, HOXA5, HSF1, HYAL1, IER5, IFI30, IGFBP7, IL10, IL12RB1, IL24, IL27RA, IL5RA, IL6, IL6R, ING3, INSR, IQGAP3, IRF6, JAK3, JUNB, JUND, KANK2, KCNK2, KDM5B, KDR, KIF14, KIFAP3, KIT, KLF10, KRIT1, LAMC1, LAMC2, LEP, LMNA, LONP1, LRG1, LTF, MAGI1, MAPK15, MATK, MBD4, MEF2D, MINDY4, MITF, MST1, MST1R, MTBP, MTSS1, MUC1, MYC, MYDGF, MYOG, NACC1, NANOS3, NDRG1, NES, NPR1, NR5A2, NTRK1, ODAM, OSR2, PBRM1, PDGFRA, PHF14, PHOX2B, PKN1, PLA2G4A, PLXNB1, PPARG, PROK2, PROX1, PRRX1, PTGS2, PTH1R, PTK2, PTN, PTPN14, PTPN2, PTPRC, PTPRM, PTPRZ1, PYGO2, RAB25, RAF1, RASAL3, RBM5, RC3H1, REST, RHOA, RIDA, RNASEH2A, RNF126, RNF139, RNF2, RNU6-664P, RPA3, RPL17, RPL23, S100A13, S100A6, S100A9, S1PR2, SCIN, SCRIB, SCX, SELENOK, SHC1, SIRT6, SKAP2, SKOR2, SLURP1, SMAD2, SMAD7, SMO, SMYD2, SPAM1, SQLE, STK11, STK3, TAC1, TAFA1, TBX20, TDGF1, TDGF1P3, TES, TICAM1, TLR9, TMEM115, TNFSF18, TNFSF4, TNFSF9, TNN, TNNC1, TRAF5, TRIB1, TWSG1, UHRF1, VGLL4, WDR6, WNT2, WNT3A, WNT5A, WNT7A, WNT9A, XCL1, ZBTB7B, ZBTB7C, ZFPM2, ZNF16]
GO:0008284	positive regulation of cell population proliferation	0,01	0,00	13,78	135,00	[ADCYAP1, AKR1B1, AKT3, AQP1, AREG, ASPM, ATF3, BRK1, BST2, CALR, CAMP, CARM1, CAV2, CAV3, CCN4, CCR2, CCR3, CD320, CD46, CD55, CD70, CDCA7L, CDK6, CHRNB2, CHTOP, CNBP, COMP, COPS9, CPAMD8, CR1, CRLF1, CTHRC1, DAND5, DHX9, DLX5, DLX6, DNMT1, EBI3, ELANE, EMP2, EPGN, EREG, FASLG, FGF22, FOXP1, FZR1, GAREM1, GATA2, GDF15, GHRHR, GHRL, GJC2, GLUL, GNAI2, GPNMB, GPR37L1, HAS2, HNRNPU, HOXA3, HSF1, HYAL1, IL10, IL12RB1, IL24, IL27RA, IL5RA, IL6, IL6R, INSR, IQGAP3, JAK3, KDM5B, KDR, KIF14, KIT, LAMC1, LAMC2, LEP, LONP1, LRG1, LTF, MAPK15, MATK, MBD4, MEF2D, MINDY4, MST1, MST1R, MYC, MYDGF, NACC1, NES, ODAM, OSR2, PDGFRA, PKN1, PROK2, PROX1, PRRX1, PTGS2, PTH1R, PTK2, PTN, PTPRC, RAB25, RASAL3, RPL17, RPL23, S100A13, S100A6, S100A9, S1PR2, SCX, SELENOK, SHC1, SIRT6, SMO, SPAM1, TAC1, TBX20, TDGF1, TDGF1P3, TICAM1, TLR9, TNFSF4, TNFSF9, TNNC1, TRAF5, WNT2, WNT3A, WNT5A, WNT7A, XCL1, ZFPM2, ZNF16]
GO:0043043	peptide biosynthetic process	0,05	0,00	13,32	102,00	[AASDH, ABTB1, AGO2, APEH, ATF3, BSG, CALR, CELF4, CIRBP, CNBP, COA3, CTIF, DALRD3, DAP3, DAPK3, DARS2, DCP1A, DHX9, EEF1A1, EEF1D, EEF2, EEFSEC, EFNA1, EIF3E, EIF3G, EIF3H, EIF3L, EIF4E3, ELANE, ELAVL1, ELOF1, EXOSC4, EXOSC7, FARSA, GADD45GIP1, GARS1, GDF15, GGCT, GSPT1, GUF1, IGF2BP3, IL6, ILF3, IMPACT, IREB2, JMJD4, KBTBD8, KHSRP, LARS2, LSM3, LSM4, LSM5, LSM7, MALSU1, METTL18, MEX3D, MPV17L2, MRPL13, MRPL22, MRPL24, MRPL34, MRPL4, MRPL42, MRPL45, MRPL54, MRPL55, MRPS10, MRPS14, MRPS25, MRPS36, MYC, NANOS3, NDRG1, NDUFA7, NIBAN1, NOA1, PABPC1, PDE12, PRKCSH, QARS1, RC3H1, RHOA, RIDA, RNF139, ROCK1, RPL11, RPL17, RPL17-C18orf32, RPL23, RPL26, RPL32, RPL37A, RPL8, RPS28, RPUSD3, SHFL, SRP9, TPR, TYMS, UBA52, UPF1, ZNF706]
GO:0006412	translation	0,05	0,00	13,35	98,00	[ABTB1, AGO2, APEH, ATF3, CALR, CELF4, CIRBP, CNBP, COA3, CTIF, DALRD3, DAP3, DAPK3, DARS2, DCP1A, DHX9, EEF1A1, EEF1D, EEF2, EEFSEC, EFNA1, EIF3E, EIF3G, EIF3H, EIF3L, EIF4E3, ELAVL1, ELOF1, EXOSC4, EXOSC7, FARSA, GADD45GIP1, GARS1, GDF15, GSPT1, GUF1, IGF2BP3, IL6, ILF3, IMPACT, IREB2, JMJD4, KBTBD8, KHSRP, LARS2, LSM3, LSM4, LSM5, LSM7, MALSU1, METTL18, MEX3D, MPV17L2, MRPL13, MRPL22, MRPL24, MRPL34, MRPL4, MRPL42, MRPL45, MRPL54, MRPL55, MRPS10, MRPS14, MRPS25, MRPS36, MYC, NANOS3, NDRG1, NDUFA7, NIBAN1, NOA1, PABPC1, PDE12, PRKCSH, QARS1, RC3H1, RHOA, RIDA, RNF139, ROCK1, RPL11, RPL17, RPL17-C18orf32, RPL23, RPL26, RPL32, RPL37A, RPL8, RPS28, RPUSD3, SHFL, SRP9, TPR, TYMS, UBA52, UPF1, ZNF706]
GO:0043462	regulation of ATPase activity	0,04	0,00	21,25	17,00	[ATP1B1, CHTOP, DHX9, DNAJB1, DNM2, HNRNPU, LTF, MCM2, MYL3, POT1, PXK, TLR9, TNNC1, TNNT2, TOR1AIP1, TOR1AIP2, UHRF1]
GO:0032781	positive regulation of ATPase activity	0,04	0,00	24,49	12,00	[ATP1B1, CHTOP, DHX9, DNAJB1, DNM2, HNRNPU, MYL3, POT1, TNNT2, TOR1AIP1, TOR1AIP2, UHRF1]

							[ABCA7, ABCB1, ABCB4, ABHD14B, ABHD17A, ABHD6, ABL2, ABRA, ACOX2, ADAMTS3, ADAR, ADCY10, ADCY8, ADCYAP1, ADCYAP1R1, ADGRB1, ADGRL1, ADIPOR1, ADORA1, AGO2, AGR2, AHR, AKAP8, AKAP9, AKR1B1, AKT3, AMIGO3, AMTN, ANGEL2, ANGPT1, ANGPTL4, ANKIB1, ANKLE1, ANKRD17, ANLN, AP3D1, APC2, APPL1, AQP1, AREG, ARF4, ARHGEF11, ARHGEF18, ARHGEF2, ARHGEF3, ARID3A, ARIH2, ARL6IP5, ARPC4, ARPC4-TTLL3, ARPC5, ASAP1, ASB4, ASH1L, ASNS, ASPM, ASXL3, ATAD2, ATF3, ATG7, ATP1B1, ATP5F1A, ATP8A1, AZIN1, BABAM1, BAP1, BMPER, BRD4, BRINP2, BRK1, BRPF1, BST2, BUD31, C18orf32, C3, C4BPB, CACNA1A, CACNA1D, CACYBP, CADPS2, CALCA, CALCR, CALR, CAMK1, CAMP, CAND2, CAPN2, CARM1, CAV1, CAV2, CAV3, CC2D1A, CCL25, CCN3, CCN4, CCR1, CCR2, CCR3, CCT3, CD247, CD320, CD34, CD46, CD55, CD5L, CD70, CDC25A, CDC34, CDCA7L, CDH2, CDK6, CELF4, CEP135, CFAP69, CFHR1, CFHR2, CFHR4, CFHR5, CFTR, CHERP, CHI3L1, CHRNA3, CHRNB2, CHTOP, CIDEA, CIITA, CIRBP, CKS1B, CLEC16A, CLEC3B, CLEC4G, CLOCK, CNBP, CNN2, CNST, CNTN6, COA3, COLEC10, COLEC12, COLGALT1, COMP, COP1, COPS9, CPAMD8, CPNE9, CR1, CRABP2, CRACD, CRB3, CRBN, CREB3L3, CREB3L4, CREB5, CRHR2, CRLF1, CRTC1, CRTC2, CSNK1G2, CSPG5, CSRP1, CTHRC1, CTIF, CXCL8, CXXC1, CYRIB, DAG1, DAND5, DAPK3, DAZAP1, DBF4, DBI, DCAF6, DCP1A, DCSTAMP, DCUN1D4, DDA1, DDX49, DENND1B, DENND6A, DERL1, DHX9, DIRAS1, DLX5, DLX6, DMTF1, DNAJB9, DNM2, DNM3, DNMT1, DOCK3, DOCK4, DSCC1, DTL, DYRK3, E2F4, EBAG9, EBI3, EDEM1, EEF1D, EEF2, EEPD1, EFNA1, EFNA3, EIF3E, ELANE, ELAVL1, ELF3, ELL, ELMO1, ELOF1, ELP6, EMP2, ENAM, ENPP2, ENY2, EPGN, EPHA5, EPOR, EREG, ETV1, EVX1, EXOC1, EXOSC4, EXOSC7, F2RL3, FAM107A, FAM83H, FASLG, FBLN2, FCER2, FEM1A, FEZF2, FGF22, FH, FLNB, FOXH1, FOXP1, FSTL3, FYCO1, FZD1, FZR1, G0S2, GADD45B, GAREM1, GARS1, GATA2, GBA, GC, GDF15, GHRHR, GHRL, GIPC1, GJC2, GLMP, GLUL, GNAI2, GNL3, GORAB, GPIHBP1, GPNMB, GPR37, GPR37L1, GPR62, GPT, GPX1, GRHL2, GRIN2A, GRSF1, GSDMD, GSDME, GSX2, GTF2F1, GUF1, H1-8, H3-3B, HAS2, HAX1, HDAC9, HDGFL2, HMCES, HNRNPA2B1, HNRNPU, HOOK2, HOPX, HOXA1, HOXA11, HOXA13, HOXA2, HOXA3, HOXA5, HOXA7, HRH1, HSF1, HYAL1, HYAL2, HYAL3, ICAM1, ICAM3, IER2, IER3IP1, IER5, IL10, IL12RB1, IL19, IL20, IL24, IL27RA, IL5RA, IL6, IL6R, ILF2, ILF3, IMPACT, INAVA, ING3, INSR, INSRR, IP6K2, IQCF1, IQGAP3, IQSEC1, IRAK2, IRF5, IRF6, ITGB8, ITPKB, JAK3, JCHAIN, JMJD4, JTB, JUNB, JUND, KCNK2, KCNN1, KCNN3, KCP, KDM5B, KDR, KEAP1, KHSRP, KIF14, KIF26B, KIFAP3, KIT, KLF1, KLF10, KLF14, KLF15, KLHDC10, KLHL18, KLHL7, KMO, LAMC1, LAMC2, LAMTOR2, LDHA, LDLR, LEFTY1, LEFTY2, LEP, LGR6, LHX4, LIMCH1, LIMD1, LIPG, LITAF, LMCD1, LMNA, LMOD2, LMOD3, LONP1, LPGAT1, LPIN2, LRG1, LRRC24, LRRD1, LRRN1, LRRN3, LSM3, LSM4, LSM5, LSM7, LTF, LYL1, MACC1, MADCAM1, MAFA, MAGI1, MAP2K2, MAP2K7, MAPK15, MAPKAPK3, MAPRE2, MATK, MBD1, MBD4, MDFIC, MED16, MED26, MED30, MEF2B, MEF2D, MET, MEX3D, MIB1, MINDY4, MIOS, MITF, MOB1B, MOCOS, MPC2, MPND, MPV17L2, MST1, MST1R, MTBP, MTCL1, MTURN, MUC1, MUC16, MYC, MYDGF, MYOC, MYOG, MYOM1, NACC1, NANOS3, NCKIPSD, NDC80, NDRG1, NDUFA13, NEK2, NEK4, NEK7, NES, NEUROD6, NFIC, NFIX, NIBAN1, NMU, NOD1, NOTCH3, NPC1, NPR1, NPRL2, NPSR1, NPY, NR2C2, NR5A2, NRF1, NSMCE2, NTRK1, NVL, NWD1, OAZ1, OBSCN, OCIAD1, OCIAD2, ODAM, OLFM2, OPN3, OSR2, OXTR, PABPC1, PALM, PARP1, PARP3, PAX4, PBX4, PDE12, PDGFRA, PFKFB2, PFKFB4, PHOX2B, PIAS4, PIK3R2, PIN1, PKN1, PKP1, PLA2G4A, PLIN3, PLIN5, PLK5, PLVAP, PLXNA1, PLXNA2, PLXNA4, PLXNB1, PLXND1, PODXL, POLR2B, POLR2E, POT1, POU2F1, PPARG, PPBP, PPP1R9A, PPP2R5A, PRDX2, PRDX6, PRKACA, PRKAR2A, PRKCD, PRKCSH, PROK2, PROX1, PRRX1, PSEN2, PSMA8, PSMD4, PTGS2, PTH1R, PTK2, PTN, PTP4A3, PTPN2, PTPN23, PTPRC, PTPRZ1, QRICH1, RAB25, RAB31, RAB3A, RAB3D, RAB7A, RAD18, RAD21, RAD23A, RAF1, RALBP1, RASAL3, RAX2, RBM5, RC3H1, REST, RETN, RFXANK, RHOA, RIDA, RIMS2, RIOK3, RIT2, RNASEH2A, RNASEL, RNF139, RNF165, RNF19A, RNF2, RNU6-664P, ROCK1, RPA3, RPL11, RPL17, RPL23, RPL26, RPUSD3, RSPO2, RUFY3, RUVBL1, RYBP, S100A1, S100A12, S100A13, S100A14, S100A4, S100A6, S100A9, S1PR2, SAP18, SBNO2, SCAP, SCIN, SCRIB, SCX, SEC13, SEC16B, SELE, SELENOK, SELP, SEM1, SEMA3B, SEMA3F, SEMA3G, SEMA4A, SEMA6B, SEPTIN7, SETD2, SF3A2, SGTA, SH2D2A, SH2D3A, SH3GL1, SHARPIN, SHC1, SHCBP1L, SHISA5, SHQ1, SIRT6, SKOR2, SLAIN2, SLC25A23, SLC26A6, SLC27A1, SLC30A8, SLC30A9, SLC38A3, SLC44A2, SLC4A4, SLC6A1, SLC6A6, SMAD2, SMAD7, SMARCA4, SMARCC1, SMCHD1, SMO, SMYD3, SNAP47, SNAPIN, SOAT1, SOCS1, SPAM1, SRI, SS18, SSBP4, STAP1, STAP2, STIMATE, STK11, STK3, STXBP2, SUCO, SULT1E1, SYBU, SYDE1, SYT11, SYT17, SYT2, SYT4, TAC1, TADA1, TADA3, TAF1D, TASOR, TBX20, TBXA2R, TCF3, TDGF1, TDGF1P3, TFEC, THOC1, TICAM1, TIMM17A, TLE6, TLR9, TMEM106B, TMEM161A, TMEM259, TMEM33, TMEM79, TMEM9, TMF1, TNFSF14, TNFSF18, TNFSF4, TNFSF9, TNNC1, TNP2, TNR, TOMM7, TP53BP2, TPR, TRA2A, TRAF5, TREX1, TRH, TRIB1, TRIM11, TRIM46, TWF2, TWSG1, TXK, UBA52, UBL5, UBR5, UHRF1, UNC13A, UPF1, USP19, UTP25, VAPA, VASH2, VAV1, VGLL4, VPS28, WASHC5, WASL, WFS1, WIPF3, WIZ, WNT16, WNT2, WNT3A, WNT5A, WNT7A, XCL1, XCL2, XPC, YES1, ZBTB18, ZBTB7B, ZBTB7C, ZC3H3, ZDHHC3, ZFAT, ZFPM2, ZGLP1, ZMYND10, ZNF16, ZNF24, ZNF281, ZNF502, ZNF521, ZXDC]
	GO:0048518	positive regulation of biological process	0,02	0,00	11,05	724,00	[ABCA7, ABCB1, ABCB4, ABHD14B, ABHD17A, ABL2, ABRA, ACOX2, ADAMTS3, ADCY10, ADCY8, ADCYAP1, ADCYAP1R1, ADGRB1, ADGRL1, ADIPOR1, ADORA1, AGO2, AGR2, AHR, AKAP8, AKAP9, AKR1B1, AKT3, AMIGO3, ANGPT1, ANKIB1, ANKLE1, ANKRD17, ANLN, AP3D1, APPL1, AQP1, AREG, ARF4, ARHGEF11, ARHGEF18, ARHGEF2, ARHGEF3, ARID3A, ARIH2, ARL6IP5, ARPC4, ARPC4-TTLL3, ARPC5, ASAP1, ASB4, ASH1L, ASNS, ASPM, ASXL3, ATAD2, ATF3, ATG7, ATP1B1, ATP5F1A, ATP8A1, AZIN1, BABAM1, BAP1, BMPER, BRD4, BRINP2, BRK1, BRPF1, BST2, BUD31, C18orf32, C3, CACNA1A, CACYBP, CADPS2, CALCA, CALCR, CALR, CAMK1, CAMP, CAND2, CAPN2, CARM1, CAV1, CAV2, CAV3, CC2D1A, CCL25, CCN3, CCN4, CCR1, CCR2, CCR3, CCT3, CD247, CD320, CD34, CD46, CD55, CD5L, CD70, CDC25A, CDC34, CDCA7L, CDH2, CDK6, CELF4, CEP135, CFAP69, CFTR, CHERP, CHI3L1, CHRNA3, CHRNB2, CHTOP, CIITA, CIRBP, CKS1B, CLEC16A, CLEC3B, CLOCK, CNBP, CNST, CNTN6, COA3, COLEC12, COLGALT1, COMP, COP1, COPS9, CPAMD8, CPNE9, CR1, CRABP2, CRACD, CRB3, CRBN, CREB3L3, CREB3L4, CREB5, CRHR2, CRLF1, CRTC1, CRTC2, CSNK1G2, CSPG5, CSRP1, CTHRC1, CTIF, CXCL8, CXXC1, CYRIB, DAG1, DAND5, DAPK3, DAZAP1, DBF4, DCAF6, DCP1A, DCSTAMP, DCUN1D4, DDA1, DDX49, DENND6A, DERL1, DHX9, DIRAS1, DLX5, DLX6, DMTF1, DNM2, DNM3, DNMT1, DOCK3, DOCK4, DSCC1, DTL, DYRK3, E2F4, EBAG9, EBI3, EDEM1, EEF1D, EEF2, EFNA1, EFNA3, EIF3E, ELANE, ELAVL1, ELF3, ELL, ELOF1, ELP6, EMP2, ENPP2, ENY2, EPGN, EPHA5, EPOR, EREG, ETV1, EVX1, EXOC1, EXOSC4, EXOSC7, F2RL3, FAM107A, FAM83H, FASLG, FBLN2, FCER2, FEZF2, FGF22, FLNB, FOXH1, FOXP1, FSTL3, FYCO1, FZD1, FZR1, G0S2, GADD45B, GAREM1, GARS1, GATA2, GBA, GC, GDF15, GHRHR, GHRL, GIPC1, GJC2, GLMP, GLUL, GNAI2, GNL3, GORAB, GPNMB, GPR37, GPR37L1, GPR62, GPT, GPX1, GRHL2, GRIN2A, GRSF1, GSDME, GSX2, GTF2F1, GUF1, H1-8, H3-3B, HAS2, HAX1, HDAC9, HDGFL2, HMCES, HNRNPA2B1, HNRNPU, HOPX, HOXA1, HOXA11, HOXA13, HOXA2, HOXA3, HOXA5, HOXA7, HRH1, HSF1, HYAL1, HYAL2, HYAL3, ICAM1, IER2, IER3IP1, IER5, IL10, IL12RB1, IL19, IL20, IL24, IL27RA, IL5RA, IL6, IL6R, ILF2, ILF3, IMPACT, INAVA, ING3, INSR, INSRR, IP6K2, IQCF1, IQGAP3, IQSEC1, IRAK2, IRF5, IRF6, ITPKB, JAK3, JMJD4, JTB, JUNB, JUND, KCNK2, KCNN1, KCNN3, KCP, KDM5B, KDR, KEAP1, KHSRP, KIF14, KIF26B, KIFAP3, KIT, KLF1, KLF10, KLF14, KLF15, KLHDC10, KLHL18, KMO, LAMC1, LAMC2, LAMTOR2, LDHA, LDLR, LEFTY1, LEFTY2, LEP, LGR6, LHX4, LIMCH1, LIMD1, LITAF, LMCD1, LMNA, LMOD2, LMOD3, LONP1, LPGAT1, LPIN2, LRG1, LRRC24, LRRD1, LRRN1, LRRN3, LSM3, LSM4, LSM5, LSM7, LTF, LYL1, MACC1, MADCAM1, MAFA, MAGI1, MAP2K2, MAP2K7, MAPK15, MAPKAPK3, MAPRE2, MATK, MBD1, MBD4, MDFIC, MED16, MED26, MED30, MEF2B, MEF2D, MET, MEX3D, MIB1, MINDY4, MIOS, MITF, MOB1B, MOCOS, MPC2, MPND, MPV17L2, MST1, MST1R, MTBP, MTCL1, MTURN, MUC1, MYC, MYDGF, MYOC, MYOG, MYOM1, NACC1, NANOS3, NCKIPSD, NDC80, NDRG1, NDUFA13, NEK2, NEK4, NEK7, NES, NEUROD6, NFIC, NFIX, NIBAN1, NMU, NOD1, NOTCH3, NPC1, NPR1, NPRL2, NPSR1, NR2C2, NR5A2, NRF1, NSMCE2, NTRK1, NVL, OAZ1, OBSCN, OCIAD1, OCIAD2, ODAM, OLFM2, OPN3, OSR2, OXTR, PABPC1, PALM, PARP1, PARP3, PAX4, PBX4, PDE12, PDGFRA, PFKFB2, PFKFB4, PHOX2B, PIAS4, PIK3R2, PIN1, PKN1, PLA2G4A, PLIN5, PLK5, PLVAP, PLXNA1, PLXNA2, PLXNA4, PLXNB1, PLXND1, PODXL, POT1, POU2F1, PPARG, PPBP, PPP1R9A, PPP2R5A, PRDX2, PRDX6, PRKACA, PRKAR2A, PRKCD, PRKCSH, PROK2, PROX1, PRRX1, PSEN2, PSMA8, PSMD4, PTGS2, PTH1R, PTK2, PTN, PTP4A3, PTPN2, PTPN23, PTPRC, PTPRZ1, QRICH1, RAB25, RAB31, RAB3A, RAB3D, RAB7A, RAD18, RAD21, RAD23A, RAF1, RALBP1, RASAL3, RAX2, RBM5, RC3H1, REST, RETN, RFXANK, RHOA, RIDA, RIMS2, RIT2, RNASEH2A, RNASEL, RNF139, RNF165, RNF19A, RNF2, RNU6-664P, ROCK1, RPA3, RPL11, RPL17, RPL23, RPL26, RPUSD3, RSPO2, RUFY3, RUVBL1, RYBP, S100A1, S100A12, S100A13, S100A14, S100A4, S100A6, S100A9, S1PR2, SAP18, SBNO2, SCIN, SCRIB, SCX, SEC13, SEC16B, SELE, SELENOK, SELP, SEM1, SEMA3B, SEMA3F, SEMA3G, SEMA4A, SEMA6B, SEPTIN7, SF3A2, SGTA, SH2D3A, SH3GL1, SHARPIN, SHC1, SHCBP1L, SHISA5, SIRT6, SKOR2, SLAIN2, SLC26A6, SLC27A1, SLC30A8, SLC30A9, SLC38A3, SLC44A2, SLC4A4, SLC6A6, SMAD2, SMAD7, SMARCA4, SMARCC1, SMCHD1, SMO, SMYD3, SNAP47, SNAPIN, SOAT1, SOCS1, SPAM1, SRI, SS18, SSBP4, STAP1, STAP2, STIMATE, STK11, STK3, STXBP2, SUCO, SULT1E1, SYBU, SYDE1, SYT11, SYT17, SYT2, SYT4, TAC1, TADA1, TADA3, TASOR, TBX20, TCF3, TDGF1, TDGF1P3, TFEC, THOC1, TICAM1, TIMM17A, TLR9, TMEM106B, TMEM161A, TMEM259, TMEM33, TMEM9, TMF1, TNFSF14, TNFSF18, TNFSF4, TNFSF9, TNNC1, TNP2, TNR, TOMM7, TP53BP2, TPR, TRA2A, TRAF5, TRH, TRIB1, TRIM46, TWF2, TWSG1, TXK, UBA52, UBL5, UBR5, UHRF1, UNC13A, UPF1, USP19, VAPA, VAV1, VGLL4, VPS28, WASHC5, WASL, WFS1, WIZ, WNT16, WNT2, WNT3A, WNT5A, WNT7A, XCL1, XCL2, XPC, YES1, ZBTB18, ZBTB7B, ZBTB7C, ZC3H3, ZDHHC3, ZFAT, ZFPM2, ZGLP1, ZMYND10, ZNF16, ZNF24, ZNF281, ZNF521, ZXDC]
	GO:0048522	positive regulation of cellular process	0,01	0,00	11,28	668,00	

GO:0048519	negative regulation of biological process	0,01	0,00	11,32	656,00	[AASS, ABCA7, ABHD17A, ABHD6, ABL2, ACP5, ADAM15, ADAM22, ADAMTS9, ADAR, ADCY8, ADCYAP1, ADCYAP1R1, ADGRB1, ADIPOR1, ADORA1, AGO2, AGR2, AHR, AKAP8, AKR1B1, AKT3, ANGEL2, ANGPT1, ANGPTL4, ANKLE1, ANKRD17, AOAH, APC2, APCDD1, APPL1, AQP1, AREG, ARF4, ARHGAP28, ARHGEF18, ARHGEF2, ARID3A, ARL6IP5, ASAP1, ASH1L, ASNS, ASPM, ASXL3, ASZ1, ATAD2, ATCAY, ATF3, ATG7, ATP5F1A, ATRIP, ATXN7, AZIN1, BABAM1, BAP1, BATF3, BECN2, BEX4, BHLHE40, BMPER, BMT2, BRINP2, BSG, BST2, C3, C4BPB, CACNA1A, CACTIN, CACYBP, CALCA, CALCR, CALR, CAMSAP2, CAPZA2, CARM1, CAV1, CAV2, CAV3, CC2D1A, CCL25, CCN3, CCN4, CCR1, CCR2, CCR5, CD247, CD34, CD46, CD55, CDC34, CDH2, CDK6, CDKN2D, CELF4, CENPF, CHERP, CHRNB2, CIDEA, CIITA, CIRBP, CISH, CLEC16A, CLEC4G, CLK2, CLOCK, CNBP, CNIH4, CNN1, CNN2, CNTN4, COL28A1, COL7A1, COLEC12, COMP, COPS9, CPAMD8, CR1, CRACD, CRBN, CREB3L4, CREG1, CRHR2, CRLF1, CRTC1, CSN2, CSRP1, CTHRC1, CTIF, CXCL8, CXXC1, CYP51A1, CYRIB, DAD1, DAG1, DAND5, DAPK3, DBI, DCAF1, DCP1A, DCST1, DCSTAMP, DEPTOR, DHX9, DNAJB1, DNAJB9, DNM2, DNM3, DNMT1, DOCK4, DOT1L, DPT, DTL, DYRK3, E2F4, EEF1AKNMT, EFNA1, EFNA3, EIF3E, EIF3H, ELANE, ELAVL1, ELF3, ENY2, EPGN, EPPK1, EPS15L1, ERC2, EREG, ETV3, EVI5L, EXOSC4, EXOSC7, F2RL3, FAM107A, FAM3C, FAM3D, FANCD2, FASLG, FBXO43, FCMR, FEM1A, FERD3L, FEZF2, FHIT, FHOD3, FLNB, FOXH1, FOXP1, FOXP2, FSTL3, FYCO1, FZD6, FZR1, GADD45B, GARS1, GATA2, GATAD2A, GATAD2B, GBA, GDF15, GHRHR, GHRL, GIPC1, GJC2, GMIP, GNAI2, GON4L, GPNMB, GPR108, GPR161, GPR25, GPR37, GPR37L1, GPX1, GREM2, GRHL2, GRIN2A, GRINA, GRM7, GSDME, GSPT1, H1-8, H2AW, H3-3B, HAX1, HDAC9, HDGF, HESX1, HNRNPA2B1, HNRNPM, HNRNPU, HOMER3, HOOK2, HOPX, HOXA2, HOXA5, HOXA7, HSF1, HYAL1, HYAL2, HYAL3, ICAM1, IFI30, IFT122, IGF2BP3, IGFBP7, IL10, IL17RD, IL19, IL24, IL27RA, IL6, ILF3, IMPACT, ING3, INKA1, INTS3, INTS7, IP6K1, IP6K2, IQGAP3, IREB2, IRF6, ITGB8, ITIH1, ITPKB, ITPR1, IVNS1ABP, JAGN1, JAK3, JAZF1, KANK2, KANK3, KCNK2, KCTD1, KCTD6, KDM4B, KDM5B, KDR, KHSRP, KIF14, KIFAP3, KIT, KLF10, KLF15, KLF16, KLHL20, KRIT1, L3MBTL4, LAPTM4B, LDLR, LEFTY1, LEP, LHX4, LHX9, LIMCH1, LIMD1, LITAF, LMCD1, LMNA, LMOD2, LMOD3, LONP1, LRRC14, LSM3, LSM4, LSM5, LSM7, LSM8, LTF, LY6E, LZTFL1, MAEL, MAF1, MAGI1, MALSU1, MAP2K2, MAP4, MAPK15, MBD1, MBD3, MBD4, MCM2, MDFIC, MET, MEX3D, MFSD12, MIB1, MIDN, MIER2, MINDY4, MITF, MLLT1, MOCOS, MRPL13, MST1, MTBP, MTSS1, MUC1, MYC, MYDGF, MYOC, MYOG, NACC1, NANOS3, NAXE, NDC80, NDRG1, NDUFA13, NEK2, NES, NFE2L3, NFIC, NFIX, NIBAN1, NISCH, NME6, NMU, NOTCH3, NPC1, NPR1, NPRL2, NPSR1, NPVF, NR2C2, NR2F6, NRBP2, NTRK1, NUBP1, NUP210, OAZ1, OGG1, OPN3, OSR2, OXR1, OXTR, P2RY11, PABPC1, PALM, PALM3, PARP1, PARP3, PAX4, PBRM1, PBXIP1, PCBP4, PDE12, PDGFRA, PDK4, PEG10, PGLYRP2, PGPEP1, PHF14, PHOX2B, PIAS2, PIAS4, PIK3R2, PIN1, PKN1, PKP1, PLIN5, PLK5, PLXNA1, PLXNA2, PLXNA4, PLXNB1, PLXND1, PODXL, POLR2B, POLR2E, PON3, POT1, POU2F1, PPAN-P2RY11, PPARG, PPP1R17, PPP1R9A, PPP2R5A, PRDX2, PRKACA, PRKAR2A, PRKCD, PROK2, PROX1, PRRX1, PSCA, PSEN2, PSMA8, PSMD4, PSMG2, PTGER1, PTGS2, PTH1R, PTK2, PTN, PTPN14, PTPN2, PTPN23, PTPRC, PTPRG, PTPRM, PTPRS, PTPRZ1, PXK, QARS1, QSOX1, RAB7A, RAD18, RAD21, RAF1, RASAL3, RASL11B, RBBP8, RBM15B, RBM5, RC3H1, RCOR3, REST, RETN, RGS16, RGS22, RGS7, RGS8, RHOA, RIDA, RIOK3, RIT2, RLN3, RMI2, RNASEL, RNF113A, RNF125, RNF126, RNF139, RNF2, RNU6-664P, ROCK1, RPL11, RPL17, RPL17-C18orf32, RPL23, RPL26, RPL32, RPL37A, RPL8, RPS28, RRM2B, RSPO2, RUFY3, RYBP, S100A1, S100A9, S1PR2, SAP18, SBNO2, SCAP, SCIN, SCRIB, SCX, SDE2, SEC13, SEM1, SEMA3B, SEMA3F, SEMA3G, SEMA4A, SEMA6B, SERPINC1, SET, SFMBT1, SGTA, SH2D2A, SHARPIN, SHC1, SHFL, SHISA3, SIN3B, SIRT6, SKAP2, SKOR2, SLC25A23, SLC27A1, SLC30A1, SLC6A1, SLURP1, SMAD2, SMAD7, SMARCA4, SMARCC1, SMCHD1, SMG5, SMG7, SMO, SMYD2, SMYD3, SNAPIN, SND1, SNX13, SOCS1, SOSTDC1, SPAM1, SPINK2, SPINK8, SRGAP3, SRI, SRP9, ST3GAL1, STAB1, STAP1, STK11, STK3, STK38, SYT11, SYT4, TAC1, TASOR, TAX1BP1, TBX20, TBXA2R, TCF3, TCTA, TDGF1, TDGF1P3, TES, TFEC, TFPI2, TGIF1, THAP5, THOC1, TICAM1, TIMP4, TIPRL, TLE2, TLE6, TLR9, TMEM115, TMEM161A, TMEM259, TMEM38A, TMF1, TNFAIP8L1, TNFRSF11B, TNFSF14, TNFSF18, TNFSF4, TNN, TNNC1, TNR, TP53BP2, TPR, TPRA1, TRAF5, TRAIP, TREX1, TRH, TRIB1, TRIM11, TRIM46, TRPS1, TUBB4A, TWF2, TWSG1, TYMS, UBA3, UBA52, UBA7, UBQLN4, UBR5, UHRF1, UPF1, USP14, USP19, USP4, VGLL4, VPS28, WASL, WDR6, WFS1, WNT16, WNT3A, WNT5A, WNT7A, WNT9A, XCL1, XCR1, XPC, YES1, YJU2, YOD1, YY1AP1, ZBTB14, ZBTB18, ZBTB37, ZBTB7A, ZBTB7B, ZBTB7C, ZC3H7A, ZC3HC1, ZCCHC17, ZFPM2, ZGLP1, ZHX2, ZNF16, ZNF177, ZNF24, ZNF266, ZNF281, ZNF555, ZNF556, ZNF557, ZNF558, ZNF559, ZNF572, ZNF653, ZNF706, ZNF846]
GO:0048523	negative regulation of cellular process	0,00	0,00	11,57	594,00	[AASS, ABCA7, ABHD17A, ABHD6, ABL2, ACP5, ADAM15, ADAM22, ADAMTS9, ADAR, ADCY8, ADCYAP1, ADCYAP1R1, ADGRB1, ADIPOR1, ADORA1, AGO2, AGR2, AHR, AKR1B1, AKT3, ANGEL2, ANGPT1, ANGPTL4, ANKLE1, ANKRD17, APC2, APCDD1, APPL1, AQP1, AREG, ARF4, ARHGAP28, ARHGEF18, ARHGEF2, ARID3A, ARL6IP5, ASH1L, ASNS, ASPM, ATAD2, ATCAY, ATF3, ATG7, ATP5F1A, ATRIP, ATXN7, BABAM1, BAP1, BATF3, BECN2, BEX4, BHLHE40, BMPER, BMT2, BRINP2, BSG, BST2, C3, CACNA1A, CACTIN, CACYBP, CALCA, CALR, CAMSAP2, CAPZA2, CARM1, CAV1, CAV2, CAV3, CC2D1A, CCL25, CCN3, CCN4, CCR2, CCR5, CD34, CD46, CDC34, CDH2, CDK6, CDKN2D, CELF4, CENPF, CHERP, CIDEA, CIITA, CIRBP, CISH, CLEC16A, CLEC4G, CLK2, CLOCK, CNBP, CNIH4, CNN1, CNN2, CNTN4, COL28A1, COL7A1, COMP, COPS9, CPAMD8, CR1, CRACD, CRBN, CREB3L4, CREG1, CRLF1, CSN2, CSRP1, CTHRC1, CXCL8, CXXC1, CYP51A1, CYRIB, DAD1, DAG1, DAND5, DAPK3, DBI, DCAF1, DCP1A, DCST1, DCSTAMP, DEPTOR, DHX9, DNAJB1, DNAJB9, DNM2, DNM3, DNMT1, DOT1L, DPT, DTL, DYRK3, E2F4, EEF1AKNMT, EFNA1, EIF3E, EIF3H, ELANE, ELAVL1, ELF3, ENY2, EPGN, EPPK1, EPS15L1, ERC2, EREG, ETV3, EVI5L, EXOSC4, EXOSC7, F2RL3, FAM107A, FAM3C, FAM3D, FANCD2, FASLG, FBXO43, FCMR, FERD3L, FEZF2, FHIT, FHOD3, FOXH1, FOXP1, FOXP2, FSTL3, FYCO1, FZD6, FZR1, GADD45B, GARS1, GATA2, GATAD2A, GATAD2B, GBA, GDF15, GHRL, GIPC1, GJC2, GNAI2, GON4L, GPNMB, GPR108, GPR161, GPR37, GPR37L1, GPX1, GREM2, GRHL2, GRINA, GRM7, GSDME, H1-8, H2AW, H3-3B, HAX1, HDAC9, HDGF, HESX1, HNRNPA2B1, HNRNPU, HOMER3, HOOK2, HOPX, HOXA2, HOXA5, HOXA7, HSF1, HYAL1, HYAL2, ICAM1, IFI30, IFT122, IGF2BP3, IGFBP7, IL10, IL17RD, IL19, IL24, IL27RA, IL6, ILF3, IMPACT, ING3, INKA1, INTS3, INTS7, IP6K2, IREB2, IRF6, ITIH1, ITPKB, ITPR1, IVNS1ABP, JAGN1, JAK3, JAZF1, KANK2, KANK3, KCNK2, KCTD1, KCTD6, KDM4B, KDM5B, KDR, KHSRP, KIF14, KIFAP3, KIT, KLF10, KLF15, KLF16, KLHL20, KRIT1, L3MBTL4, LAPTM4B, LDLR, LEFTY1, LEP, LHX4, LHX9, LIMCH1, LIMD1, LITAF, LMCD1, LMNA, LMOD2, LMOD3, LONP1, LRRC14, LSM3, LSM4, LSM5, LSM7, LSM8, LTF, LZTFL1, MAEL, MAF1, MAGI1, MALSU1, MAP4, MAPK15, MBD1, MBD3, MBD4, MCM2, MDFIC, MET, MEX3D, MFSD12, MIB1, MIDN, MIER2, MINDY4, MITF, MLLT1, MOCOS, MRPL13, MST1, MTBP, MTSS1, MUC1, MYC, MYDGF, MYOC, MYOG, NACC1, NANOS3, NDC80, NDRG1, NDUFA13, NEK2, NES, NFE2L3, NFIC, NFIX, NIBAN1, NISCH, NME6, NOTCH3, NPC1, NPR1, NPRL2, NPSR1, NPVF, NR2C2, NR2F6, NRBP2, NTRK1, NUBP1, OAZ1, OGG1, OPN3, OSR2, OXR1, PABPC1, PALM, PALM3, PARP1, PARP3, PAX4, PBRM1, PBXIP1, PCBP4, PDE12, PDGFRA, PDK4, PEG10, PGLYRP2, PGPEP1, PHF14, PHOX2B, PIAS2, PIAS4, PIK3R2, PIN1, PKN1, PKP1, PLIN5, PLK5, PLXNA1, PLXNA2, PLXNA4, PLXNB1, PLXND1, PODXL, POLR2B, POLR2E, PON3, POT1, POU2F1, PPARG, PPP1R17, PPP1R9A, PPP2R5A, PRDX2, PRKACA, PRKAR2A, PRKCD, PROK2, PROX1, PRRX1, PSCA, PSEN2, PSMA8, PSMD4, PSMG2, PTGS2, PTH1R, PTK2, PTN, PTPN14, PTPN2, PTPN23, PTPRC, PTPRG, PTPRM, PTPRS, PTPRZ1, QARS1, QSOX1, RAB7A, RAD18, RAD21, RAF1, RASAL3, RASL11B, RBBP8, RBM15B, RBM5, RC3H1, RCOR3, REST, RGS16, RGS22, RGS7, RGS8, RHOA, RIDA, RIOK3, RIT2, RMI2, RNF113A, RNF125, RNF126, RNF139, RNF2, RNU6-664P, ROCK1, RPL11, RPL17, RPL23, RPL26, RRM2B, RUFY3, RYBP, S100A1, S100A9, S1PR2, SAP18, SBNO2, SCIN, SCRIB, SCX, SDE2, SEM1, SEMA3B, SEMA3F, SEMA3G, SEMA4A, SEMA6B, SERPINC1, SET, SFMBT1, SGTA, SHC1, SHFL, SHISA3, SIN3B, SIRT6, SKAP2, SKOR2, SLC25A23, SLC27A1, SLC30A1, SLC6A1, SLURP1, SMAD2, SMAD7, SMARCA4, SMARCC1, SMCHD1, SMO, SMYD2, SMYD3, SNAPIN, SNX13, SOCS1, SOSTDC1, SPAM1, SPINK2, SPINK8, SRGAP3, SRI, SRP9, ST3GAL1, STAP1, STK11, STK3, STK38, SYT11, SYT4, TASOR, TAX1BP1, TBX20, TBXA2R, TCF3, TCTA, TDGF1, TDGF1P3, TES, TFEC, TFPI2, TGIF1, THAP5, THOC1, TICAM1, TIMP4, TIPRL, TLE2, TLE6, TLR9, TMEM115, TMEM161A, TMEM259, TMEM38A, TMF1, TNFAIP8L1, TNFSF14, TNFSF18, TNFSF4, TNN, TNNC1, TNR, TP53BP2, TPR, TPRA1, TRAF5, TRAIP, TREX1, TRH, TRIB1, TRIM11, TRIM46, TRPS1, TUBB4A, TWF2, TWSG1, TYMS, UBA3, UBA52, UBQLN4, UBR5, UHRF1, UPF1, USP14, USP19, USP4, VGLL4, VPS28, WASL, WDR6, WFS1, WNT16, WNT3A, WNT5A, WNT7A, WNT9A, XCL1, XCR1, XPC, YJU2, YOD1, YY1AP1, ZBTB14, ZBTB18, ZBTB37, ZBTB7A, ZBTB7B, ZBTB7C, ZC3HC1, ZCCHC17, ZFPM2, ZGLP1, ZHX2, ZNF16, ZNF177, ZNF24, ZNF266, ZNF281, ZNF555, ZNF556, ZNF557, ZNF558, ZNF559, ZNF572, ZNF653, ZNF706, ZNF846]
GO:0050673	epithelial cell proliferation	0,03	0,00	14,81	64,00	[AKR1B1, AKT3, ANGPT1, ANGPTL8, AREG, ATP5F1A, BMPER, CALCA, CAV1, CAV2, CCN3, CCR3, CD34, CDK6, CPAMD8, DAND5, DLX5, DLX6, EPGN, EPPK1, EREG, GATA2, GHRL, GLUL, GPX1, HAS2, HOXA5, HYAL1, IL10, IL6, IQGAP3, IRF6, KDM5B, KDR, KIT, KRIT1, LAMC1, LEP, LRG1, MBD4, MST1, MTSS1, MYC, MYDGF, ODAM, OSR2, PPARG, PROK2, PROX1, PTN, PTPRM, PYGO2, RIDA, SIRT6, SLURP1, SMO, SPAM1, STK11, UHRF1, WNT16, WNT2, WNT3A, WNT5A, WNT7A]
GO:0050679	positive regulation of epithelial cell proliferation	0,03	0,00	16,98	36,00	[AKR1B1, AKT3, AREG, CAV2, CCR3, CPAMD8, DAND5, DLX5, DLX6, EPGN, GATA2, GHRL, GLUL, HAS2, HYAL1, IL10, IQGAP3, KDM5B, KDR, LAMC1, LRG1, MBD4, MST1, MYC, MYDGF, ODAM, OSR2, PROX1, PTN, SIRT6, SMO, SPAM1, WNT2, WNT3A, WNT5A, WNT7A]
GO:0035095	behavioral response to nicotine	0,04	0,00	57,14	4,00	[CHRNA3, CHRNA5, CHRNB2, GRM2]
GO:0060084	synaptic transmission involved in micturition	0,03	0,00	100,00	3,00	[CHRNA3, CHRNB2, CHRNB4]
GO:0071526	semaphorin-plexin signaling pathway	0,05	0,00	25,00	11,00	[MET, PLXNA1, PLXNA2, PLXNA4, PLXNB1, PLXND1, SEMA3B, SEMA3F, SEMA3G, SEMA4A, SEMA6B]
GO:0017154	semaphorin receptor activity	0,04	0,00	40,00	6,00	[MET, PLXNA1, PLXNA2, PLXNA4, PLXNB1, PLXND1]

GO:1902287	semaphorin-plexin signaling pathway involved in axon guidance	0,03	0,00	46,15	6,00	[PLXNA1, PLXNA2, PLXNA4, PLXNB1, PLXND1, SEMA3F]
GO:0031579	membrane raft organization	0,04	0,00	30,77	8,00	[ABCA7, CAV1, CAV2, CAV3, EMP2, NAXE, NPC1, PTPRC]
GO:0044857	plasma membrane raft organization	0,03	0,00	55,56	5,00	[ABCA7, CAV1, CAV2, CAV3, EMP2]
GO:0070836	caveola assembly	0,02	0,00	80,00	4,00	[CAV1, CAV2, CAV3, EMP2]
GO:0006935	chemotaxis	0,01	0,00	14,51	102,00	[ANGPT1, BSG, CALCA, CALR, CCL25, CCN3, CCR1, CCR2, CCR3, CCR5, CCR9, CCRL2, CHL1, CNTN4, CNTN6, COLEC10, CREB3L4, CRPPA, CXCL6, CXCL8, CXCR6, CYRIB, DAG1, DLX5, DOCK4, EFNA1, EFNA3, ELANE, ENAH, ENPP2, EPHA5, ETV1, EVX1, EXT1, FEZF2, GPNMB, HOXA2, HRH1, IL10, IL6, IL6R, KDR, KIT, LAMA1, LAMA3, LAMB2, LAMC1, LAMC2, LGR6, LHX4, LHX9, LMNB2, LRTM1, MET, MST1, NOTCH3, NRTN, NTRK1, PDGFRA, PIP5K1C, PLP2, PLXNA1, PLXNA2, PLXNA4, PLXNB1, PLXND1, PPBP, PRKCD, PRKCSH, PROK2, PSPN, PTK2, PTN, PTPN2, PTPRM, RAB13, RALBP1, RHOA, RNF165, S100A12, S100A14, S100A9, SCRIB, SEMA3B, SEMA3F, SEMA3G, SEMA4A, SEMA6B, SHC1, SMO, STAP1, TAFA4, TNFSF18, TNR, USP14, VAV1, WNT3A, WNT5A, XCL1, XCL2, XCR1, ZSWIM4]
GO:0007411	axon guidance	0,03	0,00	16,01	49,00	[BSG, CHL1, CNTN4, CNTN6, CRPPA, DAG1, DLX5, EFNA1, EFNA3, ENAH, EPHA5, ETV1, EVX1, EXT1, FEZF2, HOXA2, LAMA1, LAMA3, LAMB2, LAMC1, LAMC2, LGR6, LHX4, LHX9, LMNB2, LRTM1, NOTCH3, NRTN, NTRK1, PLXNA1, PLXNA2, PLXNA4, PLXNB1, PLXND1, PSPN, PTK2, PTPRM, RNF165, SEMA3B, SEMA3F, SEMA3G, SEMA4A, SEMA6B, SHC1, SMO, TNR, WNT3A, WNT5A, ZSWIM4]
GO:0007409	axonogenesis	0,04	0,00	14,12	72,00	[ADGRB1, AFG3L2, BSG, CDH2, CHL1, CHRNB2, CNTN4, CNTN6, CRABP2, CRPPA, CXXC1, DAG1, DLX5, DNM2, EFNA1, EFNA3, ENAH, EPHA5, ETV1, EVX1, EXT1, FEZF2, FYCO1, HOXA2, LAMA1, LAMA3, LAMB2, LAMC1, LAMC2, LGR6, LHX4, LHX9, LMNB2, LRTM1, MAP1S, NOTCH3, NRTN, NTRK1, PHOX2B, PKN1, PLXNA1, PLXNA2, PLXNA4, PLXNB1, PLXND1, PSPN, PTK2, PTPRM, PTPRS, PTPRZ1, RAB3A, RAB8A, RHOA, RNF165, RUFY3, S100A6, SEMA3B, SEMA3F, SEMA3G, SEMA4A, SEMA6B, SHC1, SMO, STK11, TNN, TNR, TRIM46, TWF2, WNT3A, WNT5A, WNT7A, ZSWIM4]
GO:0046903	secretion	0,04	0,00	12,34	196,00	[ABCB4, ADCY8, ADCYAP1, ADGRE3, ADGRE5, ADORA1, AGR2, ALDOA, AP1M1, APEH, AQP1, ARHGAP45, ARL8B, ARPC5, ATG7, ATP8A1, BST2, C1orf35, C3, CACNA1A, CACNA1D, CACNA1E, CACNA2D2, CADPS2, CAMP, CAV1, CCN3, CCR1, CCR2, CD55, CFTR, CHI3L1, CHRNA3, CHRNA5, CHRNB2, CHRNB4, CLEC3B, CLOCK, CNN2, COMP, COPG1, COPG2, CORIN, CPAMD8, CR1, CREG1, CSN2, CSN3, CSPG5, CXXC1, CYB5R1, CYP51A1, CYRIB, DEGS1, DGAT1, EEF1A1, EEF2, ELANE, ENY2, EPHA5, ERC2, EXOC1, EXOC1L, EXOC4, F5, FAM3C, FAM3D, FLNB, GATA2, GHRHR, GHRL, GIPC1, GLUL, GNAI2, GPNMB, GRM2, GRM7, GSDMD, HOOK2, HYAL3, ICA1, IER3IP1, IL6, ILDR2, ILF2, IMPDH1, IMPDH2, ITPR1, JAGN1, KDM5B, KIT, KMO, LAMTOR2, LEFTY2, LEP, LRG1, LSM4, LTF, LY6E, MAFA, MANF, MBD4, MCEMP1, MIDN, MINDY4, MON1A, MPC2, MTX1, MYC, MYOM1, NAPRT, NBEAL2, NISCH, NMU, NPR1, NPVF, OXTR, PFKFB2, PIGR, PIK3C3, PIP5K1C, PKN1, PKP1, PLA2G4A, PLPPR3, PPAT, PPBP, PPP1R9A, PRDX6, PRKCD, PRKCSH, PTPN23, PTPRC, QSOX1, RAB11B, RAB12, RAB13, RAB25, RAB31, RAB3A, RAB3D, RAB43, RAB7A, RAB8A, RAF1, REST, RETN, RHOA, RIMS2, ROCK1, S100A12, S100A13, S100A9, SCCPDH, SCFD2, SCIN, SCRIB, SCRN1, SELL, SELP, SERPINC1, SLC26A6, SLC30A1, SLC30A8, SLC44A2, SLC4A4, SLC6A1, SMAD2, SNAP47, SNAPIN, SNX10, SPAM1, SRI, STEAP2, STXBP2, SYBU, SYN2, SYT11, SYT17, SYT2, SYT4, TAC1, TEX264, TMEM63A, TMEM79, TMF1, TRH, TUBB, TVP23A, UBE2Q1, UNC13A, USE1, VAPA, WASHC3, WNT7A, ZBTB7B]
GO:0023061	signal release	0,01	0,00	15,18	78,00	[ADCY8, ADCYAP1, ADORA1, CACNA1A, CACNA1D, CACNA1E, CACNA2D2, CADPS2, CCN3, CFTR, CHRNA3, CHRNA5, CHRNB2, CHRNB4, CLOCK, CPAMD8, CSPG5, CXXC1, ENY2, EPHA5, ERC2, FAM3D, FLNB, GHRHR, GHRL, GIPC1, GLUL, GNAI2, GPNMB, GRM2, ICA1, IL6, ILDR2, ITPR1, JAGN1, KDM5B, KMO, LEP, LSM4, MAFA, MIDN, MPC2, NISCH, NMU, NPVF, OXTR, PFKFB2, PIP5K1C, PLA2G4A, PPP1R9A, PTPN23, RAB11B, RAB3A, RAB43, RAF1, REST, RETN, RIMS2, SCRIB, SLC30A1, SLC30A8, SMAD2, SNAP47, SNAPIN, SRI, STXBP2, SYBU, SYN2, SYT11, SYT17, SYT2, SYT4, TAC1, TMF1, TRH, UBE2Q1, UNC13A, WNT7A]
GO:0042886	amide transport	0,03	0,00	15,21	54,00	[ABCB1, ABCB4, ADCY8, ADCYAP1, ADORA1, BSG, CACNA1A, CACNA1D, CACNA1E, CACNA2D2, CCN3, CFTR, CLEC4M, CLOCK, CPAMD8, ENY2, EPHA5, FAM3D, FLNB, GHRHR, GHRL, GLUL, GNAI2, ICA1, IL6, ILDR2, ITPR1, JAGN1, LEP, LSM4, MAFA, MIDN, MPC2, NMU, PFKFB2, PLEKHA8, RAB11B, RAB43, RAF1, REST, RIMS2, SLC14A1, SLC14A2, SLC19A2, SLC25A32, SLC26A6, SLC27A1, SLC30A8, SLC38A3, SMAD2, SRI, SYBU, TRH, UBE2Q1]
GO:0006810	transport	0,03	0,00	11,16	600,00	[ABCA7, ABCB1, ABCB4, ABCB5, ABL2, ABRA, ACBD3, ADAMTS9, ADCY10, ADCY8, ADCYAP1, ADCYAP1R1, ADGRB1, ADGRE3, ADGRE5, ADORA1, AFG3L2, AGR2, AHCTF1, AKAP8, AKAP9, ALDOA, ALKBH7, ANGPT1, ANKLE1, ANO8, AP1M1, AP1M2, AP3D1, APBA3, APEH, APOO, APPL1, AQP1, AQP4, AREG, ARF4, ARF5, ARHGAP45, ARHGEF2, ARIH2, ARL6IP5, ARL8B, ARPC4, ARPC4-TTLL3, ARPC5, ARRDC2, ARRDC5, ATG4D, ATG7, ATP10D, ATP13A1, ATP1B1, ATP2B2, ATP5F1A, ATP5F1D, ATP5MC3, ATP5PD, ATP6V1C1, ATP6V1F, ATP6V1G3, ATP8A1, ATP8B2, AZIN1, BAP1, BBS9, BECN2, BEST2, BET1, BLZF1, BRK1, BSG, BSN, BST2, C1orf35, C1orf43, C3, C4BPB, CABYR, CACNA1A, CACNA1D, CACNA1E, CACNA1S, CACNA2D2, CACNA2D3, CADPS2, CALCA, CALCR, CALR, CAMK1, CAMP, CAPZA2, CAV1, CAV2, CAV3, CCDC51, CCN3, CCR1, CCR2, CCR5, CCT3, CD247, CD320, CD55, CD5L, CDC37, CDH2, CENPF, CEP41, CETN2, CFHR4, CFTR, CHCHD4, CHERP, CHI3L1, CHRNA3, CHRNA5, CHRNB2, CHRNB4, CHTOP, CLEC16A, CLEC3B, CLEC4M, CLOCK, CNGA1, CNIH3, CNIH4, CNN2, CNST, COL7A1, COLEC12, COMP, COPE, COPG1, COPG2, CORIN, COX18, COX7B2, CPAMD8, CPSF1, CR1, CRBN, CREG1, CROT, CRTC2, CSN1S1, CSN2, CSN3, CSNK1G2, CSPG5, CSRP1, CXCL8, CXXC1, CYB5R1, CYP51A1, CYRIB, DBI, DDX39A, DEGS1, DENND1B, DENND1C, DENND3, DERL1, DESI2, DGAT1, DHX9, DNAH11, DNM2, DNM3, DYNC1I1, EDEM1, EEF1A1, EEF2, EEPD1, ELANE, ELAVL1, ELMO1, EMP2, ENPP2, ENY2, EPG5, EPHA5, EPS15L1, ERC2, EVI5L, EXOC1, EXOC1L, EXOC4, EXT1, F2RL3, F5, FAM3C, FAM3D, FAM91A1, FASLG, FCHO1, FLNB, FLVCR1, FYCO1, FZR1, GABRA2, GABRA4, GABRG1, GATA2, GC, GET3, GHRHR, GHRL, GIPC1, GJC2, GLUL, GNAI2, GPIHBP1, GPNMB, GRIN2A, GRIP2, GRM2, GRM3, GRM7, GSDMD, GUK1, HAS2, HAX1, HCN2, HCN3, HNRNPA2B1, HNRNPU, HOMER3, HOOK2, HSF1, HYAL2, HYAL3, ICA1, ICAM1, ICAM3, ICAM5, IER3IP1, IFT122, IGF2BP3, IL6, ILDR2, ILF2, IMPDH1, IMPDH2, INSR, IP6K2, IPO9, IREB2, ITPR1, JAGN1, JCHAIN, KCND2, KCNK2, KCNK9, KCNN1, KCNN3, KCNQ3, KCNS2, KCNV1, KDM5B, KHSRP, KIF15, KIFAP3, KIT, KLF15, KLHL20, KMO, KXD1, LAMTOR2, LAPTM4B, LDLR, LEFTY2, LEP, LIPG, LMNA, LONP1, LRG1, LRP12, LRRC6, LRRC8E, LSM4, LTF, LY6E, MAFA, MAGI1, MAL2, MANF, MAP1LC3C, MAP1S, MAP2K2, MAPK15, MAPKAPK3, MARCHF2, MBD1, MBD4, MCEMP1, MCUR1, MDFIC, MEP1B, MET, MFSD12, MFSD3, MIB1, MIDN, MINDY4, MKLN1, MON1A, MPC2, MPPE1, MRPL13, MST1R, MTCL1, MTX1, MVB12A, MYC, MYO1F, MYO5B, MYOM1, NACA2, NAPG, NAPRT, NAXE, NBEAL2, NCALD, NCF2, NCKIPSD, NDUFA13, NDUFS7, NECAP2, NIPAL1, NIPAL2, NISCH, NMU, NPC1, NPR1, NPSR1, NPVF, NPY, NRBP2, NUP210, OAZ1, OCIAD1, OCIAD2, OPN3, OSBPL1A, OSBPL3, OXTR, PACC1, PEAR1, PEX1, PFKFB2, PIEZO2, PIGR, PIK3C3, PIK3R2, PIN1, PIP5K1C, PKN1, PKP1, PLA2G4A, PLEKHA8, PLIN3, PLP2, PLPPR2, PLPPR3, PPARG, PPAT, PPBP, PPFIA4, PPP1R9A, PRDX6, PRELID3A, PRG4, PRKACA, PRKCD, PRKCSH, PSEN2, PSMA8, PSMD4, PTGS2, PTK2, PTPN14, PTPN23, PTPRC, PXK, QSOX1, RAB11B, RAB12, RAB13, RAB25, RAB31, RAB3A, RAB3D, RAB43, RAB7A, RAB8A, RABGAP1L, RABIF, RAF1, RALBP1, RANBP3, RBM15B, RBSN, REEP6, REST, RETN, RFT1, RHBG, RHOA, RIMS2, RIT2, RNASEL, RNF126, RNF139, RNF2, RNU6-664P, ROCK1, RPL11, RPL17, RPL17-C18orf32, RPL23, RPL26, RPL32, RPL37A, RPL8, RPS28, RTBDN, RTP3, RUFY3, S100A1, S100A12, S100A13, S100A6, S100A9, SCAMP3, SCAMP4, SCAP, SCCPDH, SCFD2, SCIN, SCRIB, SCRN1, SEC13, SEC16B, SEC61A1, SELE, SELENOK, SELL, SELP, SEM1, SERPINC1, SETD2, SGTA, SH2D2A, SH3GL1, SLC10A4, SLC13A1, SLC14A1, SLC14A2, SLC19A2, SLC1A6, SLC25A13, SLC25A20, SLC25A23, SLC25A26, SLC25A32, SLC25A40, SLC25A41, SLC25A42, SLC25A44, SLC26A6, SLC27A1, SLC27A3, SLC30A1, SLC30A8, SLC30A9, SLC35B4, SLC35E1, SLC38A3, SLC39A1, SLC39A3, SLC39A4, SLC39A6, SLC41A3, SLC44A2, SLC45A4, SLC4A4, SLC50A1, SLC52A1, SLC52A2, SLC5A5, SLC6A1, SLC6A11, SLC6A20, SLC6A6, SLC9C2, SLMAP, SMAD2, SMG5, SMG7, SMO, SNAP47, SNAPIN, SNRPD1, SNX10, SNX13, SNX31, SOAT1, SPAM1, SPCS1, SRI, SRP72, SRP9, SSR2, STAB1, STAP1, STEAP1, STEAP2, STEAP4, STIMATE, STK11, STX10, STX6, STXBP2, SYBU, SYN2, SYT11, SYT17, SYT2, SYT4, TAC1, TAFA4, TEX264, TG, THOC1, THOC7, TIMM17A, TIMM29, TIMM44, TLR9, TMCC1, TMED1, TMEM106B, TMEM115, TMEM165, TMEM241, TMEM38A, TMEM63A, TMEM79, TMEM9, TMF1, TNNC1, TNNT2, TNPO3, TOMM7, TP53BP2, TPR, TRAPPC9, TREX1, TRH, TRIM46, TRIP10, TSNARE1, TSPAN13, TUBB, TVP23A, UBA52, UBE2Q1, UBL5, UBR5, UBXN6, UNC13A, UPF1, USE1, USP46, VAMP4, VAPA, VAV1, VPS13B, VPS28, VPS50, VPS52, WASHC3, WASHC5, WASL, WFS1, WIPF3, WNT3A, WNT5A, WNT7A, XCL1, XCR1, XPR1, YES1, YIPF2, YOD1, YTHDC1, ZBTB7B, ZC3H3, ZDHHC3]

GO:0071702	organic substance transport	0,02	0,00	11,90	327,00	[ABCA7, ABCB1, ABCB4, ABRA, ADAMTS9, ADCY8, ADCYAP1, ADORA1, AHCTF1, AKAP8, ANGPT1, ANKLE1, AP1M1, AP1M2, AP3D1, APBA3, APOO, APPL1, AQP1, ARF4, ARF5, ARHGEF2, ARIH2, ARL6IP5, ARL8B, ARRDC2, ARRDC5, ATG4D, ATG7, ATP10D, ATP13A1, ATP1B1, ATP6V1C1, ATP6V1F, ATP6V1G3, ATP8A1, ATP8B2, AZIN1, BAP1, BBS9, BET1, BLZF1, BSG, C3, CACNA1A, CACNA1D, CACNA1E, CACNA2D2, CADPS2, CALR, CAMK1, CAV1, CCN3, CD320, CDC37, CENPF, CEP41, CETN2, CFHR4, CFTR, CHCHD4, CHRNA3, CHRNB2, CHTOP, CLEC4M, CLOCK, CNIH4, CNST, COMP, COPE, COPG1, COPG2, COX18, CPAMD8, CPSF1, CR1, CROT, CXXC1, CYB5R1, CYP51A1, DBI, DDX39A, DENND1B, DERL1, DESI2, DHX9, DNM2, EDEM1, EEPD1, ELAVL1, ENY2, EPG5, EPHA5, EVI5L, EXOC1, EXOC4, FAM3D, FAM91A1, FASLG, FLNB, FLVCR1, FYCO1, FZR1, GET3, GHRHR, GHRL, GIPC1, GLUL, GNAI2, GPIHBP1, GPNMB, GRIP2, GRM2, GRM7, GUK1, HAX1, HNRNPA2B1, HOMER3, HOOK2, HSF1, HYAL2, ICA1, IER3IP1, IGF2BP3, IL6, ILDR2, INSR, IPO9, ITPR1, JAGN1, KDM5B, KHSRP, KLF15, KLHL20, KMO, LDLR, LEP, LIPG, LMNA, LRRC8E, LSM4, LY6E, MAFA, MAGI1, MAP1LC3C, MAPK15, MBD1, MBD4, MDFIC, MFSD12, MIDN, MINDY4, MON1A, MPC2, MRPL13, MTCL1, MTX1, MVB12A, MYC, MYO5B, MYOM1, NACA2, NAPG, NAXE, NDUFA13, NECAP2, NISCH, NMU, NPC1, NUP210, OAZ1, OPN3, OSBPL1A, OSBPL3, OXTR, PEX1, PFKFB2, PIK3C3, PIK3R2, PIN1, PKN1, PLA2G4A, PLEKHA8, PPARG, PPBP, PRELID3A, PRKACA, PRKCD, PTGS2, PTPN14, PTPN23, RAB11B, RAB12, RAB13, RAB25, RAB31, RAB3A, RAB3D, RAB43, RAB7A, RAB8A, RABGAP1L, RABIF, RAF1, RALBP1, RANBP3, RBM15B, RBSN, REST, RETN, RFT1, RIMS2, RNASEL, RNF2, RNU6-664P, RPL11, RPL17, RPL17-C18orf32, RPL23, RPL26, RPL32, RPL37A, RPL8, RPS28, RTBDN, RTP3, RUFY3, S100A13, SCAMP3, SCAMP4, SCFD2, SCRIB, SEC13, SEC16B, SEC61A1, SELENOK, SEM1, SETD2, SGTA, SLC10A4, SLC14A1, SLC14A2, SLC19A2, SLC1A6, SLC25A13, SLC25A20, SLC25A23, SLC25A26, SLC25A32, SLC25A41, SLC25A42, SLC25A44, SLC26A6, SLC27A1, SLC27A3, SLC30A8, SLC35B4, SLC38A3, SLC44A2, SLC45A4, SLC4A4, SLC50A1, SLC52A1, SLC52A2, SLC6A1, SLC6A11, SLC6A20, SLC6A6, SMAD2, SMG5, SMG7, SMO, SNAP47, SNAPIN, SNX10, SNX13, SNX31, SPCS1, SRI, SRP72, SRP9, SSR2, STX10, STX6, STXBP2, SYBU, SYT11, SYT17, SYT2, SYT4, TAC1, THOC1, THOC7, TIMM17A, TIMM29, TIMM44, TMED1, TMEM115, TMEM241, TMEM9, TMF1, TNPO3, TOMM7, TP53BP2, TPR, TRH, TSNARE1, TVP23A, UBA52, UBE2Q1, UBL5, UBR5, UPF1, USE1, VAMP4, VPS13B, VPS28, VPS50, VPS52, WASHC3, WASHC5, YES1, YOD1, YTHDC1, ZC3H3, ZDHHC3]
GO:0071705	nitrogen compound transport	0,00	0,00	12,48	288,00	[ABCB1, ABCB4, ABRA, ADAMTS9, ADCY8, ADCYAP1, ADORA1, AHCTF1, AKAP8, ANGPT1, ANKLE1, AP1M1, AP1M2, AP3D1, APBA3, APPL1, AQP1, ARF4, ARF5, ARHGEF2, ARIH2, ARL6IP5, ARL8B, ARRDC2, ARRDC5, ATG4D, ATG7, ATP13A1, ATP1B1, ATP6V1C1, ATP6V1F, ATP6V1G3, ATP8A1, AZIN1, BAP1, BBS9, BET1, BLZF1, BSG, CACNA1A, CACNA1D, CACNA1E, CACNA2D2, CADPS2, CALR, CAMK1, CAV1, CCN3, CD320, CDC37, CENPF, CEP41, CETN2, CFTR, CHCHD4, CHRNA3, CHRNB2, CHTOP, CLEC4M, CLOCK, CNIH4, CNST, COMP, COPE, COPG1, COPG2, COX18, CPAMD8, CPSF1, CR1, CYP51A1, DDX39A, DENND1B, DERL1, DESI2, DHX9, DNM2, EDEM1, ELAVL1, ENY2, EPG5, EPHA5, EVI5L, EXOC1, EXOC4, FAM3D, FAM91A1, FLNB, FLVCR1, FYCO1, FZR1, GET3, GHRHR, GHRL, GIPC1, GLUL, GNAI2, GPIHBP1, GRIP2, GRM2, GRM7, GUK1, HAX1, HNRNPA2B1, HOMER3, HOOK2, HSF1, HYAL2, ICA1, IER3IP1, IGF2BP3, IL6, ILDR2, IPO9, ITPR1, JAGN1, KHSRP, KLHL20, KMO, LEP, LMNA, LRRC8E, LSM4, LY6E, MAFA, MAGI1, MAP1LC3C, MAPK15, MBD1, MBD4, MDFIC, MFSD12, MIDN, MINDY4, MON1A, MPC2, MRPL13, MTCL1, MTX1, MVB12A, MYC, MYO5B, MYOM1, NACA2, NAPG, NDUFA13, NECAP2, NISCH, NMU, NUP210, OAZ1, OXTR, PEX1, PFKFB2, PIK3C3, PIK3R2, PIN1, PKN1, PLEKHA8, PPARG, PRKACA, PRKCD, PTGS2, PTPN14, PTPN23, RAB11B, RAB12, RAB13, RAB25, RAB31, RAB3A, RAB3D, RAB43, RAB7A, RAB8A, RABGAP1L, RABIF, RAF1, RALBP1, RANBP3, RBM15B, RBSN, REST, RHBG, RIMS2, RNF2, RNU6-664P, RPL11, RPL17, RPL17-C18orf32, RPL23, RPL26, RPL32, RPL37A, RPL8, RPS28, RTBDN, RTP3, RUFY3, S100A13, SCAMP3, SCAMP4, SCFD2, SCRIB, SEC13, SEC16B, SEC61A1, SELENOK, SEM1, SETD2, SGTA, SLC14A1, SLC14A2, SLC19A2, SLC1A6, SLC25A13, SLC25A20, SLC25A23, SLC25A32, SLC25A41, SLC25A42, SLC25A44, SLC26A6, SLC27A1, SLC30A8, SLC35B4, SLC38A3, SLC44A2, SLC52A1, SLC52A2, SLC6A1, SLC6A11, SLC6A20, SLC6A6, SMAD2, SMG5, SMG7, SMO, SNAP47, SNAPIN, SNX10, SNX13, SNX31, SPCS1, SRI, SRP72, SRP9, SSR2, STX10, STX6, STXBP2, SYBU, SYT11, SYT17, SYT2, SYT4, THOC1, THOC7, TIMM17A, TIMM29, TIMM44, TMED1, TMEM115, TMEM9, TNPO3, TOMM7, TP53BP2, TPR, TRH, TSNARE1, TVP23A, UBA52, UBE2Q1, UBL5, UBR5, UPF1, USE1, VAMP4, VPS13B, VPS28, VPS50, VPS52, WASHC3, WASHC5, YOD1, YTHDC1, ZC3H3, ZDHHC3]
GO:0002698	negative regulation of immune effector process	0,04	0,01	19,64	22,00	[AHR, ANGPT1, APPL1, BST2, C4BPB, CCR2, CD46, CD55, CLEC4G, CR1, IL10, JAK3, PARP3, PGLYRP2, PTPRC, RC3H1, SMAD7, THOC1, TNFSF18, TNFSF4, XCL1, ZBTB7B]
GO:0002822	regulation of adaptive immune response based on somatic recombination of immune receptors built from immunoglobulin superfamily domains	0,05	0,01	17,14	30,00	[AHR, C3, C4BPB, CCR2, CD46, CD55, CLEC4G, CR1, CYRIB, DENND1B, FCER2, HMCES, IL10, IL12RB1, IL27RA, IL6, JAK3, MYDGF, PARP3, PKN1, PLA2G4A, PTPRC, RC3H1, RNU6-664P, SMAD7, THOC1, TNFSF18, TNFSF4, XCL1, ZBTB7B]
GO:0002823	negative regulation of adaptive immune response based on somatic recombination of immune receptors built from immunoglobulin superfamily domains	0,00	0,01	30,91	17,00	[AHR, C4BPB, CD46, CD55, CLEC4G, CR1, IL27RA, JAK3, PARP3, PTPRC, RC3H1, SMAD7, THOC1, TNFSF18, TNFSF4, XCL1, ZBTB7B]
GO:0002890	negative regulation of immunoglobulin mediated immune response	0,05	0,01	37,50	6,00	[C4BPB, CD46, CD55, CR1, PARP3, THOC1]
R-HSA:372790	Signaling by GPCR	0,00	0,00	14,77	104,00	[ABHD6, ADCY8, ADCYAP1, ADCYAP1R1, ADGRE1, ADGRE3, ADGRE5, ADORA1, AKT3, ARHGEF11, ARHGEF18, ARHGEF2, ARHGEF3, C3, CALCA, CALCR, CCL25, CCR1, CCR2, CCR3, CCR5, CCR9, CCRL2, CD55, CRHR2, CXCL6, CXCL8, CXCR6, DGKB, F2RL3, FZD1, FZD6, GHRHR, GHRL, GNA15, GNAI2, GNAL, GNAT1, GNG11, GNGT1, GNRHR, GPR25, GPR37, GPR37L1, GRM2, GRM3, GRM7, GRM8, HRH1, HRH4, ITPR1, LPAR2, MGLL, NMU, NPBWR2, NPSR1, NPY, OBSCN, OPN1SW, OPN3, OXTR, P2RY11, PCP2, PDE1C, PDE4A, PDE4C, PIK3R2, PLA2G4A, PLPPR2, PLPPR3, PLXNB1, PPBP, PRKACA, PRKAR2A, PRKCD, PROK2, PTGER1, PTH1R, RGS16, RGS22, RGS7, RGS8, RGSL1, RHOA, RLN3, ROCK1, S1PR2, S1PR4, S1PR5, SMO, TAC1, TBXA2R, TRH, TRHR, VAV1, WNT16, WNT2, WNT3A, WNT5A, WNT7A, WNT9A, XCL1, XCL2, XCR1]
R-HSA:388396	GPCR downstream signalling	0,03	0,00	13,99	88,00	[ABHD6, ADCYAP1, ADCYAP1R1, ADORA1, AKT3, ARHGEF11, ARHGEF18, ARHGEF2, ARHGEF3, C3, CALCA, CALCR, CCL25, CCR1, CCR2, CCR3, CCR5, CCR9, CRHR2, CXCL6, CXCL8, CXCR6, DGKB, F2RL3, GHRHR, GHRL, GNA15, GNAI2, GNAL, GNAT1, GNG11, GNGT1, GNRHR, GPR25, GPR37, GPR37L1, GRM2, GRM3, GRM7, GRM8, HRH1, HRH4, ITPR1, LPAR2, MGLL, NMU, NPBWR2, NPSR1, NPY, OBSCN, OPN1SW, OPN3, OXTR, P2RY11, PCP2, PDE1C, PDE4A, PDE4C, PIK3R2, PLA2G4A, PLXNB1, PPBP, PRKACA, PRKAR2A, PRKCD, PROK2, PTGER1, PTH1R, RGS16, RGS22, RGS7, RGS8, RGSL1, RHOA, RLN3, ROCK1, S1PR2, S1PR4, S1PR5, TAC1, TBXA2R, TRH, TRHR, VAV1, XCL1, XCL2, XCR1]
R-HSA:418594	G alpha (i) signalling events	0,03	0,00	15,72	50,00	[ADCY8, ADORA1, C3, CCL25, CCR1, CCR2, CCR3, CCR5, CCR9, CXCL6, CXCL8, CXCR6, GNA15, GNAI2, GNAL, GNAT1, GNG11, GNGT1, GPR37, GPR37L1, GRM2, GRM3, GRM7, GRM8, HRH4, ITPR1, LPAR2, NMU, NPBWR2, NPY, OPN1SW, OPN3, PCP2, PDE1C, PDE4A, PDE4C, PLA2G4A, PPBP, PRKACA, PRKAR2A, PRKCD, RGS16, RGS22, RGS7, RGS8, RGSL1, RLN3, S1PR2, S1PR4, S1PR5]
R-HSA:500792	GPCR ligand binding	0,02	0,00	14,99	70,00	[ADCYAP1, ADCYAP1R1, ADGRE1, ADGRE3, ADGRE5, ADORA1, C3, CALCA, CALCR, CCL25, CCR1, CCR2, CCR3, CCR5, CCR9, CCRL2, CD55, CRHR2, CXCL6, CXCL8, CXCR6, F2RL3, FZD1, FZD6, GHRHR, GHRL, GNG11, GNGT1, GNRHR, GPR37, GPR37L1, GRM2, GRM3, GRM7, GRM8, HRH1, HRH4, LPAR2, NMU, NPBWR2, NPSR1, NPY, OPN1SW, OPN3, OXTR, P2RY11, PLPPR2, PLPPR3, PPBP, PROK2, PTGER1, PTH1R, RLN3, S1PR2, S1PR4, S1PR5, SMO, TAC1, TBXA2R, TRH, TRHR, WNT16, WNT2, WNT3A, WNT5A, WNT7A, WNT9A, XCL1, XCL2, XCR1]
GO:0003014	renal system process	0,03	0,00	19,12	26,00	[ADCY8, ADORA1, AKR1B1, AQP1, AQP4, CD34, CHRNA3, CHRNB2, CHRNB4, CORIN, EMP2, GNAI2, HAS2, HYAL2, JCHAIN, MINDY4, MYO5B, NPR1, PKN1, PRKACA, PRKAR2A, RHOA, RRM2B, SLC4A4, TAC1, WFS1]
GO:0003091	renal water homeostasis	0,04	0,00	25,58	11,00	[ADCY8, AKR1B1, AQP1, AQP4, HAS2, HYAL2, MINDY4, MYO5B, PRKACA, PRKAR2A, WFS1]
GO:0003097	renal water transport	0,04	0,00	57,14	4,00	[AQP1, HAS2, HYAL2, MINDY4]
GO:0046878	positive regulation of saliva secretion	0,03	0,00	100,00	3,00	[AQP1, MINDY4, TAC1]

GO:0006396	RNA processing	0,03	0,00	13,00	137,00	[ADAR, AGO2, APOBEC4, BMT2, BUD31, CACTIN, CCDC130, CELF4, CELF5, CHERP, CHTOP, CIRBP, CLK2, COLEC12, CPSF1, CWC15, DALRD3, DAZAP1, DCAF13, DDX39A, DDX49, DHX9, DUS3L, ELAVL1, ELP2, ELP6, EXOSC4, EXOSC7, GARS1, GRSF1, GTF2F1, GTPBP3, HNRNPA2B1, HNRNPM, HNRNPU, HSF1, IGF2BP3, IL6, INTS3, INTS7, ISY1, ISY1-RAB43, IVNS1ABP, KHDC4, KHDRBS3, KHSRP, KRI1, LIN9, LSM3, LSM4, LSM5, LSM7, LSM8, MAP2K2, MCM2, METTL18, METTL4, MRPL13, NSA2, NVL, PABPC1, PCBP4, PDE12, PIN1, POLR2B, POLR2E, POP1, PPAN, PPAN-P2RY11, PPP4R2, PRCC, PRDX6, PRKACA, PUF60, QTRT1, RAVER1, RBM15B, RBM28, RBM5, RBM6, REST, RIOK3, RNASEL, RNF113A, RNF113B, RP9, RPL11, RPL17, RPL17-C18orf32, RPL23, RPL26, RPL32, RPL37A, RPL8, RPP14, RPRD1A, RPS28, RPUSD3, RRNAD1, RRP9, RSL1D1, SAFB, SAFB2, SAP18, SEM1, SF3A2, SF3A3, SMAD2, SNRPB2, SNRPD1, SNRPN, SPPL2B, SUGP1, SUGP2, TFB2M, THOC1, THOC7, THUMPD3, TRA2A, TRMT1, TRMT1L, TRNT1, TSEN15, UBA52, UBL5, USP4, UTP23, UTP25, UTP3, WDR18, WDR6, XAB2, YJU2, YTHDC1, ZBTB7A, ZC3H3, ZC3H7A]
GO:0008380	RNA splicing	0,03	0,00	14,71	70,00	[BUD31, CACTIN, CCDC130, CELF4, CELF5, CHERP, CIRBP, CLK2, COLEC12, CPSF1, CWC15, DAZAP1, DDX39A, DHX9, ELAVL1, GRSF1, GTF2F1, HNRNPA2B1, HNRNPM, HNRNPU, ISY1, ISY1-RAB43, IVNS1ABP, KHDC4, KHDRBS3, KHSRP, LIN9, LSM3, LSM4, LSM5, LSM7, LSM8, METTL4, PABPC1, PCBP4, PIN1, POLR2B, POLR2E, PPP4R2, PRCC, PRDX6, PUF60, RAVER1, RBM15B, RBM28, RBM5, RBM6, REST, RNF113A, RNF113B, RP9, SAP18, SEM1, SF3A2, SF3A3, SNRPB2, SNRPD1, SNRPN, SUGP1, SUGP2, THOC1, THOC7, TRA2A, TSEN15, UBL5, USP4, XAB2, YJU2, YTHDC1, ZBTB7A]
GO:0000375	RNA splicing, via transesterification reactions	0,03	0,00	15,18	56,00	[BUD31, CACTIN, CELF4, CELF5, CHERP, CIRBP, COLEC12, CPSF1, CWC15, DAZAP1, DDX39A, DHX9, ELAVL1, GTF2F1, HNRNPA2B1, HNRNPM, HNRNPU, ISY1, ISY1-RAB43, KHDC4, KHDRBS3, KHSRP, LIN9, LSM3, LSM4, LSM5, LSM7, LSM8, PABPC1, PCBP4, PIN1, POLR2B, POLR2E, PRCC, PRDX6, PUF60, RAVER1, RBM15B, RBM5, RBM6, REST, RNF113A, SAP18, SF3A2, SF3A3, SNRPB2, SNRPD1, SNRPN, SUGP1, TRA2A, UBL5, USP4, XAB2, YJU2, YTHDC1, ZBTB7A]
GO:0000398	mRNA splicing, via spliceosome	0,04	0,00	15,03	55,00	[BUD31, CACTIN, CELF4, CELF5, CHERP, CIRBP, COLEC12, CPSF1, CWC15, DAZAP1, DDX39A, DHX9, ELAVL1, GTF2F1, HNRNPA2B1, HNRNPM, HNRNPU, ISY1, ISY1-RAB43, KHDC4, KHDRBS3, LIN9, LSM3, LSM4, LSM5, LSM7, LSM8, PABPC1, PCBP4, PIN1, POLR2B, POLR2E, PRCC, PRDX6, PUF60, RAVER1, RBM15B, RBM5, RBM6, REST, RNF113A, SAP18, SF3A2, SF3A3, SNRPB2, SNRPD1, SNRPN, SUGP1, TRA2A, UBL5, USP4, XAB2, YJU2, YTHDC1, ZBTB7A]
GO:0009416	response to light stimulus	0,02	0,00	15,79	57,00	[ABCA7, AQP1, ASNS, BHLHE40, BSG, CCDC66, CDC25A, CDKN2D, CHRNB2, CIRBP, CLOCK, CNGA1, COPS9, CRB1, CRTC1, DNM2, DTL, ELANE, EXT1, FBXL12, FBXL6, GNAT1, GNGT1, GPR52, GPX1, GRIN2A, H2AW, HOXA1, HRH1, HYAL1, HYAL2, HYAL3, IMPACT, JUND, KIT, MAP2K7, MAPRE2, MINDY4, MYC, NMU, NR2F6, OGG1, OPN1SW, OPN3, PARP1, PDC, PRKCD, PTGS2, PTN, REEP6, RPL26, SDE2, SPAM1, STK11, TMEM161A, TREX1, XPC]
GO:0009411	response to UV	0,04	0,00	17,90	29,00	[AQP1, CDC25A, CDKN2D, CIRBP, COPS9, DTL, ELANE, GPX1, H2AW, HYAL1, HYAL2, HYAL3, IMPACT, MAP2K7, MINDY4, MYC, OPN1SW, OPN3, PARP1, PRKCD, PTGS2, PTN, RPL26, SDE2, SPAM1, STK11, TMEM161A, TREX1, XPC]
GO:0071482	cellular response to light stimulus	0,02	0,00	19,08	29,00	[AQP1, CDC25A, CNGA1, COPS9, CRB1, GNAT1, GNGT1, GPR52, H2AW, HYAL1, HYAL2, HYAL3, IMPACT, MAPRE2, MINDY4, MYC, OPN1SW, OPN3, PARP1, PRKCD, PTGS2, PTN, RPL26, SDE2, SPAM1, STK11, TMEM161A, TREX1, XPC]
GO:0034644	cellular response to UV	0,01	0,00	22,77	23,00	[AQP1, CDC25A, COPS9, H2AW, HYAL1, HYAL2, HYAL3, IMPACT, MINDY4, MYC, OPN1SW, OPN3, PARP1, PRKCD, PTGS2, PTN, RPL26, SDE2, SPAM1, STK11, TMEM161A, TREX1, XPC]
GO:0007267	cell-cell signaling	0,02	0,00	12,41	227,00	[ABHD6, ADCY8, ADCYAP1, ADGRB1, ADGRE5, ADORA1, AGO2, AKAP9, AKR1B1, APBA3, APC2, APCDD1, AREG, ASPM, BSG, BSN, C3, CACNA1A, CACNA1D, CACNA1E, CACNA2D2, CADPS2, CALCA, CAMK1, CAV1, CCN3, CCN4, CCR1, CCR2, CCR5, CD34, CD70, CDH2, CDK14, CELF4, CELSR3, CFTR, CHRNA3, CHRNA5, CHRNB2, CHRNB4, CLOCK, CNIH4, CNTN4, CPAMD8, CRB1, CRHR2, CRTC1, CSNK1G2, CSPG5, CTHRC1, CXCL6, CXXC1, DAG1, DAPK3, DGKB, DLX5, DTNA, EFNA1, EFNA3, ENY2, EPHA5, ERC2, EREG, EXOC4, EXT1, FAM107A, FAM3D, FASLG, FCRL2, FLNB, FZD1, FZD6, FZR1, GABRA2, GABRA4, GABRG1, GDF15, GHRHR, GHRL, GIPC1, GJC2, GLUL, GNA15, GNAI2, GPNMB, GRIN2A, GRM2, GRM3, GRM7, GRM8, HCN2, HESX1, HOXA5, HRH1, HRH4, ICA1, IL6, ILDR2, ITPR1, JAGN1, KCND2, KCNN1, KCNQ3, KDM5B, KIT, KLF10, KLF15, KMO, LEP, LGR6, LIMD1, LRRC4, LSM4, LY6E, LY6H, MAFA, MDFIC, MIDN, MITF, MPC2, MPZL1, MYOC, NISCH, NMU, NPVF, NPY, NTRK1, OR10H1, OR10H2, OR10H3, OR10H4, OR10H5, OXTR, PFKFB2, PIAS4, PIN1, PIP5K1C, PLA2G4A, PPP1R9A, PRICKLE2, PRKACA, PRKAR2A, PSMA8, PSMD4, PTGS2, PTN, PTPN23, PTPRS, PXK, PYGO2, RAB11B, RAB3A, RAB43, RAB8A, RAF1, REST, RETN, RGS8, RHOA, RIMS2, RIT2, RNF138, RNF19A, RNU6-664P, RSPO2, RUVBL1, S100A9, S1PR2, SCRIB, SEM1, SEMA3B, SH3GL1, SHISA3, SLC1A6, SLC25A23, SLC30A1, SLC30A8, SLC6A1, SLC6A6, SLURP1, SLURP2, SMAD2, SMARCA4, SMO, SNAP47, SNAPIN, SOSTDC1, SRI, STAB1, STK11, STK3, STXBP2, SYBU, SYN2, SYT11, SYT17, SYT2, SYT4, TAC1, TLE2, TLE6, TMED1, TMEM9, TMF1, TNFSF18, TNFSF9, TNN, TNNC1, TNR, TPGS1, TRH, TSPAN12, UBA52, UBE2Q1, UBR5, UNC13A, USP46, VGLL4, WNT16, WNT2, WNT3A, WNT5A, WNT7A, WNT9A, XCL1, ZDHHC3]
GO:0099536	synaptic signaling	0,04	0,00	13,23	107,00	[ABHD6, ADCY8, ADCYAP1, ADGRB1, ADORA1, AKAP9, APBA3, BSG, BSN, CACNA1A, CACNA1E, CADPS2, CAMK1, CCR2, CDH2, CELF4, CHRNA3, CHRNA5, CHRNB2, CHRNB4, CNIH4, CNTN4, CRHR2, CRTC1, CSPG5, DAG1, DGKB, DTNA, ERC2, EXOC4, EXT1, FAM107A, FLNB, FZR1, GABRA2, GABRA4, GABRG1, GHRL, GIPC1, GLUL, GNA15, GNAI2, GRIN2A, GRM2, GRM3, GRM7, GRM8, HRH1, HRH4, KCND2, KCNN1, KCNQ3, KIT, KMO, LRRC4, LY6E, LY6H, NISCH, NMU, NPY, NTRK1, OR10H1, OR10H2, OR10H3, OR10H4, OR10H5, OXTR, PIP5K1C, PPP1R9A, PRKACA, PRKAR2A, PTGS2, PTN, PTPRS, PXK, RAB3A, RAB8A, RETN, RGS8, RIMS2, RIT2, RNF19A, S1PR2, SCRIB, SH3GL1, SLC1A6, SLC30A1, SLC6A1, SLC6A6, SLURP1, SLURP2, SNAP47, SNAPIN, STXBP2, SYBU, SYN2, SYT11, SYT2, SYT4, TAC1, TNR, TPGS1, UNC13A, USP46, WNT3A, WNT7A, ZDHHC3]
GO:0099537	trans-synaptic signaling	0,04	0,00	13,31	105,00	[ABHD6, ADCY8, ADCYAP1, ADGRB1, ADORA1, AKAP9, BSG, CACNA1A, CACNA1E, CADPS2, CAMK1, CCR2, CDH2, CELF4, CHRNA3, CHRNA5, CHRNB2, CHRNB4, CNIH4, CNTN4, CRHR2, CRTC1, CSPG5, DGKB, ERC2, FAM107A, FLNB, FZR1, GHRL, GIPC1, GLUL, GNAI2, GRIN2A, GRM2, GRM3, GRM7, GRM8, HRH1, KIT, KMO, LRRC4, NISCH, NMU, NTRK1, OXTR, PPP1R9A, PRKACA, PTGS2, PTN, PTPRS, PXK, RAB3A, RAB8A, RETN, RIMS2, RNF19A, S1PR2, SH3GL1, SLC30A1, SLC6A1, SLC6A6, SNAP47, SNAPIN, SYBU, SYT11, SYT4, TAC1, TNR, UNC13A, USP46, WNT3A, WNT7A, ZDHHC3]
GO:0050804	modulation of chemical synaptic transmission	0,01	0,00	15,35	70,00	[ABHD6, ADCY8, ADCYAP1, ADGRB1, ADORA1, AKAP9, APBA3, BSG, BSN, CACNA1A, CACNA1E, CADPS2, CAMK1, CCR2, CDH2, CELF4, CHRNA3, CHRNA5, CHRNB2, CHRNB4, CNIH4, CNTN4, CRHR2, CRTC1, CSPG5, DGKB, DTNA, ERC2, EXOC4, EXT1, FAM107A, FLNB, FZR1, GABRA2, GABRA4, GABRG1, GHRL, GIPC1, GLUL, GNAI2, GRIN2A, GRM2, GRM3, GRM7, GRM8, HRH1, HRH4, KCND2, KCNN1, KCNQ3, KIT, KMO, LRRC4, LY6E, LY6H, NISCH, NMU, NPY, NTRK1, OR10H1, OR10H2, OR10H3, OR10H4, OR10H5, OXTR, PIP5K1C, PPP1R9A, PRKACA, PRKAR2A, PTGS2, PTN, PTPRS, PXK, RAB3A, RAB8A, RETN, RIMS2, RIT2, RNF19A, S1PR2, SCRIB, SH3GL1, SLC1A6, SLC30A1, SLC6A1, SLC6A6, SLURP1, SLURP2, SNAP47, SNAPIN, STXBP2, SYBU, SYN2, SYT11, SYT2, SYT4, TAC1, TNR, TPGS1, UNC13A, USP46, WNT3A, WNT7A, ZDHHC3]
GO:0007268	chemical synaptic transmission	0,04	0,00	13,35	104,00	

GO:0023051	regulation of signaling	0,00	0,00	11,89	442,00	[ABCA7, ABHD6, ABL2, ABRA, ADAMTS3, ADAR, ADCY8, ADCYAP1, ADCYAP1R1, ADGRB1, ADIPOR1, ADORA1, AGR2, AKAP9, AKR1B1, AKT3, ANGPT1, ANKRD17, APC2, APCDD1, APPL1, AREG, ARHGAP28, ARHGAP39, ARHGAP45, ARHGEF11, ARHGEF18, ARHGEF2, ARHGEF3, ARL6IP5, ASH1L, ASPM, ATF3, ATP1B1, ATP2B2, ATRIP, BECN2, BMPER, BMT2, BRD4, BRPF1, BSG, BST2, BUD31, C18orf32, C3, CACNA1A, CACNA1D, CACNA1E, CACNA2D2, CACTIN, CALCA, CALCR, CALR, CARM1, CAV1, CAV2, CAV3, CC2D1A, CCL25, CCN3, CCN4, CCR1, CCR2, CD46, CD55, CDC34, CDH2, CDK14, CDKN2D, CELF4, CFTR, CHERP, CHI3L1, CHN2, CHRNA3, CHRNA5, CHRNB2, CHRNB4, CIDEA, CISH, CLEC16A, CLOCK, CNGA1, CNIH3, CNIH4, CNTN4, CNTN6, CORIN, CREB3L4, CRHR2, CRTC1, CSNK1G2, CSPG5, CTHRC1, CXCL8, CXXC1, CYRIB, DAG1, DAND5, DAP3, DAPK3, DCST1, DENND3, DENND4B, DEPTOR, DGKB, DIRAS1, DLX5, DNAJB9, DNM2, DOT1L, DYRK3, EEF1D, EFNA1, ELANE, ELF3, ELOF1, ELP2, EMP2, ENY2, EPGN, EPHA5, EPOR, EPS15L1, ERC2, EREG, EXO1, F2RL3, FAM107A, FAM3D, FASLG, FGF22, FLNB, FOXH1, FOXP1, FSTL3, FZD6, FZR1, G0S2, GADD45B, GAREM1, GARS1, GBA, GDF15, GHRHR, GHRL, GIPC1, GLUL, GMIP, GNAI2, GNAT1, GORAB, GPNMB, GPR108, GPR161, GPR37, GPR37L1, GPR62, GPX1, GREM2, GRIN2A, GRINA, GRM2, GRM3, GRM7, GRM8, GSDME, GSX2, H3-3B, HAX1, HDAC9, HOMER3, HOXA13, HRH1, HRH4, HYAL2, ICA1, ICAM1, IFT122, IGFBP7, IL10, IL17RD, IL19, IL24, IL6, IL6R, INAVA, ING3, INSR, IQGAP3, IQSEC1, IRAK2, ITPKB, ITPR1, IVNS1ABP, JAGN1, JAK3, KANK2, KCP, KCTD6, KCTD8, KDM5B, KDR, KIT, KLF14, KLF15, KLHDC10, KMO, LAMTOR2, LEFTY1, LEFTY2, LEP, LGR6, LIMD1, LITAF, LMCD1, LMNA, LRG1, LRRC14, LRRC4, LRRD1, LSM4, LTF, LY6E, LY6H, MAP2K2, MAP2K7, MAPKAPK3, MAPRE2, MBD3, MBD4, MDFIC, MET, MGLL, MIDN, MIOS, MOCOS, MPC2, MST1, MST1R, MTURN, MUC1, MVB12A, MYC, MYDGF, MYO9B, MYOC, NANOS3, NCLN, NDC80, NDUFA13, NISCH, NMU, NOD1, NOTCH3, NPR1, NPRL2, NPVF, NTRK1, OBSCN, OCIAD1, OCIAD2, OXTR, PALM, PALM3, PARP1, PDC, PDE4A, PDGFRA, PEG10, PFKFB2, PHF14, PIAS2, PIAS4, PIK3R2, PIN1, PIP5K1C, PKN1, PLIN5, PLXNB1, PPARG, PPP1R9A, PRDX1, PRDX2, PRKACA, PRKAR2A, PRKCD, PROK2, PROX1, PRRX1, PSCA, PSMA8, PSMD4, PTGS2, PTK2, PTN, PTP4A3, PTPN2, PTPN23, PTPRC, PTPRS, PXK, QARS1, RAB3A, RAB7A, RAB8A, RAF1, RALBP1, RALGPS2, RASAL3, RASL11B, RBBP8, RC3H1, REST, RETN, RGS16, RGS22, RGS7, RGS8, RHOA, RIMS2, RIOK3, RIT2, RMI2, RNASEL, RNF113A, RNF125, RNF126, RNF165, RNF19A, RNU6-664P, ROCK1, RPA3, RPL11, RPL17, RPL23, RPL26, RRM2B, RSPO2, RUVBL1, S100A12, S100A13, S100A4, S100A9, S1PR2, SAFB2, SCRIB, SEC13, SELENOK, SELP, SEM1, SH3GL1, SHARPIN, SHC1, SHISA3, SHISA5, SKOR2, SLA, SLC25A23, SLC30A1, SLC30A8, SLC44A2, SLC6A1, SLC6A6, SLURP2, SMAD2, SMAD7, SMARCA4, SMO, SMYD2, SNAP47, SNAPIN, SNX13, SOCS1, SOSTDC1, SPPL2B, SRGAP3, SRI, STAP1, STIMATE, STK11, STK3, STK38, SYBU, SYDE1, SYT11, SYT4, TAC1, TAF2, TAF4B, TAFA1, TAFA4, TAX1BP1, TBX20, TDGF1, TDGF1P3, THOC1, TICAM1, TLE2, TLE6, TLR9, TMEM161A, TMEM33, TMEM65, TMEM9, TMF1, TNFAIP8L1, TNFSF14, TNN, TNR, TP53BP2, TPR, TRAF5, TRAIP, TREX1, TRH, TRIB1, TRIP10, TSPAN12, TWSG1, TXK, UBA52, UBR5, UNC13A, USP46, VAPA, VAV1, VGLL4, WFS1, WNT16, WNT3A, WNT5A, WNT7A, XCL1, XCL2, YJU2, ZBTB7A, ZBTB7B, ZC3H3, ZC3HC1, ZDHHC3, ZNF653]
GO:0007165	signal transduction	0,01	0,00	11,13	737,00	[ABCA7, ABHD17A, ABHD6, ABL2, ABRA, ADAM15, ADAMTS3, ADAR, ADCY10, ADCY8, ADCYAP1, ADCYAP1R1, ADGRB1, ADGRE1, ADGRE3, ADGRE5, ADGRL1, ADGRL3, ADIPOR1, ADORA1, AFP, AGO2, AGR2, AHR, AKAP8, AKAP9, AKR1B1, AKT3, AMBN, ANGPT1, ANGPTL1, ANGPTL8, ANKRD17, APC2, APCDD1, APPL1, AQP1, AREG, ARF4, ARHGAP28, ARHGAP39, ARHGAP45, ARHGEF11, ARHGEF18, ARHGEF2, ARHGEF3, ARID3A, ARL6IP5, ARPC4, ARPC4-TTLL3, ARPC5, ASB14, ASB15, ASB4, ASH1L, ASPM, ATF3, ATP1B1, ATP6V1C1, ATP6V1F, ATP6V1G3, ATRIP, BABAM1, BECN2, BMPER, BMT2, BRD4, BRK1, BRPF1, BSG, BSN, BST2, BUD31, C18orf32, C3, CACNA1A, CACNA1D, CACTIN, CALCA, CALCR, CALR, CALR3, CAMK1, CAPS, CARM1, CAV1, CAV2, CAV3, CC2D1A, CCL25, CCN3, CCN4, CCR1, CCR2, CCR3, CCR5, CCR9, CCRL2, CD247, CD320, CD34, CD46, CD55, CD70, CDC34, CDC37, CDC42BPA, CDH2, CDK14, CDKN2D, CELF4, CELSR3, CENPF, CHERP, CHI3L1, CHL1, CHN2, CHRNA3, CHRNA5, CHRNB2, CHRNB4, CIDEA, CIITA, CISH, CLEC16A, CLEC4M, CLOCK, CNGA1, CNIH3, CNIH4, CNN2, CNTN6, COL1A2, COLEC10, COLEC12, COMP, CPAMD8, CR1, CRABP2, CREB3L3, CREB3L4, CRHR2, CRLF1, CRTC1, CSNK1G2, CSPG5, CTHRC1, CXCL6, CXCL8, CXCR6, CXXC1, CYRIB, DAG1, DAND5, DAP3, DAPK3, DCST1, DENND1B, DENND3, DENND4B, DEPTOR, DERL1, DGKB, DIRAS1, DLX5, DNAJB9, DNM2, DNMT1, DOCK3, DOCK4, DOCK6, DOT1L, DTL, DTNA, DYRK3, E2F4, EBI3, EDEM1, EEF1D, EEPD1, EFNA1, EFNA3, ELANE, ELF3, ELMO1, ELOF1, ELP2, EMP2, EPG5, EPGN, EPHA5, EPOR, EPS15L1, EREG, EXO1, EXOC1, EXT1, F2RL3, FAM3C, FAM3D, FAM83A, FAM83H, FANCD2, FASLG, FCER2, FCRL1, FCRL2, FCRL4, FCRL5, FGF22, FHIT, FLNB, FOXH1, FOXP1, FSTL3, FZD1, FZD6, FZR1, G0S2, GABRA2, GABRA4, GABRG1, GADD45B, GAREM1, GARS1, GBA, GDF15, GGCT, GHRHR, GHRL, GIPC1, GMIP, GNA15, GNAI2, GNAL, GNAT1, GNG11, GNGT1, GNRHR, GORAB, GPNMB, GPR108, GPR141, GPR161, GPR25, GPR37, GPR37L1, GPR52, GPR62, GPR85, GPX1, GREM2, GRIN2A, GRINA, GRIP2, GRM2, GRM3, GRM7, GRM8, GSDME, GSX2, GTF2F1, H3-3B, HAX1, HDAC9, HDGF, HERPUD2, HESX1, HHAT, HNRNPA2B1, HNRNPM, HOMER3, HOXA13, HRH1, HRH4, HSF1, HSH2D, HYAL2, ICAM1, ICAM3, IFI30, IFT122, IGFBP7, IL10, IL12RB1, IL17RB, IL17RC, IL17RD, IL17RE, IL19, IL20, IL24, IL27RA, IL5RA, IL6, IL6R, IMPA2, INAVA, ING3, INSR, INSRR, INTS3, INTS7, IP6K2, IQGAP3, IQSEC1, IQUB, IRAK2, IRF5, IRF6, ITGB8, ITPKB, ITPR1, IVNS1ABP, JAGN1, JAK3, JUNB, KANK2, KBTBD2, KCNK2, KCP, KCTD6, KCTD8, KDR, KIFAP3, KIT, KLF14, KLF15, KLF16, KLHDC10, KLHL7, KRIT1, LAMA1, LAMA3, LAMTOR2, LEFTY1, LEFTY2, LEP, LGR6, LIMD1, LITAF, LMCD1, LMNA, LONP1, LPAR2, LRG1, LRP12, LRRC14, LRRC2, LRRC30, LRRD1, LSM4, LTF, LY6E, LY6H, MACC1, MADCAM1, MAEL, MAFA, MAGI1, MANF, MAP2K2, MAP2K7, MAPK15, MAPK4, MAPKAPK3, MAPRE2, MAST1, MAST3, MATK, MBD3, MBD4, MDFIC, MET, MGLL, MIB1, MINDY4, MIOS, MITF, MKLN1, MOB1B, MOCOS, MPZL1, MST1, MST1R, MTSS1, MTURN, MUC1, MUC16, MVB12A, MYC, MYDGF, MYO9B, MYOC, MYOM1, NANOS3, NCALD, NCF2, NCKIPSD, NCLN, NDC80, NDRG1, NDUFA13, NISCH, NMU, NOD1, NOTCH3, NPBWR2, NPR1, NPRL2, NPSR1, NPVF, NPY, NR2C2, NR2F6, NR5A2, NRBP2, NRTN, NTRK1, OBSCN, OCIAD1, OCIAD2, OPN1SW, OPN3, OR10H1, OR10H2, OR10H3, OR10H4, OR10H5, OR10X1, OR13G1, OR14I1, OR1I1, OR1M1, OR2AJ1, OR2AK2, OR2G6, OR2L13, OR2L2, OR2L3, OR2L5, OR2L8, OR2M2, OR2M3, OR2M5, OR2M7, OR2T1, OR2T11, OR2T12, OR2T2, OR2T27, OR2T29, OR2T33, OR2T35, OR2T4, OR2T5, OR2T6, OR2T8, OR6F1, OR7A10, OR7A17, OR7A5, OR7C1, OR7C2, OR7D2, OR7D4, OR7E24, OR7G1, OR7G2, OR7G3, OXTR, P2RY11, PALM, PALM3, PARP1, PCBP4, PDC, PDE1C, PDE4A, PDE4C, PDGFRA, PDK4, PEAR1, PEG10, PHF14, PIAS2, PIAS4, PIGR, PIK3C3, PIK3R2, PIN1, PIP5K1C, PKN1, PKP1, PLIN5, PLK5, PLP2, PLPP2, PLPPR2, PLPPR3, PLVAP, PLXNA1, PLXNA2, PLXNA4, PLXNB1, PLXND1, POLR2B, POLR2E, POU2F1, PPAN-P2RY11, PPARG, PPBP, PPP1R12B, PPP1R17, PPP1R9A, PPP2R5A, PPP4R1, PRDX1, PRDX2, PRICKLE2, PRKACA, PRKAR2A, PRKCD, PRKCSH, PROK2, PROX1, PRRX1, PSCA, PSEN2, PSMA8, PSMD4, PSMG2, PSPN, PTGER1, PTGS2, PTH1R, PTK2, PTN, PTP4A3, PTPN2, PTPN7, PTPRC, PTPRG, PTPRM, PTPRS, PTPRZ1, PYGO2, QARS1, QRICH1, RAB12, RAB13, RAB7A, RABIF, RAF1, RALBP1, RALGPS2, RAPGEF5, RASAL2, RASAL3, RASL11B, RASSF1, RASSF6, RBBP8, RC3H1, RETN, RFXANK, RGL1, RGS16, RGS22, RGS7, RGS8, RHOA, RHPN1, RIMS2, RIOK3, RIT1, RIT2, RLN3, RMI2, RNASEH2A, RNASEL, RNF113A, RNF125, RNF126, RNF138, RNF165, RNU6-664P, ROCK1, RPA3, RPL11, RPL17, RPL23, RPL26, RPS6KC1, RRM2B, RSPO2, RUVBL1, S100A1, S100A12, S100A13, S100A14, S100A4, S100A6, S100A9, S1PR2, S1PR4, S1PR5, SAFB, SAFB2, SCAP, SCX, SDE2, SEC13, SELE, SELENOK, SELP, SEM1, SEMA3B, SEMA3F, SEMA3G, SEMA4A, SEMA6B, SH2D2A, SH2D3A, SH3GL1, SHARPIN, SHC1, SHISA3, SHISA5, SKAP2, SKOR2, SLA, SLC25A23, SLC27A1, SLC44A2, SLC6A20, SLURP1, SLURP2, SMAD2, SMAD7, SMARCA4, SMARCC1, SMO, SMYD2, SNX13, SOCS1, SOSTDC1, SPPL2B, SRGAP3, SRI, SS18, STAP1, STAP2, STIMATE, STK11, STK3, STK38, SYDE1, TAC1, TADA3, TAF2, TAF4B, TAFA1, TAFA4, TATDN2, TAX1BP1, TBX20, TBXA2R, TDGF1, TDGF1P3, TG, THOC1, TICAM1, TIMP4, TIPRL, TLE2, TLE6, TLR9, TMED1, TMEM161A, TMEM33, TMEM38A, TMEM9, TMF1, TNFAIP8L1, TNFRSF11B, TNFSF14, TNFSF18, TNFSF4, TNFSF9, TNN, TP53BP2, TPR, TPRA1, TRAF5, TRAIP, TREX1, TRH, TRHR, TRIB1, TRIL, TRIP10, TSPAN12, TSSK6, TWSG1, TXK, TYK2, UBA52, UBR5, UNC13A, VAPA, VAV1, VGLL4, VN1R5, WASL, WFS1, WIPF3, WNT16, WNT2, WNT3A, WNT5A, WNT7A, WNT9A, XCL1, XCL2, XCR1, XPC, XPR1, YES1, YJU2, YOD1, ZBTB7A, ZBTB7B, ZC3H3, ZC3HC1, ZDHHC3, ZNF653]
GO:0023056	positive regulation of signaling	0,04	0,00	12,06	227,00	[ABCA7, ABRA, ADAMTS3, ADCY8, ADCYAP1, ADCYAP1R1, ADIPOR1, ADORA1, AGR2, AKR1B1, AKT3, ANGPT1, ANKRD17, AREG, ARHGEF3, ARL6IP5, ASPM, ATF3, BMPER, BRD4, BST2, C18orf32, C3, CALCR, CALR, CAV1, CAV2, CC2D1A, CCL25, CCN3, CCN4, CCR1, CCR2, CDH2, CFTR, CHERP, CHI3L1, CLEC16A, CNTN6, CRHR2, CRTC1, CSNK1G2, CXXC1, DAPK3, DIRAS1, DLX5, EEF1D, EFNA1, ELANE, ELF3, EMP2, EPGN, EPOR, EREG, F2RL3, FAM107A, FASLG, FGF22, FLNB, FOXP1, G0S2, GADD45B, GAREM1, GBA, GDF15, GHRHR, GHRL, GIPC1, GLUL, GNAI2, GORAB, GPNMB, GPR37, GPR37L1, GPR62, GPX1, GRIN2A, GSDME, GSX2, HAX1, HYAL2, ICAM1, IL10, IL19, IL6, IL6R, INAVA, ING3, INSR, IQGAP3, IRAK2, ITPKB, KCP, KDR, KIT, KLF14, KLHDC10, KMO, LAMTOR2, LEFTY1, LEFTY2, LEP, LGR6, LITAF, LMCD1, LRG1, LRRD1, LSM4, LTF, MAP2K2, MAP2K7, MAPKAPK3, MAPRE2, MBD4, MDFIC, MET, MIOS, MOCOS, MPC2, MST1R, MTURN, MYDGF, MYOC, NANOS3, NDC80, NMU, NOD1, NPR1, NPRL2, NTRK1, OCIAD1, OCIAD2, OXTR, PARP1, PDGFRA, PFKFB2, PIAS4, PIK3R2, PIN1, PKN1, PLXNB1, PPP1R9A, PRDX2, PRKCD, PROK2, PROX1, PRRX1, PSMA8, PSMD4, PTGS2, PTK2, PTN, PTP4A3, PTPN2, PTPN23, PTPRC, RAF1, RC3H1, RETN, RHOA, RIMS2, RIT2, RNF165, RNU6-664P, ROCK1, RPL11, RPL17, RPL23, RPL26, RSPO2, RUVBL1, S100A12, S100A13, S100A4, S100A9, S1PR2, SCRIB, SEC13, SELP, SEM1, SHARPIN, SHC1, SHISA5, SKOR2, SLC30A8, SLC44A2, SMAD2, SMARCA4, SMO, SNAP47, SOCS1, SRI, STAP1, STIMATE, STK11, STK3, SYBU, SYT11, TAC1, TBX20, TDGF1, TDGF1P3, TICAM1, TLR9, TMEM33, TMEM9, TMF1, TNFSF14, TNR, TPR, TRAF5, TRH, TWSG1, TXK, UBA52, UBR5, VAPA, VAV1, WNT16, WNT3A, WNT5A, WNT7A, XCL1, XCL2, ZBTB7B, ZC3H3, ZDHHC3]

GO:0010646	regulation of cell communication	0,00	0,00	11,88	437,00	[ABCA7, ABHD6, ABL2, ABRA, ADAMTS3, ADAR, ADCY8, ADCYAP1, ADCYAP1R1, ADGRB1, ADIPOR1, ADORA1, AGR2, AKAP9, AKR1B1, AKT3, ANGPT1, ANKRD17, APC2, APCDD1, APPL1, AREG, ARHGAP28, ARHGAP39, ARHGAP45, ARHGEF11, ARHGEF18, ARHGEF2, ARHGEF3, ARL6IP5, ASH1L, ASPM, ATF3, ATRIP, BECN2, BMPER, BMT2, BRD4, BRPF1, BSG, BST2, BUD31, C18orf32, C3, CACNA1A, CACNA1D, CACNA1E, CACNA2D2, CACTIN, CALCA, CALCR, CALR, CARM1, CAV1, CAV2, CAV3, CC2D1A, CCL25, CCN3, CCN4, CCR1, CCR2, CD46, CD55, CDC34, CDH2, CDK14, CDKN2D, CELF4, CFTR, CHERP, CHI3L1, CHN2, CHRNA3, CHRNA5, CHRNB2, CHRNB4, CIDEA, CISH, CLEC16A, CLOCK, CNGA1, CNIH3, CNIH4, CNTN4, CNTN6, CREB3L4, CRHR2, CRTC1, CSNK1G2, CSPG5, CTHRC1, CXCL8, CXXC1, CYRIB, DAG1, DAND5, DAPK3, DCST1, DENND3, DENND4B, DEPTOR, DGKB, DIRAS1, DLX5, DNAJB9, DNM2, DOT1L, DYRK3, EEF1D, EFNA1, ELANE, ELF3, ELOF1, ELP2, EMP2, ENY2, EPGN, EPHA5, EPOR, EPS15L1, ERC2, EREG, EXO1, F2RL3, FAM107A, FAM3D, FASLG, FGF22, FLNB, FOXH1, FOXP1, FSTL3, FZD6, FZR1, G0S2, GADD45B, GAREM1, GARS1, GBA, GDF15, GHRHR, GHRL, GIPC1, GLUL, GMIP, GNAI2, GNAT1, GORAB, GPNMB, GPR108, GPR161, GPR37, GPR37L1, GPR62, GPX1, GREM2, GRIN2A, GRINA, GRM2, GRM3, GRM7, GRM8, GSDME, GSX2, H3-3B, HAX1, HDAC9, HOMER3, HOXA13, HRH1, HRH4, HYAL2, ICA1, ICAM1, IFT122, IGFBP7, IL10, IL17RD, IL19, IL24, IL6, IL6R, INAVA, ING3, INSR, IQGAP3, IQSEC1, IRAK2, ITPKB, ITPR1, IVNS1ABP, JAGN1, JAK3, KANK2, KCP, KCTD6, KCTD8, KDM5B, KDR, KIT, KLF14, KLF15, KLHDC10, KMO, LAMTOR2, LEFTY1, LEFTY2, LEP, LGR6, LIMD1, LITAF, LMCD1, LMNA, LRG1, LRRC14, LRRC4, LRRD1, LSM4, LTF, LY6E, LY6H, MAP2K2, MAP2K7, MAPKAPK3, MAPRE2, MBD3, MBD4, MDFIC, MET, MGLL, MIDN, MIOS, MOCOS, MPC2, MST1, MST1R, MTURN, MUC1, MVB12A, MYC, MYDGF, MYO9B, MYOC, NANOS3, NCLN, NDC80, NDUFA13, NISCH, NMU, NOD1, NOTCH3, NPR1, NPRL2, NPVF, NTRK1, OBSCN, OCIAD1, OCIAD2, OXTR, PALM, PALM3, PARP1, PDC, PDE4A, PDGFRA, PEG10, PFKFB2, PHF14, PIAS2, PIAS4, PIK3R2, PIN1, PIP5K1C, PKN1, PLIN5, PLXNB1, PPARG, PPP1R9A, PRDX1, PRDX2, PRKACA, PRKAR2A, PRKCD, PROK2, PROX1, PRRX1, PSCA, PSMA8, PSMD4, PTGS2, PTK2, PTN, PTP4A3, PTPN2, PTPN23, PTPRC, PTPRS, PXK, QARS1, RAB3A, RAB7A, RAB8A, RAF1, RALBP1, RALGPS2, RASAL3, RASL11B, RBBP8, RC3H1, REST, RETN, RGS16, RGS22, RGS7, RGS8, RHOA, RIMS2, RIOK3, RIT2, RMI2, RNASEL, RNF113A, RNF125, RNF126, RNF165, RNF19A, RNU6-664P, ROCK1, RPA3, RPL11, RPL17, RPL23, RPL26, RRM2B, RSPO2, RUVBL1, S100A12, S100A13, S100A4, S100A9, S1PR2, SAFB2, SEC13, SELENOK, SELP, SEM1, SH3GL1, SHARPIN, SHC1, SHISA3, SHISA5, SKOR2, SLA, SLC25A23, SLC30A1, SLC30A8, SLC44A2, SLC6A1, SLC6A6, SLURP2, SMAD2, SMAD7, SMARCA4, SMO, SMYD2, SNAP47, SNAPIN, SNX13, SOCS1, SOSTDC1, SPPL2B, SRGAP3, SRI, STAP1, STIMATE, STK11, STK3, STK38, SYBU, SYDE1, SYT11, SYT4, TAC1, TAF2, TAF4B, TAFA1, TAFA4, TAX1BP1, TBX20, TDGF1, TDGF1P3, THOC1, TICAM1, TLE2, TLE6, TLR9, TMEM161A, TMEM33, TMEM9, TMF1, TNFAIP8L1, TNFSF14, TNN, TNR, TP53BP2, TPR, TRAF5, TRAIP, TREX1, TRH, TRIB1, TRIP10, TSPAN12, TWSG1, TXK, UBA52, UBR5, UNC13A, USP46, VAPA, VAV1, VGLL4, WFS1, WNT16, WNT3A, WNT5A, WNT7A, XCL1, XCL2, YJU2, ZBTB7A, ZBTB7B, ZC3H3, ZC3HC1, ZDHHC3, ZNF653]
GO:0010647	positive regulation of cell communication	0,04	0,00	12,04	226,00	[ABCA7, ABRA, ADAMTS3, ADCY8, ADCYAP1, ADCYAP1R1, ADIPOR1, ADORA1, AGR2, AKR1B1, AKT3, ANGPT1, ANKRD17, AREG, ARHGEF3, ARL6IP5, ASPM, ATF3, BMPER, BRD4, BST2, C18orf32, C3, CALCR, CALR, CAV1, CAV2, CC2D1A, CCL25, CCN3, CCN4, CCR1, CCR2, CDH2, CFTR, CHERP, CHI3L1, CLEC16A, CNTN6, CRHR2, CRTC1, CSNK1G2, CXXC1, DAPK3, DIRAS1, DLX5, EEF1D, EFNA1, ELANE, ELF3, EMP2, EPGN, EPOR, EREG, F2RL3, FAM107A, FASLG, FGF22, FLNB, FOXP1, G0S2, GADD45B, GAREM1, GBA, GDF15, GHRHR, GHRL, GIPC1, GLUL, GNAI2, GORAB, GPNMB, GPR37, GPR37L1, GPR62, GPX1, GRIN2A, GSDME, GSX2, HAX1, HYAL2, ICAM1, IL10, IL19, IL6, IL6R, INAVA, ING3, INSR, IQGAP3, IRAK2, ITPKB, KCP, KDR, KIT, KLF14, KLHDC10, KMO, LAMTOR2, LEFTY1, LEFTY2, LEP, LGR6, LITAF, LMCD1, LRG1, LRRD1, LSM4, LTF, MAP2K2, MAP2K7, MAPKAPK3, MAPRE2, MBD4, MDFIC, MET, MIOS, MOCOS, MPC2, MST1R, MTURN, MYDGF, MYOC, NANOS3, NDC80, NMU, NOD1, NPR1, NPRL2, NTRK1, OCIAD1, OCIAD2, OXTR, PARP1, PDGFRA, PFKFB2, PIAS4, PIK3R2, PIN1, PKN1, PLXNB1, PPP1R9A, PRDX2, PRKCD, PROK2, PROX1, PRRX1, PSMA8, PSMD4, PTGS2, PTK2, PTN, PTP4A3, PTPN2, PTPN23, PTPRC, RAF1, RC3H1, RETN, RHOA, RIMS2, RIT2, RNF165, RNU6-664P, ROCK1, RPL11, RPL17, RPL23, RPL26, RSPO2, RUVBL1, S100A12, S100A13, S100A4, S100A9, S1PR2, SEC13, SELP, SEM1, SHARPIN, SHC1, SHISA5, SKOR2, SLC30A8, SLC44A2, SMAD2, SMARCA4, SMO, SNAP47, SOCS1, SRI, STAP1, STIMATE, STK11, STK3, SYBU, SYT11, TAC1, TBX20, TDGF1, TDGF1P3, TICAM1, TLR9, TMEM33, TMEM9, TMF1, TNFSF14, TNR, TPR, TRAF5, TRH, TWSG1, TXK, UBA52, UBR5, VAPA, VAV1, WNT16, WNT3A, WNT5A, WNT7A, XCL1, XCL2, ZBTB7B, ZC3H3, ZDHHC3]
GO:0050793	regulation of developmental process	0,01	0,00	12,04	311,00	[ADAMTS9, ADCYAP1, ADGRB1, ADGRL1, ADIPOR1, AFG3L2, AGO2, AGR2, AKR1B1, AKT3, ALDOA, AMIGO3, AMTN, ANGPTL4, ANKLE1, ANKRD17, AP3D1, APC2, AQP1, AREG, ARHGEF2, ASAP1, ASB4, ASPM, BHLHE40, BMPER, BRINP2, C3, CALCA, CALR, CAMK1, CAMP, CAMSAP2, CAPN2, CARM1, CAV1, CAV3, CCN3, CCN4, CCR1, CCR2, CCR3, CD34, CD46, CDH2, CDK6, CELF4, CELSR3, CENPF, CHERP, CHI3L1, CHRNA3, CHRNB2, CLOCK, CNTN4, COMP, CPNE9, CR1, CRABP2, CRTC1, CSMD3, CSPG5, CSRP1, CTHRC1, CXCL8, CXXC1, CYRIB, DAG1, DAND5, DAPK3, DCSTAMP, DMTF1, DNM2, DNM3, DNMT1, EFNA1, EFNA3, ELAVL1, EMP2, ENAM, ENPP2, EPB41L3, EPPK1, EREG, FASLG, FERD3L, FEZF2, FGD5, FLVCR1, FOXP1, FSTL3, FYCO1, FZD1, FZD6, FZR1, GARS1, GATA2, GDF15, GHRHR, GHRL, GJC2, GLUL, GPNMB, GPR37L1, GRHL2, GSX2, H1-8, H3-3B, HAS2, HAX1, HDAC9, HESX1, HMCES, HNRNPU, HOOK2, HOPX, HOXA11, HOXA2, HOXA5, HOXA7, HSF1, HYAL1, HYAL3, ICAM1, IL10, IL12RB1, IL17RD, IL20, IL6, IL6R, IMPACT, ING3, INSR, IQGAP3, ITGB8, ITPKB, JAK3, JUNB, JUND, KCNK2, KDM5B, KDR, KEAP1, KIF14, KIT, KLF10, KRIT1, LAMA1, LAMA3, LDLR, LEP, LIMD1, LMNA, LMOD3, LONP1, LRG1, LRP12, LRRC24, LRRN1, LRRN3, LTF, MAEL, MBD1, MBD4, MIB1, MINDY4, MITF, MKLN1, MST1, MTURN, MYC, MYDGF, MYL12A, MYOC, MYOG, NANOS3, NAXE, NEK4, NOTCH3, NPR1, NPRL2, NR2C2, NTRK1, OCIAD1, OLFM2, OSR2, OXTR, P4HTM, PALM, PARP1, PARP3, PAX4, PDGFRA, PEAK3, PGLYRP2, PHF14, PHOX2B, PIN1, PKN1, PLXNA1, PLXNA2, PLXNA4, PLXNB1, PLXND1, PPARG, PPP1R9A, PRDX2, PRICKLE2, PRKACA, PROK2, PROX1, PRRX1, PSMA8, PSMD4, PTGS2, PTK2, PTN, PTPN2, PTPRC, PTPRM, PTPRS, PTPRZ1, RAF1, RALBP1, RC3H1, REST, RETN, RHOA, RIMS2, RNASEH2A, RNU6-664P, ROCK1, RSL1D1, RSPO2, RUFY3, S100A1, S100A9, S1PR2, S1PR5, SCIN, SCX, SEM1, SEMA3B, SEMA3F, SEMA3G, SEMA4A, SEMA6B, SEPTIN7, SFMBT1, SIGLEC15, SIRT6, SKOR2, SLC25A23, SLC6A6, SMAD2, SMAD7, SMO, SOCS1, SOSTDC1, SPAM1, ST7, STAB1, STK11, STK3, STRIP2, SUCO, SULT1E1, SYDE1, SYT17, SYT2, SYT4, TBX20, TBXA2R, TCF3, TCTA, TG, THOC1, TLE6, TLR9, TMEM106B, TMEM79, TNFRSF11B, TNFSF18, TNFSF4, TNFSF9, TNN, TNR, TRIB1, TRIM11, TRIM46, TRPS1, TSPAN12, TWF2, TWSG1, UNC13A, USP19, UTP25, VASH2, VGLL4, WNT2, WNT3A, WNT5A, WNT7A, WNT9A, ZBTB7B, ZBTB7C, ZFPM2, ZHX2, ZNF16, ZNF277, ZNF706]
GO:0051239	regulation of multicellular organismal process	0,02	0,00	11,88	337,00	[ABCA7, ABHD6, ACP5, ADAMTS9, ADCYAP1, ADGRB1, ADIPOR1, ADORA1, AFG3L2, AGO2, AKAP8, AKAP9, AKR1B1, AKT3, AMIGO3, AMTN, ANGPT1, ANGPTL4, AP3D1, APPL1, AQP1, AREG, ARHGEF2, ASPM, ATP1B1, ATP2B2, ATP5F1A, BAP1, BHLHE40, BMPER, BST2, C3, CACNA1D, CACNA2D2, CACTIN, CALCA, CALCR, CALR, CAMP, CAPN2, CAV1, CAV3, CCN3, CCN4, CCR1, CCR2, CCR3, CD34, CD46, CD55, CDK6, CELF4, CHI3L1, CHRNA3, CHRNB2, CIDEA, CLOCK, CNIH4, CNN1, COMP, CORIN, CPAMD8, CR1, CRABP2, CSRP1, CXCL6, CXCL8, CXXC1, CYP51A1, CYRIB, DAG1, DAND5, DAPK3, DCSTAMP, DENND1B, DHX9, DMTF1, DOCK4, EBI3, EFNA1, EFNA3, ELANE, ELAVL1, EMP2, ENAM, ENPP2, EPPK1, EREG, FASLG, FBXO32, FERD3L, FEZF2, FH, FLNB, FLVCR1, FOXP1, FSTL3, FYCO1, G0S2, GARS1, GATA2, GBA, GDF15, GHRHR, GHRL, GJC2, GLUL, GNAI2, GPIHBP1, GPNMB, GPR37L1, GRHL2, GSDMD, GSX2, H3-3B, HAS2, HAX1, HDAC9, HESX1, HMCES, HOMER3, HOOK2, HOPX, HOXA11, HOXA5, HOXA7, HRH1, HSF1, HYAL1, HYAL2, ICAM1, IGF2BP3, IL10, IL12RB1, IL17RD, IL19, IL20, IL27RA, IL5RA, IL6, IL6R, INAVA, INSR, IP6K1, IQGAP3, IQSEC1, IRF5, ITGB8, ITPKB, ITPR1, JAK3, KCND2, KCNK2, KDM5B, KDR, KEAP1, KHSRP, KIF14, KIT, KLF10, KRIT1, LAMA1, LAMA3, LAPTM4B, LDLR, LEP, LIPG, LITAF, LMCD1, LMNA, LMOD3, LONP1, LRG1, LRRC24, LRRN1, LRRN3, LTF, MAEL, MAGI1, MAPRE2, MBD1, MBD4, MET, MGLL, MINDY4, MITF, MST1, MTURN, MUC1, MYBPH, MYC, MYDGF, MYL3, MYOG, NANOS3, NAXE, NMU, NOD1, NPR1, NPRL2, NPVF, NR2C2, NTRK1, OSR2, OXTR, P4HTM, PARP1, PARP3, PDGFRA, PDK4, PGLYRP2, PHF14, PHOX2B, PIN1, PKN1, PLXNA1, PLXNA2, PLXNA4, PLXNB1, PLXND1, POLR2E, PPARG, PPP1R12B, PRDX2, PRKACA, PRKCD, PROK2, PROX1, PTGER1, PTGS2, PTK2, PTN, PTPN2, PTPN23, PTPRC, PTPRG, PTPRM, PTPRS, PTPRZ1, RAB25, RC3H1, REST, RETN, RHOA, RIMS2, RIOK3, RNF125, RNF2, RNU6-664P, ROCK1, RSPO2, RUFY3, S100A1, S100A13, S100A9, S1PR2, SCIN, SCRIB, SCX, SELENOK, SEMA3B, SEMA3F, SEMA3G, SEMA4A, SEMA6B, SEPTIN7, SERPINC1, SETD2, SFMBT1, SH3GL1, SIGLEC15, SIRT6, SLC25A44, SLC27A1, SMAD2, SMAD7, SMO, SOCS1, SOSTDC1, SPAM1, SRI, STAB1, STK11, STK3, SUCO, SYDE1, SYT11, TAC1, TAFA4, TAX1BP1, TBX20, TBXA2R, TCTA, TDGF1, TDGF1P3, TG, THOC1, TICAM1, TLE6, TLR9, TMEM38A, TMEM65, TMF1, TNFRSF11B, TNFSF18, TNFSF4, TNFSF9, TNNC1, TNNI1, TNNT2, TNR, TRAIP, TREX1, TRIB1, TRIL, TRIM11, TRIM46, TRPS1, TSPAN12, TWF2, TWSG1, TXK, UBA7, USP19, UTP25, VASH2, VGLL4, WNT2, WNT3A, WNT5A, WNT7A, WNT9A, XCL1, ZBTB7B, ZFPM2, ZNF16, ZNF706]
GO:0051094	positive regulation of developmental process	0,03	0,00	12,64	168,00	[ADGRB1, ADGRL1, AGO2, AGR2, AKR1B1, AKT3, AMIGO3, AMTN, ANGPTL4, AP3D1, AQP1, AREG, ARHGEF2, ASB4, ASPM, BMPER, BRINP2, C3, CALCA, CALR, CAMK1, CAMP, CAPN2, CARM1, CAV3, CCN4, CCR1, CCR3, CD34, CD46, CDH2, CHI3L1, CPNE9, CR1, CRABP2, CRTC1, CSPG5, CTHRC1, CXCL8, DAG1, DAND5, DCSTAMP, DNM2, ENAM, ENPP2, FEZF2, FYCO1, GARS1, GATA2, GDF15, GHRHR, GHRL, GJC2, GSX2, HAS2, HAX1, HMCES, HNRNPU, HOOK2, HOPX, HOXA11, HOXA5, HSF1, HYAL1, IL10, IL12RB1, IL20, IL6, IL6R, IMPACT, INSR, IQGAP3, ITGB8, ITPKB, JUNB, JUND, KDM5B, KDR, KIT, KLF10, LEP, LMNA, LMOD3, LONP1, LRG1, LRRC24, LRRN1, LRRN3, LTF, MBD4, MINDY4, MST1, MTURN, MYC, MYDGF, MYOC, MYOG, NANOS3, NR2C2, NTRK1, OLFM2, OSR2, OXTR, PARP1, PAX4, PHOX2B, PIN1, PKN1, PLXNA1, PLXNA2, PLXNA4, PLXNB1, PLXND1, PPARG, PPP1R9A, PROX1, PTGS2, PTN, PTPRC, PTPRZ1, RALBP1, REST, RETN, RHOA, RIMS2, RNASEH2A, RUFY3, S100A1, S1PR2, SCIN, SCX, SEMA4A, SIRT6, SLC6A6, SMAD2, SMAD7, SMO, SOCS1, SPAM1, STK11, STK3, SUCO, SULT1E1, SYDE1, SYT17, SYT2, SYT4, TBX20, TBXA2R, TCF3, TLE6, TMEM106B, TMEM79, TNFSF4, TNFSF9, TRIB1, TWF2, UNC13A, UTP25, VASH2, WNT2, WNT3A, WNT5A, WNT7A, ZBTB7B, ZBTB7C, ZFPM2, ZNF16]

GO:0051241	negative regulation of multicellular organismal process	0,04	0,00	12,82	136,00	[ABHD6, ACP5, ADAMTS9, ADCYAP1, ADGRB1, ADIPOR1, ADORA1, AKAP8, ANGPT1, BST2, CACTIN, CALCA, CALCR, CALR, CAV3, CCN3, CCN4, CCR1, CCR2, CD34, CDK6, CIDEA, CR1, CXXC1, CYP51A1, DAND5, DOCK4, EFNA1, EFNA3, ELANE, EPPK1, FASLG, FLNB, FSTL3, FYCO1, GATA2, GBA, GDF15, GHRL, GNAI2, GPNMB, GPR37L1, GRHL2, HDAC9, HOMER3, HOXA5, HOXA7, IL10, IL17RD, IL19, IL27RA, IL6, IP6K1, JAK3, KCNK2, KHSRP, KRIT1, LAPTM4B, LDLR, LEP, LMNA, LTF, MBD1, MYC, NANOS3, NAXE, NMU, NPR1, NPVF, OXTR, PARP3, PDGFRA, PGLYRP2, PHF14, PIN1, PKN1, PPARG, PRDX2, PRKCD, PTGER1, PTGS2, PTN, PTPN2, PTPN23, PTPRC, PTPRG, PTPRM, PTPRS, RC3H1, REST, RHOA, RNF125, ROCK1, RSPO2, RUFY3, SEMA3B, SEMA3F, SEMA3G, SEMA4A, SEMA6B, SFMBT1, SMAD7, SMO, SOCS1, SOSTDC1, SRI, STAB1, STK11, STK3, SYT11, TAC1, TAX1BP1, TBXA2R, TCTA, THOC1, TLR9, TNFRSF11B, TNFSF18, TNFSF4, TNR, TRAIP, TRIB1, TRIM11, TRIM46, TWSG1, UBA7, USP19, VGLL4, WNT3A, WNT5A, WNT7A, WNT9A, XCL1, ZBTB7B, ZFPM2, ZNF706]
GO:0022603	regulation of anatomical structure morphogenesis	0,04	0,00	12,86	130,00	[ADAMTS9, ADGRB1, AGO2, AKR1B1, AKT3, ALDOA, ANGPTL4, AQP1, AREG, BMPER, C3, CALR, CAMP, CAV3, CCR2, CCR3, CD34, CDH2, CELSR3, CHI3L1, CHRNA3, CHRNB2, CPNE9, CRABP2, CSPG5, CTHRC1, CXCL8, CXXC1, CYRIB, DAG1, DAND5, DAPK3, DNM2, DNM3, EFNA1, EFNA3, EMP2, ENPP2, EPB41L3, FASLG, FGD5, FOXP1, FYCO1, FZD1, FZD6, GARS1, GATA2, GHRL, GLUL, GPNMB, HAS2, HOOK2, HOXA11, HOXA5, HYAL1, ICAM1, IL10, IL6, ITGB8, KDR, KIT, KRIT1, LEP, LIMD1, LRG1, MINDY4, MKLN1, MYDGF, MYL12A, MYOC, NANOS3, NAXE, NPR1, PALM, PEAK3, PKN1, PLXNA1, PLXNA2, PLXNA4, PLXNB1, PLXND1, PPARG, PPP1R9A, PRICKLE2, PROK2, PSMA8, PSMD4, PTK2, PTN, PTPRM, PTPRS, RALBP1, RC3H1, RHOA, RIMS2, RNU6-664P, ROCK1, RSPO2, RUFY3, S100A1, SCX, SEM1, SEMA3B, SEMA3F, SEMA3G, SEMA4A, SEMA6B, SEPTIN7, SIRT6, SKOR2, SMO, SPAM1, STAB1, STK11, STRIP2, SYT17, SYT2, SYT4, TBXA2R, TNFRSF11B, TNR, TRIM46, TSPAN12, TWF2, UNC13A, VASH2, WNT2, WNT3A, WNT5A, WNT7A]
GO:0050793	regulation of developmental process	0,01	0,00	12,04	311,00	[ADAMTS9, ADCYAP1, ADGRB1, ADGRL1, ADIPOR1, AFG3L2, AGO2, AGR2, AKR1B1, AKT3, ALDOA, AMIGO3, AMTN, ANGPTL4, ANKLE1, ANKRD17, AP3D1, APC2, AQP1, AREG, ARHGEF2, ASAP1, ASB4, ASPM, BHLHE40, BMPER, BRINP2, C3, CALCA, CALR, CAMK1, CAMP, CAMSAP2, CAPN2, CARM1, CAV1, CAV3, CCN3, CCN4, CCR1, CCR2, CCR3, CD34, CD46, CDH2, CDK6, CELF4, CELSR3, CENPF, CHERP, CHI3L1, CHRNA3, CHRNB2, CLOCK, CNTN4, COMP, CPNE9, CR1, CRABP2, CRTC1, CSMD3, CSPG5, CSRP1, CTHRC1, CXCL8, CXXC1, CYRIB, DAG1, DAND5, DAPK3, DCSTAMP, DMTF1, DNM2, DNM3, DNMT1, EFNA1, EFNA3, ELAVL1, EMP2, ENAM, ENPP2, EPB41L3, EPPK1, EREG, FASLG, FERD3L, FEZF2, FGD5, FLVCR1, FOXP1, FSTL3, FYCO1, FZD1, FZD6, FZR1, GARS1, GATA2, GDF15, GHRHR, GHRL, GJC2, GLUL, GPNMB, GPR37L1, GRHL2, GSX2, H1-8, H3-3B, HAS2, HAX1, HDAC9, HESX1, HMCES, HNRNPU, HOOK2, HOPX, HOXA11, HOXA2, HOXA5, HOXA7, HSF1, HYAL1, HYAL3, ICAM1, IL10, IL12RB1, IL17RD, IL20, IL6, IL6R, IMPACT, ING3, INSR, IQGAP3, ITGB8, ITPKB, JAK3, JUNB, JUND, KCNK2, KDM5B, KDR, KEAP1, KIF14, KIT, KLF10, KRIT1, LAMA1, LAMA3, LDLR, LEP, LIMD1, LMNA, LMOD3, LONP1, LRG1, LRP12, LRRC24, LRRN1, LRRN3, LTF, MAEL, MBD1, MBD4, MIB1, MINDY4, MITF, MKLN1, MST1, MTURN, MYC, MYDGF, MYL12A, MYOC, MYOG, NANOS3, NAXE, NEK4, NOTCH3, NPR1, NPRL2, NR2C2, NTRK1, OCIAD1, OLFM2, OSR2, OXTR, P4HTM, PALM, PARP1, PARP3, PAX4, PDGFRA, PEAK3, PGLYRP2, PHF14, PHOX2B, PIN1, PKN1, PLXNA1, PLXNA2, PLXNA4, PLXNB1, PLXND1, PPARG, PPP1R9A, PRDX2, PRICKLE2, PRKACA, PROK2, PROX1, PRRX1, PSMA8, PSMD4, PTGS2, PTK2, PTN, PTPN2, PTPRC, PTPRM, PTPRS, PTPRZ1, RAF1, RALBP1, RC3H1, REST, RETN, RHOA, RIMS2, RNASEH2A, RNU6-664P, ROCK1, RSL1D1, RSPO2, RUFY3, S100A1, S100A9, S1PR2, S1PR5, SCIN, SCX, SEM1, SEMA3B, SEMA3F, SEMA3G, SEMA4A, SEMA6B, SEPTIN7, SFMBT1, SIGLEC15, SIRT6, SKOR2, SLC25A23, SLC6A6, SMAD2, SMAD7, SMO, SOCS1, SOSTDC1, SPAM1, ST7, STAB1, STK11, STK3, STRIP2, SUCO, SULT1E1, SYDE1, SYT17, SYT2, SYT4, TBX20, TBXA2R, TCF3, TCTA, TG, THOC1, TLE6, TLR9, TMEM106B, TMEM79, TNFRSF11B, TNFSF18, TNFSF4, TNFSF9, TNN, TNR, TRIB1, TRIM11, TRIM46, TRPS1, TSPAN12, TWF2, TWSG1, UNC13A, USP19, UTP25, VASH2, VGLL4, WNT2, WNT3A, WNT5A, WNT7A, WNT9A, ZBTB7B, ZBTB7C, ZFPM2, ZHX2, ZNF16, ZNF277, ZNF706]
GO:0022603	regulation of anatomical structure morphogenesis	0,04	0,00	12,86	130,00	[ADAMTS9, ADGRB1, AGO2, AKR1B1, AKT3, ALDOA, ANGPTL4, AQP1, AREG, BMPER, C3, CALR, CAMP, CAV3, CCR2, CCR3, CD34, CDH2, CELSR3, CHI3L1, CHRNA3, CHRNB2, CPNE9, CRABP2, CSPG5, CTHRC1, CXCL8, CXXC1, CYRIB, DAG1, DAND5, DAPK3, DNM2, DNM3, EFNA1, EFNA3, EMP2, ENPP2, EPB41L3, FASLG, FGD5, FOXP1, FYCO1, FZD1, FZD6, GARS1, GATA2, GHRL, GLUL, GPNMB, HAS2, HOOK2, HOXA11, HOXA5, HYAL1, ICAM1, IL10, IL6, ITGB8, KDR, KIT, KRIT1, LEP, LIMD1, LRG1, MINDY4, MKLN1, MYDGF, MYL12A, MYOC, NANOS3, NAXE, NPR1, PALM, PEAK3, PKN1, PLXNA1, PLXNA2, PLXNA4, PLXNB1, PLXND1, PPARG, PPP1R9A, PRICKLE2, PROK2, PSMA8, PSMD4, PTK2, PTN, PTPRM, PTPRS, RALBP1, RC3H1, RHOA, RIMS2, RNU6-664P, ROCK1, RSPO2, RUFY3, S100A1, SCX, SEM1, SEMA3B, SEMA3F, SEMA3G, SEMA4A, SEMA6B, SEPTIN7, SIRT6, SKOR2, SMO, SPAM1, STAB1, STK11, STRIP2, SYT17, SYT2, SYT4, TBXA2R, TNFRSF11B, TNR, TRIM46, TSPAN12, TWF2, UNC13A, VASH2, WNT2, WNT3A, WNT5A, WNT7A]
GO:0035239	tube morphogenesis	0,00	0,00	14,60	131,00	[ADAM15, ADAMTS9, ADGRB1, AGO2, AGR2, AKR1B1, AKT3, ANGPT1, ANGPTL1, ANGPTL4, ANGPTL6, AQP1, AREG, ASB4, BMPER, BSG, C1GALT1, C3, CAMP, CAV1, CAV3, CCN3, CCR2, CCR3, CD34, CDH2, CHI3L1, COMP, CTHRC1, CXCL8, DAG1, DAND5, EFNA1, EFNA3, EMP2, ENPP2, EPGN, EREG, EXT1, FASLG, FOXH1, FOXP1, FZD6, GARS1, GATA2, GHRL, GLUL, GPNMB, GPX1, GREB1L, GRHL2, HAS2, HDAC9, HESX1, HOOK2, HOXA1, HOXA11, HOXA13, HOXA3, HOXA5, HOXA7, HYAL1, IFT122, IL10, IL6, ITGB8, JUNB, KDM5B, KDR, KIF26B, KRIT1, LAMA1, LDLR, LEP, LRG1, MBD4, MET, MIB1, MINDY4, MST1, MTSS1, MYC, MYDGF, NANOS3, NAXE, NPR1, PDGFRA, PKN1, PLXND1, PODXL, PPARG, PRKACA, PROK2, PROX1, PRRX1, PTGS2, PTK2, PTN, PTPRM, RNASEH2A, RNU6-664P, ROCK1, RSPO2, S100A1, SCRIB, SDCCAG8, SEMA4A, SETD2, SH2D2A, SHC1, SIRT6, SMAD2, SMAD7, SMO, SOSTDC1, SPAM1, STAB1, STK3, TBX20, TBXA2R, TDGF1, TDGF1P3, THSD7A, TNNC1, TSPAN12, VASH2, WNT2, WNT3A, WNT5A, WNT7A, ZFPM2]
GO:0001525	angiogenesis	0,01	0,00	15,17	83,00	[ADAM15, ADAMTS9, ADGRB1, AGO2, AKT3, ANGPT1, ANGPTL1, ANGPTL4, ANGPTL6, AQP1, BMPER, BSG, C1GALT1, C3, CAMP, CAV1, CCN3, CCR2, CCR3, CD34, CHI3L1, CXCL8, DAG1, DAND5, EFNA1, EFNA3, EMP2, ENPP2, EPGN, EREG, FASLG, GARS1, GATA2, GHRL, GLUL, GPNMB, GPX1, HDAC9, HOOK2, HOXA3, HOXA5, HOXA7, HYAL1, IL10, IL6, ITGB8, KDR, KRIT1, LEP, LRG1, MBD4, MINDY4, MYDGF, NANOS3, NAXE, NPR1, PDGFRA, PLXND1, PPARG, PROK2, PTGS2, PTK2, PTN, PTPRM, RNU6-664P, ROCK1, S100A1, SEMA4A, SETD2, SH2D2A, SHC1, SIRT6, SPAM1, STAB1, TBX20, TBXA2R, TDGF1, TDGF1P3, THSD7A, TSPAN12, VASH2, WNT5A, WNT7A]
GO:0048514	blood vessel morphogenesis	0,00	0,00	15,37	99,00	[ADAM15, ADAMTS9, ADGRB1, AGO2, AKT3, ANGPT1, ANGPTL1, ANGPTL4, ANGPTL6, AQP1, ASB4, BMPER, BSG, C1GALT1, C3, CAMP, CAV1, CCN3, CCR2, CCR3, CD34, CDH2, CHI3L1, COMP, CXCL8, DAG1, DAND5, EFNA1, EFNA3, EMP2, ENPP2, EPGN, EREG, FASLG, FOXH1, GARS1, GATA2, GHRL, GLUL, GPNMB, GPX1, HAS2, HDAC9, HOOK2, HOXA1, HOXA13, HOXA3, HOXA5, HOXA7, HYAL1, IL10, IL6, ITGB8, JUNB, KDR, KRIT1, LAMA1, LDLR, LEP, LRG1, MBD4, MINDY4, MYDGF, NANOS3, NAXE, NPR1, PDGFRA, PLXND1, PPARG, PROK2, PROX1, PRRX1, PTGS2, PTK2, PTN, PTPRM, RNASEH2A, RNU6-664P, ROCK1, S100A1, SEMA4A, SETD2, SH2D2A, SHC1, SIRT6, SMAD7, SMO, SPAM1, STAB1, TBX20, TBXA2R, TDGF1, TDGF1P3, THSD7A, TSPAN12, VASH2, WNT5A, WNT7A, ZFPM2]
GO:0045765	regulation of angiogenesis	0,00	0,00	18,58	55,00	[ADAMTS9, ADGRB1, AGO2, AKT3, ANGPTL4, AQP1, BMPER, C3, CAMP, CCR2, CCR3, CD34, CHI3L1, CXCL8, DAND5, EFNA1, EFNA3, EMP2, ENPP2, FASLG, GARS1, GATA2, GHRL, GLUL, GPNMB, HOOK2, HOXA5, HYAL1, IL10, IL6, ITGB8, KDR, KRIT1, LEP, LRG1, MINDY4, MYDGF, NANOS3, NAXE, NPR1, PLXND1, PPARG, PROK2, PTN, PTPRM, ROCK1, S100A1, SEMA4A, SIRT6, SPAM1, STAB1, TBXA2R, TSPAN12, VASH2, WNT5A]
GO:0032879	regulation of localization	0,00	0,00	12,35	352,00	[ABCA7, ABCB1, ABCB4, ABHD17A, ABHD6, ABL2, ADAM15, ADAMTS9, ADCY8, ADCYAP1, ADCYAP1R1, ADGRB1, ADIPOR1, ADORA1, AGO2, AGR2, AKAP9, AKR1B1, AKT3, ALKBH7, ANGPT1, AP3D1, APPL1, AQP1, AREG, ARHGEF2, ARIH2, ARL6IP5, ATCAY, ATP1B1, ATP5F1A, ATP8A1, AZIN1, BAP1, BEX4, BMPER, BSG, BSN, BST2, C3, CACNA1A, CACNA1D, CACNA1E, CACNA1S, CACNA2D2, CACNA2D3, CADPS2, CALCA, CALCR, CALR, CAMK1, CAV1, CAV3, CCDC66, CCL25, CCN3, CCN4, CCR1, CCR2, CCR5, CCT3, CD247, CDH2, CDK6, CEP135, CFAP69, CFTR, CHERP, CHRNA3, CHRNA5, CHRNB2, CHRNB4, CIDEA, CLOCK, CNIH3, CNIH4, CNN2, CNST, CORIN, CPAMD8, CRBN, CREB3L4, CSPG5, CSRP1, CXCL8, CXXC1, CYP51A1, CYRIB, DAG1, DAND5, DAPK3, DBI, DHX9, DNAH11, DNM2, DNM3, DOCK4, EDEM1, EEPD1, EFNA1, ELANE, ELP6, EMP2, ENPP2, ENY2, EPHA5, EPPK1, EREG, EXOC1, F2RL3, FAM107A, FAM3D, FAM83H, FASLG, FEZF2, FGF22, FLNB, FOXP1, FYCO1, FZR1, GATA2, GHRHR, GHRL, GIPC1, GJC2, GLUL, GNAI2, GNL3, GPNMB, GRIN2A, GRM2, GRM7, GSX2, HAS2, HAX1, HCN2, HCN3, HDAC9, HNRNPU, HOMER3, HOOK2, HOXA7, HYAL1, HYAL2, HYAL3, ICA1, ICAM1, IER3IP1, IL24, IL27RA, IL6, IL6R, INSR, IQCF1, IQSEC1, ITPR1, JAGN1, KCND2, KCNN1, KCNN3, KCNQ3, KCNS2, KCNV1, KDM5B, KDR, KIAA1614, KIT, KLF15, KMO, KRIT1, LAMA1, LAMA3, LAMC2, LEP, LGR6, LIMCH1, LIPG, LMNA, LONP1, LSM4, LZTFL1, MADCAM1, MAGI1, MAP2K2, MAPK15, MAPRE2, MBD1, MDFIC, MEST, MET, MIB1, MIDN, MINDY4, MISP, MITF, MKLN1, MPC2, MST1, MTCL1, MYC, MYOC, MYOM1, NANOS3, NAXE, NDC80, NISCH, NMU, NPR1, NPSR1, NPVF, NVL, OAZ1, OPN3, OXTR, PARP1, PDGFRA, PFKFB2, PIK3C3, PIK3R2, PIN1, PKN1, PLA2G4A, PLIN3, PLIN5, PLVAP, PLXNA1, PLXNA2, PLXNA4, PLXNB1, PLXND1, PODXL, PPARG, PPP1R9A, PPP2R5A, PRKACA, PRKCD, PRKCSH, PROX1, PSEN2, PTGS2, PTK2, PTN, PTP4A3, PTPN14, PTPN2, PTPN23, PTPRC, PTPRG, PTPRM, PXK, RAB11B, RAB12, RAB13, RAB25, RAB31, RAB3A, RAB3D, RAB43, RAB7A, RAB8A, RAF1, REEP6, REST, RETN, RHOA, RIMS2, RIT2, RNASEL, RNF139, RNF2, RNU6-664P, ROCK1, RUFY3, RUVBL1, S100A1, S100A14, S100A9, SCIN, SCRIB, SEC16B, SELE, SELENOK, SELP, SEMA3B, SEMA3F, SEMA3G, SEMA4A, SEMA6B, SETD2, SH3GL1, SHQ1, SLC25A23, SLC26A6, SLC30A1, SLC30A8, SLC38A3, SLC6A1, SLMAP, SLURP1, SMAD7, SMO, SNAPIN, SPAM1, SRGAP3, SRI, STAP1, STIMATE, STK11, STX10, STX6, STXBP2, SYBU, SYDE1, SYT11, SYT17, SYT2, SYT4, TAC1, TBXA2R, TDGF1, TDGF1P3, TLR9, TMEM38A, TMF1, TNFSF18, TNN, TNNC1, TNNT2, TOMM7, TP53BP2, TPR, TRH, TRIB1, TRIM46, TSPAN13, UBL5, UBR5, USP46, VAMP4, VPS28, WASL, WFS1, WNT3A, WNT5A, WNT7A, XCL1, XCL2, XCR1, YES1, YOD1, ZDHHC3, ZSWIM4]

GO:0040012	regulation of locomotion	0,01	0,00	13,79	143,00	[ABHD6, ABL2, ADAM15, ADAMTS9, ADGRB1, ADIPOR1, ADORA1, AGO2, AKT3, ANGPT1, APPL1, ARHGEF2, ATP5F1A, ATP8A1, BEX4, BMPER, BST2, CALR, CAV1, CCL25, CCN3, CCN4, CCR1, CCR2, CDK6, CFAP69, CNN2, CREB3L4, CXCL8, CYRIB, DAG1, DAND5, DAPK3, DOCK4, EFNA1, ELANE, ELP6, EMP2, ENPP2, EPPK1, EREG, FAM107A, FAM83H, FEZF2, FGF22, FOXP1, FYCO1, FZR1, GATA2, GHRL, GLUL, GNAI2, GPNMB, GSX2, HAS2, HDAC9, HOXA7, HYAL1, HYAL2, ICAM1, IL24, IL27RA, IL6, IL6R, INSR, IQCF1, IQSEC1, KDR, KIT, KRIT1, LAMA1, LAMA3, LAMC2, LGR6, LIMCH1, LMNA, MADCAM1, MAPK15, MAPRE2, MET, MITF, MST1, MYC, MYOC, NANOS3, NISCH, PDGFRA, PIN1, PKN1, PLVAP, PLXNA1, PLXNA2, PLXNA4, PLXNB1, PLXND1, PODXL, PPARG, PROX1, PTGS2, PTK2, PTN, PTPN2, PTPN23, PTPRC, PTPRG, PTPRM, RAB25, RAF1, RHOA, ROCK1, RUFY3, S100A14, S100A9, SELE, SELENOK, SELP, SEMA3B, SEMA3F, SEMA3G, SEMA4A, SEMA6B, SLURP1, SMAD7, SMO, SPAM1, SRGAP3, STAP1, SYDE1, TAC1, TBXA2R, TDGF1, TDGF1P3, TNFSF18, TNN, TRIB1, USP14, WASL, WNT3A, WNT5A, WNT7A, XCL1, XCL2, ZSWIM4]
GO:0048870	cell motility	0,01	0,00	12,62	229,00	[ABHD6, ABL2, ADAM15, ADAMTS9, ADCY8, ADGRB1, ADGRL3, ADIPOR1, ADORA1, AGO2, AKT3, ANGPT1, ANLN, APC2, APPL1, ARF4, ARHGEF2, ARPC5, ASH1L, ASPM, ASTN1, ATP1B1, ATP5F1A, ATP8A1, AVL9, BEX4, BMPER, BRK1, BSG, BST2, CALCA, CALR, CATSPERD, CAV1, CCL25, CCN3, CCN4, CCR1, CCR2, CCR3, CCR5, CCR9, CCRL2, CD34, CDC42BPA, CDH2, CDK6, CFAP69, CNN2, COL1A2, CREB3L4, CTHRC1, CXCL6, CXCL8, CXCR6, CYRIB, DAG1, DAND5, DAPK3, DNAH1, DNAH11, DNAH14, DOCK4, EFNA1, ELANE, ELMO1, ELP6, EMP2, ENAH, ENPP2, EPPK1, EREG, EVX1, EXT1, FAM107A, FAM83H, FCAMR, FEZF2, FGF22, FOXP1, FSCN3, FYCO1, FZR1, GATA2, GBA, GIPC1, GLUL, GNAI2, GPNMB, GPX1, GSX2, HAS2, HDAC9, HOXA5, HOXA7, HRH1, HYAL1, HYAL2, ICAM1, IER2, IL10, IL24, IL27RA, IL6, IL6R, ING3, INSR, IQCF1, IQSEC1, ITGB8, JAGN1, JCHAIN, KANK2, KDR, KIT, KRIT1, LAMA1, LAMA3, LAMB2, LAMB3, LAMC1, LAMC2, LAMTOR2, LEP, LGR6, LIMCH1, LIMD1, LMNA, LMNB2, LRP12, LRRC6, MADCAM1, MAPK15, MAPRE2, MBD1, MET, MISP, MITF, MST1, MST1R, MYC, MYOC, NANOS3, NAV1, NISCH, PDGFRA, PHOX2B, PIK3R2, PIN1, PIP5K1C, PKN1, PLVAP, PLXNA1, PLXNA2, PLXNA4, PLXNB1, PLXND1, PODXL, PODXL2, PPARG, PPBP, PRKCD, PRKCSH, PROX1, PSTPIP2, PTGS2, PTK2, PTN, PTP4A3, PTPN23, PTPRC, PTPRG, PTPRM, RAB13, RAB25, RAF1, RHOA, ROCK1, RUFY3, S100A12, S100A14, S100A2, S100A9, SCRIB, SCYL3, SDCCAG8, SELE, SELENOK, SELL, SELP, SEMA3B, SEMA3F, SEMA3G, SEMA4A, SEMA6B, SETD2, SHC1, SLC25A23, SLURP1, SMAD7, SMO, SPAM1, SRGAP3, STAP1, STRIP2, SYDE1, TAC1, TAFA4, TBX20, TBXA2R, TDGF1, TDGF1P3, TEKT5, TMF1, TNFSF18, TNN, TNR, TPGS1, TRIB1, TRIM46, TSSK6, VAV1, WASL, WNT5A, WNT7A, XCL1, XCL2, XCR1, YES1]
GO:0090132	epithelium migration	0,00	0,00	17,83	56,00	[ADAMTS9, ADGRB1, ADIPOR1, AKT3, ANGPT1, ANLN, ATP5F1A, BMPER, CALCA, CALR, CCN3, DAND5, EFNA1, EMP2, ENPP2, EPPK1, FOXP1, GATA2, GIPC1, GLUL, GPX1, GRHL2, HAS2, HDAC9, HYAL1, IQSEC1, KANK2, KDR, KIT, KRIT1, MAPRE2, MET, NANOS3, PKN1, PLXND1, PPARG, PROX1, PTGS2, PTK2, PTN, PTP4A3, PTPN23, PTPRG, PTPRM, RAB13, RAB25, ROCK1, S100A2, SEMA4A, SPAM1, TAC1, TBXA2R, TDGF1, TDGF1P3, WNT5A, WNT7A]
GO:0016477	cell migration	0,01	0,00	12,71	206,00	[ABHD6, ADAM15, ADAMTS9, ADGRB1, ADGRL3, ADIPOR1, ADORA1, AGO2, AKT3, ANGPT1, ANLN, APC2, APPL1, ARF4, ARHGEF2, ARPC5, ASPM, ASTN1, ATP1B1, ATP5F1A, ATP8A1, AVL9, BEX4, BMPER, BSG, BST2, CALCA, CALR, CAV1, CCL25, CCN3, CCN4, CCR1, CCR2, CCR3, CCR5, CCR9, CCRL2, CD34, CDC42BPA, CDH2, CNN2, COL1A2, CREB3L4, CTHRC1, CXCL6, CXCL8, CXCR6, CYRIB, DAG1, DAND5, DAPK3, DOCK4, EFNA1, ELANE, ELMO1, ELP6, EMP2, ENPP2, EPPK1, EVX1, EXT1, FAM107A, FAM83H, FCAMR, FEZF2, FGF22, FOXP1, FSCN3, FYCO1, FZR1, GATA2, GBA, GIPC1, GLUL, GNAI2, GPNMB, GPX1, GSX2, HAS2, HDAC9, HOXA5, HOXA7, HRH1, HYAL1, HYAL2, ICAM1, IL10, IL24, IL27RA, IL6, IL6R, INSR, IQSEC1, ITGB8, JAGN1, JCHAIN, KANK2, KDR, KIT, KRIT1, LAMA1, LAMA3, LAMB2, LAMB3, LAMC1, LAMC2, LAMTOR2, LEP, LGR6, LIMCH1, LIMD1, LMNA, LMNB2, LRP12, MADCAM1, MAPK15, MAPRE2, MBD1, MET, MISP, MITF, MST1, MST1R, MYC, MYOC, NANOS3, NAV1, NISCH, PDGFRA, PHOX2B, PIK3R2, PIP5K1C, PKN1, PLVAP, PLXNA1, PLXNA2, PLXNA4, PLXNB1, PLXND1, PODXL, PODXL2, PPARG, PPBP, PRKCD, PROX1, PSTPIP2, PTGS2, PTK2, PTN, PTP4A3, PTPN23, PTPRC, PTPRG, PTPRM, RAB13, RAB25, RHOA, ROCK1, RUFY3, S100A12, S100A14, S100A2, S100A9, SCRIB, SCYL3, SDCCAG8, SELE, SELENOK, SELL, SELP, SEMA3B, SEMA3F, SEMA3G, SEMA4A, SEMA6B, SETD2, SHC1, SLC25A23, SLURP1, SMAD7, SMO, SPAM1, SRGAP3, STAP1, STRIP2, SYDE1, TAC1, TAFA4, TBX20, TBXA2R, TDGF1, TDGF1P3, TNFSF18, TNN, TNR, TRIB1, TRIM46, VAV1, WASL, WNT5A, WNT7A, XCL1, XCL2, XCR1, YES1]
GO:0051270	regulation of cellular component movement	0,01	0,00	13,73	148,00	[ABHD6, ABL2, ADAM15, ADAMTS9, ADGRB1, ADIPOR1, ADORA1, AGO2, AKAP9, AKT3, ANGPT1, APPL1, ARHGEF2, ATP5F1A, ATP8A1, BEX4, BMPER, BST2, CALR, CAV1, CAV3, CCL25, CCN3, CCN4, CCR1, CCR2, CDK6, CFAP69, CNIH4, CNN2, CREB3L4, CXCL8, CYRIB, DAG1, DAND5, DAPK3, DNAH11, DOCK4, EFNA1, ELANE, ELP6, EMP2, ENPP2, EPPK1, EREG, FAM107A, FAM83H, FEZF2, FGF22, FOXP1, FYCO1, FZR1, GATA2, GLUL, GNAI2, GPNMB, GSX2, HAS2, HDAC9, HOXA7, HYAL1, HYAL2, ICAM1, IL24, IL27RA, IL6, IL6R, INSR, IQCF1, IQSEC1, KDR, KIT, KRIT1, LAMA1, LAMA3, LAMC2, LGR6, LIMCH1, LMNA, MADCAM1, MAPK15, MAPRE2, MET, MITF, MST1, MYC, MYOC, NANOS3, NISCH, PDGFRA, PIN1, PKN1, PLVAP, PLXNA1, PLXNA2, PLXNA4, PLXNB1, PLXND1, PODXL, PPARG, PROX1, PTGS2, PTK2, PTN, PTPN23, PTPRC, PTPRG, PTPRM, RAB25, RAF1, RHOA, ROCK1, RUFY3, S100A14, S100A9, SELE, SELENOK, SELP, SEMA3B, SEMA3F, SEMA3G, SEMA4A, SEMA6B, SLURP1, SMAD7, SMO, SPAM1, SRGAP3, SRI, STAP1, STK11, SYDE1, TAC1, TBXA2R, TDGF1, TDGF1P3, TNFSF18, TNN, TNNC1, TNNT2, TRIB1, TRIM46, WASL, WNT5A, WNT7A, XCL1, XCL2, ZSWIM4]
GO:2000145	regulation of cell motility	0,01	0,00	13,82	137,00	[ABHD6, ABL2, ADAM15, ADAMTS9, ADGRB1, ADIPOR1, ADORA1, AGO2, AKT3, ANGPT1, APPL1, ARHGEF2, ATP5F1A, ATP8A1, BEX4, BMPER, BST2, CALR, CAV1, CCL25, CCN3, CCN4, CCR1, CCR2, CDK6, CFAP69, CNN2, CREB3L4, CXCL8, CYRIB, DAG1, DAND5, DAPK3, DOCK4, EFNA1, ELANE, ELP6, EMP2, ENPP2, EPPK1, EREG, FAM107A, FAM83H, FGF22, FOXP1, FYCO1, FZR1, GATA2, GLUL, GNAI2, GPNMB, GSX2, HAS2, HDAC9, HOXA7, HYAL1, HYAL2, ICAM1, IL24, IL27RA, IL6, IL6R, INSR, IQCF1, IQSEC1, KDR, KIT, KRIT1, LAMA1, LAMA3, LAMC2, LGR6, LIMCH1, LMNA, MADCAM1, MAPK15, MAPRE2, MET, MITF, MST1, MYC, MYOC, NANOS3, NISCH, PDGFRA, PIN1, PKN1, PLVAP, PLXNA1, PLXNA2, PLXNA4, PLXNB1, PLXND1, PODXL, PPARG, PROX1, PTGS2, PTK2, PTN, PTPN23, PTPRC, PTPRG, PTPRM, RAB25, RAF1, RHOA, ROCK1, RUFY3, S100A14, S100A9, SELE, SELENOK, SELP, SEMA3B, SEMA3F, SEMA3G, SEMA4A, SEMA6B, SLURP1, SMAD7, SMO, SPAM1, SRGAP3, STAP1, SYDE1, TAC1, TBXA2R, TDGF1, TDGF1P3, TNFSF18, TNN, TRIB1, WASL, WNT5A, WNT7A, XCL1, XCL2]
GO:0001667	ameboidal-type cell migration	0,01	0,00	15,53	68,00	[ADAMTS9, ADGRB1, ADIPOR1, AGO2, AKT3, ANGPT1, ANLN, APPL1, ATP5F1A, BMPER, CALCA, CALR, CCN3, CDH2, DAND5, EFNA1, EMP2, ENPP2, EPPK1, FOXP1, GATA2, GIPC1, GLUL, GPX1, HAS2, HDAC9, HYAL1, HYAL2, IQSEC1, KANK2, KDR, KIT, KRIT1, LAMTOR2, MAPRE2, MET, NANOS3, PHOX2B, PKN1, PLXND1, PPARG, PROX1, PTGS2, PTK2, PTN, PTP4A3, PTPN23, PTPRG, PTPRM, RAB13, RAB25, ROCK1, S100A2, SEMA3B, SEMA3F, SEMA3G, SEMA4A, SEMA6B, SMO, SPAM1, SRGAP3, SYDE1, TAC1, TBXA2R, TDGF1, TDGF1P3, WNT5A, WNT7A]
GO:0010632	regulation of epithelial cell migration	0,01	0,00	17,65	42,00	[ADAMTS9, ADGRB1, ADIPOR1, AKT3, ANGPT1, ATP5F1A, BMPER, CALR, DAND5, EFNA1, EMP2, ENPP2, EPPK1, FOXP1, GATA2, GLUL, HAS2, HDAC9, HYAL1, IQSEC1, KDR, KRIT1, MAPRE2, MET, NANOS3, PPARG, PROX1, PTGS2, PTK2, PTN, PTPN23, PTPRG, PTPRM, RAB25, SEMA4A, SPAM1, TAC1, TBXA2R, TDGF1, TDGF1P3, WNT5A, WNT7A]
GO:0030334	regulation of cell migration	0,01	0,00	14,02	130,00	[ABHD6, ADAM15, ADAMTS9, ADGRB1, ADIPOR1, ADORA1, AGO2, AKT3, ANGPT1, APPL1, ARHGEF2, ATP5F1A, ATP8A1, BEX4, BMPER, BST2, CALR, CAV1, CCL25, CCN3, CCN4, CCR1, CCR2, CNN2, CREB3L4, CXCL8, CYRIB, DAG1, DAND5, DAPK3, DOCK4, EFNA1, ELANE, ELP6, EMP2, ENPP2, EPPK1, FAM107A, FAM83H, FGF22, FOXP1, FYCO1, FZR1, GATA2, GLUL, GNAI2, GPNMB, GSX2, HAS2, HDAC9, HOXA7, HYAL1, HYAL2, ICAM1, IL24, IL27RA, IL6, IL6R, INSR, IQSEC1, KDR, KIT, KRIT1, LAMA1, LAMA3, LAMC2, LGR6, LIMCH1, LMNA, MADCAM1, MAPK15, MAPRE2, MET, MITF, MST1, MYC, MYOC, NANOS3, NISCH, PDGFRA, PKN1, PLVAP, PLXNA1, PLXNA2, PLXNA4, PLXNB1, PLXND1, PODXL, PPARG, PROX1, PTGS2, PTK2, PTN, PTPN23, PTPRC, PTPRG, PTPRM, RAB25, RHOA, ROCK1, RUFY3, S100A14, S100A9, SELE, SELENOK, SELP, SEMA3B, SEMA3F, SEMA3G, SEMA4A, SEMA6B, SLURP1, SMAD7, SMO, SPAM1, SRGAP3, STAP1, SYDE1, TAC1, TBXA2R, TDGF1, TDGF1P3, TNFSF18, TNN, TRIB1, WASL, WNT5A, WNT7A, XCL1, XCL2]
GO:0043542	endothelial cell migration	0,04	0,00	16,38	38,00	[ADAMTS9, ADGRB1, AKT3, ANGPT1, ATP5F1A, BMPER, CALCA, CALR, CCN3, DAND5, EFNA1, EMP2, FOXP1, GATA2, GIPC1, GLUL, GPX1, HDAC9, KDR, KRIT1, MET, NANOS3, PLXND1, PPARG, PROX1, PTGS2, PTK2, PTN, PTP4A3, PTPRM, RAB13, S100A2, SEMA4A, TBXA2R, TDGF1, TDGF1P3, WNT5A, WNT7A]
GO:0048646	anatomical structure formation involved in morphogenesis	0,02	0,00	13,08	153,00	[ADAM15, ADAMTS9, ADGRB1, AGO2, AKR1B1, AKT3, AMTN, ANGPT1, ANGPTL4, ANGPTL6, AQP1, AREG, BMPER, BSG, C1GALT1, C3, CAMK1, CAMP, CAPN2, CAV1, CAV3, CCDC136, CCN3, CCR2, CCR3, CD34, CHI3L1, COL7A1, CRB1, CSRP1, CTHRC1, CXCL8, DAG1, DAND5, DCSTAMP, DLX5, DLX6, DMTF1, EFNA1, EFNA3, EMP2, ENAM, ENPP2, EPB41L3, EPGN, EREG, EXOC4, EXT1, FASLG, FHOD3, FOXH1, FZD6, GARS1, GATA2, GBA, GDF15, GHRL, GLUL, GPNMB, GPX1, GRHL2, HDAC9, HESX1, HOXA1, HOXA11, HOXA3, HOXA5, HOXA7, HYAL1, IFT122, IGFN1, IL10, IL6, ITGB8, JUNB, KBTBD8, KDR, KIF26B, KLHL7, KRIT1, LAMA3, LAMB3, LEP, LMOD2, LMOD3, LONP1, LRG1, MBD4, MIB1, MINDY4, MYDGF, MYOG, NANOS3, NAXE, NBEAL2, NPR1, OBSCN, PDGFRA, PKN1, PLXNA2, PLXND1, PODXL, PPARG, PRKACA, PROK2, PROX1, PTGS2, PTK2, PTN, PTPN14, PTPRM, RC3H1, RFX2, RNASEH2A, RNU6-664P, ROCK1, S100A1, SBNO2, SCRIB, SCX, SDCCAG8, SEMA4A, SETD2, SH2D2A, SHC1, SIRT6, SKOR2, SMAD2, SMO, SPAM1, SPINK2, STAB1, STK3, TBX20, TBXA2R, TCTA, TDGF1, TDGF1P3, THBS3, THSD7A, TMF1, TNNT2, TSPAN12, TWSG1, VASH2, WNT16, WNT2, WNT3A, WNT5A, WNT7A]

GO:0022603	regulation of anatomical structure morphogenesis	0,04	0,00	12,86	130,00	[ADAMTS9, ADGRB1, AGO2, AKR1B1, AKT3, ALDOA, ANGPTL4, AQP1, AREG, BMPER, C3, CALR, CAMP, CAV3, CCR2, CCR3, CD34, CDH2, CELSR3, CHI3L1, CHRNA3, CHRNB2, CPNE9, CRABP2, CSPG5, CTHRC1, CXCL8, CXXC1, CYRIB, DAG1, DAND5, DAPK3, DNM2, DNM3, EFNA1, EFNA3, EMP2, ENPP2, EPB41L3, FASLG, FGD5, FOXP1, FYCO1, FZD1, FZD6, GARS1, GATA2, GHRL, GLUL, GPNMB, HAS2, HOOK2, HOXA11, HOXA5, HYAL1, ICAM1, IL10, IL6, ITGB8, KDR, KIT, KRIT1, LEP, LIMD1, LRG1, MINDY4, MKLN1, MYDGF, MYL12A, MYOC, NANOS3, NAXE, NPR1, PALM, PEAK3, PKN1, PLXNA1, PLXNA2, PLXNA4, PLXNB1, PLXND1, PPARG, PPP1R9A, PRICKLE2, PROK2, PSMA8, PSMD4, PTK2, PTN, PTPRM, PTPRS, RALBP1, RC3H1, RHOA, RIMS2, RNU6-664P, ROCK1, RSPO2, RUFY3, S100A1, SCX, SEM1, SEMA3B, SEMA3F, SEMA3G, SEMA4A, SEMA6B, SEPTIN7, SIRT6, SKOR2, SMO, SPAM1, STAB1, STK11, STRIP2, SYT17, SYT2, SYT4, TBXA2R, TNFRSF11B, TNR, TRIM46, TSPAN12, TWF2, UNC13A, VASH2, WNT2, WNT3A, WNT5A, WNT7A]
GO:0035295	tube development	0,01	0,00	13,63	152,00	[ADAM15, ADAMTS9, ADGRB1, AGO2, AGR2, AKR1B1, AKT3, ANGPT1, ANGPTL1, ANGPTL4, ANGPTL6, AQP1, AREG, ASB4, BMPER, BSG, C1GALT1, C3, CAMP, CAV1, CAV3, CCN3, CCR2, CCR3, CD34, CDH2, CHI3L1, COMP, CRLF1, CTHRC1, CXCL8, DAG1, DAND5, EFNA1, EFNA3, EMP2, ENPP2, EPGN, EREG, EXT1, FASLG, FERD3L, FLNB, FOXH1, FOXP1, FSTL3, FZD6, GARS1, GATA2, GHRL, GLUL, GORAB, GPNMB, GPR161, GPX1, GREB1L, GRHL2, HAS2, HDAC9, HESX1, HOOK2, HOPX, HOXA1, HOXA11, HOXA13, HOXA3, HOXA5, HOXA7, HSD11B1, HYAL1, IFT122, IL10, IL6, ING3, INKA1, ITGB8, JUNB, KDM5B, KDR, KIF26B, KIT, KRIT1, LAMA1, LDLR, LEP, LRG1, MBD4, MET, MIB1, MINDY4, MST1, MTSS1, MYC, MYDGF, NANOS3, NAXE, NPR1, NPY, OXTR, PDGFRA, PHF14, PKN1, PLXNA2, PLXND1, PODXL, PPARG, PRKACA, PROK2, PROX1, PRRX1, PTGS2, PTK2, PTN, PTPRM, RAB3A, RIDA, RNASEH2A, RNU6-664P, ROCK1, RSPO2, S100A1, SCRIB, SDCCAG8, SEMA4A, SETD2, SH2D2A, SHC1, SIRT6, SMAD2, SMAD7, SMO, SOAT1, SOSTDC1, SPAM1, STAB1, STK3, TBX20, TBXA2R, TDGF1, TDGF1P3, THSD7A, TNNC1, TSPAN12, TYMS, VASH2, VPS52, WNT2, WNT3A, WNT5A, WNT7A, ZFPM2, ZNF358]
GO:0035239	tube morphogenesis	0,00	0,00	14,60	131,00	[ADAM15, ADAMTS9, ADGRB1, AGO2, AGR2, AKR1B1, AKT3, ANGPT1, ANGPTL1, ANGPTL4, ANGPTL6, AQP1, AREG, ASB4, BMPER, BSG, C1GALT1, C3, CAMP, CAV1, CAV3, CCN3, CCR2, CCR3, CD34, CDH2, CHI3L1, COMP, CTHRC1, CXCL8, DAG1, DAND5, EFNA1, EFNA3, EMP2, ENPP2, EPGN, EREG, EXT1, FASLG, FOXH1, FOXP1, FZD6, GARS1, GATA2, GHRL, GLUL, GPNMB, GPX1, GREB1L, GRHL2, HAS2, HDAC9, HESX1, HOOK2, HOXA1, HOXA11, HOXA13, HOXA3, HOXA5, HOXA7, HYAL1, IFT122, IL10, IL6, ITGB8, JUNB, KDM5B, KDR, KIF26B, KRIT1, LAMA1, LDLR, LEP, LRG1, MBD4, MET, MIB1, MINDY4, MST1, MTSS1, MYC, MYDGF, NANOS3, NAXE, NPR1, PDGFRA, PKN1, PLXND1, PODXL, PPARG, PRKACA, PROK2, PROX1, PRRX1, PTGS2, PTK2, PTN, PTPRM, RNASEH2A, RNU6-664P, ROCK1, RSPO2, S100A1, SCRIB, SDCCAG8, SEMA4A, SETD2, SH2D2A, SHC1, SIRT6, SMAD2, SMAD7, SMO, SOSTDC1, SPAM1, STAB1, STK3, TBX20, TBXA2R, TDGF1, TDGF1P3, THSD7A, TNNC1, TSPAN12, VASH2, WNT2, WNT3A, WNT5A, WNT7A, ZFPM2]
GO:0072359	circulatory system development	0,01	0,00	13,46	156,00	[ADAM15, ADAMTS9, ADGRB1, AGO2, AHR, AKT3, ANGPT1, ANGPTL1, ANGPTL4, ANGPTL6, ANKRD17, AQP1, ASB4, BMPER, BORCS8, BSG, C1GALT1, C3, CACYBP, CALCA, CALR, CAMP, CAV1, CAV3, CCN3, CCR2, CCR3, CD34, CDH2, CHI3L1, COL1A2, COMP, CXCL8, DAG1, DAND5, DNAH11, DNMT1, EFNA1, EFNA3, EMP2, ENPP2, EPGN, EPOR, EREG, EXT1, FASLG, FHOD3, FLVCR1, FOXH1, GARS1, GATA2, GHRL, GLUL, GPNMB, GPX1, GREB1L, GRHL2, HAS2, HDAC9, HNRNPU, HOOK2, HOPX, HOXA1, HOXA13, HOXA3, HOXA5, HOXA7, HYAL1, IFT122, IL10, IL6, IL6R, INSR, ITGB8, JUNB, KCNK2, KDR, KIT, KRIT1, LAMA1, LDLR, LEFTY1, LEP, LMNA, LONP1, LRG1, LY6E, LYL1, MBD1, MBD3, MBD4, MEF2D, MIB1, MINDY4, MYDGF, MYL3, NANOS3, NAXE, NDUFV2, NPR1, OXTR, PDGFRA, PIN1, PKN1, PLXND1, PPARG, PROK2, PROX1, PRRX1, PTGS2, PTK2, PTN, PTPN14, PTPRM, RAF1, REST, RNASEH2A, RNU6-664P, ROCK1, S100A1, SCX, SEMA4A, SETD2, SGCB, SH2D2A, SHC1, SIRT6, SMAD2, SMAD7, SMO, SMYD2, SPAM1, SRI, STAB1, STK11, STK3, TBX20, TBXA2R, TDGF1, TDGF1P3, THSD7A, TMEM65, TNNC1, TNNI1, TNNT2, TREX1, TSPAN12, VASH2, VGLL4, WNT16, WNT2, WNT3A, WNT5A, WNT7A, ZBTB14, ZFPM2]
GO:0001944	vasculature development	0,00	0,00	15,15	115,00	[ADAM15, ADAMTS9, ADGRB1, AGO2, AHR, AKT3, ANGPT1, ANGPTL1, ANGPTL4, ANGPTL6, ANKRD17, AQP1, ASB4, BMPER, BSG, C1GALT1, C3, CALCA, CAMP, CAV1, CCN3, CCR2, CCR3, CD34, CDH2, CHI3L1, COL1A2, COMP, CXCL8, DAG1, DAND5, DNMT1, EFNA1, EFNA3, EMP2, ENPP2, EPGN, EREG, FASLG, FLVCR1, FOXH1, GARS1, GATA2, GHRL, GLUL, GPNMB, GPX1, HAS2, HDAC9, HOOK2, HOXA1, HOXA13, HOXA3, HOXA5, HOXA7, HYAL1, IL10, IL6, IL6R, ITGB8, JUNB, KDR, KIT, KRIT1, LAMA1, LDLR, LEP, LRG1, LYL1, MBD4, MIB1, MINDY4, MYDGF, NANOS3, NAXE, NPR1, PDGFRA, PLXND1, PPARG, PROK2, PROX1, PRRX1, PTGS2, PTK2, PTN, PTPN14, PTPRM, RNASEH2A, RNU6-664P, ROCK1, S100A1, SEMA4A, SETD2, SGCB, SH2D2A, SHC1, SIRT6, SMAD7, SMO, SPAM1, STAB1, STK11, TBX20, TBXA2R, TDGF1, TDGF1P3, THSD7A, TREX1, TSPAN12, VASH2, WNT2, WNT5A, WNT7A, ZBTB14, ZFPM2]
GO:0001568	blood vessel development	0,00	0,00	15,01	109,00	[ADAM15, ADAMTS9, ADGRB1, AGO2, AHR, AKT3, ANGPT1, ANGPTL1, ANGPTL4, ANGPTL6, ANKRD17, AQP1, ASB4, BMPER, BSG, C1GALT1, C3, CAMP, CAV1, CCN3, CCR2, CCR3, CD34, CHI3L1, COL1A2, COMP, CXCL8, DAG1, DAND5, EFNA1, EFNA3, EMP2, ENPP2, EPGN, EREG, FASLG, FLVCR1, FOXH1, GARS1, GATA2, GHRL, GLUL, GPNMB, GPX1, HAS2, HDAC9, HOOK2, HOXA1, HOXA13, HOXA3, HOXA5, HOXA7, HYAL1, IL10, IL6, IL6R, ITGB8, JUNB, KDR, KRIT1, LAMA1, LDLR, LEP, LRG1, LYL1, MBD4, MIB1, MINDY4, MYDGF, NANOS3, NAXE, NPR1, PDGFRA, PLXND1, PPARG, PROK2, PROX1, PRRX1, PTGS2, PTK2, PTN, PTPRM, RNASEH2A, RNU6-664P, ROCK1, S100A1, SEMA4A, SETD2, SH2D2A, SHC1, SIRT6, SMAD7, SMO, SPAM1, STAB1, TBX20, TBXA2R, TDGF1, TDGF1P3, THSD7A, TREX1, TSPAN12, VASH2, WNT2, WNT5A, WNT7A, ZBTB14, ZFPM2]
GO:0001525	angiogenesis	0,01	0,00	15,17	83,00	[ADAM15, ADAMTS9, ADGRB1, AGO2, AKT3, ANGPT1, ANGPTL1, ANGPTL4, ANGPTL6, AQP1, BMPER, BSG, C1GALT1, C3, CAMP, CAV1, CCN3, CCR2, CCR3, CD34, CHI3L1, COL1A2, COMP, CXCL8, DAG1, DAND5, EFNA1, EFNA3, EMP2, ENPP2, EPGN, EREG, FASLG, GARS1, GATA2, GHRL, GLUL, GPNMB, GPX1, HDAC9, HOOK2, HOXA3, HOXA5, HOXA7, HYAL1, IL10, IL6, ITGB8, KDR, KRIT1, LEP, LRG1, MBD4, MINDY4, MYDGF, NANOS3, NAXE, NPR1, PDGFRA, PLXND1, PPARG, PROK2, PTGS2, PTK2, PTN, PTPRM, RNU6-664P, ROCK1, S100A1, SEMA4A, SETD2, SH2D2A, SHC1, SIRT6, SPAM1, STAB1, TBX20, TBXA2R, TDGF1, TDGF1P3, THSD7A, TSPAN12, VASH2, WNT5A, WNT7A]
GO:0048514	blood vessel morphogenesis	0,00	0,00	15,37	99,00	[ADAM15, ADAMTS9, ADGRB1, AGO2, AKT3, ANGPT1, ANGPTL1, ANGPTL4, ANGPTL6, AQP1, ASB4, BMPER, BSG, C1GALT1, C3, CAMP, CAV1, CCN3, CCR2, CCR3, CD34, CDH2, CHI3L1, COMP, CXCL8, DAG1, DAND5, EFNA1, EFNA3, EMP2, ENPP2, EPGN, EREG, FASLG, FOXH1, GARS1, GATA2, GHRL, GLUL, GPNMB, GPX1, HAS2, HDAC9, HOOK2, HOXA1, HOXA13, HOXA3, HOXA5, HOXA7, HYAL1, IL10, IL6, ITGB8, JUNB, KDR, KRIT1, LAMA1, LDLR, LEP, LRG1, MBD4, MINDY4, MYDGF, NANOS3, NAXE, NPR1, PDGFRA, PLXND1, PPARG, PROK2, PROX1, PRRX1, PTGS2, PTK2, PTN, PTPRM, RNASEH2A, RNU6-664P, ROCK1, S100A1, SEMA4A, SETD2, SH2D2A, SHC1, SIRT6, SMAD7, SMO, SPAM1, STAB1, TBX20, TBXA2R, TDGF1, TDGF1P3, THSD7A, TSPAN12, VASH2, WNT5A, WNT7A, ZFPM2]
GO:0045765	regulation of angiogenesis	0,00	0,00	18,58	55,00	[ADAMTS9, ADGRB1, AGO2, AKT3, ANGPTL4, AQP1, BMPER, C3, CAMP, CCR2, CCR3, CD34, CHI3L1, CXCL8, DAND5, EFNA1, EFNA3, EMP2, ENPP2, FASLG, GARS1, GATA2, GHRL, GLUL, GPNMB, HOOK2, HOXA5, HYAL1, IL10, IL6, ITGB8, KDR, KRIT1, LEP, LRG1, MINDY4, MYDGF, NANOS3, NAXE, NPR1, PLXND1, PPARG, PROK2, PTN, PTPRM, ROCK1, S100A1, SEMA4A, SIRT6, SPAM1, STAB1, TBXA2R, TSPAN12, VASH2, WNT5A]
GO:0045766	positive regulation of angiogenesis	0,03	0,00	17,82	31,00	[AGO2, AKT3, ANGPTL4, AQP1, BMPER, C3, CAMP, CCR3, CD34, CHI3L1, CXCL8, DAND5, GARS1, GATA2, GHRL, HOOK2, HYAL1, IL10, IL6, ITGB8, KDR, LRG1, MINDY4, MYDGF, NANOS3, S100A1, SIRT6, SPAM1, TBXA2R, VASH2, WNT5A]

GO:0010033	response to organic substance	0,00	0,00	12,46	440,00	[ABCA7, ABCB4, ABL2, ACP5, ADAM15, ADAMTS3, ADAR, ADCY8, ADCYAP1, ADCYAP1R1, ADH5, ADIPOR1, ADSS2, AGR2, AHR, AKAP8, AKAP9, AKR1A1, AKR1B1, ANGPT1, APPL1, AQP1, AQP4, AREG, ARHGEF18, ARHGEF2, ARL6IP5, ASNS, ATF3, ATG7, ATIC, ATP6V1C1, ATP6V1F, ATP6V1G3, BMPER, BRINP2, BSG, BST2, CACNA1A, CACNA1S, CACTIN, CACYBP, CALCA, CALCR, CALR, CALR3, CAMP, CAPN2, CARM1, CATSPERD, CAV1, CAV2, CAV3, CCL25, CCR1, CCR2, CCR3, CCR5, CCR9, CCRL2, CD55, CD70, CDC34, CDKN2D, CFTR, CHERP, CHI3L1, CHRNA3, CHRNB2, CIDEA, CIITA, CISH, CLEC3B, CLOCK, CNN2, COL1A2, COLEC12, COMP, CREB3L3, CREB3L4, CRHR2, CRLF1, CSN1S1, CXCL6, CXCL8, CXCR6, CXXC1, CYC1, CYRIB, DAG1, DAND5, DAPK3, DCST1, DCSTAMP, DERL1, DHX9, DLX5, DNAJB1, DNAJB9, DNM2, DNMT1, EBI3, EDEM1, EDEM3, EEF1A1, EEF2, ELANE, ELOF1, ENY2, EPG5, EPHA5, EPHX1, EPOR, EREG, ETV3, EXT1, FAM107A, FASLG, FBXO32, FCER2, FGF22, FLNB, FMO1, FOXH1, FOXP1, FOXP2, FSTL3, FZR1, GAREM1, GARS1, GATA2, GBA, GDF15, GHRHR, GHRL, GIPC1, GLUL, GNA15, GNAI2, GNAL, GNRHR, GPIHBP1, GPT, GREM2, GRIN2A, GRM2, GSDME, GTF2F1, H3-3B, HAS2, HAX1, HCN2, HCN3, HDAC9, HDGF, HERPUD2, HNRNPA2B1, HNRNPM, HNRNPU, HOOK2, HOXA13, HOXA2, HRH1, HRH4, HSF1, HYAL1, HYAL2, HYAL3, ICAM1, IER2, IFI30, IGFBP7, IL10, IL12RB1, IL17RB, IL17RC, IL17RD, IL17RE, IL19, IL20, IL24, IL27RA, IL5RA, IL6, IL6R, ILDR2, IMPACT, IMPDH2, INAVA, ING3, INSR, INSRR, IP6K2, IQGAP3, IRAK2, IRF5, IRF6, ITGB8, JAGN1, JAK3, JUNB, JUND, KANK2, KBTBD2, KCP, KCTD6, KDM5B, KDR, KEAP1, KHSRP, KIT, KLF1, KLF10, KLF15, KLF16, KLHL20, KMO, LAMTOR2, LDHA, LDLR, LEFTY1, LEFTY2, LEP, LITAF, LMNA, LONP1, LPIN2, LRG1, LTF, LY6E, LY6H, MAFA, MANF, MAP2K7, MAPKAPK3, MBD1, MBD3, MBD4, MCM2, MGST3, MINDY4, MPC2, MST1R, MUC1, MYC, MYDGF, MYOG, NANOS3, NDUFA13, NOD1, NPC1, NPRL2, NR5A2, NTRK1, OGG1, OR10H1, OR10H2, OR10H3, OR10H4, OR10H5, OXTR, P2RY11, PALM, PALM3, PARP1, PAX4, PDE12, PDGFRA, PDK4, PEG10, PFKFB2, PHOX2B, PIAS2, PIAS4, PIK3C3, PIK3R2, PIN1, PKLR, PKN1, PLK5, PLP2, PLVAP, PMVK, POLR2B, POLR2E, POU2F1, PPAN-P2RY11, PPARG, PPAT, PPBP, PRDX2, PRKACA, PRKAR2A, PRKCD, PSMA8, PSMD4, PTGER1, PTGS2, PTK2, PTN, PTP4A3, PTPN14, PTPN2, PTPN23, PTPN7, PTPRC, PTPRZ1, QRICH1, RAB11B, RAB12, RAB13, RAB31, RAB43, RAB8A, RAF1, RASL11B, RBBP8, RC3H1, REST, RETN, RGS8, RHOA, RIDA, RIOK3, RNASEH2A, RNASEL, RNF113A, RNF125, RNF126, RNF139, RNF165, RNU6-664P, ROCK1, RPL17, RPL23, RRM2B, S100A14, S100A9, SAFB, SAFB2, SBNO2, SCAP, SCX, SEC61A1, SELE, SELP, SEM1, SETD2, SGTA, SH2D2A, SHARPIN, SHC1, SHFL, SKOR2, SLA, SLC26A6, SLC27A1, SLC30A8, SLC5A5, SLC6A1, SLURP2, SMAD2, SMAD7, SMARCA4, SMARCC1, SMO, SMYD3, SNRPN, SNX10, SOAT1, SOCS1, SOSTDC1, SPAM1, SPPL2B, SQLE, SRI, STAP1, STEAP2, STK11, SYBU, TAC1, TADA3, TAF2, TATDN2, TAX1BP1, TBX20, TBXA2R, TDGF1, TDGF1P3, TGIF1, TICAM1, TIMP4, TLR9, TMEM161A, TMEM259, TMEM33, TMEM38A, TMF1, TNFRSF11B, TNFSF14, TNFSF18, TNFSF4, TNFSF9, TNNC1, TPR, TRAF5, TRAIP, TREX1, TRH, TRIB1, TSPAN12, TWF2, TWSG1, TXK, TYK2, TYMS, UBA52, UBR5, UBXN6, UPF1, UQCRC1, USP14, USP19, USP46, VAV1, VN1R5, WFS1, WNT2, WNT3A, WNT5A, WNT7A, WNT9A, XCL1, XCL2, XCR1, YES1, YOD1, ZBTB7A, ZBTB7B, ZNF16]
GO:0070887	cellular response to chemical stimulus	0,00	0,00	12,09	426,00	[ABCA7, ABCB4, ABL2, ACER1, ADAM15, ADAMTS3, ADAR, ADCY10, ADCY8, ADCYAP1, ADH5, ADIPOR1, AGR2, AHR, AKAP8, AKAP9, AKR1A1, AKR1B1, ANGPT1, APPL1, AQP1, AQP4, AREG, ARHGEF18, ARHGEF2, ARL6IP5, ASNS, ATF3, ATG7, ATIC, ATP6V1C1, ATP6V1F, ATP6V1G3, BMPER, BRINP2, BSG, BST2, CACNA1A, CACNA1S, CACTIN, CACYBP, CALCA, CALR, CALR3, CAMP, CAPN2, CARM1, CAV1, CAV2, CAV3, CCL25, CCN3, CCR1, CCR2, CCR3, CCR5, CCR9, CCRL2, CD34, CD55, CD70, CDC34, CFTR, CHERP, CHI3L1, CHRNA3, CHRNB2, CIDEA, CIITA, CISH, CLEC3B, CLOCK, CNN2, COL1A2, COLEC12, COMP, CPNE9, CREB3L3, CREB3L4, CRHR2, CRLF1, CXCL6, CXCL8, CXCR6, CXXC1, DAG1, DAND5, DAPK3, DCST1, DCSTAMP, DERL1, DHX9, DLX5, DNAJB9, DNM2, DNMT1, DOCK4, EBI3, EDEM1, EEF1A1, EEF2, ELOF1, ENY2, EPG5, EPHA5, EPHX1, EPOR, EREG, ETV3, EXT1, FAM107A, FASLG, FBXO32, FCER2, FGF22, FLNB, FMO1, FMO2, FMO3, FMO4, FOXH1, FOXP1, FSTL3, FZR1, GAREM1, GARS1, GBA, GDF15, GHRHR, GHRL, GIPC1, GNA15, GNAI2, GNAL, GNRHR, GPR37, GPR37L1, GPT, GPX1, GREM2, GRIN2A, GSDME, GTF2F1, GUK1, H3-3B, HAS2, HAX1, HCN2, HCN3, HDAC9, HDGF, HERPUD2, HESX1, HNRNPA2B1, HNRNPM, HNRNPU, HOOK2, HOXA13, HOXA2, HRH1, HRH4, HSF1, HYAL1, HYAL2, HYAL3, ICAM1, IFI30, IGFBP7, IL10, IL12RB1, IL17RB, IL17RC, IL17RD, IL17RE, IL19, IL20, IL24, IL27RA, IL5RA, IL6, IL6R, IMPACT, IMPDH2, ING3, INSR, INSRR, IP6K2, IQGAP3, IRAK2, IRF5, IRF6, ITGB8, ITPKB, JAGN1, JAK3, JUNB, JUND, KANK2, KCND2, KCNK2, KCP, KCTD6, KDM5B, KDR, KEAP1, KHSRP, KIT, KLF1, KLF10, KLF15, KLF16, KMO, LAMTOR2, LDLR, LEFTY1, LEFTY2, LEP, LIMD1, LITAF, LMNA, LONP1, LOXHD1, LPIN2, LRG1, LRRC8E, LTF, LY6E, LY6H, MAPRE2, MBD4, MCM2, MET, MGST3, MINDY4, MPC2, MST1, MST1R, MUC1, MYC, MYDGF, MYOG, NANOS3, NCF2, NDRG1, NDUFA13, NOD1, NPC1, NPRL2, NR5A2, NTRK1, OGG1, OR10H1, OR10H2, OR10H3, OR10H4, OR10H5, OXR1, P2RY11, PALM, PALM3, PARP1, PDE12, PDE4A, PDGFRA, PDK4, PEG10, PHOX2B, PIAS2, PIAS4, PIK3R2, PIN1, PIP5K1C, PKLR, PKN1, PLA2G4A, PLK5, PLP2, PLVAP, PLXNA4, POLR2B, POLR2E, PON3, POU2F1, PPAN-P2RY11, PPARG, PPAT, PPBP, PPP1R9A, PRDX1, PRDX2, PRDX6, PRKACA, PRKAR2A, PRKCD, PSMA8, PSMD4, PTGER1, PTGS2, PTK2, PTN, PTP4A3, PTPN14, PTPN2, PTPN23, PTPN7, PTPRC, PTPRZ1, PYCR2, QRICH1, RAB11B, RAB12, RAB13, RAB31, RAB43, RAB8A, RAF1, RASL11B, RC3H1, RCSD1, REST, RGS8, RHOA, RIOK3, RNASEH2A, RNASEL, RNF113A, RNF125, RNF126, RNF165, ROCK1, RPL17, RPL23, S100A12, S100A14, S100A9, SAFB, SAFB2, SBNO2, SCX, SEM1, SEMA3B, SHARPIN, SHC1, SKOR2, SLA, SLC25A23, SLC26A6, SLC27A1, SLC38A3, SLC5A5, SLURP2, SMAD2, SMAD7, SMARCA4, SMARCC1, SMO, SMYD3, SNX10, SOCS1, SOSTDC1, SPAM1, SPPL2B, SRI, STAP1, STK11, SULT1B1, SYBU, SYT11, SYT17, SYT2, SYT4, TAC1, TADA3, TAFA4, TATDN2, TAX1BP1, TBX20, TBXA2R, TDGF1, TDGF1P3, TGIF1, TICAM1, TMEM161A, TMEM33, TMEM38A, TMF1, TNFRSF11B, TNFSF14, TNFSF18, TNFSF4, TNFSF9, TNNC1, TPR, TRAF5, TRAIP, TREX1, TRH, TRIB1, TSPAN12, TWF2, TWSG1, TXK, TXNDC2, TXNRD3, TYK2, UBA52, UBR5, UPF1, USP19, VAV1, WFS1, WNT16, WNT2, WNT3A, WNT5A, WNT7A, WNT9A, XCL1, XCL2, XCR1, YES1, YOD1, ZBTB7A, ZBTB7B, ZNF16, ZNF277]
GO:0071495	cellular response to endogenous stimulus	0,03	0,00	12,52	189,00	[ADCY8, ADCYAP1, ADIPOR1, AHR, AKAP8, AKAP9, AKR1B1, APPL1, AQP1, AREG, ARHGEF18, ARHGEF2, ASNS, ATG7, ATP6V1C1, ATP6V1F, ATP6V1G3, BMPER, CACNA1A, CACNA1S, CALCA, CALR, CAMP, CAPN2, CARM1, CAV1, CAV2, CAV3, CFTR, CHERP, CIDEA, CLEC3B, CLOCK, COL1A2, COMP, CRHR2, CXCL8, DAND5, DLX5, DNM2, DNMT1, EBI3, EEF1A1, EEF2, EXT1, FAM107A, FBXO32, FGF22, FOXH1, FOXP1, FSTL3, FZR1, GAREM1, GARS1, GDF15, GHRHR, GHRL, GIPC1, GNA15, GNAI2, GNAL, GNRHR, GPT, GREM2, GRIN2A, GTF2F1, H3-3B, HAS2, HCN2, HCN3, HDAC9, HNRNPM, HNRNPU, HOXA13, HRH1, HRH4, HSF1, HYAL1, HYAL2, ICAM1, IGFBP7, IL17RD, IMPACT, ING3, INSR, INSRR, ITGB8, JAK3, KANK2, KCP, KCTD6, KDM5B, KIT, KLF1, KLF10, KLF15, KLF16, LAMTOR2, LEFTY1, LEFTY2, LEP, LPIN2, LRG1, MBD4, MINDY4, MYC, NOD1, NPC1, NR5A2, NTRK1, OR10H1, OR10H2, OR10H3, OR10H4, OR10H5, P2RY11, PALM, PARP1, PDGFRA, PDK4, PEG10, PHOX2B, PIAS2, PIK3R2, PIN1, PKLR, PKN1, POLR2B, POLR2E, PPAN-P2RY11, PPARG, PPAT, PRKACA, PRKAR2A, PRKCD, PTGER1, PTGS2, PTK2, PTN, PTPN2, RAB12, RAB13, RAB31, RAB8A, RASL11B, REST, RGS8, RHOA, RNF165, ROCK1, RPL17, RPL23, SAFB, SAFB2, SCX, SHC1, SKOR2, SLC26A6, SLC27A1, SLC5A5, SMAD2, SMAD7, SMARCA4, SMARCC1, SMYD3, SOCS1, SOSTDC1, SPAM1, STK11, TAC1, TADA3, TBX20, TDGF1, TDGF1P3, TMEM38A, TMF1, TNFSF4, TNNC1, TRH, TWSG1, UBA52, UBR5, WNT2, WNT5A, WNT7A, XCL1, YES1, ZBTB7A, ZBTB7B]
GO:1901698	response to nitrogen compound	0,01	0,00	13,32	163,00	[ADCY8, ADIPOR1, ADSS2, AHR, AKAP9, AKR1B1, APPL1, AQP1, AREG, ARHGEF2, ASNS, ATG7, ATP6V1C1, ATP6V1F, ATP6V1G3, BSG, CACNA1A, CACNA1S, CACYBP, CALCR, CAMP, CAPN2, CARM1, CAV1, CAV2, CAV3, CFTR, CHRNA3, CHRNB2, CIITA, COL1A2, COLEC12, CRHR2, CYC1, DAG1, DAND5, DERL1, DHX9, DNAJB9, DNM2, DNMT1, EDEM1, EDEM3, EEF2, EPG5, EREG, EXT1, FZR1, GDF15, GHRHR, GHRL, GNA15, GNAI2, GNAL, GNRHR, GPIHBP1, GPT, GRIN2A, GRM2, HCN2, HCN3, HDAC9, HRH1, HRH4, HSF1, ICAM1, IL10, IL6, IMPACT, INAVA, INSR, INSRR, IRF5, JAK3, JUND, KBTBD2, KLF1, KLF10, KLF15, KLF16, LAMTOR2, LDHA, LDLR, LEP, LPIN2, LY6E, LY6H, MBD1, MGST3, MINDY4, MUC1, MYC, NOD1, NPC1, NTRK1, OGG1, OR10H1, OR10H2, OR10H3, OR10H4, OR10H5, OXTR, P2RY11, PALM, PARP1, PAX4, PDE12, PDGFRA, PDK4, PIK3C3, PIK3R2, PKLR, PKN1, PPAN-P2RY11, PPARG, PPAT, PRKACA, PRKAR2A, PRKCD, PTGER1, PTGS2, PTK2, PTN, PTPN2, RAB12, RAB13, RAB31, RAB8A, RETN, RGS8, RHOA, RIOK3, RNF139, ROCK1, RPL17, RPL23, RRM2B, SCAP, SGTA, SH2D2A, SHC1, SLC26A6, SLC27A1, SLC5A5, SLC6A1, SLURP2, SMARCC1, SOCS1, TAC1, TICAM1, TIMP4, TMEM259, TMEM38A, TNFSF4, TREX1, TYMS, UBXN6, UQCRC1, USP14, USP19, WFS1, YOD1, ZBTB7B]
GO:1901700	response to oxygen-containing compound	0,00	0,00	12,90	236,00	[ABCB4, ABL2, ACP5, ADAM15, ADCY8, ADCYAP1, ADCYAP1R1, ADH5, ADIPOR1, AHR, AKAP8, AKAP9, AKR1A1, AKR1B1, APPL1, AQP1, AREG, ARHGEF2, ASNS, ATG7, ATP6V1C1, ATP6V1F, ATP6V1G3, BRINP2, BSG, CACNA1A, CACTIN, CACYBP, CALCR, CALR, CAMP, CAPN2, CARM1, CATSPERD, CAV1, CAV2, CCR5, CD55, CDKN2D, CFTR, CHRNA3, CHRNB2, COL1A2, COLEC12, CRHR2, CSN1S1, CXCL6, CXCL8, CXXC1, CYC1, DAG1, DAND5, DNM2, DNMT1, EDEM1, EDEM3, EEF2, ELANE, ENY2, EPHA5, EREG, EXT1, FASLG, FBXO32, FMO1, FOXP1, FOXP2, FZR1, GBA, GDF15, GHRHR, GHRL, GLUL, GNA15, GNAI2, GNAL, GNRHR, GPIHBP1, GPR37, GPR37L1, GPT, GPX1, GRIN2A, GRM2, HCN2, HCN3, HDAC9, HOXA2, HRH1, HRH4, HSF1, HYAL1, HYAL2, ICAM1, IGFBP7, IL10, IL24, IL6, ILDR2, IMPACT, INAVA, INSR, INSRR, IP6K2, IRAK2, IRF5, JAGN1, JAK3, JUND, KANK2, KBTBD2, KLF1, KLF10, KLF15, KLF16, KMO, LAMTOR2, LDHA, LDLR, LEP, LITAF, LONP1, LPIN2, LTF, LY6E, LY6H, MAFA, MAPKAPK3, MBD1, MBD3, MBD4, MET, MINDY4, MPC2, MUC1, MYC, MYOG, NANOS3, NDUFA13, NOD1, NTRK1, OGG1, OR10H1, OR10H2, OR10H3, OR10H4, OR10H5, OXR1, OXTR, P2RY11, PALM, PALM3, PARP1, PAX4, PDGFRA, PDK4, PFKFB2, PIK3C3, PIK3R2, PKLR, PKN1, PMVK, PPAN-P2RY11, PPARG, PPAT, PPBP, PRDX1, PRDX2, PRKACA, PRKAR2A, PRKCD, PTGER1, PTGS2, PTK2, PTN, PTPN2, RAB11B, RAB12, RAB13, RAB31, RAB43, RAB8A, RAF1, RBBP8, RETN, RGS8, RHOA, ROCK1, RPL17, RPL23, S100A14, S100A9, SBNO2, SCAP, SELE, SELP, SH2D2A, SHC1, SLC26A6, SLC27A1, SLC30A8, SLC5A5, SLC6A1, SLURP2, SMAD2, SMARCA4, SMARCC1, SMO, SMYD3, SOCS1, SPAM1, SRI, STAP1, SYBU, TAC1, TBXA2R, TICAM1, TIMP4, TMEM161A, TNFSF4, TNNC1, TREX1, TRH, TRIB1, TWF2, TYMS, UPF1, USP46, WNT2, WNT3A, WNT5A, WNT7A, WNT9A, YES1, ZBTB7B, ZNF277]

GO:0010243	response to organonitrogen compound	0,01	0,00	13,29	151,00	[ADCY8, ADIPOR1, ADSS2, AHR, AKAP9, AKR1B1, APPL1, AQP1, AREG, ARHGEF2, ASNS, ATG7, ATP6V1C1, ATP6V1F, ATP6V1G3, BSG, CACNA1A, CACNA1S, CACYBP, CALCR, CAMP, CAPN2, CARM1, CAV1, CAV2, CAV3, CFTR, CHRNB2, COL1A2, CRHR2, CYC1, DAG1, DAND5, DERL1, DNAJB9, DNM2, DNMT1, EDEM1, EDEM3, EEF2, EREG, EXT1, FZR1, GDF15, GHRHR, GHRL, GNA15, GNAI2, GNAL, GNRHR, GPIHBP1, GPT, GRIN2A, GRM2, HCN2, HCN3, HDAC9, HRH1, HRH4, HSF1, ICAM1, IL10, IL6, IMPACT, INAVA, INSR, INSRR, IRF5, JAK3, JUND, KBTBD2, KLF1, KLF10, KLF15, KLF16, LAMTOR2, LDHA, LDLR, LEP, LPIN2, MBD1, MGST3, MINDY4, MUC1, MYC, NOD1, NPC1, NTRK1, OGG1, OR10H1, OR10H2, OR10H3, OR10H4, OR10H5, OXTR, P2RY11, PALM, PARP1, PAX4, PDGFRA, PDK4, PIK3C3, PIK3R2, PKLR, PKN1, PPAN-P2RY11, PPARG, PPAT, PRKACA, PRKAR2A, PRKCD, PTGER1, PTGS2, PTK2, PTN, PTPN2, RAB12, RAB13, RAB31, RAB8A, RETN, RGS8, RHOA, RNF139, ROCK1, RPL17, RPL23, RRM2B, SCAP, SGTA, SH2D2A, SHC1, SLC26A6, SLC27A1, SLC5A5, SLC6A1, SMARCC1, SOCS1, TAC1, TICAM1, TIMP4, TMEM259, TMEM38A, TYMS, UBXN6, UQCRC1, USP14, USP19, WFS1, YOD1, ZBTB7B]
GO:0034097	response to cytokine	0,00	0,00	13,83	177,00	[ABL2, ACP5, ADAR, ADIPOR1, ANGPT1, APPL1, AQP4, ARHGEF2, ATIC, BST2, CACTIN, CACYBP, CALCA, CAMP, CAPN2, CAV1, CCL25, CCR1, CCR2, CCR3, CCR5, CCR9, CCRL2, CD70, CDC34, CHI3L1, CIITA, CISH, CNN2, COL1A2, CRLF1, CXCL6, CXCL8, CXCR6, DAPK3, DCST1, DCSTAMP, DHX9, EBI3, ELOF1, EPOR, EREG, ETV3, EXT1, FASLG, FCER2, FLNB, FOXH1, GBA, GIPC1, GREM2, GSDME, HAS2, HAX1, HDGF, HNRNPA2B1, HNRNPU, HOOK2, HYAL1, HYAL2, HYAL3, ICAM1, IFI30, IL10, IL12RB1, IL17RB, IL17RC, IL17RD, IL17RE, IL19, IL20, IL24, IL27RA, IL5RA, IL6, IL6R, IMPDH2, IP6K2, IRAK2, IRF5, IRF6, JAGN1, JAK3, JUNB, KDM5B, KEAP1, KHSRP, KIT, KLHL20, KMO, LEP, LONP1, MAP2K7, MAPKAPK3, MBD4, MCM2, MST1R, MUC1, MYC, MYDGF, MYOG, NDUFA13, NOD1, NPRL2, NR5A2, OXTR, PALM3, PDE12, PIAS4, PLP2, PLVAP, POU2F1, PPARG, PPBP, PRKACA, PRKCD, PSMA8, PSMD4, PTGS2, PTP4A3, PTPN14, PTPN2, PTPN23, PTPN7, PTPRC, PTPRZ1, RAB43, RC3H1, RHOA, RNASEH2A, RNASEL, RNF113A, RNF125, S100A9, SBNO2, SEC61A1, SELE, SELP, SEM1, SETD2, SHARPIN, SHC1, SHFL, SLA, SLC26A6, SLC27A1, SLC30A8, SMAD7, SMARCA4, SNX10, SOCS1, SPAM1, SPPL2B, STAP1, TAX1BP1, TDGF1, TDGF1P3, TIMP4, TNFRSF11B, TNFSF14, TNFSF18, TNFSF4, TNFSF9, TPR, TRAF5, TRAIP, TREX1, TXK, TYK2, TYMS, UBA52, UPF1, VAV1, WNT5A, XCL1, XCL2, XCR1]
GO:0071310	cellular response to organic substance	0,00	0,00	12,44	359,00	[ABCA7, ABCB4, ABL2, ADAM15, ADAMTS3, ADAR, ADCY8, ADCYAP1, ADIPOR1, AGR2, AHR, AKAP8, AKAP9, AKR1B1, ANGPT1, APPL1, AQP1, AQP4, AREG, ARHGEF18, ARHGEF2, ARL6IP5, ASNS, ATF3, ATG7, ATIC, ATP6V1C1, ATP6V1F, ATP6V1G3, BMPER, BRINP2, BST2, CACNA1A, CACNA1S, CACTIN, CACYBP, CALCA, CALR, CALR3, CAMP, CAPN2, CARM1, CAV1, CAV2, CAV3, CCL25, CCR1, CCR2, CCR3, CCR5, CCR9, CCRL2, CD55, CD70, CDC34, CFTR, CHERP, CHI3L1, CIDEA, CIITA, CISH, CLEC3B, CLOCK, CNN2, COL1A2, COLEC12, COMP, CREB3L3, CREB3L4, CRHR2, CRLF1, CXCL6, CXCL8, CXCR6, CXXC1, DAG1, DAND5, DAPK3, DCST1, DCSTAMP, DERL1, DHX9, DLX5, DNAJB9, DNM2, DNMT1, EBI3, EDEM1, EEF1A1, EEF2, ELOF1, ENY2, EPG5, EPHA5, EPOR, EREG, ETV3, EXT1, FAM107A, FASLG, FBXO32, FCER2, FGF22, FLNB, FOXH1, FOXP1, FSTL3, FZR1, GAREM1, GARS1, GBA, GDF15, GHRHR, GHRL, GIPC1, GNA15, GNAI2, GNAL, GNRHR, GPT, GREM2, GRIN2A, GSDME, GTF2F1, H3-3B, HAS2, HAX1, HCN2, HCN3, HDAC9, HDGF, HERPUD2, HNRNPA2B1, HNRNPM, HNRNPU, HOOK2, HOXA13, HOXA2, HRH1, HRH4, HSF1, HYAL1, HYAL2, HYAL3, ICAM1, IFI30, IGFBP7, IL10, IL12RB1, IL17RB, IL17RC, IL17RD, IL17RE, IL19, IL20, IL24, IL27RA, IL5RA, IL6, IL6R, IMPACT, IMPDH2, ING3, INSR, INSRR, IP6K2, IQGAP3, IRAK2, IRF5, IRF6, ITGB8, JAGN1, JAK3, JUNB, KANK2, KCP, KCTD6, KDM5B, KDR, KEAP1, KHSRP, KIT, KLF1, KLF10, KLF15, KLF16, KMO, LAMTOR2, LDLR, LEFTY1, LEFTY2, LEP, LITAF, LMNA, LONP1, LPIN2, LRG1, LTF, MBD4, MCM2, MINDY4, MPC2, MST1R, MUC1, MYC, MYDGF, MYOG, NDUFA13, NOD1, NPC1, NPRL2, NR5A2, NTRK1, OR10H1, OR10H2, OR10H3, OR10H4, OR10H5, P2RY11, PALM, PALM3, PARP1, PDE12, PDGFRA, PDK4, PEG10, PHOX2B, PIAS2, PIAS4, PIK3R2, PIN1, PKLR, PKN1, PLK5, PLP2, PLVAP, POLR2B, POLR2E, POU2F1, PPAN-P2RY11, PPARG, PPAT, PPBP, PRDX2, PRKACA, PRKAR2A, PRKCD, PSMA8, PSMD4, PTGER1, PTGS2, PTK2, PTN, PTP4A3, PTPN14, PTPN2, PTPN23, PTPN7, PTPRC, PTPRZ1, QRICH1, RAB11B, RAB12, RAB13, RAB31, RAB43, RAB8A, RAF1, RASL11B, RC3H1, REST, RGS8, RHOA, RIOK3, RNASEH2A, RNASEL, RNF113A, RNF125, RNF126, RNF165, ROCK1, RPL17, RPL23, S100A9, SAFB, SAFB2, SBNO2, SCX, SEM1, SHARPIN, SHC1, SKOR2, SLA, SLC26A6, SLC27A1, SLC5A5, SMAD2, SMAD7, SMARCA4, SMARCC1, SMO, SMYD3, SNX10, SOCS1, SOSTDC1, SPAM1, SPPL2B, SRI, STAP1, STK11, SYBU, TAC1, TADA3, TATDN2, TAX1BP1, TBX20, TBXA2R, TDGF1, TDGF1P3, TGIF1, TICAM1, TMEM33, TMEM38A, TMF1, TNFRSF11B, TNFSF14, TNFSF18, TNFSF4, TNFSF9, TNNC1, TPR, TRAF5, TRAIP, TREX1, TRH, TRIB1, TSPAN12, TWF2, TWSG1, TXK, TYK2, UBA52, UBR5, UPF1, VAV1, WFS1, WNT2, WNT3A, WNT5A, WNT7A, WNT9A, XCL1, XCL2, XCR1, YES1, YOD1, ZBTB7A, ZBTB7B, ZNF16]
GO:1901699	cellular response to nitrogen compound	0,01	0,00	14,12	108,00	[ADCY8, ADIPOR1, AHR, AKAP9, AKR1B1, APPL1, AQP1, ARHGEF2, ATG7, ATP6V1C1, ATP6V1F, ATP6V1G3, CACNA1A, CACNA1S, CAMP, CAPN2, CAV1, CAV2, CAV3, CFTR, CHRNA3, CHRNB2, CIITA, COL1A2, COLEC12, CRHR2, DAND5, DHX9, DNM2, DNMT1, EPG5, FZR1, GDF15, GHRHR, GHRL, GNA15, GNAI2, GNAL, GNRHR, GPT, GRIN2A, HCN2, HCN3, HDAC9, HRH1, HRH4, HSF1, ICAM1, IMPACT, INSR, INSRR, JAK3, KLF1, KLF10, KLF15, KLF16, LAMTOR2, LEP, LPIN2, LY6E, LY6H, MINDY4, MYC, NOD1, NTRK1, OR10H1, OR10H2, OR10H3, OR10H4, OR10H5, P2RY11, PALM, PARP1, PDE12, PDGFRA, PDK4, PIK3R2, PKLR, PKN1, PPAN-P2RY11, PPARG, PPAT, PRKACA, PRKAR2A, PRKCD, PTGER1, PTGS2, PTK2, PTPN2, RAB12, RAB13, RAB31, RAB8A, RGS8, RIOK3, ROCK1, RPL17, RPL23, SHC1, SLC26A6, SLC27A1, SLC5A5, SLURP2, SMARCA4, SMARCC1, SMO, SMYD3, SOCS1, SRI, STAP1, SYBU, TBXA2R, TICAM1, TMEM38A, TREX1, ZBTB7B]
GO:1901701	cellular response to oxygen-containing compound	0,02	0,00	12,96	167,00	[ABCB4, ABL2, ADAM15, ADCY8, ADH5, ADIPOR1, AHR, AKAP8, AKAP9, AKR1A1, AKR1B1, APPL1, AQP1, AREG, ARHGEF2, ATP6V1C1, ATP6V1F, ATP6V1G3, BRINP2, CACNA1A, CACTIN, CAMP, CAPN2, CAV1, CAV2, CCR5, CD55, CFTR, CHRNA3, CHRNB2, COL1A2, COLEC12, CRHR2, CXCL6, CXCL8, CXXC1, DAG1, DAND5, DNM2, DNMT1, ENY2, EPHA5, FBXO32, FZR1, GDF15, GHRHR, GHRL, GNA15, GNAI2, GNAL, GNRHR, GPR37, GPR37L1, GPT, GRIN2A, HCN2, HCN3, HDAC9, HOXA2, HRH1, HRH4, HSF1, ICAM1, IL10, IL24, IL6, IMPACT, INSR, INSRR, IP6K2, IRAK2, JAGN1, JAK3, KANK2, KLF1, KLF10, KLF15, KLF16, KMO, LAMTOR2, LDLR, LEP, LITAF, LONP1, LPIN2, LTF, LY6E, LY6H, MBD4, MET, MINDY4, MPC2, MYC, MYOG, NANOS3, NDUFA13, NOD1, NTRK1, OR10H1, OR10H2, OR10H3, OR10H4, OR10H5, OXR1, P2RY11, PALM, PARP1, PDGFRA, PDK4, PIK3R2, PKLR, PKN1, PPAN-P2RY11, PPARG, PPAT, PPBP, PRDX1, PRDX2, PRKACA, PRKAR2A, PRKCD, PTGER1, PTGS2, PTK2, PTN, PTPN2, RAB11B, RAB12, RAB13, RAB31, RAB43, RAB8A, RAF1, RGS8, RHOA, ROCK1, RPL17, RPL23, SBNO2, SHC1, SLC26A6, SLC27A1, SLC5A5, SLURP2, SMARCA4, SMARCC1, SMO, SMYD3, SOCS1, SRI, STAP1, SYBU, TBXA2R, TICAM1, TNFSF4, TNNC1, TREX1, TRIB1, TWF2, UPF1, WNT2, WNT3A, WNT5A, WNT9A, YES1, ZBTB7B, ZNF277]
GO:0071417	cellular response to organonitrogen compound	0,03	0,00	13,66	96,00	[ADCY8, ADIPOR1, AHR, AKAP9, AKR1B1, APPL1, AQP1, ARHGEF2, ATG7, ATP6V1C1, ATP6V1F, ATP6V1G3, CACNA1A, CACNA1S, CAMP, CAPN2, CAV1, CAV2, CAV3, CFTR, COL1A2, CRHR2, DAND5, DNM2, DNMT1, FZR1, GDF15, GHRHR, GHRL, GNA15, GNAI2, GNAL, GNRHR, GPT, GRIN2A, HCN2, HCN3, HDAC9, HRH1, HRH4, HSF1, ICAM1, IMPACT, INSR, INSRR, JAK3, KLF1, KLF10, KLF15, KLF16, LAMTOR2, LEP, LPIN2, MINDY4, MYC, NOD1, NTRK1, OR10H1, OR10H2, OR10H3, OR10H4, OR10H5, P2RY11, PALM, PARP1, PDGFRA, PDK4, PIK3R2, PKLR, PKN1, PPAN-P2RY11, PPARG, PPAT, PRKACA, PRKAR2A, PRKCD, PTGER1, PTGS2, PTK2, PTPN2, RAB12, RAB13, RAB31, RAB8A, RGS8, ROCK1, RPL17, RPL23, SHC1, SLC26A6, SLC27A1, SLC5A5, SMARCC1, SOCS1, TMEM38A, ZBTB7B]
GO:0071345	cellular response to cytokine stimulus	0,00	0,00	13,82	164,00	[ABL2, ADAR, ADIPOR1, ANGPT1, APPL1, AQP4, ARHGEF2, ATIC, BST2, CACTIN, CACYBP, CALCA, CAMP, CAPN2, CAV1, CCL25, CCR1, CCR2, CCR3, CCR5, CCR9, CCRL2, CD70, CDC34, CHI3L1, CIITA, CISH, CNN2, COL1A2, CRLF1, CXCL6, CXCL8, CXCR6, DAPK3, DCST1, DCSTAMP, DHX9, EBI3, ELOF1, EPOR, EREG, ETV3, EXT1, FASLG, FCER2, FLNB, FOXH1, GBA, GIPC1, GREM2, GSDME, HAS2, HAX1, HDGF, HNRNPA2B1, HNRNPU, HOOK2, HYAL1, HYAL2, HYAL3, ICAM1, IFI30, IL10, IL12RB1, IL17RB, IL17RC, IL17RD, IL17RE, IL19, IL20, IL24, IL27RA, IL5RA, IL6, IL6R, IMPDH2, IP6K2, IRAK2, IRF5, IRF6, JAGN1, JAK3, JUNB, KDM5B, KEAP1, KHSRP, KIT, KMO, LEP, LONP1, MBD4, MCM2, MST1R, MUC1, MYC, MYDGF, MYOG, NDUFA13, NOD1, NPRL2, NR5A2, PALM3, PDE12, PIAS4, PLP2, PLVAP, POU2F1, PPARG, PPBP, PRKACA, PRKCD, PSMA8, PSMD4, PTGS2, PTP4A3, PTPN14, PTPN2, PTPN23, PTPN7, PTPRC, PTPRZ1, RAB43, RC3H1, RHOA, RNASEH2A, RNASEL, RNF113A, RNF125, S100A9, SBNO2, SEM1, SHARPIN, SHC1, SLA, SLC26A6, SLC27A1, SMAD7, SMARCA4, SNX10, SOCS1, SPAM1, SPPL2B, STAP1, TAX1BP1, TDGF1, TDGF1P3, TNFRSF11B, TNFSF14, TNFSF18, TNFSF4, TNFSF9, TPR, TRAF5, TRAIP, TREX1, TXK, TYK2, UBA52, UPF1, VAV1, WNT5A, XCL1, XCL2, XCR1]

ID	Term	Term PValue Corrected with Benjamini-Hochberg	Group pValue Corrected with Benjamini-Hochberg	% Associated Genes	Nr. Genes	Associated Genes Found
R-HSA:2453902	The canonical retinoid cycle in rods (twilight vision)	0,03	0,03	17,39	4,00	[HSD17B6, NAPEPLD, RDH16, SDR9C7]
R-HSA:392517	Rap1 signalling	0,01	0,01	25,00	4,00	[PRKG1, RAP1B, RASGRP2, SIPA1]
WP:1422	Sphingolipid pathway	0,05	0,04	13,33	4,00	[ASAH2, CERK, PPP1CA, SGMS1]
WP:143	Fatty acid beta-oxidation	0,01	0,01	17,65	6,00	[CHKB, CPT1A, CPT1B, DLD, LIPF, PNPLA2]
WP:2848	Differentiation Pathway	0,03	0,03	12,50	6,00	[DKK1, FGF4, HGF, INHBA, INS, WNT7B]
WP:2878	PPAR-alpha pathway	0,01	0,01	19,23	5,00	[CCND1, CDK4, CPT1A, NR1H3, PPARA]
WP:383	Striated Muscle Contraction Pathway	0,03	0,03	13,16	5,00	[ACTA2, ACTN3, MYBPC3, TNNI2, TNNT3]
WP:3844	PI3K-AKT-mTOR signaling pathway and therapeutic opportunities	0,02	0,02	16,67	5,00	[ATG13, BAD, GRB10, HRAS, PIK3CG]
WP:3869	Cannabinoid receptor signaling	0,02	0,02	17,24	5,00	[DAGLA, MAPK11, MAPK12, NAPEPLD, PRKAR2B]
GO:0010642	negative regulation of platelet-derived growth factor receptor signaling pathway	0,03	0,03	21,43	3,00	[LRP1, PTPN12, PTPRJ]
WP:3933	Kennedy pathway from sphingolipids	0,04	0,03	20,00	3,00	[CHKA, CHKB, PTDSS2]
WP:3935	Leptin Insulin Overlap	0,04	0,04	17,65	3,00	[DGKZ, INS, PIK3CG]
WP:45	G1 to S cell cycle control	0,03	0,03	10,94	7,00	[CCND1, CDK4, CREB311, MDM2, ORC5, POLA2, PRIM1]
WP:47	Hedgehog Signaling Pathway Netpath	0,04	0,03	18,75	3,00	[GLI1, GLI3, GRK2]
WP:4722	Glycerolipids and Glycerophospholipids	0,01	0,01	20,83	5,00	[CHKB, DGKZ, PNPLA2, PNPLA3, PTDSS2]
WP:4877	Host-pathogen interaction of human coronaviruses - MAPK signaling	0,01	0,02	16,67	6,00	[DDIT3, IFITM1, IFITM3, MAP3K11, MAPK11, MAPK12]
WP:5046	NAD Metabolism in Oncogene-induced Senescence and Mitochondrial Dysfunction-Associated Senescence	0,03	0,03	16,67	4,00	[NAMPT, RELA, SCO2, SIRT3]
WP:5053	Development of ureteric collection system	0,03	0,03	12,77	6,00	[CCND1, CELSR1, GLI1, GLI3, GRIP1, WT1]
R-HSA:5362517	Signaling by Retinoic Acid	0,02	0,02	13,95	6,00	[CPT1A, CPT1B, DLD, PDHX, RDH16, SDR16C5]
GO:0022841	potassium ion leak channel activity	0,04	0,03	18,75	3,00	[KCNK12, KCNK4, KCNK7]
GO:0033273	response to vitamin	0,02	0,02	10,09	11,00	[CAT, CCND1, CYP27B1, EGFR, FADS1, GLYAT, MDM2, PDHX, PENK, RELA, TSPO]
GO:0035269	protein O-linked mannosylation	0,05	0,04	16,67	3,00	[B4GAT1, LARGE2, RXYLT1]
GO:0042832	defense response to protozoan	0,03	0,03	16,00	4,00	[BATF2, CCDC88B, HRAS, TSPAN32]
GO:0045899	positive regulation of RNA polymerase II transcription preinitiation complex assembly	0,02	0,02	30,00	3,00	[CAND1, PSMC2, PSMC3]
GO:0048633	positive regulation of skeletal muscle tissue growth	0,00	0,00	75,00	3,00	[ACTN3, IGF2, NACA]
GO:0048843	negative regulation of axon extension involved in axon guidance	0,04	0,03	14,81	4,00	[SEMA3A, SEMA3C, SEMA3D, SEMA3E]
GO:0050994	regulation of lipid catabolic process	0,02	0,02	12,12	8,00	[BSCL2, CDK4, CPT1A, INS, LGALS12, PIK3CG, PNPLA2, PPARA]
GO:0051412	response to corticosterone	0,01	0,02	21,74	5,00	[AVPR1A, CCND1, FOSL1, NPAS4, TH]
GO:0070885	negative regulation of calcineurin-NFAT signaling cascade	0,04	0,03	18,75	3,00	[ACTN3, DYRK2, TBC1D10C]
GO:0090336	positive regulation of brown fat cell differentiation	0,04	0,04	17,65	3,00	[INS, NAPEPLD, VSTM2A]
R-HSA:5619102	SLC transporter disorders	0,02	0,02	10,20	10,00	[AVPR1A, NUP107, NUP160, NUP50, SLC22A12, SLC22A18, SLC26A3, SLC26A4, SLC35C1, SLC3A2]
GO:1900227	positive regulation of NLRP3 inflammasome complex assembly	0,02	0,02	30,00	3,00	[ATAT1, CD36, USP50]

Table 16: pathways derived from lost genes (LGSS)

GO:1902742	apoptotic process involved in development	0,05	0,04	11,63	5,00	[CYP27B1, FGF4, LRP5, SPI1, XKR4]
GO:1905208	negative regulation of cardiocyte differentiation	0,02	0,02	27,27	3,00	[DKK1, EGFR, FRS2]
KEGG:00360	Phenylalanine metabolism	0,04	0,04	17,65	3,00	[ALDH3B2, DDC, GLYAT]
KEGG:04137	Mitophagy	0,04	0,03	10,29	7,00	[AMBRA1, HRAS, RELA, TBC1D15, TBK1, USP15, USP8]
KEGG:04611	Platelet activation	0,01	0,01	10,48	13,00	[F2, FERMT3, GNAI1, LYN, MAPK11, MAPK12, PIK3CG, PLCB3, PPP1CA, PRKG1, RAP1B, RASGRP2, VASP]
R-HSA:1834941	STING mediated induction of host immune responses	0,04	0,03	18,75	3,00	[DTX4, STAT6, TBK1]
GO:0009414	response to water deprivation	0,02	0,02	27,27	3,00	[AVPR1A, SIPA1, TH]
R-HSA:3772470	Negative regulation of TCF-dependent signaling by WNT ligand antagonists	0,04	0,07	20,00	3,00	[DKK1, LRP5, WIF1]
WP:3658	Wnt/beta-catenin signaling pathway in leukemia	0,04	0,07	15,38	4,00	[CCND1, DKK1, LRP5, WIF1]
WP:3926	ApoE and miR-146 in inflammation and atherosclerosis	0,02	0,03	33,33	3,00	[RELA, SPI1, TRAF6]
GO:0001773	myeloid dendritic cell activation	0,05	0,03	13,33	4,00	[BATF2, SPI1, TRAF6, TSPAN32]
R-HSA:5358508	Mismatch Repair	0,04	0,03	20,00	3,00	[MSH2, MSH6, POLD4]
R-HSA:5358565	Mismatch repair (MMR) directed by MSH2:MSH6 (MutSalpha)	0,03	0,03	21,43	3,00	[MSH2, MSH6, POLD4]
KEGG:04115	p53 signaling pathway	0,01	0,03	12,33	9,00	[CCND1, CD82, CDK4, DDB2, FAS, GTSE1, MDM2, PIDD1, TNFRSF10B]
WP:707	DNA damage response	0,02	0,03	11,59	8,00	[CCND1, CDK4, DDB2, FAS, MDM2, PIDD1, RAD9A, TNFRSF10B]
GO:0010907	positive regulation of glucose metabolic process	0,01	0,01	17,07	7,00	[ACTN3, DDB1, DYRK2, IGF2, INS, MAP4K2, PPARA]
GO:0005979	regulation of glycogen biosynthetic process	0,02	0,01	15,15	5,00	[DYRK2, IGF2, INS, MAP4K2, PPP1CA]
GO:0014066	regulation of phosphatidylinositol 3-kinase signaling	0,00	0,01	10,87	15,00	[AGAP2, CAT, EGFR, F2, GLYAT, HGF, INS, LYN, NEDD4, PIK3CG, PIP4K2C, PPP2R5B, PRR5, PRR5L, RELN]
GO:0014068	positive regulation of phosphatidylinositol 3-kinase signaling	0,01	0,01	11,76	12,00	[AGAP2, CAT, F2, GLYAT, HGF, INS, LYN, NEDD4, PIK3CG, PRR5, PRR5L, RELN]
GO:0001727	lipid kinase activity	0,01	0,01	12,16	9,00	[AGAP2, AMBRA1, CD81, CERK, DGKZ, F2, LYN, PIP4K2C, TNFAIP8L3]
GO:0043550	regulation of lipid kinase activity	0,02	0,01	11,59	8,00	[AGAP2, AMBRA1, CD81, DGKZ, F2, LYN, PIP4K2C, TNFAIP8L3]
R-HSA:549132	Organic cation/anion/zwitterion transport	0,00	0,00	33,33	5,00	[SLC22A11, SLC22A12, SLC22A18, SLC22A6, SLC22A8]
R-HSA:561048	Organic anion transport	0,00	0,00	80,00	4,00	[SLC22A11, SLC22A12, SLC22A6, SLC22A8]
GO:0055093	response to hyperoxia	0,05	0,03	13,79	4,00	[CAT, CDK4, FAS, GLYAT]
GO:0033197	response to vitamin E	0,04	0,03	20,00	3,00	[CAT, CCND1, GLYAT]
GO:0060251	regulation of glial cell proliferation	0,01	0,02	18,18	6,00	[ASCL2, CHRM1, EGFR, LYN, PLAG1, TSPO]
GO:0060252	positive regulation of glial cell proliferation	0,02	0,02	22,22	4,00	[EGFR, LYN, PLAG1, TSPO]
GO:0061178	regulation of insulin secretion involved in cellular response to glucose stimulus	0,04	0,03	10,14	7,00	[ANO1, BAD, BRSK2, LRP1, LRP5, OSBP, PDHX]
GO:0035774	positive regulation of insulin secretion involved in cellular response to glucose stimulus	0,04	0,03	12,50	5,00	[ANO1, BAD, LRP1, OSBP, PDHX]
GO:0035094	response to nicotine	0,02	0,02	13,21	7,00	[BAD, GNAT3, PDHX, PENK, PPARA, RELA, TH]
GO:0071316	cellular response to nicotine	0,02	0,02	33,33	3,00	[BAD, RELA, TH]
R-HSA:209822	Glycoprotein hormones	0,02	0,03	25,00	3,00	[INHBA, INHBC, INHBE]
R-HSA:209952	Peptide hormone biosynthesis	0,03	0,03	21,43	3,00	[INHBA, INHBC, INHBE]
R-HSA:5633008	TP53 Regulates Transcription of Cell Death Genes	0,05	0,04	11,36	5,00	[FAS, PIDD1, TNFRSF10B, TNFRSF10C, TNFRSF10D]
R-HSA:6803211	TP53 Regulates Transcription of Death Receptors and Ligands	0,01	0,04	33,33	4,00	[FAS, TNFRSF10B, TNFRSF10C, TNFRSF10D]
R-HSA:5362768	Hh mutants are degraded by ERAD	0,04	0,01	10,71	6,00	[OS9, PSMA2, PSMC2, PSMC3, PSMD13, SYVN1]

R-HSA:5387390	Hh mutants abrogate ligand secretion	0,05	0,01	10,17	6,00	[OS9, PSMA2, PSMC2, PSMC3, PSMD13, SYVN1]
R-HSA:75815	Ubiquitin-dependent degradation of Cyclin D	0,04	0,01	11,54	6,00	[CCND1, CDK4, PSMA2, PSMC2, PSMC3, PSMD13]
R-HSA:1368082	RORA activates gene expression	0,05	0,03	16,67	3,00	[CPT1A, PPARA, TGS1]
R-HSA:1368108	BMAL1:CLOCK,NPAS2 activates circadian gene expression	0,04	0,03	14,81	4,00	[NAMPT, NPAS2, PPARA, TGS1]
R-HSA:400253	Circadian Clock	0,04	0,03	10,00	7,00	[CPT1A, CRY2, NAMPT, NPAS2, PPARA, PPP1CA, TGS1]
R-HSA:209776	Metabolism of amine-derived hormones	0,05	0,03	16,67	3,00	[DDC, TH, TPH2]
WP:1602	Nicotine Activity on Dopaminergic Neurons	0,03	0,03	18,18	4,00	[DDC, GNAI1, PPP1CA, TH]
WP:550	Biogenic Amine Synthesis	0,04	0,03	18,75	3,00	[DDC, HDC, TH]
GO:0033555	multicellular organismal response to stress	0,03	0,03	10,13	8,00	[MAPK8IP2, NPAS2, P2RX3, PENK, RAG1, RELN, SHANK3, TSPO]
GO:0001662	behavioral fear response	0,04	0,03	12,50	5,00	[MAPK8IP2, NPAS2, PENK, RAG1, SHANK3]
GO:2000822	regulation of behavioral fear response	0,00	0,03	36,36	4,00	[NPAS2, PENK, RAG1, SHANK3]
R-HSA:1482839	Acyl chain remodelling of PE	0,05	0,02	13,33	4,00	[PLAAT3, PLAAT4, PLAAT5, PNPLA8]
GO:0070292	N-acylphosphatidylethanolamine metabolic process	0,00	0,02	44,44	4,00	[NAPEPLD, PLAAT3, PLAAT4, PLAAT5]
GO:0046337	phosphatidylethanolamine metabolic process	0,00	0,02	21,21	7,00	[CHKA, CHKB, NAPEPLD, PLAAT3, PLAAT4, PLAAT5, PNPLA8]
R-HSA:447115	Interleukin-12 family signaling	0,05	0,07	10,53	6,00	[AIP, CFL1, IFNG, RALA, RAP1B, TALDO1]
R-HSA:8950505	Gene and protein expression by JAK-STAT signaling after Interleukin-12 stimulation	0,02	0,07	15,79	6,00	[AIP, CFL1, IFNG, RALA, RAP1B, TALDO1]
R-HSA:9020591	Interleukin-12 signaling	0,03	0,07	12,77	6,00	[AIP, CFL1, IFNG, RALA, RAP1B, TALDO1]
GO:0035722	interleukin-12-mediated signaling pathway	0,04	0,07	10,71	6,00	[AIP, CFL1, IFNG, RALA, RAP1B, TALDO1]
GO:0008271	secondary active sulfate transmembrane transporter activity	0,03	0,03	23,08	3,00	[SLC26A3, SLC26A4, SLC26A5]
GO:0015108	chloride transmembrane transporter activity	0,04	0,03	17,65	3,00	[SLC26A3, SLC26A4, SLC26A5]
GO:0015301	anion:anion antiporter activity	0,02	0,03	16,67	5,00	[SLC22A6, SLC22A9, SLC26A3, SLC26A4, SLC26A5]
GO:0019531	oxalate transmembrane transporter activity	0,02	0,03	30,00	3,00	[SLC26A3, SLC26A4, SLC26A5]
GO:0043113	receptor clustering	0,03	0,03	11,48	7,00	[CD81, LHFPL3, LRP4, MAGI2, NRXN2, RELN, SHANK3]
GO:0099068	postsynapse assembly	0,05	0,03	13,33	4,00	[LRFN4, LRP4, NRXN2, SHANK3]
GO:0072578	neurotransmitter-gated ion channel clustering	0,04	0,03	17,65	3,00	[LHFPL3, RELN, SHANK3]
GO:1904861	excitatory synapse assembly	0,04	0,03	15,38	4,00	[LRFN4, NRXN2, PLXNB2, SHANK3]
R-HSA:75067	Processing of Capped Intronless Pre-mRNA	0,04	0,02	14,29	4,00	[CLP1, CPSF7, CSTF2T, CSTF3]
R-HSA:77595	Processing of Intronless Pre-mRNAs	0,02	0,02	21,05	4,00	[CLP1, CPSF7, CSTF2T, CSTF3]
GO:0006379	mRNA cleavage	0,01	0,02	19,23	5,00	[CPSF6, CPSF7, CSTF2T, CSTF3, TUT1]
GO:0098789	pre-mRNA cleavage required for polyadenylation	0,01	0,02	30,77	4,00	[CPSF6, CPSF7, CSTF2T, TUT1]
WP:3942	PPAR signaling pathway	0,04	0,03	10,45	7,00	[CD36, CPT1A, CPT1B, FADS2, NR1H3, PPARA, SLC27A2]
GO:0032365	intracellular lipid transport	0,04	0,03	11,32	6,00	[CHKB-CPT1B, CPT1A, CPT1B, CTDSP2, OSBP, SYT7]
GO:0009437	carnitine metabolic process	0,04	0,03	18,75	3,00	[CHKB-CPT1B, CPT1A, CPT1B]
GO:1902001	fatty acid transmembrane transport	0,04	0,03	15,38	4,00	[CD36, CHKB-CPT1B, CPT1A, CPT1B]
R-HSA:5083625	Defective GALNT3 causes familial hyperphosphatemic tumoral calcinosis (HFTC)	0,04	0,04	17,65	3,00	[MUC5AC, MUC5B, MUC6]
R-HSA:5083632	Defective C1GALT1C1 causes Tn polyagglutination syndrome (TNPS)	0,05	0,04	16,67	3,00	[MUC5AC, MUC5B, MUC6]

R-HSA:5083636	Defective GALNT12 causes colorectal cancer 1 (CRCS1)	0,04	0,04	17,65	3,00	[MUC5AC, MUC5B, MUC6]
R-HSA:5621480	Dectin-2 family	0,04	0,04	14,81	4,00	[LYN, MUC5AC, MUC5B, MUC6]
KEGG:05218	Melanoma	0,00	0,00	15,28	11,00	[BAD, CCND1, CDK4, DDB2, EGFR, FGF19, FGF3, FGF4, HGF, HRAS, MDM2]
R-HSA:2219528	PI3K/AKT Signaling in Cancer	0,02	0,00	10,58	11,00	[BAD, EGFR, FGF19, FGF3, FGF4, FRS2, HGF, MDM2, NRG4, PRR5, RPS6KB2]
R-HSA:5674400	Constitutive Signaling by AKT1 E17K in Cancer	0,03	0,00	16,00	4,00	[BAD, MDM2, PRR5, RPS6KB2]
R-HSA:6811558	PI5P, PP2A and IER3 Regulate PI3K/AKT Signaling	0,02	0,00	10,38	11,00	[EGFR, FGF19, FGF3, FGF4, FRS2, HGF, INS, NRG4, PIP4K2C, PPP2R5B, TRAF6]
R-HSA:74751	Insulin receptor signalling cascade	0,02	0,00	12,96	7,00	[FGF19, FGF3, FGF4, FRS2, GRB10, HRAS, INS]
R-HSA:74752	Signaling by Insulin receptor	0,03	0,00	10,26	8,00	[FGF19, FGF3, FGF4, FRS2, GRB10, HRAS, INS, TCIRG1]
KEGG:03030	DNA replication	0,03	0,03	13,89	5,00	[FEN1, POLA2, POLD4, PRIM1, RNASEH2C]
R-HSA:69091	Polymerase switching	0,03	0,03	21,43	3,00	[POLA2, POLD4, PRIM1]
R-HSA:69109	Leading Strand Synthesis	0,03	0,03	21,43	3,00	[POLA2, POLD4, PRIM1]
R-HSA:69166	Removal of the Flap Intermediate	0,01	0,03	28,57	4,00	[FEN1, POLA2, POLD4, PRIM1]
R-HSA:69183	Processive synthesis on the lagging strand	0,01	0,03	26,67	4,00	[FEN1, POLA2, POLD4, PRIM1]
R-HSA:69186	Lagging Strand Synthesis	0,02	0,03	20,00	4,00	[FEN1, POLA2, POLD4, PRIM1]
KEGG:04931	Insulin resistance	0,01	0,02	11,11	12,00	[CD36, CPT1A, CPT1B, CREB3L1, INS, NR1H3, PPARA, PPP1CA, PYGM, RELA, RPS6KB2, SLC27A2]
WP:3942	PPAR signaling pathway	0,04	0,02	10,45	7,00	[CD36, CPT1A, CPT1B, FADS2, NR1H3, PPARA, SLC27A2]
GO:0019915	lipid storage	0,01	0,02	11,24	10,00	[B4GALNT1, BSCL2, CD36, CPT1A, CRY2, EHD1, NR1H3, PNPLA2, PPARA, VSTM2A]
GO:0010883	regulation of lipid storage	0,02	0,02	12,28	7,00	[CD36, CPT1A, EHD1, NR1H3, PNPLA2, PPARA, VSTM2A]
GO:0010878	cholesterol storage	0,02	0,02	20,00	4,00	[CD36, EHD1, NR1H3, PPARA]
GO:0010885	regulation of cholesterol storage	0,02	0,02	22,22	4,00	[CD36, EHD1, NR1H3, PPARA]
GO:1902001	fatty acid transmembrane transport	0,04	0,02	15,38	4,00	[CD36, CHKB-CPT1B, CPT1A, CPT1B]
KEGG:05210	Colorectal cancer	0,02	0,01	10,47	9,00	[BAD, CCND1, DDB2, EGFR, HRAS, MSH2, MSH6, RALA, RPS6KB2]
KEGG:05212	Pancreatic cancer	0,03	0,01	10,53	8,00	[BAD, CCND1, CDK4, DDB2, EGFR, RALA, RELA, RPS6KB2]
KEGG:05218	Melanoma	0,00	0,01	15,28	11,00	[BAD, CCND1, CDK4, DDB2, EGFR, FGF19, FGF3, FGF4, HGF, HRAS, MDM2]
KEGG:05219	Bladder cancer	0,02	0,01	14,63	6,00	[CCND1, CDK4, EGFR, HRAS, MDM2, UPK3A]
KEGG:05223	Non-small cell lung cancer	0,02	0,01	11,11	8,00	[BAD, CCND1, CDK4, DDB2, EGFR, HGF, HRAS, KIF5A]
R-HSA:2219528	PI3K/AKT Signaling in Cancer	0,02	0,01	10,58	11,00	[BAD, EGFR, FGF19, FGF3, FGF4, FRS2, HGF, MDM2, NRG4, PRR5, RPS6KB2]
WP:2828	Bladder cancer	0,02	0,01	14,63	6,00	[CCND1, CDK4, EGFR, HRAS, MDM2, UPK3A]
R-HSA:1227990	Signaling by ERBB2 in Cancer	0,04	0,02	15,38	4,00	[EGFR, HRAS, NRG4, PTPN12]
R-HSA:1250196	SHC1 events in ERBB2 signaling	0,03	0,02	18,18	4,00	[EGFR, HRAS, NRG4, PTPN12]
R-HSA:1963640	GRB2 events in ERBB2 signaling	0,04	0,02	18,75	3,00	[EGFR, HRAS, NRG4]
R-HSA:8863795	Downregulation of ERBB2 signaling	0,05	0,02	13,79	4,00	[EGFR, NRG4, PTPN12, USP8]
WP:2643	Nanoparticle-mediated activation of receptor signaling	0,05	0,02	13,79	4,00	[EGFR, HRAS, MAPK11, MAPK12]
WP:2870	Extracellular vesicle-mediated signaling in recipient cells	0,05	0,02	13,33	4,00	[EGFR, HGF, HRAS, TSPAN8]
WP:4483	Relationship between inflammation, COX-2 and EGFR	0,03	0,02	16,00	4,00	[CYP19A1, EGFR, HRAS, PIK3CG]
GO:0006956	complement activation	0,00	0,00	12,98	27,00	[CD59, CD81, F2, IGHG1, IGHG2, IGHG3, IGHG4, IGHV1-24, IGHV1-69-2, IGHV3-11, IGHV3-13, IGHV3-21, IGHV3-23, IGHV3-30, IGHV3-33, IGHV3-38, IGHV3-48, IGHV3-53, IGHV3-64, IGHV3-64D, IGHV3-66, IGHV3-7, IGHV3-74, IGHV3OR16-10, IGHV3OR16-12, IGHV3OR16-13, SERPING1]
GO:0010324	membrane invagination	0,00	0,00	15,57	26,00	[CD36, IGHG1, IGHG2, IGHG3, IGHG4, IGHV1-24, IGHV1-69-2, IGHV3-11, IGHV3-13, IGHV3-21, IGHV3-23, IGHV3-30, IGHV3-33, IGHV3-38, IGHV3-48, IGHV3-53, IGHV3-64, IGHV3-64D, IGHV3-66, IGHV3-7, IGHV3-74, IGHV3OR16-10, IGHV3OR16-12, IGHV3OR16-13, SYT12, XKR4]

GO:0002455	humoral immune response mediated by circulating immunoglobulin	0,00	0,00	13,81	25,00	[CD81, IGHG1, IGHG2, IGHG3, IGHG4, IGHV1-24, IGHV1-69-2, IGHV3-11, IGHV3-13, IGHV3-21, IGHV3-23, IGHV3-30, IGHV3-33, IGHV3-38, IGHV3-48, IGHV3-53, IGHV3-64, IGHV3-64D, IGHV3-66, IGHV3-7, IGHV3-74, IGHV3OR16-10, IGHV3OR16-12, IGHV3OR16-13, SERPING1]
GO:0006911	phagocytosis, engulfment	0,00	0,00	17,01	25,00	[CD36, IGHG1, IGHG2, IGHG3, IGHG4, IGHV1-24, IGHV1-69-2, IGHV3-11, IGHV3-13, IGHV3-21, IGHV3-23, IGHV3-30, IGHV3-33, IGHV3-38, IGHV3-48, IGHV3-53, IGHV3-64, IGHV3-64D, IGHV3-66, IGHV3-7, IGHV3-74, IGHV3OR16-10, IGHV3OR16-12, IGHV3OR16-13, XKR4]
GO:0016064	immunoglobulin mediated immune response	0,00	0,00	12,11	31,00	[CD81, IGHG1, IGHG2, IGHG3, IGHG4, IGHV1-24, IGHV1-69-2, IGHV3-11, IGHV3-13, IGHV3-21, IGHV3-23, IGHV3-30, IGHV3-33, IGHV3-38, IGHV3-48, IGHV3-53, IGHV3-64, IGHV3-64D, IGHV3-66, IGHV3-7, IGHV3-74, IGHV3OR16-10, IGHV3OR16-12, IGHV3OR16-13, IRF7, KMT5B, MSH2, MSH6, SERPING1, STAT6, TCIRG1]
GO:0030449	regulation of complement activation	0,00	0,00	12,50	16,00	[CD59, CD81, F2, IGHG1, IGHG2, IGHG3, IGHG4, IGHV3-11, IGHV3-13, IGHV3-23, IGHV3-30, IGHV3-33, IGHV3-48, IGHV3-53, IGHV3-7, SERPING1]
GO:0050864	regulation of B cell activation	0,00	0,00	14,16	31,00	[BAD, CD81, IGHG1, IGHG2, IGHG3, IGHG4, IGHV1-24, IGHV1-69-2, IGHV3-11, IGHV3-13, IGHV3-21, IGHV3-23, IGHV3-30, IGHV3-33, IGHV3-38, IGHV3-48, IGHV3-53, IGHV3-64, IGHV3-64D, IGHV3-66, IGHV3-7, IGHV3-74, IGHV3OR16-10, IGHV3OR16-12, IGHV3OR16-13, INHBA, KMT5B, LYN, MSH2, STAT6, TBC1D10C]
GO:0050871	positive regulation of B cell activation	0,00	0,00	16,09	28,00	[BAD, CD81, IGHG1, IGHG2, IGHG3, IGHG4, IGHV1-24, IGHV1-69-2, IGHV3-11, IGHV3-13, IGHV3-21, IGHV3-23, IGHV3-30, IGHV3-33, IGHV3-38, IGHV3-48, IGHV3-53, IGHV3-64, IGHV3-64D, IGHV3-66, IGHV3-7, IGHV3-74, IGHV3OR16-10, IGHV3OR16-12, IGHV3OR16-13, KMT5B, MSH2, STAT6]
KEGG:04740	Olfactory transduction	0,00	0,00	14,45	64,00	[GRK2, OR10AG1, OR10Q1, OR10V1, OR10W1, OR4A15, OR4A47, OR4A5, OR4C11, OR4C12, OR4C13, OR4C15, OR4C16, OR4C3, OR4C45, OR4C46, OR4C5, OR4C6, OR4D10, OR4D11, OR4D6, OR4D9, OR4K14, OR4P4, OR4S1, OR4S2, OR5A1, OR5AK2, OR5AN1, OR5AP2, OR5AR1, OR5AS1, OR5B12, OR5B17, OR5B2, OR5B21, OR5B3, OR5D13, OR5D14, OR5D18, OR5F1, OR5I1, OR5J2, OR5L1, OR5L2, OR5M3, OR5M8, OR5M9, OR5T1, OR5T2, OR5T3, OR6C68, OR6Q1, OR8J1, OR8J3, OR8K1, OR8K3, OR8U1, OR9G1, OR9G4, OR9I1, OR9Q2, PRKG1]
R-HSA:381753	Olfactory Signaling Pathway	0,00	0,00	15,48	61,00	[OR10AG1, OR10Q1, OR10V1, OR10W1, OR4A15, OR4A47, OR4A5, OR4C11, OR4C12, OR4C13, OR4C15, OR4C16, OR4C3, OR4C46, OR4C5, OR4C6, OR4D10, OR4D11, OR4D6, OR4D9, OR4K14, OR4P4, OR4S1, OR4S2, OR5A1, OR5A2, OR5AK2, OR5AN1, OR5AP2, OR5AR1, OR5AS1, OR5B12, OR5B17, OR5B2, OR5B21, OR5B3, OR5D13, OR5D14, OR5D18, OR5F1, OR5I1, OR5J2, OR5L1, OR5L2, OR5M3, OR5M8, OR5M9, OR5T1, OR5T2, OR5T3, OR6C68, OR6Q1, OR8J1, OR8J3, OR8K1, OR8K3, OR8U1, OR9G1, OR9G4, OR9I1, OR9Q2]
R-HSA:9709957	Sensory Perception	0,00	0,00	12,24	70,00	[CABP2, EPS8L2, HSD17B6, LRP1, NAPEPLD, OR10AG1, OR10Q1, OR10V1, OR10W1, OR4A15, OR4A47, OR4A5, OR4C11, OR4C12, OR4C13, OR4C15, OR4C16, OR4C3, OR4C46, OR4C5, OR4C6, OR4D10, OR4D11, OR4D6, OR4D9, OR4K14, OR4P4, OR4S1, OR4S2, OR5A1, OR5A2, OR5AK2, OR5AN1, OR5AP2, OR5AR1, OR5AS1, OR5B12, OR5B17, OR5B2, OR5B21, OR5B3, OR5D13, OR5D14, OR5D18, OR5F1, OR5I1, OR5J2, OR5L1, OR5L2, OR5M3, OR5M8, OR5M9, OR5T1, OR5T2, OR5T3, OR6C68, OR6Q1, OR8J1, OR8J3, OR8K1, OR8K3, OR8U1, OR9G1, OR9G4, OR9I1, OR9Q2, PCLO, RDH16, SDR9C7, SLC26A5]
GO:0009593	detection of chemical stimulus	0,00	0,00	13,41	70,00	[GNAT3, MAP4K2, OR10AG1, OR10Q1, OR10V1, OR10W1, OR4A15, OR4A47, OR4A5, OR4A8, OR4C11, OR4C12, OR4C13, OR4C15, OR4C16, OR4C3, OR4C45, OR4C46, OR4C5, OR4C6, OR4D10, OR4D11, OR4D6, OR4D9, OR4K14, OR4P4, OR4S1, OR4S2, OR5A1, OR5A2, OR5AK2, OR5AK3P, OR5AN1, OR5AP2, OR5AR1, OR5AS1, OR5B12, OR5B17, OR5B2, OR5B21, OR5B3, OR5D13, OR5D14, OR5D18, OR5D3P, OR5F1, OR5G3, OR5I1, OR5J2, OR5L1, OR5L2, OR5M3, OR5M8, OR5M9, OR5T1, OR5T2, OR5T3, OR6C68, OR6Q1, OR8J1, OR8J2, OR8J3, OR8K1, OR8K3, OR8U1, OR9G1, OR9G4, OR9I1, OR9Q2, PDHX]
GO:0050906	detection of stimulus involved in sensory perception	0,00	0,00	13,18	73,00	[ANO1, BEST1, GNAT3, KCNK4, OR10AG1, OR10Q1, OR10V1, OR10W1, OR4A15, OR4A47, OR4A5, OR4A8, OR4C11, OR4C12, OR4C13, OR4C15, OR4C16, OR4C3, OR4C45, OR4C46, OR4C5, OR4C6, OR4D10, OR4D11, OR4D6, OR4D9, OR4K14, OR4P4, OR4S1, OR4S2, OR5A1, OR5A2, OR5AK2, OR5AK3P, OR5AN1, OR5AP2, OR5AR1, OR5AS1, OR5B12, OR5B17, OR5B2, OR5B21, OR5B3, OR5D13, OR5D14, OR5D18, OR5D3P, OR5F1, OR5G3, OR5I1, OR5J2, OR5L1, OR5L2, OR5M3, OR5M8, OR5M9, OR5T1, OR5T2, OR5T3, OR6C68, OR6Q1, OR8J1, OR8J2, OR8J3, OR8K1, OR8K3, OR8U1, OR9G1, OR9G4, OR9I1, OR9Q2, PTPRR, ROM1]
GO:0007606	sensory perception of chemical stimulus	0,00	0,00	13,33	72,00	[BBS1, CD36, GNAT3, OR10AG1, OR10Q1, OR10V1, OR10W1, OR4A15, OR4A47, OR4A5, OR4A8, OR4C11, OR4C12, OR4C13, OR4C15, OR4C16, OR4C3, OR4C45, OR4C46, OR4C5, OR4C6, OR4D10, OR4D11, OR4D6, OR4D9, OR4K14, OR4P4, OR4S1, OR4S2, OR5A1, OR5A2, OR5AK2, OR5AK3P, OR5AN1, OR5AP2, OR5AR1, OR5AS1, OR5B12, OR5B17, OR5B2, OR5B21, OR5B3, OR5D13, OR5D14, OR5D18, OR5D3P, OR5F1, OR5G3, OR5I1, OR5J2, OR5L1, OR5L2, OR5M3, OR5M8, OR5M9, OR5T1, OR5T2, OR5T3, OR6C68, OR6Q1, OR8J1, OR8J2, OR8J3, OR8K1, OR8U1, OR9G1, OR9G4, OR9I1, OR9Q2, P2RX3, TRPM5]
GO:0050907	detection of chemical stimulus involved in sensory perception	0,00	0,00	14,02	68,00	[GNAT3, OR10AG1, OR10Q1, OR10V1, OR10W1, OR4A15, OR4A47, OR4A5, OR4A8, OR4C11, OR4C12, OR4C13, OR4C15, OR4C16, OR4C3, OR4C45, OR4C46, OR4C5, OR4C6, OR4D10, OR4D11, OR4D6, OR4D9, OR4K14, OR4P4, OR4S1, OR4S2, OR5A1, OR5A2, OR5AK2, OR5AK3P, OR5AN1, OR5AP2, OR5AR1, OR5AS1, OR5B12, OR5B17, OR5B2, OR5B21, OR5B3, OR5D13, OR5D14, OR5D18, OR5D3P, OR5F1, OR5G3, OR5I1, OR5J2, OR5L1, OR5L2, OR5M3, OR5M8, OR5M9, OR5T1, OR5T2, OR5T3, OR6C68, OR6Q1, OR8J1, OR8J2, OR8J3, OR8K1, OR8K3, OR8U1, OR9G1, OR9G4, OR9I1, OR9Q2]
GO:0007608	sensory perception of smell	0,00	0,00	14,69	68,00	[BBS1, OR10AG1, OR10Q1, OR10V1, OR10W1, OR4A15, OR4A47, OR4A5, OR4A8, OR4C11, OR4C12, OR4C13, OR4C15, OR4C16, OR4C3, OR4C45, OR4C46, OR4C5, OR4C6, OR4D10, OR4D11, OR4D6, OR4D9, OR4K14, OR4P4, OR4S1, OR4S2, OR5A1, OR5A2, OR5AK2, OR5AK3P, OR5AN1, OR5AP2, OR5AR1, OR5AS1, OR5B12, OR5B17, OR5B2, OR5B21, OR5B3, OR5D13, OR5D14, OR5D18, OR5D3P, OR5F1, OR5G3, OR5I1, OR5J2, OR5L1, OR5L2, OR5M3, OR5M8, OR5M9, OR5T1, OR5T2, OR5T3, OR6C68, OR6Q1, OR8J1, OR8J2, OR8J3, OR8K1, OR8K3, OR8U1, OR9G1, OR9G4, OR9I1, OR9Q2]
GO:0004984	olfactory receptor activity	0,00	0,00	15,44	67,00	[OR10AG1, OR10Q1, OR10V1, OR10W1, OR4A15, OR4A47, OR4A5, OR4A8, OR4C11, OR4C12, OR4C13, OR4C15, OR4C16, OR4C3, OR4C45, OR4C46 , OR4C5, OR4C6, OR4D10, OR4D11, OR4D6, OR4D9, OR4K14, OR4P4, OR4S1, OR4S2, OR5A1, OR5A2, OR5AK2, OR5AK3P, OR5AN1, OR5AP2, OR5AR1, OR5AS1, OR5B12, OR5B17, OR5B2, OR5B21, OR5B3, OR5D13, OR5D14, OR5D18, OR5D3P, OR5F1, OR5G3, OR5I1, OR5J2, OR5L1, OR5L2, OR5M3, OR5M8, OR5M9, OR5T1, OR5T2, OR5T3, OR6C68, OR6Q1, OR8J1, OR8J2, OR8J3, OR8K1, OR8K3, OR8U1, OR9G1, OR9G4, OR9I1, OR9Q2]
R-HSA:2404192	Signaling by Type 1 Insulin-like Growth Factor 1 Receptor (IGF1R)	0,04	0,01	11,11	6,00	[FGF19, FGF3, FGF4, FRS2, HRAS, IGF2]
R-HSA:2428924	IGF1R signaling cascade	0,04	0,01	11,32	6,00	[FGF19, FGF3, FGF4, FRS2, HRAS, IGF2]
R-HSA:2428928	IRS-related events triggered by IGF1R	0,04	0,01	11,54	6,00	[FGF19, FGF3, FGF4, FRS2, HRAS, IGF2]
R-HSA:5654687	Downstream signaling of activated FGFR1	0,02	0,01	16,13	5,00	[FGF3, FGF4, FLRT1, FRS2, HRAS]
R-HSA:5654693	FRS-mediated FGFR1 signaling	0,03	0,01	17,39	4,00	[FGF3, FGF4, FRS2, HRAS]
R-HSA:5654696	Downstream signaling of activated FGFR2	0,05	0,01	13,33	4,00	[FGF3, FGF4, FRS2, HRAS]
R-HSA:5654700	FRS-mediated FGFR2 signaling	0,03	0,01	16,00	4,00	[FGF3, FGF4, FRS2, HRAS]
R-HSA:5654712	FRS-mediated FGFR4 signaling	0,03	0,01	18,18	4,00	[FGF19, FGF4, FRS2, HRAS]
R-HSA:5654716	Downstream signaling of activated FGFR4	0,04	0,01	14,81	4,00	[FGF19, FGF4, FRS2, HRAS]
R-HSA:5655253	Signaling by FGFR2 in disease	0,05	0,01	11,63	5,00	[FGF3, FGF4, FRS2, HRAS, POLR2G]
R-HSA:6811558	PI5P, PP2A and IER3 Regulate PI3K/AKT Signaling	0,02	0,01	10,38	11,00	[EGFR, FGF19, FGF3, FGF4, FRS2, HGF, INS, NRG4, PIP4K2C, PPP2R5B, TRAF6]
R-HSA:74751	Insulin receptor signalling cascade	0,02	0,01	12,96	7,00	[FGF19, FGF3, FGF4, FRS2, GRB10, HRAS, INS]

R-HSA:74752	Signaling by Insulin receptor	0,03	0,01	10,26	8,00	[FGF19, FGF3, FGF4, FRS2, GRB10, HRAS, INS, TCIRG1]
KEGG:04622	RIG-I-like receptor signaling pathway	0,04	0,02	10,00	7,00	[IRF7, MAPK11, MAPK12, RELA, TBK1, TKFC, TRAF6]
KEGG:04917	Prolactin signaling pathway	0,02	0,02	11,43	8,00	[CCND1, ELF5, HRAS, INS, MAPK11, MAPK12, RELA, TH]
KEGG:05235	PD-L1 expression and PD-1 checkpoint pathway in cancer	0,03	0,02	10,11	9,00	[BATF2, EGFR, HRAS, IFNG, MAPK11, MAPK12, RELA, RPS6KB2, TRAF6]
R-HSA:167044	Signalling to RAS	0,02	0,02	20,00	4,00	[HRAS, MAPK11, MAPK12, RALA]
R-HSA:171007	p38MAPK events	0,01	0,02	30,77	4,00	[HRAS, MAPK11, MAPK12, RALA]
R-HSA:187687	Signalling to ERKs	0,03	0,02	14,71	5,00	[FRS2, HRAS, MAPK11, MAPK12, RALA]
R-HSA:1963640	GRB2 events in ERBB2 signaling	0,04	0,02	18,75	3,00	[EGFR, HRAS, NRG4]
WP:2643	Nanoparticle-mediated activation of receptor signaling	0,05	0,02	13,79	4,00	[EGFR, HRAS, MAPK11, MAPK12]
WP:3303	RAC1/PAK1/p38/MMP2 Pathway	0,04	0,02	10,14	7,00	[BAD, EGFR, HRAS, MAPK11, MAPK12, MSH2, RELA]
WP:3611	Photodynamic therapy-induced AP-1 survival signaling.	0,02	0,02	13,73	7,00	[CCND1, EGFR, FAS, IFNG, MAPK11, MAPK12, TRAF6]
WP:3851	TLR4 Signaling and Tolerance	0,05	0,02	13,33	4,00	[IRAK3, IRF7, TBK1, TRAF6]
WP:3858	Toll-like Receptor Signaling related to MyD88	0,02	0,02	15,63	5,00	[IRF7, RELA, TBK1, TOLLIP, TRAF6]
WP:3865	Novel intracellular components of RIG-I-like receptor (RLR) pathway	0,01	0,02	13,11	8,00	[IFNG, IRF7, MAPK11, MAPK12, RELA, TBK1, TKFC, TRAF6]